LCH Laboratoire de Constructions Hydrauliques
Laboratory of Hydraulic Constructions

ÉCOLE POLYTECHNIQUE
FÉDÉRALE DE LAUSANNE

Communication 52

Operation of complex hydropower schemes and its impact on the flow regime in the downstream river system under changing scenarios

M. Bieri

Editeur : Prof. Dr A. Schleiss

Lausanne, 2012

Communications du Laboratoire de Constructions Hydrauliques ISSN 1661-1179
Ecole Polytechnique Fédérale de Lausanne
Editeur: Prof. Dr A. Schleiss

N° 26 2006 M. Andaroodi
Standardization of civil engineering works of small high-head hydropower plants and development of an optimization tool

N° 27 2006 Symposium érosion et protection des rives lacustres
Bases de dimensionnement des mesures de protection des rives lacustres

N° 28 2007 A. Vela Giró
Bank protection at the outer side of curved channels by an undulated concrete wall

N° 29 2007 F. Jordan
Modèle de prévision et de gestion des crues - Optimisation des opérations des aménagements hydroélectriques à accumulation pour la réduction des débits de crue

N° 30 2007 P. Heller
Méthodologie pour la conception et la gestion des aménagements hydrauliques à buts multiples

N° 31 2007 P. Heller
Analyse qualitative des systèmes complexes à l'aide de la méthode de Gomez & Probst

N° 32 2007 J. García Hernández, F. Jordan, J. Dubois, J.-L. Boillat
Routing System II - Modélisation d'écoulements dans des systèmes hydrauliques

N° 33 2007 Symposium - Flussbauliche Massnahmen im Dienste des Hochwasserschutzes, der Umwelt, Gesellschaft und Wirtschaft / Mesures d'aménagement des cours d'eau pour la protection contre les crues, l'environnement, la société et l'économie

N° 34 2007 B. Rosier
Interaction of side weir overflow with bed-load transport and bed morphology in a channel

N° 35 2007 A. Amini
Contractile floating barriers for confinement and recuperation of oil slicks

N° 36 2008 T. Meile
Influence of macro-roughness of walls on steady and unsteady flow in a channel

N° 37 2008 S. A. Kantoush
Experimental study on the influence of the geometry of shallow reservoirs on flow patterns and sedimentation by suspended sediments

N° 38 2008 F. Jordan, J. García Hernández, J. Dubois, J.-L. Boillat
Minerve - Modélisation des intempéries de nature extrême du Rhône valaisan et de leurs effets

Preface

High-head storage hydropower plants are designed to concentrate their turbine operation during periods of high-energy demand in order to satisfy the latter. The sudden opening and closing of the turbines produce highly unsteady or transient flow conditions, called hydropeaking, in the river downstream of the powerhouse outlet. Hydropeaking modifies the river flow regime. Large fluctuations in discharge and water levels associated with hydropeaking may result in a loss of habitats. In the framework of river restoration projects and according to the legal requirements in Switzerland, the negative effects of hydropeaking have to be mitigated.

Innovative hydropeaking mitigation measures are subsequently required, which do not question the economic soundness of the hydropower production. Especially in complex hydropower schemes, as they exist in Switzerland, it is a challenge to identify sustainable hydropeaking mitigation measures. In this thesis research project, Dr. Martin Bieri developed a novel integrative approach to model and to assess the impact of the operation of high-head storage hydropower schemes on the downstream river system. The approach is based on an economic-ecological coupled analysis and contains several aspects including: precipitation-runoff modeling in glacierized Alpine catchment areas, optimization of hydropower operation in a free electricity exchange market, and identification of hydropeaking measures with cost estimation in order to assess them with habitat models for target species and reference river morphologies. Construction measures (e.g., retention basins, plant enhancements) are preferred to restrictions of turbine operations. From socio-economic and energy production points of view, the latter was assessed as less efficient.

Dr. Martin Bieri developed and applied his novel integrative approach to one of the probably most complex hydropower schemes in Switzerland, namely the Kraftwerke Oberhasli scheme in the Swiss Alps.

Gratitude is expressed to the *e-dric.ch* consulting engineers for their support and guidance in using the RS 3.0 based simulation tool. I would like to thank also the members of the thesis committee, Prof. Andrew Barry (president) and Prof. Paolo Perona from IIE-EPFL, Dr. Steffen Schweizer from the Kraftwerke Oberhasli AG (KWO) and Prof. Bernhard Wehrli from EAWAG for their valuable comments and suggestions. The Swiss Innovation Promotion Agency (CTI) is acknowledged for the financial support of the project 9676.1 PFIW-IW, co-financed by KWO and other private and public partners.

Prof. Dr. Anton Schleiss

Abstract

Operation of complex hydropower schemes and its impact on the flow regime in the downstream river system under changing scenarios

Hydropower is the world's most important renewable electricity source. More than 40% of European hydroelectric energy is produced in Alpine countries. High-head storage hydropower plants (HPP) contribute significantly to peak energy production as well as electricity grid regulation. Future plant management is faced with several challenges concerning modified availability of water resources due to climate change as well as new economic constraints associated with legal, political and electricity market issues.

HPP operation results in unsteady water release to the downstream river system. Hydropeaking is the primary factor of flow regime alteration, impacting the river ecosystem. Even when the biological response to hydropeaking is not fully understood, the recently adapted law on water protection prescribes its mitigation in Switzerland.

In this research project, a novel integrative approach to model and assess the impact of the operation of a complex hydropower scheme on the downstream river system is developed. It contains (1) a precipitation-runoff model extended for long-term simulations of glacierized Alpine catchment areas, (2) an operation tool for high-head storage HPP, (3) flow regime generation with cost estimation of hydropeaking mitigation measures and (4) a habitat model of reference river morphologies for a target species.

The upper Aare River (Hasliaare) in Switzerland is an Alpine stream, affected by hydropeaking from a complex hydropower scheme with several storage volumes and power houses. Since the 1930s, seasonal water transfer from summer to winter and the amplitude and frequency of daily peak discharge have been continuously increased. Furthermore, the dynamic braided river network with various mesohabitats gave way to a mainly monotonous channel. Although diversity of species and biomass of aquatic biota have drastically decreased, the potential of redevelopment remains. Investigations to improve the river morphology and the flow regime are under discussion. The upper Aare River catchment is therefore an appropriate case study for analysis of the interactions between climatic, hydrological, hydraulic, economic as well as ecological parameters.

The simulation of runoff in Alpine catchment areas is essential for optimal hydropower exploitation under normal flow conditions, but also for the analysis of flood events. The semi-distributed conceptual modeling approach *Routing System* contains a reservoir-based precipitation-runoff transformation model (GSM-SOCONT), extended by dynamic glacier simulation tool. Spatial precipitation and temperature distributions are taken into account for simulating the relevant hydrological processes, such as glacier melt, snowpack constitution and melt, soil infiltration and runoff. The model development, calibration and validation are illustrated for the 2005 flood event, where the flood reduction capacity of the HPP is discussed, as well as future long-term runoff estimations. Climate change scenarios, based on a reference climate period, take into account intra-annual temperature and precipitation variations as well as their long-term tendencies. Runoff series of daily resolution are produced by hourly updating of the meteorological, glaciological and hydrological parameters. An almost complete de-

glacierization of the upper Aare River basin is simulated for the late 21st century. The resulting reduction of glacier melt in summer and earlier snowmelt in spring change the runoff regime from glacio-nival to nival.

The implemented heuristic hydropower modeling tool in *Routing System* allows simulation of the operating mode of complex HPP. Within the case study of the upper Aare River catchment and despite the complexity of the HPP network, the influence of climate change, electricity market issues, plant enhancements as well as hydropeaking constraints is simulated and assessed. Despite the reduction of future runoff, increased flexibility due to new turbine and pumped-storage capacities allows compensation, especially in the case of volatile electricity prices, and could even partially restore the natural flow regime.

Several operational and construction measures to reduce hydropeaking are implemented in the model. Resulting flow regimes as well as the related costs are defined. Operational constraints, such as limitation of turbine discharge, increase of residual flow or limited drawdown range, generate relatively high costs compared to their environmental effectiveness. Better ecological and economic response is achieved by construction measures, such as flow deviation systems or compensation basins installed downstream of the power house outflow where the water is temporarily stored and then released to the river by a guided system.

The simulated flow regimes are rated by a river specific habitat model for representative morphologies and three life stages of the target species brown trout (*Salmo trutta fario*). This is based on results from a 2D hydrodynamic model and *in situ* investigations undertaken in the framework of a joint project of EAWAG. Steady and dynamic indicators quantify fish habitat suitability and allow comparison through economic indices of the implemented mitigation measures. For the Hasliaare River, investments for mitigation of hydropeaking are only justified by morphological improvements.

The developed approach is useful for the enhancement of complex storage hydropower schemes regarding mitigation of altered flow regimes. Despite several uncertainties, it allows operators, authorities and researchers to define and rate the impact of HPP operation on the river network, to ecologically and economically assess mitigation measures and thus to address hydropeaking in a straightforward manner.

Keywords: Hydrological modeling, hydropeaking, hydropower, Alps, flood retention, climate change, glacier melt, electricity market, plant management, optimization, mitigation measures, habitat suitability, rating.

Zusammenfassung

Der Betrieb komplexer Wasserkraftanlagen und dessen Auswirkungen auf das Abflussregime des unterhalb liegenden Fliessgewässers

Die Wasserkraft ist momentan immer noch die wichtigste erneuerbare Energiequelle weltweit. In Europa wird mehr als 40% des Stroms aus Wasserkraft im Alpenraum produziert. Speicherkraftwerke sind für die Erzeugung von Spitzenstrom und die Netzregulierung von zentraler Bedeutung. Die Wasserkraft wird in Zukunft mit grossen Herausforderungen konfrontiert, wie z.B. die durch den Klimawandel veränderte Verfügbarkeit der Ressource Wasser sowie neue Randbedingungen rechtlicher, politischer und wirtschaftlicher Art.

Der Betrieb von Speicherkraftwerken führt zu instationärer Wasserabgabe in das unterhalb liegende Fliessgewässer. Schwall und Sunk erzeugt erhebliche Veränderungen des Fliessregimes und somit des Ökosystems. Obwohl bis jetzt die biotischen Beeinträchtigungen nur ansatzweise verstanden werden, schreibt das Schweizerische Gewässerschutzgesetz eine Reduktion der negativen Auswirkungen von Schwall und Sunk vor.

In der vorliegenden Forschungsarbeit wurde ein neuartiger integrativer Ansatz zur Modellierung und Beurteilung der Auswirkungen der Wasserkraftnutzung auf unterhalb liegende Fliessgewässer erarbeitet. Die Methode beinhaltet (1) ein hydrologisches Modell für Langzeitsimulationen von alpinen, teilweise vergletscherten Einzugsgebieten, (2) ein Betriebssimulationstool für Speicherkraftwerke, (3) eine Bestimmung des Abflussregimes resultierend aus schwalldämpfenden Massnahmen und (4) ein Fischhabitatsmodell.

Der obere Aarelauf (oder Hasliaare) in der Schweiz ist ein schwallbeeinträchtigtes alpines Gewässer unterhalb eines komplexen Wasserkraftwerks, bestehend aus mehreren Speichern und Zentralen. Seit den 30er Jahren nahm der saisonale Wassertransfer vom Sommer in den Winter sowie die täglichen Abflussschwankungen durch Kraftwerksausbauten stetig zu. Zudem musste das natürlich verzweigte Gerinne mit verschiedensten Mesohabitatstypen einer monotonen kanalisierten Gewässermorphologie weichen. Dies führte zu einer Reduktion der Biomassen und zu einem Rückgang der Artenvielfalt der aquatischen Organismen. Die Wiederbesiedelungspotential wir als intakt eingestuft. Diskussionen über eine Gewässersanierung morphologischer und hydrologischer Art sind im Gange. Das Einzugsgebiet der Hasliaare ist darum als Fallstudie zur Untersuchung der Zusammenhänge zwischen klimatischen, hydrologischen, hydraulischen, wirtschaftlichen sowie ökologischen Einflussgrössen sehr gut geeignet.

Die Simulation der Abflüsse in Einzugsgebieten ist für eine optimale Bewirtschaftung der Wasserkraftanlagen unter Normal- sowie Hochwasserbedingungen von Bedeutung. Die Software *Routing System* basiert auf einem konzeptionellen Modellierungsansatz und beinhaltet ein für Langzeitsimulationen erweitertes speicherbasiertes Niederschlags-Abfluss-Transformationsmodell (GSM-SOCONT). Eine räumliche Niederschlags- und Temperaturverteilung wird zur Berechnung der vorherrschenden hydrologischen Prozesse, wie Schnee- resp. Gletscherbildung und -schmelze, Grundwasser und Oberflächenabfluss, berücksichtigt. Tagesabflüsse werden

mit einem stündlichen Zeitschritt bestimmt. Der Aufbau des Modells sowie dessen Kalibrierung und Anwendung werden anhand des 2005 Hasliaare-Hochwasserereignisses, wo der Retentionseffekt der Speicherseen untersucht wurde, sowie an Langzeitabflussvorhersagen erläutert. Die Klimaszenarien basieren auf einer Referenzperiode und berücksichtigen künftige intra- und interannuelle Niederschlags- und Temperaturänderungen. Ohne Verringerung der CO_2-Emmissionen werden bis zum Ende des 21. Jahrhunderts weitgehend alle Gletscher im untersuchten Einzugsgebiet geschmolzen sein. Der daraus folgende Rückgang der sommerlichen Gletscherschmelze und die frühere Schneeschmelze im Frühling verändern das Abflussregime von glazio-nival zu nival.

Ein heuristischer Modellierungsansatz wurde in *Routing System* zur Optimierung des Betriebs von Kraftwerkskomplexen verwendet. Im Rahmen der Fallstudie der Kraftwerke Oberhasli – und trotz der Komplexität des Systems – kann der Einfluss der Klimaänderung, Umwälzungen im Strommarkt, Ausbauvorhaben sowie ökologische Randbedingungen untersucht werden. Somit können Flexibilitätssteigerungen durch den Zubau von Turbinen- sowie Pumpspeicherkapazitäten den künftigen natürlichen Zuflussrückgang weitgehend kompensieren, sofern gleichzeitig die Volatilität der Strompreise zunimmt. Zur Aufwertung des Abflussregimes können Kraftwerkserweiterungen mit ökologischen Aufwertungsmassnahmen für besonders sensitive Teilstücke kombiniert werden.

Mehrere betriebliche und bauliche Massnahmen zur Verminderung der Auswirkungen von Schwall und Sunk sind im Modell implementiert und simuliert worden, sowie deren resultierende Ganglinien und Kosten bestimmt. Betriebliche Einschränkungen, wie z.B. eine Begrenzung des Maximalturbinenabflusses, eine Erhöhung des Restwassers oder ein limitiertes Schwall/Sunk-Verhältnis, haben unter Umständen erhebliche Ertragseinbussen zur Folge und schlagen sich in einem unausgewogenen Kosten-Nutzen-Verhältnis nieder. Aus wirtschaftlicher und ökologischer Sicht sind bauliche Massnahmen, wie Umleitstollen oder Ausgleichsbecken unterhalb der Wasserrückgabe von Kraftwerken, zu bevorzugen.

Fischbiologische Untersuchungen der EAWAG ermöglichen es, die resultierenden Ganglinien mit einem gewässerspezifischen Habitatsmodell ökologisch zu bewerten, indem für vier Referenzmorphologien die Habitatseignung für drei Entwicklungsstadien der Forelle (*Salmo trutta fario*) bestimmt wird. Stationäre und dynamische Indikatoren quantifizieren die Habitatspräferenz, was eine Kosten-Nutzen-Beurteilung der Schwallsanierungsmassnahmen erlaubt. Diese Indikatoren zeigen im Fall der Hasliaare, dass Abflusskorrekturen nur verbunden mit morphologischen Anpassungen zu einer Aufwertung des aquatischen Lebensraums führen.

Die entwickelte Methode ist für Schwallsanierungsmassnahmen unterhalb von Speicherkraftwerken anwendbar. Trotz mehrerer Unsicherheiten erlaubt sie Betreibern, Behörden und Wissenschaftlern eine ökologisch-ökonomische Modellierung und somit die Möglichkeit einer zielgerichteten und effizienten Gewässersanierung.

Schlüsselwörter: Hydrologische Modellierung, Schwall und Sunk, Wasserkraft, Alpen, Hochwasserrückhalt, Klimawandel, Gletscherschmelze, Strommarkt, Betrieb von Wasserkraftwerken, Optimierung, Verbesserungsmassnahmen, Habitatseignung, Bewertung.

Résumé

L'exploitation des aménagements hydroélectriques complexes et son impact sur le régime d'écoulement du cours d'eau aval

L'hydraulique est toujours la source d'énergie renouvelable la plus importante mondialement. Plus de 40% de l'hydro-électricité européenne provient des pays alpins. Les aménagements d'accumulation à haute chute contribuent significativement à la production d'énergie de pointe et à la régulation des réseaux électriques. Dans l'avenir, l'exploitation hydroélectrique sera confrontée à plusieurs défis relatifs d'une part à l'impact du changement climatique sur la disponibilité des ressources en eau et d'autre part aux contraintes économiques imposées par l'évolution des circonstances légales, politiques et commerciales.

La production hydroélectrique conduit à une restitution non-stationnaire de l'eau dans la rivière aval. Le marnage est la source majeure de la dégradation du régime d'écoulement et par conséquent de l'écosystème fluvial. Même si son effet sur les paramètres biologiques n'est que partiellement compris, la loi prescrit son atténuation.

Dans ce projet de recherche, une nouvelle approche intégrative de modélisation et d'évaluation de l'impact des aménagements hydroélectriques complexes sur le cours d'eau aval est développée. La méthode de diagnostic et intervention contient (1) un modèle hydrologique pour une évaluation des bassins versants glaciaires alpins à long terme, (2) un outil de gestion de l'exploitation des aménagements d'accumulation à haute chute, (3) la définition du régime d'écoulement et les coûts des mesures d'atténuation du marnage et (4) un modèle d'habitat pour des morphologies spécifiques et une espèce indicateur.

L'Aar supérieur (ou Hasliaare) en Suisse est un cours d'eau alpin soumis au marnage d'un complexe hydroélectrique composé de plusieurs retenues et centrales de production. Depuis les années 1930, le transfert d'eau estivale en hiver ainsi que l'amplitude et la fréquence des fluctuations journalières de débit ont considérablement augmenté. En outre, la morphologie naturelle en tresses présentant une multitude de mesohabitats a été transformée en canal rectiligne dans la vallée. Malgré la forte réduction de la biodiversité et biomasse des faune et flore aquatiques, le potentiel de redéveloppement a été jugé comme étant toujours existant. Des discussions concernant une réhabilitation au niveau morphologique et hydraulique sont en cours. Le bassin versant de l'Aar supérieur est donc un cas d'étude approprié pour l'analyse de l'interaction entre les paramètres climatiques, hydrologiques, hydrauliques, économiques et écologiques.

La simulation de l'apport en eau des bassins versants est essentielle pour une gestion optimale des forces hydrauliques en conditions normales, mais également en cas de crues. L'approche conceptuelle semi-distribuée de *Routing System* contient un modèle de transformation précipitations-apports constitué de différents réservoirs d'eau (GSM-SOCONT). Une distribution spatiale des précipitations et de la température est prise en compte pour la simulation des processus hydrologiques prédominants, comme la constitution de la couche de neige, la fonte de neige et de glace, l'infiltration et le ruissellement. Le développement, le calage ainsi que l'application du modèle sont discutés pour la crue de 2005, où l'effet de rétention de l'aménagement est étudié, et

pour des estimations d'apports à long terme. Les scénarios de changement climatique sont basés sur une période de référence et tiennent compte des variations intra- et interannuelles de température et de précipitations. Les apports journaliers sont simulés par une mise à jour horaire des paramètres météorologiques, glaciologiques et hydrologiques. Sans réduction des émissions en CO_2, une disparition de la quasi-totalité de la masse glaciaire est prévue pour la fin du 21ème siècle. Par conséquence, l'absence de la fonte de glace en été et la fonte de neige survenant plus tôt au printemps modifierait le régime de glacio-nival à nival.

Une approche heuristique implantée dans le logiciel *Routing System* permet la simulation du mode d'exploitation des aménagements hydroélectriques complexes. Dans le cas d'étude du bassin versant de l'Aar supérieur, et malgré la complexité du système, l'influence du climat, l'effet de la libéralisation du marché de l'électricité, les extensions de l'aménagement ainsi que les contraintes environnementales sont simulés et évalués. Au niveau économique, une augmentation de la flexibilité opérationnelle induite par des nouvelles capacités de (pompage-) turbinage permet de compenser la réduction des apports futurs, en particulier en cas d'une variabilité croissante du prix de l'électricité. Ces renforcements peuvent être combinés avec des restrictions sur les paliers écologiquement sensibles afin de restaurer le régime d'écoulement naturel.

Plusieurs mesures opérationnelles et constructives ayant pour objectif de réduire le marnage sont implantées dans le modèle. Les régimes d'écoulement résultant et leurs coûts sont définis. Des contraintes au niveau de la gestion de l'aménagement, comme la réduction de la capacité de turbinage, l'augmentation du débit résiduel ou la limitation du ratio entre les débits minimum et maximum, imposent un coût relativement important en comparaison avec l'efficacité écologique de la mesure. Un meilleur résultat au niveau écologique et économique est atteint pour des mesures constructives, comme une galerie de déviation ou un bassin de compensation à l'aval des turbines. L'eau est temporairement retenue pour être ensuite restituée, atténuant ainsi les pointes.

Le régime d'écoulement est évalué pour un modèle d'habitat spécifique pour les morphologies représentatives et trois périodes de vie de la truite (*Salmo trutta fario*), basé sur des études *in situ* réalisées dans le cadre d'un projet de recherche mené par l'EAWAG. Les indicateurs stationnaires et dynamiques quantifient la préférence d'habitat. Ils permettent une analyse coûts-avantages des mesures d'atténuation du marnage prévues. Pour le cas de l'Aar, ces indices montrent que la réhabilitation du régime d'eau doit être combinée avec une amélioration de l'état morphologique du cours d'eau pour augmenter la qualité des habitats piscicoles.

L'approche développée est utile pour l'extension des aménagements d'accumulation à haute chute ayant pour objectif une atténuation du régime d'écoulement altéré d'un cours d'eau. Malgré plusieurs sources d'incertitudes, elle permet aux opérateurs, autorités et chercheurs de définir l'impact écologique de l'exploitation, nécessaire à l'évaluation multi-objectif des interventions, et donc de traiter le marnage d'une manière directe et efficace.

Mots-clés: Modélisation hydrologique, rétention des crues, marnage, Alpes, changement climatique, fonte des glaciers, marché d'électricité, gestion des aménagements hydroélectriques, optimisation, mesures d'atténuation du marnage, préférence d'habitat, évaluation.

Contents

1

Introduction

Hydropower is still the major renewable electricity source worldwide. More than 40% of European hydroelectric power is produced in Alpine countries. High-head storage hydropower plants (HPP) contribute significantly to peak energy production as well as grid regulation in central Europe. Future operation is faced with several challenges concerning modified availability of water resources due to climate change as well as new economic constraints according to legal, political and electricity market issues. Furthermore, the sudden opening and closing of the turbines produces highly unsteady flow conditions called hydropeaking in the river downstream of the power house outlet. Degradation of the riverine ecosystem may result. River and especially flow regime restoration impacts the HPP operation. Thus, sustainability of hydropower is or will become an important issue. The hereafter developed methodology is useful for the enhancement of complex storage hydropower schemes regarding mitigation of the altered flow regime. The approach allows operators of hydropower plants, authorities or researchers to analyze affected catchment areas, to do an ecological and economic rating of construction, operational or morphological measures and thus to address hydropeaking in an optimal manner.

This chapter presents the context and formulates the main objectives of the research project. It also provides the applied methodology and describes the structure of the thesis report.

1.1 Context

The thesis is part of the project entitled *Sustainable use of hydropower – Innovative mitigation measures for hydropeaking* (9676.1 PFIW-IW) and supported by the Commission for Technology and Innovation (CTI). An interdisciplinary approach is chosen to improve the habitat conditions of river systems influenced by hydropower operations. Hydropeaking interacts with hydraulic, morphological and ecological parameters. Because of this diversity, collaboration between the Laboratory of Hydraulic Constructions of the Ecole Polytechnique Fédérale de Lausanne (LCH-EPFL), the Department of Fish Ecology and Evolution of the Swiss Federal Institute of Aquatic Science and Technology (EAWAG) and the Institute of Construction and Environment of the College of Engineering and Architecture of Fribourg (EIA-FR) was set-up. Industrial partners (Kraftwerke Oberhasli AG, Schweizerischer Wasserwirtschaftsverband SWV) support the different projects by providing adequate test and field study facilities in addition to acquisition and provision of data for case studies. The research contains the following projects (Figure 1.1):

– *Project A* is elaborated by EAWAG and provides knowledge and understanding of the impact of hydropeaking on fish in Alpine rivers with a focus on the Hasliaare River in Switzerland. This field study supplies the needed background for project B (Haas and Peter, 2009).

– *Project B* analyses in detail the possible effects of hydropeaking on fish and its habitat. The relation between hydropeaking and morphology is taken into account as well as different mitigation measures. EAWAG is responsible for this study.

– *Project C* is a join research between EIA-FR and LCH-EPFL. Physical model tests with juvenile fish allowed the study of the efficiency of fish retraction niches during hydropeaking events (Ribi, 2011).

– *Project D* is the present research and aims to assess mitigation measures reducing hydropeaking induced by operation of high-head storage hydropower plants. Climatic and hydrological concerns, energy and economic issues as well as ecological criteria are considered for an overall impact analysis.

– *Project E* contains the synthesis of the CTI project. It provides a generally applicable methodology to deal with hydropeaking due to hydropower operation in mountainous river basins. Besides ecological and biological fundamental knowledge, design guidelines for fish refuges are provided. A list of possible mitigation measures for hydropeaking and its energetic and economic application criteria are also part of the final report.

A coordination board has been created with the aim of managing the project and monitoring the progress. It is constituted of experienced engineers and scientists from the partner organizations.

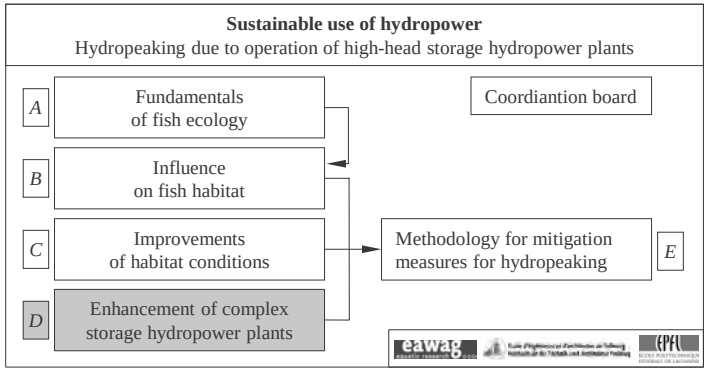

Figure 1.1: Stakeholders, research topics and collaborations of the CTI project consortium *Sustainable use of hydropower – Innovative mitigation measures for hydropeaking*

1.2 Objectives

The present research project aims to develop an approach that allows the evaluation of mitigation measures reducing the negative impacts of hydropeaking downstream of high-head storage hydropower schemes. Environmental aspects, hydraulic concerns and energy and economic issues are considered in the novel integrative method. It includes (1) a precipitation-runoff model for glacierized Alpine catchment areas, (2) an operation tool for high-head storage hydropower plants, (3) flow regime generation with cost estimation of hydropeaking mitigation measures and (4) a fish habitat model. The project is realized in four main steps (Figure 1.2):

Step A

The hydrological model is developed for runoff predictions in mountainous, glacierized catchment areas. Multiple hydrological processes, such as glacier melt, snow pack constitution and melt, soil infiltration and surface runoff, are simulated. The semi-distributed conceptual approach allows integration of routing in rivers as well as the main implementation of hydraulic structures. The flow regime of the river network can be simulated in time and space. The model is calibrated and validated, respecting the operation rules of the power plants. The simulation of the 2005 flood event allows definition of the model's performance.

Step B

An important task is dealing with climate change, influencing the climatic input parameters (temperature and precipitation) and the hydrological characteristics of the catchment area (glacier and snow cover). The existing reservoir-based precipitation-runoff transformation model (GSM-SOCONT) is extended by a dynamic glacier model for long term simulations.

Step C

The operation of a high-head storage hydropower plant can be simulated by the developed optimization tool interacting with the hydrological model. Combined daily and seasonal optimization can be performed. Systematic simulations take into account

natural and anthropogenic parameters such as climatic, economic, legal and ecological issues for different plant outlines.

Step D

The operation mode of power plants with and without hydropeaking mitigation measures and its impacts on the downstream river system for different scenarios is simulated. Mitigation measures can consist in operational, construction or morphological improvements. Measures in the framework of future plant extensions are also tested. The definition of these measures includes an economic and ecological rating for decision support.

The four steps together define an overall modeling and simulation approach on how to operate complex hydropower schemes regarding the impact on the flow regime in the downstream river system. The developed economic-ecological diagnostic and intervention method is applied to the case study of the upper Aare River catchment upstream of Lake Brienz in Switzerland (Figure 3.1). The Alpine catchment area shows common hydrological characteristics. It is operated by the complex high-head storage hydropower scheme of the Kraftwerke Oberhasli AG (KWO).

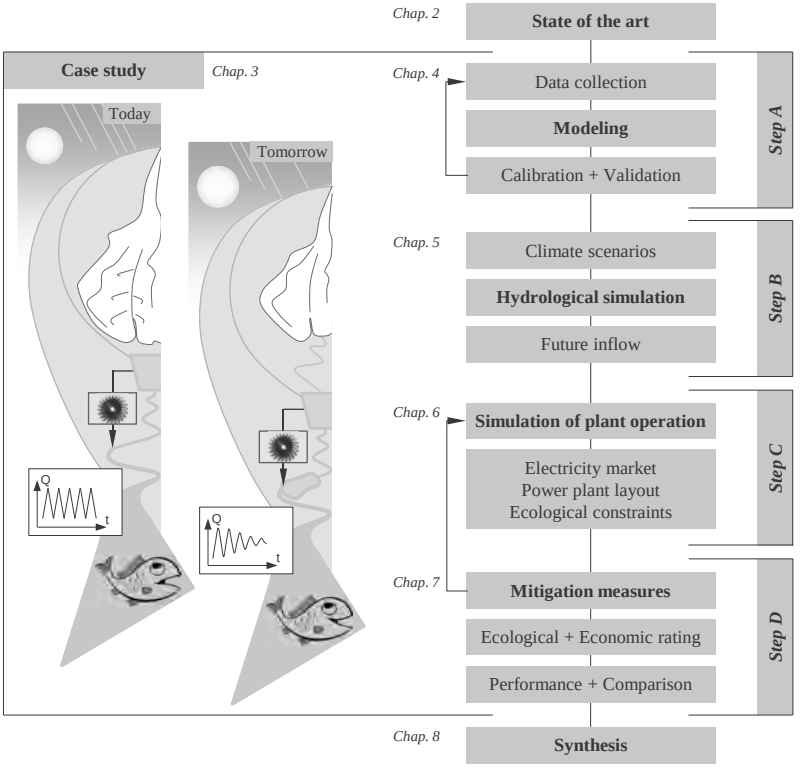

Figure 1.2. Methodology of the research project and structure of the report.

1.3 Structure

The present thesis consists of eight chapters. Chapter 4 to 7 are written as papers and have been submitted to peer-reviewed journals. They are framed by the *Introduction*, the *State of the art*, the presentation of the *Case study* and the *Synthesis*. An overall state-of-the-art of the concerned research fields, hydropower, hydropeaking, hydrological modeling and optimization techniques is given in Chapter 2, whereas more specific information can be found in the corresponding main chapters. In Chapter 3, the case study is presented, revealing the morphological, hydrological and biological particularities of the upper Aare River catchment. In the following, a short outline of the four main chapters is provided:

Chapter 4: *Analysis of flood reduction capacity of hydropower schemes by semi-distributed modeling in an Alpine catchment area*

The simulation of runoff in Alpine catchment areas is essential for the optimal operation of high-head storage hydropower plants under normal flow conditions, but also for the analysis of flood events. A semi-distributed conceptual numerical approach is presented, combining hydrological modeling and operation of hydraulic works. Its performance is shown for the 2005 flood event in the upper Aare River catchment. The influence of the hydropower scheme on flood peak reduction is presented.

Chapter 5: *Semi-distributed conceptual modeling of effects of climate change on future runoff in glacierized Alpine catchment areas*

The impact analysis of climate change on runoff in partially ice-covered Alpine catchment areas is an important task for water resources management. The dynamic glacier behavior is implemented in the semi-distributed conceptual model. Future runoff in the case study area is assessed for the period between 2010 and 2099 for five climate scenarios. Changes in glacier mass as well as the annual and daily runoff are computed and discussed, providing input data for future long-term hydropower operation.

Chapter 6: *Simulation of hydropower plant operation in mountainous areas considering climatic, economic and ecological issues*

For the simulation of future hydropower management, an autonomous operation tool is developed. It is implemented in the hydrological model and takes into account long and short-term reservoir inflow as well as electricity price. Different future hydrological and economic scenarios are simulated for three plant layouts. Ecological constraints are respected by a regulation tool reducing flow fluctuations in the downstream river system and estimating the subsequent operation losses.

Chapter 7: *Mitigation measures for fish habitat improvement in Alpine rivers affected by hydropower operations*

A novel economic-ecological diagnostic and intervention method to assess hydropeaking in a river system is presented. A hydropower operation model simulates the flow regime and defines the related costs due to operational and construction mitigation measures. A dynamic fish habitat simulation tool based on 2D hydraulic modeling and preference curves from *in situ* investigations allows assessment of the generated streamflow regime. Habitat suitability for three life stages of brown trout is defined for four river morphologies. The steady and dynamic habitat indices are

compared to the mitigation costs for the case study area of the upper Aare River catchment.

Due to reasons of coherence, some repetition in the introductory as well as case study parts of the four main chapters could not be avoided. In Chapter 8, general conclusions, recommendations and an outlook on further research are provided. In the two appendices A and B, detailed information about the simulation of normal streamflow conditions and cost estimations of construction mitigation measures are given.

2

State of the art

This chapter contains a short recall of today's situation and future challenges of hydropower with a focus on Switzerland. General introductions to the three main topics of the research project are given. The specific scientific questions and the corresponding literature are focused and discussed in the main chapters. The phenomenon of hydropeaking is explained and its impact on the environment discussed. Then an overview on hydrological modeling is given, comparing different deterministic approaches in terms of description of the catchment area and the hydrological processes. Finally, different qualitative and quantitative optimization techniques and the decision support system are discussed. The content should allow general understanding of the concerned fields.

2.1 Hydropower under changing challenges

Hydropower constituted about 16% of total electricity production worldwide in 2007 and is world's most important source of renewable energy due to its almost negligible CO_2 emissions over the full life cycle (Auer, 2010). Among the renewable sources of electrical energy, hydropower has a very long tradition with first plant constructions at the end of the 19th century. Its high efficiency level of up to 90%, low operating costs and the perspective of multiple-use facilities will maintain its lead in the renewable energy sector. The International Energy Agency (IEA) forecasts an increase of electricity production by 70% up to 2030, with hydropower at a share of 14%, wind power of 4% and photovoltaic by 1%.

Hydropower accounts for 15% of Europe's power generating capacities (Auer, 2010). However, its potential is far from being exhausted. Only 64% of the economically viable potential (870 TWh/yr) is currently used.

Especially in Alpine countries, hydropower is an important energy source. Due to topography and high precipitation, they offer optimal natural conditions for hydropower generation. At the end of the 19th century and between 1945 and 1970 a large number of hydropower plants (HPP), run-of-river as well as large-scale storage ones, were built in Switzerland. In the 70s, almost 90% of Swiss electricity production was hydropower. Due to the commissioning of nuclear power plants, this number decreased to 56% nowadays. As published by the Swiss Federal Office of Energy (SFOE) in 2011, there are 556 HPPs with a greater capacity than 300 kW in Switzerland, which produce in average about 35.8 TWh per year. 47% of that energy is produced by run-of-river, 49% by storage and 4% by pumped-storage hydropower plants.

Figure 2.1. Main water bodies of Switzerland and the gauging stations of the Swiss Federal Office of the Environment (FOEN) showing hydropeaking in their discharge series from 29.01 to 06.03.2005 (Baumann *et al.*, 2005). The gauging stations are indicated as dots.

High-head storage hydropower significantly contributes to Swiss electricity production (Schleiss, 2002, 2007). Reservoirs at high altitudes store rainfall, snowmelt and glacier melt, collecting the water during wet and warm periods to be mainly used in winter. Storage HPPs concentrate their turbine operations during periods of high energy demand and generate highly unsteady flow conditions in the downstream river system. This so-called hydropeaking is an ecologically problematic phenomenon in Alpine rivers (Minor and Möller, 2007), as shown in Figure 2.1 for Switzerland. An evaluation of discharge data series of Swiss rivers shows an amplification of hydropeaking in recent years (Pfaundler and Keusen, 2007). The increasing need of peak load energy, continuous opening of electricity markets and grid regulation demand will probably intensify the problem in the future.

2.1.1 Legal concerns

After years of extensive use of water resources with severe consequences for all living aquatic and shoreline organisms, politics and administration start to recognize the need of an overall water protection policy. The Water Framework Directive of the European Union mentions in its introduction chapter, that “water is not a commercial product like any other but, rather, a heritage which must be protected, defended and treated as such”. It commits to achieve good qualitative and quantitative status of all water bodies by 2015 and it promotes therefore “sustainable water use based on a long-term protection of available water resources” (Directive 2000/60/EC, Article 1b). Improvements of both ecological and chemical status of the surface water body should preserve the natural resources. Several countries set environmental standards for water resources to define water abstraction limits and ecologically appropriate flow release from reservoirs or time-limited licenses and license trading (Acreman and Ferguson, 2010).

In Switzerland, an even more straightforward approach was chosen. After several scientifically supported but privately motivated initiatives to achieve “sustainable hydropower” or “Green Hydropower” (Truffer *et al.*, 2003; Bratrich *et al.*, 2004), the Swiss Parliament adopted in 2009 several laws. In particular, the law on water protection (*Gewässerschutzgesetz (GSchG)*, Sr 814.20) was tightened to improve the quality of the water bodies in Switzerland. The decisions, motivated by the popular initiative *Lebendiges Wasser* (Living water), became effective the 1st of January 2011 and define two aims:

– Promotion of river revitalization by assuring the extensive use of the water.

– Reduction of the negative impacts of hydropower operation by reducing hydropeaking downstream of HPPs, reactivating sediment transport and re-establishing fish migration.

To mitigate the negative effects of hydropeaking, construction measures are preferred to operational ones, which would affect electricity production. To cover the cost of the mitigation measures, an annual amount of CHF 50 million is collected by an additional charge of 0.1 cents per kWh on the high tension transmission fees. This money feeds a fund for fully compensation of rehabilitation costs undertaken by HPP operators. The cantons are committed to define the priorities and the deadlines until 2014. The river restoration measures have to be realized in the next 20 years. The law foresees compensative exceptions to reduce residual flow for river of low ecological potential between 1500 and 1700 m a.s.l. Land acquisition for construction of compensation basins and permission procedure for pumped-storage facilities should be facilitated.

The Federal Office of the Environment (FOEN) has developed guidelines, which support the cantonal authorities for the implementation of the new laws. A recently established document contains a module designated to hydropeaking (Baumann *et al.*, 2012). Several examination and rating methods are presented to be applied by the authorities and the commissioned specialists (see Chapter 2.2.3).

2.1.2 Development of the electricity market

Liberalization of the European power market in addition to the economic crises led in a first time to over-capacities and thus to decreasing electricity prices. Due to re-

dimensioning of the power supply and the increase of the costs for fossil energy sources, electricity prices have recovered and are steadily increasing. Thus, economic efficiency of existing as well as new and enhanced HPPs is also increasing. The Swiss Federal Office of Energy (SFOE) defined a list of opportunities of hydropower in Switzerland, also applicable to other Alpine or European countries:

– The carbon tax and the request for full compensation of carbon dioxide emissions of combined cycle power plants make hydropower more competitive than fossil energy sources.

– Hydropower is not exposed to the high risk price scenarios of fossil energy (taxes and certificates). Competitive advantages are the ecological rating as well as the focus on peak load energy and grid regulation. The latter promises high gains, justifying higher investment costs for related projects. Enhancement of existing schemes and new pumped-storage facilities should focus on this issue.

– By applying the Water Framework Directive of the European Union, European hydropower will become the leading ecological energy source in the next 20 years. Similar laws in Switzerland help to make hydropower an important player in the market of green electricity. Acceptance of hydropower can be increased by internally approved labels, proof of origin in addition to marketing and promotion activities.

– Energy production in the European Union shows an increasing share of variable generation technologies. The Union of the Electricity Industry EURELECTRIC published in 2011 that wind power increased from 74.6 GW to 83.8 GW between 2009 and 2010 and solar photovoltaic from 15.2 GW to 23.0 GW in the same period. Forecasts for future growth are even more promising. Wind power is hardly predictable and solar power depends on season, daytime and weather. The gap between capacity and generation is therefore expanding, requiring even more back-up capacity. This will be especially true up to 2020, since alternative and complementary means such as large-scale storage or demand-side measures are unlikely to deliver beforehand. High-head storage hydropower can provide the needed energy at any moment and therefore regulate the power supply.

– Investments in HPP enhancements (bigger turbine units, efficiency upgrade, turbines for residual flow) are relatively cheap and have generally a minor impact on environmental issues. An annual potential of 970 GWh is mentioned by SFOE.

– Small hydropower has potential, which could be easily exploited from a technical and economic point of view. Especially the re-activation of abandoned HPPs and the use of existing infrastructure (e.g., exploitation of drinking water, waste water or residual flow) is an attractive alternative for future energy supply.

Due to the increase in energy demand (demography, mobility, etc.) and the decision to stop nuclear power production by the end of 2030, the federal government is promoting the use of hydropower to a greater extent. New HPP should be constructed and existing ones are to be enhanced and extended to increase annual power production by at least 2 TWh. Existing as well as new ecological requirements have to be taken into account. In addition, cost-covering remuneration for small hydropower (< 10 MW) should boost production by another 2 TWh.

Measures to face climate change support the trend away from fossil-fuel-based electricity. Internalization of climate costs, growth in global energy consumption and increasing scarcity of resources will create a market environment in favor of hydropower. An average rise of 4% per year from 2010 up until 2030 has been estimated (Auer, 2010). The emergence of a truly European electricity market and investments in grid enhancements will also boost hydropower in Europe.

2.1.3 Climate change

The world's climate depends on natural as well as anthropogenic influences. The hydrological cycle of the Alps is especially sensitive to weather and therefore climate change. Impacts on the duration of snow cover in addition to long-term glacier shrinkage or growth directly affect water resources management and thus the sustainability of hydropower. Several studies have measured, described and simulated the impact of climate change on water availability on mid- and long-term development and operation of hydropower schemes in mountainous areas (Schaefli *et al.*, 2007; Terrier *et al.*, 2011).

Horton *et al.* (2006) investigated different climate models for runoff estimations of several mountainous and partly glacierized catchment areas in the Swiss Alps by the GSM-SOCONT approach (Schaefli *et al.*, 2005). For the future climate between 2070 and 2099, combinations between two greenhouse gas emission scenarios (A2 and B2) and three coupled atmosphere-ocean general circulation scenarios were taken into account. For all catchments and scenarios, earlier snowmelt is computed. Mean annual runoff mainly decreases. Glacierized catchments at high altitudes are affected by higher temperature and the related glacier mass dynamics, whereas the regime of lower catchments is more influenced by changes of seasonal precipitation.

A Swiss research cluster recently developed in a joint project the *Swiss Climate Change Scenarios CH2011* (CH2011, 2011), based on a new generation of global and European-scale regional climate models. As example, Figure 2.2 shows the past and future changes in winter and summer temperature and precipitation over northeastern Switzerland as relative values to the reference climate period of 1980–2009. The climate is strongly dependent on the future greenhouse gas emissions. Even in case of successful mitigation measures reducing global emission by at least 50 % by 2050 relative to 1990 (RCP3PD), a warming of 1.4°C toward the end of the century is predicted for Switzerland. Two scenarios without mitigation (A2 and A1B) estimate the increase of temperature twice to three times as high. Mean temperature will therefore mainly increase in all regions and seasons. The mean precipitation in summer will likely decrease all over Switzerland, whereas in other seasons no clear tendency is assigned. Precipitation is expected to change from snowfall to rainfall.

Despite the increasing scientific body of literature investigating the interactions between climate change and availability of water resources for different Alpine catchments, capabilities of overall quantification of future runoff remain tenuous. One reason of this lack of knowledge is the difficulty to extrapolate hydrological results (SGHL-CHy, 2011). Various local climatic, hydrological and hydraulic characteristics need individual analysis as well as efficient measuring, modeling, simulation and evaluation tools.

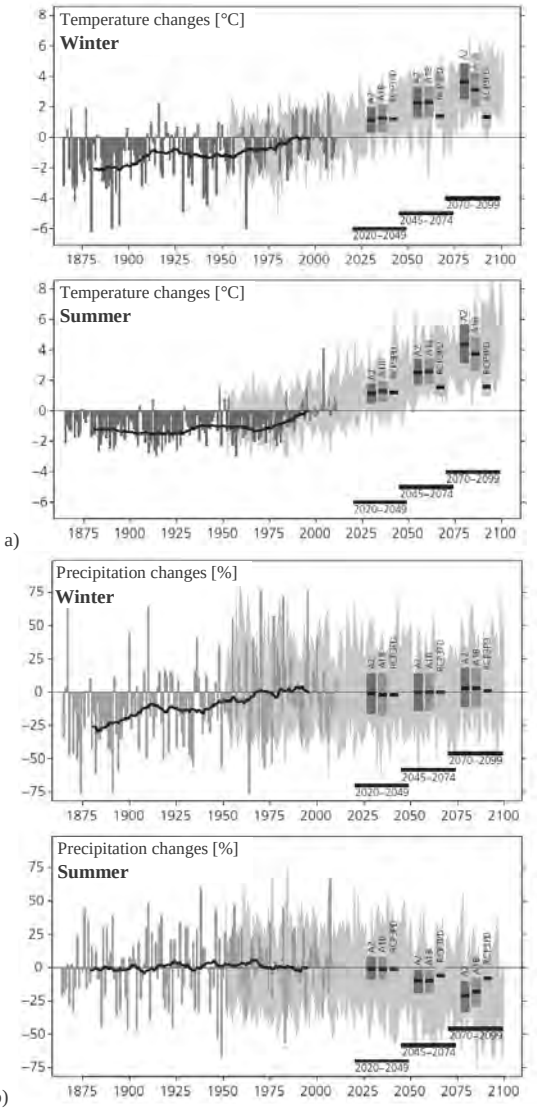

Figure 2.2. Past and future changes in winter and summer temperature [°C] (a) and precipitation [%] (b) over northeastern Switzerland, relative to the reference climate period of 1980–2009. Thin colored bars display the annual deviation; heavy black lines stand for the smoothed averages over 30 years; grey shading shows the range of annual deviations as simulated for A1B (5^{th} and 95^{th} percentile range for each year); thick colored bars display the best estimates of future simulations with associated uncertainty ranges for selected 30-year time-periods and for the greenhouse gas emission scenarios A2, A1B and RCP3PD (CH2011, 2011).

2.2 Hydropeaking

The sudden opening and closing of water releasing structures, i.e., turbines, produce highly unsteady flow conditions in the river downstream of the power house outlet. The natural flow regime of the river is considerably influenced by this so-called *hydropeaking*.

2.2.1 Hydraulic effects

In a river cross-section, hydropeaking is characterized by frequent changes between an upper and a lower flow level. The amplitude depends on the maximum and minimum discharge as well as on the river morphology, which includes the cross-sectional shape and backwater effects. In a river reach, hydropeaking creates a surge wave propagating downstream. In complex systems consisting of several storage hydropower plants and tributaries, propagation, attenuation and superposition of several positive and negative waves characterizes the unsteady flow conditions resulting from hydropeaking. The propagation of these waves is influenced by the channel slope and roughness (Favre, 1935) as well as the river morphology (Stranner, 1996). The duration of the hydropeaking impulse is defined as the duration of the turbine operation. For long operations and channelized rivers, hydropeaking can be considered as the transition between two steady flow conditions. For shorter impulses and under complex conditions, hydropeaking produces dynamic effects. Besides the operation of storage hydropower plants, unsteady open channel flow conditions can also result from other anthropogenic activities or natural events, as presented in Table 2.1.

Table 2.1. Natural and anthropogenic influences on unsteady streamflow conditions (Meile, 2008).

	Anthropogenic activities	Natural events
often	– Hydropeaking due to storage hydropower plants (surge waves) – Surge waves produced by operation of navigation locks – Flushing of water intakes	– Daily flow cycles in snow- and ice-covered river basins due to temperature – Tidal effect in estuaries – Floods (heavy rainfall of climate-dependent frequency)
rare	– Surge waves due to emergency stopping of turbines of run-of-river plants – Flushing of reservoirs and desilting basins – Dambreak waves	– Flash floods due to debris jam, break-up – Flash floods due to ice jam, break-up – Landslides and glacier breakdowns into reservoirs producing overtopping

River hydrology is altered due to rapid and significant fluctuations of discharge, resulting in changed hydraulic parameters such as water level, flow velocity and bed shear stress (Petts and Amoros, 1996; Meile *et al.*, 2011). Modified streamflow also impacts the riverine thermal regime (Zolezzi *et al.*, 2011). Turbines can selectively release hypolimnetic (cold) or epilimnetic (warm) water from thermally stratified reservoirs, harming aquatic organisms (Olden and Naiman, 2010). Morphology is less affected by hydropeaking. Not yet answered is the question of how seasonal and sub-daily flow fluctuations shape ecological patterns and processes in riverine ecosystems.

2.2.2 Ecological effects

Hydropeaking has an influence on almost all living organisms depending on the river ecosystem (Pellaud, 2007). The negative effects have been known for a long time (Vibert, 1939) namely on benthic macro-invertebrates, fish, periphyton and moss, aquatic macrophytes and riverbank vegetation. Literature surveys (Baumann and Klaus, 2003; Pellaud, 2007) confirm the situation of macro-invertebrates driven ashore due to rapid water level dropping or an increase of catastrophic drift during sudden increases in discharge, water levels and flow velocities.

In a hydropeaking impacted river, biomass and richness of species generally diminish. As example, fish is affected at several life stages. A change of abundance and composition of adult fish is reported in different studies (Pellaud, 2007). Juvenile fish are endangered by drift and stranding. The natural reproduction of fish can be disturbed or even completely hindered (Baumann and Klaus, 2003). Furthermore, a relationship between habitat quality, fish size, season, flow-ramping rates and habituation to stranding rates was revealed by stranding experiments with juvenile brown trout (Halleraker *et al.*, 2003) or between stranding and river morphology for juvenile grayling (Tuhtan et al., 2012). Flodmark et al. (2004) analyzed the impact of rapidly changing water levels and temperature on growth of juvenile brown trout. The effect is potentially detrimental and is more severe for slow- than fast-growing fish.

Besides aquatic animals, also riparian vegetation depends on river flow regime (Merritt *et al.*, 2010). Its composition, structure and abundance are influenced by the selective pressure, resulting in adaptations to specific flow attributes. Thus, hydropeaking alters the vegetation communities. However, streamflow restoration may reverse this process.

Despite the increasing knowledge of the interactions between hydropeaking and habitat, it is currently still difficult to predict and quantify the biotic responses to hydropeaking. This can be explained by the fact that rivers often suffer from poor morphology and problematic water quality (Baumann and Meile, 2004).

2.2.3 Methods for flow regime analysis

Degradation of the river ecosystem by hydropeaking is a proven result. Nowadays, an assessment of the flow regime should be integrated as part of all sorts of river restoration projects. Commonly used hydraulic indicators for describing hydropeaking are often based on discharge or water level (Table 2.2). Several methods for describing flow regime and quantification of its deviation from the natural state due to seasonal water transfer and hydropeaking are known (Pfaundler and Keusen, 2007; Meile *et al.*, 2011). Other metrics used to assess subdaily flow fluctuations, as Richards-Baker flashiness index (RBF), ratio of the range of the diurnal cycle to total daily discharge (percentage of total flow; PTF) and the coefficient of diel variation (CDV), are discussed and applied in Zimmerman *et al.* (2010).

Table 2.2. Basic parameters and deduced indicators and indices for describing sub-daily flow fluctuations of flow regime in rivers, e.g., hydropeaking (VAW-LCH 2006).

Basic parameters	Defined parameters		Deduced indicators / indices	
$Q(t,x)$ Discharge	$Q_{max,j}$	Maximum daily discharge	$Q_{max,j} / Q_{min,j}$	Drawdown range
	$Q_{min,j}$	Minimum daily discharge	$\Delta Q_j = Q_{max,j} - Q_{min,j}$	Drawdown difference
	$Q_{mean,j}$	Mean daily discharge	$\Delta Q_j / Q_{mean,j}$	Hydropeaking indicator
	$Q_{mean\ yr\ a}$	Mean annual discharge	$Q_{max,j} / Q_{mean\ yr\ a}$	
	dQ/dt	Discharge variation rate	dQ/dt distribution	
$P(t,x)$ Water level	$P_{max,j}$	Maximum daily flow level	$\Delta P_j = P_{max,j} - P_{min,j}$	Flow level difference
	$P_{min,j}$	Minimum daily flow level	dP/dt distribution	
	dP/dt	Water level variation rate		

These or other hydrologically-based parameters (Richter *et al.*, 1997; Black *et al.*, 2005) are useful for comparison and preliminary analysis. The most common and practically applied coefficients and indicators are briefly explained hereafter.

Pardé-coefficient

Annual distribution in discharge is described by the monthly Pardé-coefficents PC, defined as the mean monthly discharge $Q_{mean\ month\ m,a}$ (month $m \in [1;12]$) divided by the mean annual discharge $Q_{mean\ yr\ a}$ of the year a:

$$PC_{m,a} = \frac{Q_{mean\ month\ m,a}}{Q_{mean\ yr\ a}}. \tag{2.1}$$

Drawdown range

Time series with higher resolution are required due to multiple daily peaks. Subdaily flow variations can be expressed by the ratio between maximum $Q_{max,j}$ and minimum $Q_{min,j}$ daily discharge, called drawdown range.

***Hydropeaking indicator* HP_1**

The drawdown range approach was extended to the difference between $Q_{max,j}$ and $Q_{min,j}$ normalized by the mean daily discharge $Q_{mean,j}$ (Meile *et al.*, 2011). The hydropeaking indicator HP_1 is a dimensionless daily indicator (day $j \in [1;365(366)]$):

$$HP_{1,j} = \frac{Q_{max,j} - Q_{min,j}}{Q_{mean,j}} \tag{2.2}$$

Hydropeaking depends on season, meteorological conditions and hydropower operation as well as river and catchment scales. Thus, flow characteristics (velocities, flow depths and shear stress) depend on both discharge changes and mean flow. Monthly mean values of the HP_1 define seasonal and annual trends and allow comparison between different interventions for mitigation.

***Flow-ramping rate* $\mathbf{HP_2}$**

Gradient in flow change (up or down ramping) is described by the flow change rate HP_2 (Meile *et al.*, 2011), corresponding to the difference between two successive discharges $Q_{i\text{-}1}$ and Q_i divided by the observation time interval ($t_i - t_{i\text{-}1}$):

$$HP_{2,i} = \frac{Q_i - Q_{i-1}}{t_i - t_{i-1}} \tag{2.3}$$

Flow-ramping depends on resolution of the available time series. Pellaud (2007) considers hourly time steps as sufficient but finer resolution has an advantage.

***Hydropeaking ratio* r_{HP}**

The legal ordinance (*GSchV*, Art. 41d) proposes a discharge analysis of a sample of 10 weeks during the low flow season (winter) over five years. To avoid single extreme events and the influence of low production during weekends, peak discharge Q_{peak} is defined as the 80th percentile of the daily maximum discharge series $Q_{max,j}$ and the off-peak discharge $Q_{off\text{-}peak}$ as the 20th percentile of the daily minimum discharge series $Q_{min,j}$. The hydropeaking ratio r_{HP} is the 80th percentile of the daily drawdown ranges $Q_{max,j}/Q_{min,j}$ over the sampling period of five times 70 days (day $j \in [1; 5{\cdot}70]$):

$$\begin{aligned} Q_{peak} &= x_{80th}(Q_{max,j}) \\ Q_{off\text{-}peak} &= x_{20th}(Q_{min,j}) \\ r_{HP} &= x_{80th}(Q_{max,j} / Q_{min,j}) \end{aligned} \tag{2.4}$$

Interaction between hydropeaking and riparian ecology is complex and the current metrics are still rudimentary. New methods to provide a fully integrated predictive capacity of effects of hydropeaking are needed to evaluate future developments, as e.g., river restoration, changed turbine activities due to economic constraints and mitigation measures.

2.2.4 Economic issues and mitigation measures

A restricted turbine operation mode may be theoretically an efficient measure from an environmental point of view. It often risks the economic sustainability of electricity production by high-head storage hydropower plants, having the task to furnish peak energy during high demand periods and to regulate the electricity grid. The main parameters, which allow quantifying the energetic and economic impacts of a restricted turbine operation mode, are the installed power and energy production of the power houses as well as the energy prices depending on contract- or market-based demand. Several measures to mitigate the effects of hydropeaking are applied:

Operational measures

Restrictions in the turbine operation mode can reduce peak release. Such measures often endanger the energetic and economic viability of the plant. Technical constraints may make several measures impossible to be applied. The list of potential operational measures includes the increase of residual flow, discharge limitations, the anti-cyclical operation of different HPPs as well as a successive increase and decrease of discharge.

Construction measures

To reduce hydropeaking of several hydropower plants simultaneously, managed compensation basins could be located directly downstream of power houses or integrated in the river at strategic locations (Meile, 2006). Innovative ideas such as multipurpose schemes or joint operations of run-of-river hydropower and high-head storage HPPs are interesting approaches to minimize economic losses. Managed compensation basins with significant storage volumes can influence on the maximum and minimum daily discharge of the downstream river reach even for long duration operations (VAW-LCH, 2006). Flow change rate can also be improved depending on the management of the basin.

Morphological measures

Morphological measures increase the flow resistance and the natural retention capacity of rivers. Thus, an attenuation and deformation of the surge wave front is expected (Meile, 2008). Furthermore, they allow an increase in the flow variability and creation of refuges for fish, macrozoo- and phyto-benthos. The complex interaction between flow and river morphology has to be considered in order to reduce the bank and bed falling dry. For long duration hydropeaking impulses, no significant influence on minimum and maximum daily discharge is expected.

2.2.5 Environmental flows

A goal of today's river restoration projects is to give once again more space to rivers. Improvements of the flood evacuation capacity and the morphology (Willi, 2002) should result. Such projects are ecologically effective if simultaneously the quality and the flow regime are in an acceptable range (Peter, 2004). Anthropogenic influence on the natural flow regime is one of the main reasons for the declining health of rivers (Poff *et al.*, 1997).

Sustainability in the framework of freshwater management can be achieved by respecting the "environmental flows". These flows correspond to the water left in rivers or restored to developed rivers for ecological and societal development (Arthington *et al.*, 2010). More than 200 methods and approaches to quantify the water requirements of aquatic biota have been developed and applied to achieve environmental flows (Richter *et al.*, 2006). The inherent variability of streamflow and poor understanding of alteration dynamics and assessment need further investigations and modeling approaches.

2.3 Modeling of catchment areas

Flood forecasting, optimization of water resources management and sediment transport issues need robust short- and long-term discharge estimation tools. Despite the increasing knowledge about hydrological phenomena and the development of powerful mathematical models, no unique overall modeling approach exists. Models are applied to specific conditions according to scale, flow regime (flood or low flow) and available datasets. Precipitation-runoff models are simplified representations of the hydrological cycle, simulating the relevant processes, e.g., ice melt, snowpack constitution and melt, infiltration, runoff and streamflow.

Depending on the type of input and output data, hydrological models can be classified as *deterministic* or *stochastic* (Figure 2.3). Stochastic modeling estimates probability distributions of the model outputs by taking into account one or more input parameter, with a random character over time. The probabilistic character is based on trend and fluctuations in the presence of noise observed in historical time series. A large number of simulations can produce distributions of potential outcomes (e.g., Monte-Carlo simulations). In deterministic modeling, a simulation with an input data set defines the result for every occurrence.

Models can simulate single events or time sequences, designated as *event-based* or *continuous-time*, respectively. In an event-based simulation, the accuracy of the output depends on the reliability of the initial conditions which have to be defined and supplied as input data for each event. In a continuous-time simulation, the effect of any assumed initial conditions decreases rapidly as time advances.

Hydrological models use different approaches for spatial discretization and process description (Figure 2.3). Refsgaard (1996) classifies hydrological models as *physically-based*, *conceptual* or *empirical* according to the modeling of the hydrological phenomena. Furthermore, models can be *distributed* or *lumped/semi-distributed* (Ajami *et al.*, 2004) according to the discretization of the catchment area. Most physically-based models are distributed and most conceptual models are lumped. In Chapter 2.3.1 and 2.3.2, the modeling approaches are explained in detail and the scale dependency is discussed.

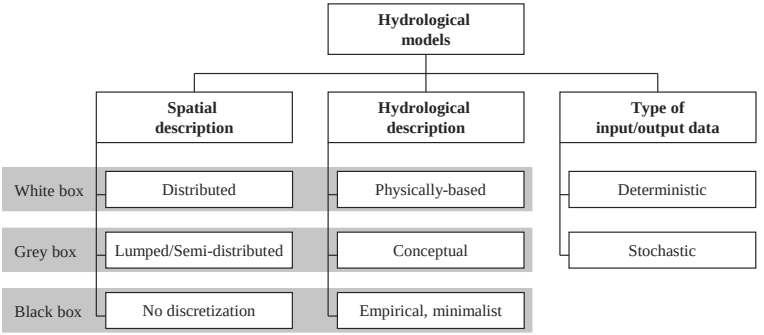

Figure 2.3. Classification of hydrological models according to the discretization of the catchment area (spatial description), the simulation of the hydrological phenomena (hydrological description) as well as the type of input and output data.

2.3.1 Hydrological Models

Physically-based models

Physically-based models (white box) are based on equations which have been developed to describe physical, chemical and biological phenomenon (Freeze and Harlan, 1969). The spatial variability of these characteristics is accounted among the different computational grid points of the model (Abbott and Refsgaard, 1996). The input parameters come from *in situ* measurements or from experimental studies. Distributed models show generally better performance than lumped ones (Carpenter and Georgakakos, 2006). However, the large amount of input data makes this approach only applicable to small scale problems. Progress in understanding of physical phenomenon and increasing processing power increase its efficiency and performance. Different conceptual models have been developed:

– *SHE* (Système Hydrologique Européen) allows simulation of nearly all hydrological processes for any geographic region (Abbott *et al.*, 1986a; b).

– *MIKE SHE* is based on the SHE approach and has been applied to several small and medium size catchments (Feyen *et al.*, 2000).

– *TOPMODEL* (TOPography based hydrological MODEL) is a quasi-physically-based model developed by Beven and Kirkby (1979). Due to its application to several river basins around the world, its performance is discussed in Beven (1997).

– *WaSiM-ETH* (Water balance Simulation Model) is a fully distributed model with physically-based process description (Klok *et al.*, 2001).

– *TOPKAPI* (TOPographic Kinematic APproximation and Integration) uses the kinematic wave approach to simulate subsurface flow, overland flow due to saturation excess and channel flow (Todini *et al.*, 2002). It was modified for simulation of high-mountainous and glacierized catchment areas (Finger *et al.*, 2011).

Conceptual models

Conceptual models (grey box) take into account the spatial variability of the catchment area's characteristics. The dominant hydrological processes are described by simplified equations. For calibration of the physically-based parameters, field data is needed. Several conceptual modeling approaches are known:

– *SAC-SMA* (SACramento Soil Moisture Accounting) simulates runoff using precipitation and potential evapotranspiration as input. Transfer rules between the different reservoirs allow simulation of the main hydrological processes.

– *MORDOR* (MOdèle à Réservoirs de Détermination Objective du Ruissellement) reproduces snowpack accumulation and ablation as well as transformation from rainfall to runoff by daily temperature and precipitation series (Garçon, 1996).

– *HBV (*Hydrologiska Byrans Vattenbalansavdelning) was initially developed for runoff simulation in the framework of hydrological forecast (Lindström *et al.*, 1997). Several improvements make this tool still widely applied.

– *SWAT* (Soil and Water Assessment Tool) is a dynamic rainfall-runoff model (Jeong *et al.*, 2010). Runoff is simulated by combining two different methods (SCS number and Green-and-Ampt-Mein-Larson excess rainfall method).

– *PREVAH* (PREcipitation-runoff-EVAportranspiration-Hydrotope) reproduces the main hydrological processes of mountainous catchment areas and has therefore been applied to several Alpine river basins (Gurtz *et al.*, 1999; Viviroli *et al.*, 2009).

– *GSM-SOCONT* (Glacier Snow Melt – Soil CONTribution) was developed in the framework of modeling and simulation of glacierized watersheds and has found several applications in Alpine areas (Schaefli *et al.*, 2005).

Empirical and minimalist models

Empirical or minimalist models (black box) apply statistical or mathematical concepts to link input to output variables. Understanding of physical processes is not needed. Several approaches have been presented in literature:

– *Box-Jenkins* is an autoregressive model using constant or time-dependent parameters (Hipel *et al.*, 1977).

– *ARMAX* (AutoRegressive Moving Average with eXogenous inputs) uses linear modeling for rainfall-runoff simulations (Karlsson and Yakowitz, 1987). Increased performance is achieved for combinations with Kalman filter or other models.

– *MIAGE* is a spatially lumped nonlinear differential model to describe the link between the volume of water that is stored on the basin and the river runoff at the seasonal scale (Perona and Burlando, 2008; Perona *et al.*, 2008).

– *Unit Hydrograph* (UH) simulates the basin's response to a unit average effective rainfall. It was then extended to instantaneous (IUH) and geomorphologic (GIUH) unit hydrograph and has become one of the most applied approaches for runoff simulations (Rinaldo and Rodriguez-Iturbe, 1996; Rinaldo *et al.*, 2006)

– *Artificial Neural Networks* (ANN) have been developed for neural systems in biology. In the meanwhile, this data-driven self-adaptive method is widely applied for problem resolution due to the few a priori assumptions.

2.3.2 Scale-dependent discharge prediction

The dimensions of the modeling area and therefore the scale-dependency of the modeling approach are key elements for appropriate discharge simulations. From this point of view, some models have advantages regarding outline and scale of the modeled catchment area:

Large scale

Large catchment areas (>50'000 km^2) have a relatively long response time. The result of heavy rainfall at the outlet can appear after a long period and during several days. The input parameters of the model are limited to discharge measurements on the upper part of the main river and on its confluences. The discharges are finally obtained by the resolution of the hydrodynamic equations (dynamic wave).

Intermediate scale

Intermediate catchment areas (1'000-50'000 km^2) use besides the discharge measurements also hydro-meteorological data sets especially rain- and snowfall as well as temperature. The shorter response time needs a link between these measurements, taking into account ice and snowmelt. The amount of input data is therefore quite important, respecting spatial and time distribution. Various approaches have been developed using neural networks, statistical (decomposition and multiple regression MLR, Box-Jenkins or ARMAX), adaptive (Kalman filter) and conceptual models.

Small scale

Small catchment areas (<1'000 km^2) can show very short response time. Real time adjustments are quite difficult. The smaller the area in question is, the more robust a hydrological model has to be for calculating realistic behavior of the catchment area, especially during flood events. The idea is to reduce the uncertainty to the one of the meteorological forecast. Scenarios in deterministic or stochastic modeling are possible ways to deal with the problem of the high reactivity of the catchment area. Thus, meteorological radar data can be used.

2.3.3 Semi-distributed conceptual modeling of Alpine catchment areas

Several studies compared performances of different modeling approaches for case studies. Most of them conclude that the optimal modeling and simulation tool for a given case mainly depends on data availability (Figure 2.4). Increasing complexity does not always improve performance. General conclusions are therefore not possible. The model has to be chosen regarding scale and data availability.

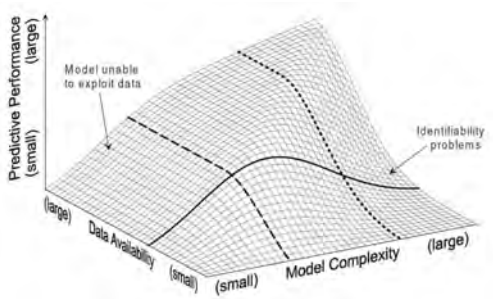

Figure 2.4. Schematic representation of the relationship between data availability, model complexity and predictive performance (Grayson and Blöschl, 2001).

Routing System is a hydrological-hydraulic modeling tool for simulation of operated high-mountainous catchment areas (Dubois, 2005; García Hernández *et al.*, 2007). It was developed at the Laboratory of Hydraulic Constructions (LCH) of Ecole Polytechnique Fédérale de Lausanne (EPFL) in the Object Oriented Programming (OOP) language Visual Basic .NET (VB.NET). The hydrological forecasting is based on the semi-distributed conceptual GSM-SOCONT approach (Schaefli *et al.*, 2005). Spatial precipitation and temperature distributions are taken into account for simulating the dominant hydrological processes, as glacier melt, snowpack constitution and melt, soil infiltration and runoff, as indicated in the upper part of Figure 2.5. Each basin is

divided into ice- and non ice-coverd elevation bands, segregating rain and snow from corresponding precipitation and temperature. Contrary to most models, *Routing System* is able to take into account also hydraulic structures, such as water intakes, reservoirs, turbines, pumps, gates and regulations, as indicated in the lower part of Figure 2.5. Thus, it allows simulation of the operation mode of hydropower plants and its impact on the downstream river system for different scenarios. New developments include data transfer from the linked database, manual calibration with analysis of performance and visualization as well as export of all computed results for analysis and post-processing.

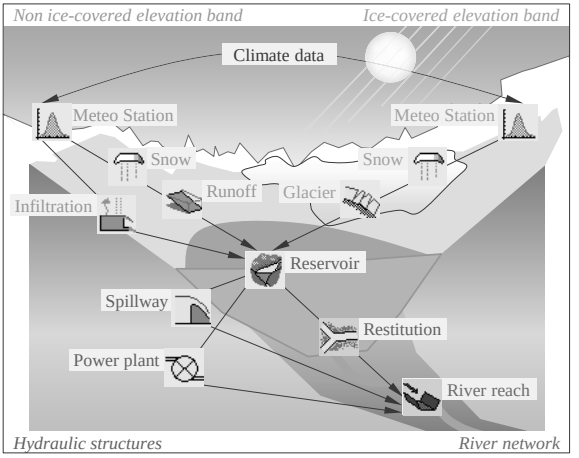

Figure 2.5. Function sketch of *Routing System* for high-mountainous catchment areas, indicating the meteorological data input by local Meteo Stations, the hydrological elements in the ice- and non ice-covered elevation bands (Snow, Glacier, Infiltration and Runoff), the hydraulic elements of the HPP (Reservoir, Spillway, Power Plant and Restitution for residual flow) as well as the downstream river network for streamflow simulation (River reach).

The development of a flood prediction and management tool for the upper Rhône River basin upstream of Lake Geneva in Switzerland was the objective of two recently published thesis based on *Routing System*, Jordan (2007) and García Hernández (2011), in the framework of the MINERVE project (Modélisation des Intempéries de Nature Extrême dans le Rhône Valaisan et leurs Effets). It integrates all hydroelectricity production data of the existing hydropower plants. A decision-support system was implemented using the hydrological model and weather forecasts for real-time optimization of the preventive turbine and gate operations of the ten major hydropower schemes (García Hernández, 2011; Jordan *et al.*, 2012).

Prediction of low or normal flow or re-simulation of historic events, as needed for the present study, has no need of real-time interaction. But, both water resources management and flood prediction should be able to estimate appropriately discharge in time and space. Thus, most flood forecast models can also be used for low water predictions. *Routing System* was chosen for the present research project due to its modeling and simulation abilities, proven by a preliminary analysis presented in Appendix A (Bieri and Schleiss, 2011). Furthermore, developments in code can be done thanks to code availability.

2.4 Methods of decision support and optimization

2.4.1 Qualitative methods

There are several qualitative decision support systems for different kinds of particular problems. Existing methods have often to be adapted for the application in a specific context.

Participatory methods

A multi-objective project needs the participation of a maximal number of the concerned parties. Nowadays participatory methods are even implemented in legal processes. The project, the involved parties and the links between project and parties have to be defined first (Luyet, 2005). A specific method for management of hydraulic projects has been developed (Leach and Pelkey, 2001). The actors have to be chosen by a method based on seven criteria (Mason and Mitroff, 1981; Banville *et al.*, 1998). Only by applying these identification rules the integrity can be guaranteed. This method has been adapted and completed by several authors (Kapoor, 2001; Luyet, 2005). Participation levels with different competences are defined as well as a number of general rules to support a successful decision making process.

Expert judgment

An expert judgment (e.g., Delphi method) is similar to a participatory method. Decisions are taken by specialists, whose performances are usually higher than those of non-experts. Good decisions are only possible by a formal communication method between the experts (Rowe and Wright, 1996). Anonymous communication structures as well as iterative procedures guided by a group coordinator leading to a consensus are the main pillars of successful objective decision making. The precision and the reliability of the results cannot be easily defined. Thus, the consensus of experts is an approach that comes close to the objective optimum (Landeta, 2006).

System dynamics

System dynamics take into account temporal aspects for decision making. The approach solves a problem in a complex and non-linear system analytically (Park *et al.*, 2004). The definition of the impact of every factor on others allows the identification of retroaction and loops (Maani and Maharaj, 2004). Modeling by system dynamics is divided into four steps: conceptualization, formulation, test and implementation (Luna-Reyes and Andersen, 2003). Qualitative models are often explained by diagrams, where the links show the causality of the relations. The use of system dynamics asks for a well-developed data set. Human variables are complicated to model and the interactions not easily defined.

Heller (2007) qualifies the applicability of the different methods in various contexts. System dynamics is generally the most appropriate. If social aspects have to be taken into account, a participatory method has to be implemented in a second step of the analysis for guaranteeing the acceptance by the concerned parties. The presented methods are limited on comparison of alternatives and neglect the aspect of optimization. They just attempt to achieve a compromise and a consensus. Heller *et al.* (2010) applied the method of Gomez and Probst (1995) to analyze the system of a multipurpose run-of-river hydropower plant. The holistic method, initially developed

for economic contexts, allows a global overview on a complex system for adequate decision making (Figure 2.6).

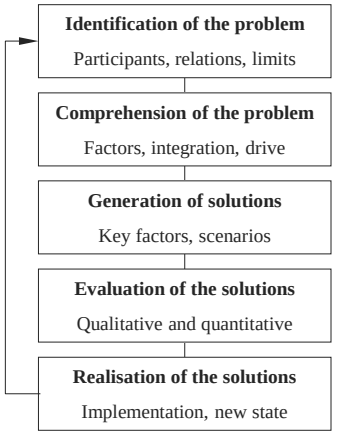

Figure 2.6. Main steps of decision making by the method of Gomez and Probst (1995).

2.4.2 Mixed methods

Mixed methods link qualitative aspects to quantitative ones. In case of multi-criteria criteria decision making (MCDM), decision makers often face problems with incomplete and vague information. Fuzzy set approaches, recognized as an important problem modeling and solution techniques, are suitable when modeling of human knowledge is necessary and when human evaluations are needed. Fuzzy set theory in MCDM has been successfully applied to many problems in recent years (Kahraman, 2008).

Multi-criteria analysis

Multi-criteria decision making is a modeling and methodological tool is well suited for dealing with complex problems. It neglects aspects of system modeling and is confined to the objective of the optimal solution. The technique consists in four potentially cyclic steps (Mena, 2000): list of potential solutions, list of considered criteria, table of performances and aggregation of the performances. Most applications have the first three steps in common, showing mainly an objective character. For the last step, various methods exist to define the aggregation function, because of the bias between the performances and the consequent subjectivity (Schärlig, 1985).

Fuzzy sets

Fuzzy sets are systems where the links between the variables are not known or not sophisticatedly quantifiable. Fuzzy logic was invented by Zadeh (1965). Since then, the theory has been used for various applications. The goal of fuzzy logic is to quantify imprecise responses, which allows implementation in software tools. Fundamentals of the theory are the expressions of interference rule and attribution functions.

2.4.3 Quantitative methods

After having defined the problem, its components and the relation between them, the output of the system has to be quantified. A quantitative method allows for optimization, which defines the set of model variables leading to the highest general performance. The comparison of different alternatives is done by an objective function.

Complex problems, such as optimization of dynamic processes described by partial differential equations, cannot be analytically solved. The problems can be continuous or discrete, depending on the type of equations to be solved. The simulation and the optimization can be linked by two different means (Bock *et al.*, 2007):

– *Black box approaches* treat the two tools separately. An outer optimization loop calculates the objective function by iterating over the decision variables only, whereas an inner simulation loop iteratively determines the state variables describing the dynamic system behavior (Figure 2.7a).

– *Simultaneous approaches* closely couple the optimization aspect of the overall algorithm with the computation of the state variables of the dynamic system in the simulation. With an adequate resolution algorithm, this method is rapidly executable (Figure 2.7b).

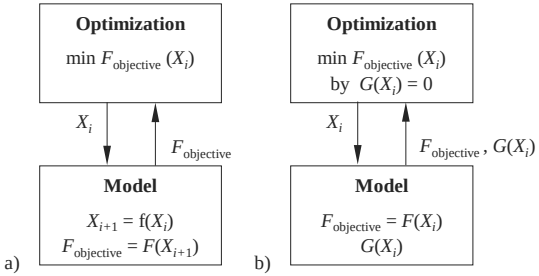

Figure 2.7. Interaction between optimization tool and model for black box (a) and simultaneous approach (b) (Heller 2007), with objective function ($F_{objective}$), external constraints (G), input variable at time step i X_i and input variable at time step (i+1) X_{i+1}.

An optimization of a problem is characterized by the mathematical equations used in the model. The objective function and its conditions are defined by linearity or non-linearity. The variables can be continuous or integer. Thus, the optimization has to be done by an adequate solver:

Mathematical optimization methods

Mathematical optimization methods can be used in strictly and well defined environments, where the solving algorithm is known as either polynomial or exponential. The following rules are generally applicable (Heller, 2007):

– Linear models can be easily solved and the optimum is fast defined.

– Non-linear models with continuous variables can be solved by mathematical methods. Limits of validity of the results and of problem formulation exist.

– Non-linear models with discrete variables cannot generally be solved by mathematical methods. Heuristic approaches have to be applied.

Heuristic optimization methods

Heuristic methods (artificial intelligence, expert systems) are flexible and close to programming tools. They generate solutions which have been tested by simulations. The different types of problem settings lead to various algorithms, as e.g., genetic algorithms, neuronal networks, expert systems, fuzzy methods, simulated annealing, dynamic and goal programming. In hydrology and hydraulics, several of these methods have been applied (Chang and Moore, 1997; Cheng, 1999; Faber and Stedinger, 2001; Sharma *et al.*, 2004; Chandramouli and Deka, 2005; Chang, 2008).

Between mathematical and heuristic optimization techniques, a large number of hybrid models have been developed.

2.4.4 Multi-objective optimization

For multi-objective optimization of complex systems, a problem description by a qualitative method is recommended (Heller, 2007), as shown in Figure 2.8. The alternative to be tested is defined by internal variables and depends on external variables. For every set of internal variables, a simulation with the corresponding models (global model) is undertaken. The performance or efficiency is expressed by objective functions. Economic, ecological, social or other indicators allow a rating and therefore an optimization of different alternatives. When faced with multiple objectives, Pareto curves (Pareto, 1896) define the boundary along which multiple different solutions lie and help users to compare and decide.

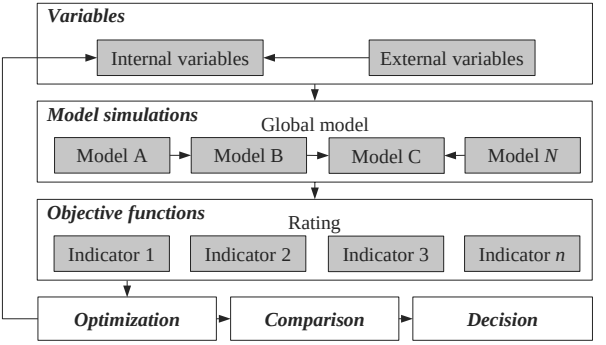

Figure 2.8. Flowchart of a decision making procedure: The effect of external and internal variables of the alternative is defined by model simulations (A...*N*) and their output rated by indicators (1...*n*). An optimization procedure allows the definition of the optimal alternative(s) for comparison and decision making (Heller, 2007).

3 Case study

The present research deals with impact of hydropower operation on river systems. The developed approaches should be tested on a sample, specifically defined but representative for a larger number of real cases. The upper Aare River catchment in Switzerland was chosen as case study area. The following chapter reveals the relevance of this decision by discussing existing studies in different research fields as well as proper statistical analysis of available data series.

3.1 Introduction

The upper Aare River catchment (Figure 3.1) is a glacierized Alpine river basin. It is located between 564 m a.s.l. (Lake Brienz) and 4274 m a.s.l. (Finsteraarhorn) and has a surface area of 554 km^2. About 20% of this area is covered by six main glaciers as well as several smaller ice patches. The natural flow regime of the upper Aare River, also-called Hasliaare, is therefore glacial or glacio-nival (Weingartner and Aschwanden, 1986). The river finds its source in the glaciers of Unteraar and Oberaar and flows nowadays through several artificial reservoirs (Oberaar, Grimsel and Räterichsboden), in which most of the water is temporally accumulated to be released by the turbines in the Grimsel, Handeck and Innertkirchen power houses. In Innertkirchen, the water is given back to the Aare River immediately downstream of the confluence with the Gadmerwasser River, draining the eastern part of the catchment area. After the Aareschlucht canyon the Aare River reaches the main valley of Meiringen and enters Lake Brienz at Brienzwiler.

At the end of the 19th century, the area of the Grimsel and Susten was recognized as well suited for hydropower exploitation. Heavy rainfall, large storage areas, solid

granitic bedrock as well as steep slopes provide optimal conditions for high-head storage hydropower. The first concrete dams for the reservoirs of Grimsel ($94 \cdot 10^6$ m^3) and Gelmer ($13 \cdot 10^6$ m^3) and the Handeck power house were built between 1925 and 1932. Then Lake Räterichsboden ($25 \cdot 10^6$ m^3) and Oberaar ($57 \cdot 10^6$ m^3) with their operation facilities followed. In the 1960s, the operation of the eastern Susten catchment started with the water release by Innertkirchen 2 HPP after the confluence of Gadmerwasser and Hasliaare River. The Grimsel 2 pumped-storage plant between Lake Oberaar and Grimsel allows flexible generation and absorption of energy since 1980. The result is a complex scheme with nine power plants and several reservoirs, representing as an average 8.1% of the total installed power of Swiss storage hydropower schemes and producing 10.1% of the corresponding electrical energy (Table 3.1). In the recently started upgrading program *KWOplus*, several technical, economic and ecological improvements of the scheme are foreseen, such as the increase of the electric power of turbo-machines and the increase of the retention volumes of the largest reservoir of Grimsel.

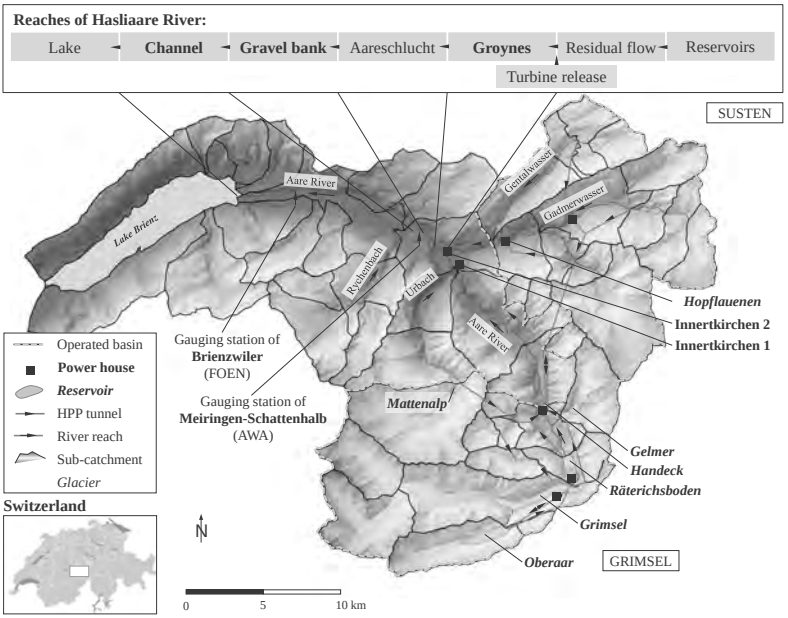

Figure 3.1. Catchment area of the upper Aare River upstream of Lake Brienz with the river network, the operated river basin with the hydropower scheme (main reservoirs and power houses), glaciers, main sub-catchment areas and the two river gauging stations Meiringen-Schattenhalb and Brienzwiler.

The unsteady water release by Innertkirchen 1 and 2 HPPs leads to hydropeaking in the Hasliaare River between Innertkirchen and Lake Brienz. The altered flow regime in addition to the degraded morphology due to river training works during the last century have led to poor habitat conditions for aquatic biota.

Besides the advantages of a well-defined but complex study area, the plant operator, the Kraftwerke Oberhasli AG (KWO), was willing to support the research project. Hydraulic and hydrological characteristics of the catchment area, technical and

operational information about the hydropower scheme, operation rules, historical data and other information have been made accessible for the present research project.

Table 3.1. Installed power and mean annual energy production of the storage hydropower schemes (without pumped-storage) in Switzerland (CH) and the Kraftwerke Oberhasli AG (KWO) (published by the Swiss Federal Office of Energy (SFOE), 2011).

	Installed power (generator)		Mean annual energy production	
	[MW]	[% of CH]	[GWh]	[% of CH]
Switzerland (CH)	8'073	100.0	17'382	100.0
Kraftwerke Oberhasli AG (KWO)	653	8.1	1'753	10.1

Available data

The study site is well documented. Several national and local authorities and services as well as privates provide useful and rich historical data sets from *in situ* measurements:

- *Topography:* Spatial discretization of the catchment area, including glacier extension of 1993, is defined by a digital elevation model (DEM) with a grid size of 25 m (Swisstopo).
- *Climate data:* The meteorological data is provided by the Swiss Federal Office of Meteorology and Climatology (MeteoSwiss). On the one hand, temperature and precipitation data have been sampled every ten minutes by an automatic monitoring network (ANETZ) all over Switzerland since 1980. On the other hand, a large number of gauging stations (NIME) measure daily precipitation.
- *Streamflow:* Discharge, water level elevation and temperature of the Hasliaare River are measured every ten minutes at the Brienzwiler gauging station by the Federal Office for the Environment (FOEN). For the time periods of 1925-1929 and 1974-2010, data are available. Since September 2006, discharge of the Aare River has been measured by the *Amt für Wasser und Abfall* of Bern Canton (AWA) at Meiringen-Schattenhalb after Aareschlucht.
- *Hydropower scheme:* KWO made accessible the detailed hydraulic characteristics of the hydropower scheme, operation rules and historical operation data for the last 30 years of exploitation. Daily turbine and pump volumes in addition to water levels in the four main reservoirs were obtained as well as hourly averages for 2005. These datasets allowed calculating the inflow into the main lakes and compensation basins operated by KWO.
- *River ecology:* For the projects A and B of the present CTI project, several *in situ* investigations are undertaken for defining habitat suitability of fish, including electro-fishing as well as detailed analysis and documentation of the river morphology.

Furthermore, several studies related to hydrological (floods, residual flow), hydraulic (sediment load, habitats), biological (fish, benthos, wetlands, connectivity) as well as landscape issues have been carried out for the upper Aare River catchment in the framework of the enhancement project *KWOplus* (Schweizer *et al.*, 2009; Schweizer *et al.*, 2010; Schweizer *et al.*, 2012a; Schweizer *et al.*, 2012b). Further data of peak flow

estimations during 2005 flood event, glacier mass estimations as well as field investigations for analysis of fish and benthos are used for this study and mentioned in the corresponding chapters.

3.2 Morphology

In the 19th century, the dynamic braided river network of the Hasliaare River was transformed into a mainly monotonous channel for secure flood evacuation during summer months. The natural variety of steep and shallow benches was replaced by rubblework walls or rip-rap. The floodplains and wetlands were drained for agricultural use. Gravel banks with their specific fauna and pioneer flora have mainly disappeared. The main stream course was shortened by about 3 km. Dikes on both river sides avoid inundation. Several tributaries were deviated. Nowadays, the lower part of the valley is drained by a channel parallel to the main river. The bed width of the lower part of the Aare River has been reduced to 12 m, allowing sediment transport to the mouth in Lake Brienz. The bed slope varies between 0.5 and 0.8%.

Based on variability of water surface width, bank slope and mesohabitat, Haas and Peter (2009) identify three main morphologies for the Hasliaare River between Innertkirchen and Lake Brienz (Figure 3.1):

– *Reach 1 "Groynes"* (Figure 3.2a) is 0.8 km long. The morphology from the water release of KWO to the upstream end of the Aareschlucht canyon is dominated by groynes on both sides of the river. Between the steep rip-rap structures, shallow flow fields are located. High flow velocities in the main channel, low current between the groynes and deep pools directly behind them define a typical outline of mesohabitat.

– *Reach 2 "Gravel bank"* (Figure 3.2b) is 1.3 km long. The Hasliaare River between the downstream end of the Aareschlucht canyon and Meiringen has enough space for alternating gravel banks. Shallow flow zones allow flow variety.

– *Reach 3 "Channelized river"* (Figure 3.2c) is 11.8 km long and corresponds to the remaining reach until Lake Brienz. In this reach, the Hasliaare River has a trapezoidal cross-section with steep bank slopes. The flow patterns are monotonous and obstacles in the river bed do not exist.

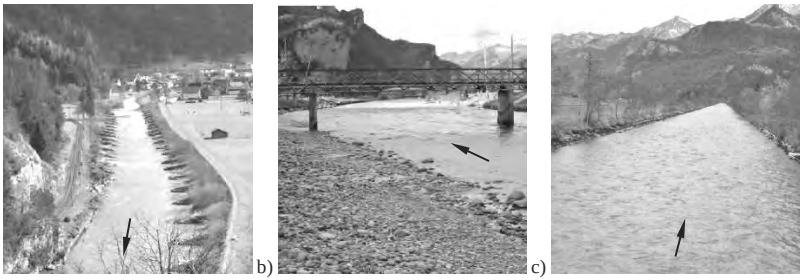

Figure 3.2. The three main morphologies of the Hasliaare River between Innertkirchen and Lake Brienz: Groynes (a), Gravel bank (b) and Channelized river (c). The arrows indicate the flow direction (Haas and Peter, 2009).

The detrimental effect on aquatic biota of sediment depositing within the interstitial spaces of stream substrate (embeddedness) has been established. Stream deposited sediment has been recognized as one of the major affecting stressors. The analysis of the river reaches 1 and 2 remains full embeddedness of the substrate as well as a cover layer of fine sediment on the gravel bed.

3.3 Hydrology

3.3.1 Flow regime

At the gauging station of Brienzwiler (570 m a.s.l.), the mean annual discharge of the Hasliaare River is of 35.0 m^3/s, as defined by the continuous time series from 1975 to 2008. Due to the 20% glacierization and the mean elevation of 2150 m a.s.l., the natural streamflow regime of the river network is based upon glacier melt and snowmelt and is therefore glacial or glacio-nival (Weingartner and Aschwanden, 1986). Mean monthly discharges of 17.1 and 64.6 m^3/s for January and June, respectively, have been measured. Peak flows of 190 and 441 m^3/s have a return period of 2 and 100 years. The latter was achieved during the 2005 flood event. Four hydrological years are chosen, before (1927) and after (1977, 1987, 1997, 2007) the construction of the Oberhasli HPP, are presented in Figure 3.3 and give the situation with and without hydropeaking.

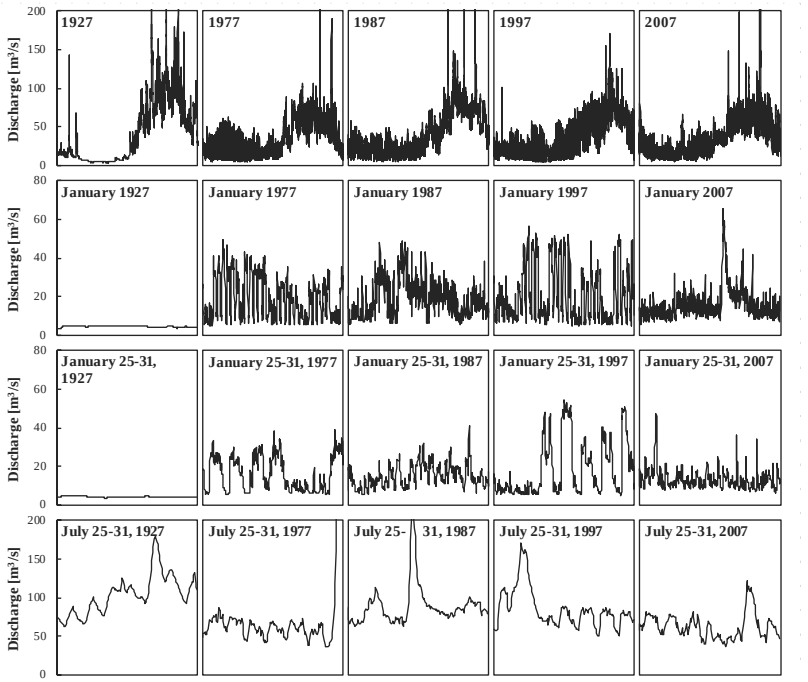

Figure 3.3: Hydrographs of the Hasliaare River at the gauging station of Brienzwiler for selected hydrological years before (1927) and after (1977, 1987, 1997, 2007) the construction of the Oberhasli HPP (FOEN). Annual hydrographs are based on 1-hour time series (*above*), monthly and weekly hydrographs on 10-minute time series (*below*).

Annual distribution

Hydropower operation influences the natural flow regime. Water intakes and reservoirs allow seasonal water transfer from summer to winter. About 60% of the catchment area is exploited by KWO, using the water from Susten and Grimsel. It is stored in the reservoirs, guided by the tunnel network and released by the turbine units of Innertkirchen 1 and 2 HPPs with a maximum capacity of 39 m^3/s and 29 m^3/s, respectively.

The averaged Pardé-coefficients PC [-] at Brienzwiler are defined for the pre- and post-construction period of the large reservoirs within the upper Aare River catchment, 1925-1929 and 1975-2008, respectively (Figure 3.4a). A significant redistribution of annual discharge from summer to winter months is observed. The mean monthly discharge has generally increased by 5% to 23% in winter (between October and May), while a decrease of 14% to 19% is measured in summer (between June and September). The annual distribution of flow has shifted towards regimes of higher winter and reduced summer flows. The analysis of selected years shows inter-annual variability without any clear tendency during the last centuries (Figure 3.4b).

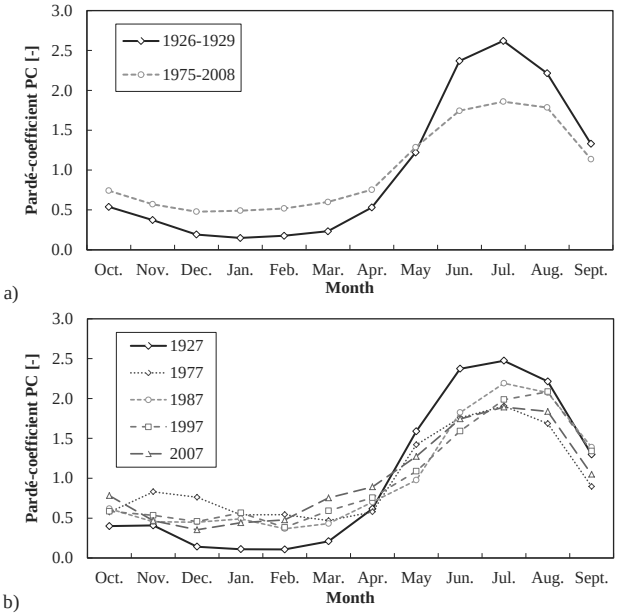

Figure 3.4. Mean values of the Pardé-coefficients of the Hasliaare River at Brienzwiler before (1926-1929) and after (1975-2008) the construction of the Oberhasli HPP (a) and monthly Pardé-coefficients for selected hydrological years (b).

The observed relative increases of flow during winter and decreases during summer are also identified for the flow duration curves (Figure 3.5). Comparison of 1925-1929 and 1975–2008 at Brienzwiler reveals a decrease in the annual maximum daily discharge from about 180 to 170 m^3/s. The mean daily discharge is lower during 120 days, mainly in summer and higher during 245 days, mainly in winter. As discussed by Meile *et al.*

(2011), the related parameters of flow depth, velocity and bed shear stress are faced to more significant modification by the increase in mean daily discharge in winter than the decrease in summer. However, bed load and frequency of armor layer break-up and thus morphological dynamics can be influenced by the decrease in mean daily discharges during summer months.

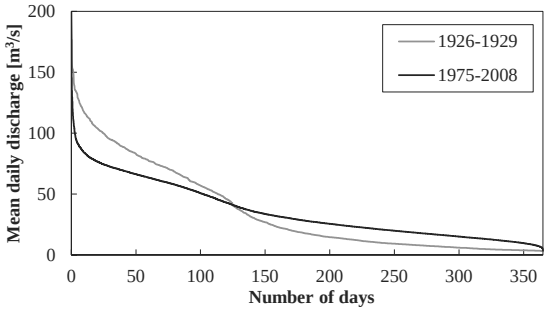

Figure 3.5. Flow duration curves for the mean daily discharge of the Hasliaare River at Brienzwiler for the period before (1926-1929) and after (1975-2008) the construction of the Oberhasli HPP.

Hydropeaking

Depending on the chosen approach, different coefficients describing hydropeaking are applied. For the Hasliaare River, various values are defined, such as drawdown ranges between 3:1 and 18:1 based on single events, mean values, percentiles as well as seasonal or specific sample time series. Besides the drawdown range, water level changes, flow-ramping time intervals and gradients or daily peak indicators are used. For this study, the approach, as developed by Meile *et al.* (2011) for the upper Rhone River in Switzerland, is applied using the hydropeaking indicators HP_1 for daily flow fluctuations (Eq. 2.2) and HP_2 for flow change (Eq. 2.3) for the time series measured in Brienzwiler.

The monthly averaged values of the hydropeaking indicator HP_1 for selected hydrological years of the pre- (1927) and post-construction period (1977, 1987, 1997, 2007) are compared in Figure 3.6a for the Hasliaare River in Brienzwiler. The mean monthly values of HP_1 are lower during winter than summer and always below 0.4 for natural flow conditions, whereas under hydropeaking conditions, the values always exceeded 0.3 with maxima between 0.9 and 1.5 for the winter period between October and March.

Statistical analysis of the daily values of HP_1 identifies the non-exceedance probability of a certain threshold value (Figure 3.6b). HP_1 remains below 0.5 for 91% of the days of natural flow conditions in 1927. Under operated conditions, the indicator is below 0.5 only during 22% (1997) and 33% (1987) of the days. For the channelized reach, HP_1 of 0.5 corresponds to water level variations between 0.4 and 0.5 m.

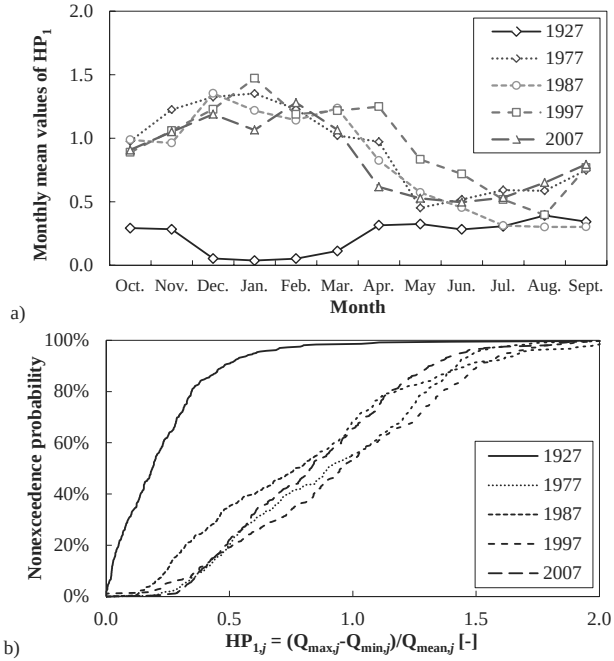

Figure 3.6. Monthly mean values of hydropeaking indicator HP_1 of the Hasliaare River at Brienzwiler of the 1-hour time series for selected hydrological years before (1927) and after (1977, 1987, 1997, 2007) the construction of the Oberhasli HPP. Mean values per month of the hydropeaking indicator HP_1 (a). Statistical analysis of the daily values of the hydropeaking indicator HP_1 (b).

Figure 3.7 (a and b) illustrates the flow change rates HP_2 with and without maximum and minimum values for selected hydrological years. Under the natural conditions of the year 1927, winter months have low flow-ramping rates, whereas summer months show higher values. The increase of the flow change rates (up and down ramping) in July is due to the natural daily discharge cycles by snow and glacier melt. For the years with hydropeaking, the flow change rates are quite similar for winter and summer. The median of the summer flow-ramping rates increases from 0.04 $m^3/s/min$ (1927) to values up to 0.11 $m^3/s/min$ (1977). Down ramping rates increased from 0.03 $m^3/s/min$ (1927) to 0.10 $m^3/s/min$ (1977).

Analyzing the level change rates (Figure 3.7c and d), no important inter-annual difference is revealed. But ramping rates of the water level in winter are higher than in summer. Due to increased residual flow, the water level of the Hasliaare River is generally higher in summer than in winter. The trapezoidal channel section mitigates flow changes for high water elevations. This phenomenon also explains the higher winter variability. Down ramping rates higher than 0.3 cm/min (Baumann and Klaus, 2003) or 0.4 cm/min (Pfaundler and Keusen, 2007) increase the risk stranding of juvenile fish and larvae.

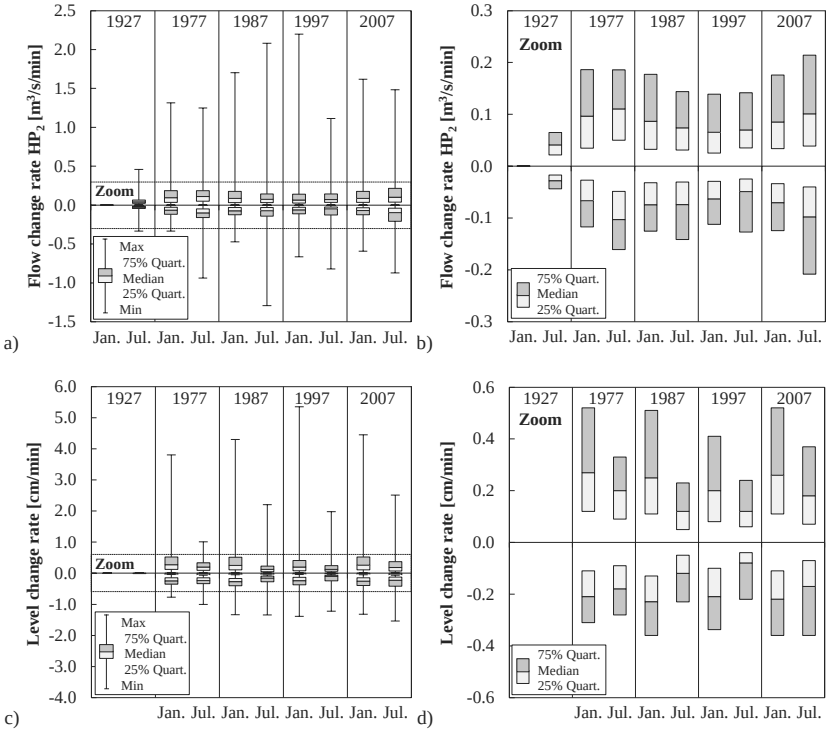

Figure 3.7. Flow change rate HP_2 (a, b) and water level change rate (c, d) of the Hasliaare River at Brienzwiler of the 10-minute time series for January (Jan.) and July (Jul.) of selected years before (1927) and after (1977, 1987, 1997, 2007) the construction of the Oberhasli HPP with (a, c) and without (b, d) indication of minimum (Min) and maximum (Max) values. For 1927 no water level data is available.

Flow routing in the Hasliaare River

Since 2006, discharge series can be compared between the gauging stations of Meiringen-Schattenhalb (AWA) and Brienzwiler (FOEN), 2.1 and 11.4 km downstream of the power house outlet in Innertkirchen. For 2007 (Table 3.2), the mean annual discharge of 30.0 m^3/s at Meiringen-Schattenhalb is 6.3 m^3/s lower than at Brienzwiler. The discharge difference is between 20% and 30% in summer and of only 10% in winter. As a consequence, upstream drawdown ranges (DR) are higher. Mean monthly values in winter achieve values up to 8.1 (February). This behavior is also shown for the hydropeaking indicator HP_1. Monthly means in Meiringen varies between 2.0 (January) and 0.9 (July), whereas the annual mean of 1.4 is considerably greater than 1.1 in Brienzwiler. In Brienzwiler the flow-ramping rates are between 43% and 69% lower.

Figure 3.8 shows flow propagation between Meiringen and Brienzwiler. Propagation time is about 1 hour depending on the discharge. Due to the short distance between the gauges of less than 10 km and the long turbine operations, no attenuation of the peak is shown. However, the downstream hydrograph is smoother due to routing effects. Flow gradients are less steep, as shown for the flow-ramping rates. The influence of macro-roughness (groynes) between the turbine outlet in Innertkirchen and

Meiringen-Schattenhalb was studied (LCH, 2010) and reveals attenuation of peak front without reduction of its amplitude. Despite the lack of long-term data series, the more fluctuating flow regime in Meiringen is more relevant regarding biological constraints than the one in Brienzwiler.

Table 3.2. Comparison of monthly and annual mean values of daily hydropeaking indicators from 10-minute discharge series of Hasliaare River from October 2006 to September 2007 at gauging station Meiringen-Schattenhalb (**S**) and Brienzwiler (**B**).

Monthly mean of …		Oct.	Nov.	Dec.	Jan.	Feb.	Mar.	Apr.	May	Jun.	Jul.	Aug.	Sept.	**Year**
Q [m^3/s]	**S**	25.7	15.6	11.6	13.8	16.2	24.8	27.5	38.4	45.5	56.6	52.9	29.9	**30.0**
	B	28.4	17.0	12.8	16.0	17.3	27.3	32.3	46.1	63.5	68.1	66.6	38.0	**36.3**
$(Q_S - Q_B)/Q_S$ [%]		10	9	10	16	7	10	18	20	40	20	26	27	**21**
Q_{max}/Q_{min} [-]	**S**	5.5	7.0	6.4	6.1	8.1	7.0	3.6	2.8	2.8	2.7	3.1	4.4	**4.9**
(= DR)	**B**	3.5	4.1	4.2	3.7	5.0	4.4	2.5	2.0	1.9	2.0	2.3	2.9	**3.2**
$(DR_S - DR_B)/DR_S$ [%]		-36	-42	-34	-40	-39	-38	-31	-27	-33	-26	-27	-34	**-36**
HP_1 [-]	**S**	1.4	2.0	2.1	2.0	2.0	1.6	1.1	1.0	0.9	0.9	1.0	1.3	**1.4**
	B	1.1	1.4	1.6	1.4	1.6	1.3	0.8	0.7	0.6	0.6	0.7	1.0	**1.1**
$(HP_{1S} - HP_{1B})/HP_{1S}$ [%]		-21	-29	-24	-31	-21	-20	-24	-28	-35	-27	-23	-25	**-25**
HP_2 [$m^3/s/min$]	**S**	1.7	2.0	1.3	1.6	1.6	1.5	1.6	1.6	1.5	1.5	1.4	1.4	**1.6**
Up ramping	**B**	0.8	0.8	0.8	0.7	0.8	0.8	0.7	0.7	0.8	0.8	0.8	0.7	**0.8**
$(HP_{2S} - HP_{2B})/HP_{2S}$ [%]		-54	-59	-43	-56	-46	-48	-52	-54	-46	-48	-47	-48	**-51**
HP_2 [$m^3/s/min$]	**S**	-0.9	-1.2	-0.8	-0.8	-0.8	-0.8	-1.2	-1.2	-1.1	-1.2	-1.0	-0.9	**-1.0**
Down ramping	**B**	-0.4	-0.4	-0.3	-0.3	-0.3	-0.4	-0.5	-0.5	-0.6	-0.5	-0.5	-0.4	**-0.4**
$(HP_{2S} - HP_{2B})/HP_{2S}$ [%]		-58	-69	-62	-60	-59	-56	-61	-57	-50	-55	-50	-52	**-57**

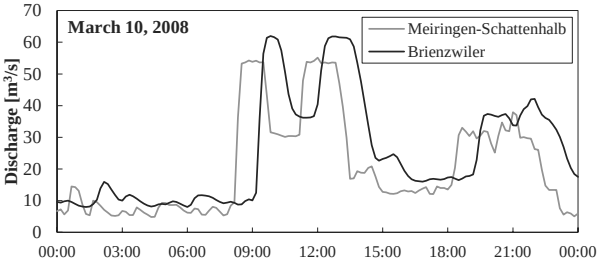

Figure 3.8. Measured discharge of the Hasliaare River at gauging stations Meiringen-Schattenhalb (AWA) and Brienzwiler (FOEN) for the 10th of March 2008 (day of benthos drift measurements).

3.3.2 Temperature

Water temperature has an important impact on water quality and habitat conditions of aquatic biota. It defines chemical and physical properties of the water, as surface tension, density, viscosity or solubility, and thus the biological ones, as metabolism and respiration of riverine species.

The impact of storage hydropower on water temperature has been studied by different approaches. Water deviation by tunnels extracts less thermal energy than streamflow, where friction increases temperature. The impact of water storage on temperature is time- and space-dependent. Residual flow heats up faster than the natural

flow and is therefore more sensitive to external influences. In summer, released water from deep reservoirs is generally colder, whereas in winter the water release from the turbines is warmer than the water of non-operated catchments (Figure 3.9). The impact depends on the relation between the turbine discharge and residual flow of the upstream river reach.

The mean monthly water temperature for the Hasliaare River at Brienzwiler for 1975-2008 lies between 3.5 °C in January and 7.7 °C in July. No data series are available for the period before the construction of the HPP. Different studies estimate the increase of temperature in winter by about 1.0 to 1.3 °C and the decrease in summer by about 1.0 to 1.9 °C (Haas and Peter, 2009). These amplitudes are not a priori critical for aquatic biota. However, hydropeaking affects the frequency of the temperature fluctuations and can have an impact on habitat conditions, especially for monotonous river morphologies.

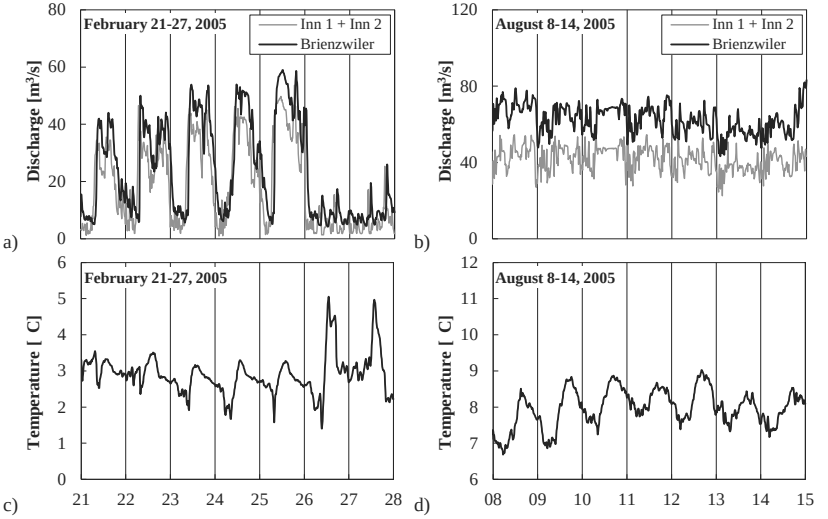

Figure 3.9. Discharge of the Hasliaare River at Brienzwiler and cumulative discharge of Innertkirchen 1 and 2 HPPs for one week in February 2005 (a) and one week in August 2005 (b) as well as water temperature for the same periods at Brienzwiler (c, d).

3.3.3 Suspended sediment load

Turbidity is an important parameter for abiotic and biotic conditions in Alpine rivers. High percentage of melt water from glaciers in summer increases fine sediment load. Due to settlement in the artificial storage volumes of KWO in the upper Aare catchment, the mean annual sediment concentration in the downstream river system decreases by about 70%. However, the seasonal shift of water due to hydropower operation slightly increases the naturally low load in winter (Finger *et al.*, 2006). Considerably lower values are measured in summer. Relational trends of freshwater fish activity to turbidity values and time was developed (Newcombe and Jensen, 1996). For the Hasliaare River, winter concentration can be critical for spawning and egg evolution.

3.4 Habitat conditions

Aquatic life habitat is essential for aquatic community assemblages and life histories. The condition and type of habitat influence species diversity, growth rates and abundance of aquatic fauna and flora. Several studies have been performed for analysis and understanding of the ecosystem of the Hasliaare River. Fish as well as benthos are especially relevant regarding hydropeaking.

3.4.1 Fish

An *in situ* study based on electrofishing (Haas and Peter, 2009) describes the fish habitat of the Hasliaare River between Innertkirchen and Brienzwiler. Despite the vicinity of Lake Brienz, only four different fish species are detected. Brown trout (*Salmo trutta fario*) is the only widespread one. Besides the lack of richness of species, biomass and density are also very low. The highest size range is found in the river reach with groynes, thanks to the morphological diversity and the proximity to the residual flow reaches. In the gravel bank reach mainly small fish are found, whereas the channelized reach is only poorly populated due to the missing instream structure.

The missing lateral connectivity due to steep and/or stepped connections avoids biological interaction between the main river and its tributaries. Due to their natural state, the latter would be an important hotspot for reproduction and a pool of diversity for fish. The field investigations show that main reproduction takes place in the residual flow reach upstream of the turbine outlets in Innertkirchen as well as in the connected tributaries without hydropeaking. The concentrations of spawning and juvenile fish are 40 and 5 times, respectively, higher than in the main river.

Incubation tests show that growth of brown trout is possible with the altered flow regime, despite the high turbidity and suspended load. However, spawning ground is missing between Innertkirchen and Lake Brienz. Despite hydropeaking, the lake trout (*Salmo trutta lacustris*) is able to ascend to the spawning grounds upstream of the turbine outlets in the residual flow reaches.

3.4.2 Benthos

In the winters of 2007 and 2008, field investigations documented the river ecological aspects of the Hasliaare River (Limnex, 2009). Hydropeaking by the power plants of Innertkichen 1 and 2 affects measurably the habitat conditions of macrozoobenthos as well as the drift behavior of benthos and other organic and inorganic material in the Hasliaare. Abundance and biomass of macrozoobenthos are lower than in rivers of similar morpho-hydrological characteristics and altitude without hydropeaking. In March, 55% to 90% of reference biomass is achieved, corresponding to less available nutrition for predators. Despite hydropeaking, an high potential of development is detected, especially for natural morphologies.

Flow peaks induce drift of invertebrates. Tests show catastrophic drift only for abrupt and high peaks in the channelized reach. Despite the low frequency of such maximum peaks, drift losses are defined as considerable during winter, the main reproduction time of such species, explaining why today’s abundance and biomass of macrozoobenthos are below the expected values for the Hasliaare River.

3.5 Conclusion

Since the 1930s, the natural flow regime of the river network in the upper Aare River catchment has been altered by high-head storage hydropower. Seasonal water transfer from summer to winter and an increased frequency of daily peak discharge events result.

The quality of the aquatic habitat of the Hasliaare River has drastically decreased during the last 150 years (Haas and Peter, 2009). The dynamic braided river network with various mesohabitats gave way to a mainly straight and monotonous channel without any instream structure. The water temperature and the turbidity are linked to the daily and seasonal hydrograph affected by hydropower operations.

Abundance and biomass of fish have decreased. Besides the fish as the key ecological indicator, benthos is also affected by hydropeaking and the poor river morphology. Despite today's situation of aquatic biota, the potential for biological development of the Hasliaare River has been highlighted. Investigations to improve the river morphology and the flow regime are therefore recommended.

Thus, the upper Aare River catchment (Figure 3.10) is an interesting case study for analysis of the interactions between climatic, hydrological, hydraulic, economic as well as ecological parameters of a glacierized Alpine river basin.

Figure 3.10. The upper Aare River catchment with Oberaar, Grimsel, Räterichsboden and Gelmer reservoirs (from background to front) as well as the Rhone Valley (Valais Canton) on the left and the Bernese Alps with snow peaks and glaciers in the background (www.kwo.ch, 01.2012).

4

Analysis of flood reduction capacity of hydropower schemes by semi-distributed modeling in an Alpine catchment area

The simulation of runoff in Alpine catchment areas is essential for the optimal operation of high-head storage hydropower plants (HPP) under normal flow conditions, but also in case of flood events. A semi-distributed conceptual numerical approach is presented, combining hydrological modeling and operation of hydraulic works. Spatial precipitation and temperature distributions were taken into account for the simulation of the dominant hydrological processes, such as glacier melt, snowpack constitution and melt, soil infiltration and runoff. The object-oriented modeling tool *Routing System* allowed runoff generation, simulation of the operating mode of complex HPP and its impact on the downstream river network for different scenarios. The chapter presents the hydrological modeling approach and its application for the upper Aare River catchment in Switzerland, where about half of the area is operated by the Oberhasli hydropower scheme. The development, calibration and validation of the hydrological model are discussed. Finally, the retention effect of the existing reservoirs and their management, including preventive turbine operations, on flood routing in the Aare River upstream of Lake Brienz is presented for the 2005 historical flood event.

4.1 Introduction

Flood events are all over the world and since ever highly damaging natural disasters. River training works as well as retention basins can increase capacity increase or reduce peak flow. Besides flood reduction, reservoirs can be combined with energy and/or irrigation purposes. In mountainous areas, the presence of storage hydropower multireservoir systems strongly influences the flow regime of the downstream located river system, depending on the drained area, the water storage capacities and their location within the basin. Peak flow during floods is therefore affected by filling rate of the reservoirs (Cheng and Chau, 2004). Besides the meteorological and hydrological parameters, the implementation and regulation of hydraulic structures is therefore crucial in order to simulate runoff in catchment areas. A large number of prediction models exist. Typical applications concern flood forecasting in large river basins for emergency planning (Koussis *et al.*, 2003; Thielen *et al.*, 2009a) and inflow forecasting for optimized reservoir operations (Turcotte *et al.*, 2004). Moreover, forecasting for flood warning is societally relevant issue (Moore *et al.*, 2005; Thielen *et al.*, 2009b), where the economic impact has to be assessed by taking into account risk and uncertainty (Arduino *et al.*, 2005; Demeritt *et al.*, 2007).

Most of the approaches lack the simulation of complex high-head hydropower schemes with large reservoirs for seasonal storage and low turbine capacities for peak-load, such as present in Alpine countries. Thus, the conceptual semi-distributed modeling tool *Routing System* (Dubois, 2005)was developed for hydrological forecast in high mountainous, operated catchment areas. Tri-dimensional rainfall, temperature and evapotranspiration distributions are used for simulating the hydrological processes by the GSM-SOCONT approach (Schaefli *et al.*, 2005). The model is able to produce glacier melt, snowpack constitution and melt, soil infiltration and runoff. The advantage of this object-oriented modeling tool is the consideration of flood routing in rivers as well as the operation of hydraulic structures such as water intakes, water transfer tunnels, reservoirs with water releasing structures and powerhouses. The multi-objective evaluation of runoff simulations at multiple locations in river basins was therefore the main advantage of the developed approach. It was successfully applied for several Alpine catchments in Switzerland and abroad, for example in the Rhone valley upstream of Lake Geneva (Jordan, 2007; García Hernández, 2011).

In the present study, the developed approach was applied to the upper Aare River catchment in Switzerland (Figure 4.1), which is operated by a highly complex storage hydropower scheme. During the flood event of August 2005, the Aare River inundated the whole valley between Meiringen and Brienzwiler. The peak flow of 444 m^3/s was the highest measured discharge in Brienzwiler since 1905, corresponding statistically to a return period of about 100 years. Despite a levee break and flooding of agricultural land, major damages were avoided. In the context of a post-assessment of the event by the authorities and because half of the river catchment is used for hydropower generation, the influence of the hydropower plants (HPP) on flood had to be estimated by systematic simulations.

To analyze the contribution of the different sub-catchments to runoff in the river system, a hydrological model was needed. Thus, the hydrographs of the 1987 and 2005 flood events were back evaluated in a first step. The results are assessed in terms of the

Nash and Sutcliffe efficiency (NSE), volume ratio and peak flow ratio. The calibrated and validated model was used to study the influence of the initial water level in the main reservoirs of the hydropower scheme on streamflow in the river system during the flood of 2005 (Bieri *et al.*, 2010). All hydroelectricity production data of the existing HPPs as well as the corresponding meteorological datasets were implemented. The contribution of the hydraulic scheme to flood routing was analyzed by comparison to simulations without considering reservoirs and HPPs. Finally, the potential of active flood management of the Oberhasli scheme is highlighted and discussed for several scenarios, taking into account different flow forecast time horizons as well as initial water levels in the four main reservoirs.

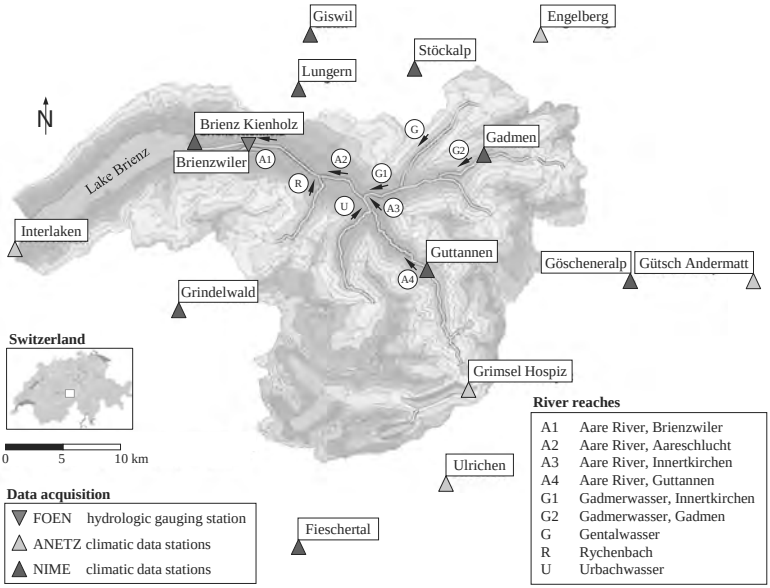

Figure 4.1. The upper Aare River catchment with elevation bands of 300 m altitude, main river reaches and ground-based weather and hydrological gauging stations.

4.2 Case study

4.2.1 Study site

The study site is the upper Aare River catchment (also-called Hasliaare) upstream of Lake Brienz in Switzerland. At the end of the 19th century, the area of the Grimsel and Susten was recognized as appropriate for hydropower exploitation. Heavy rainfalls, large retention areas, solid granitic bedrock as well as large differences in altitudes over short horizontal distances provide optimal conditions for storage hydropower (Schweizer *et al.*, 2008). The first concrete dams of Gelmer and Grimsel were built by the Kraftwerke Oberhasli AG (KWO) hydropower company between 1925 and 1932. Since then, a complex scheme with nine power houses and several reservoirs has been constructed (Figure 4.2). The largest reservoirs are Lake Oberaar ($57 \cdot 10^6$ m^3), Grimsel ($94 \cdot 10^6$ m^3), Gelmer ($13 \cdot 10^6$ m^3) and Räterichsboden ($25 \cdot 10^6$ m^3).

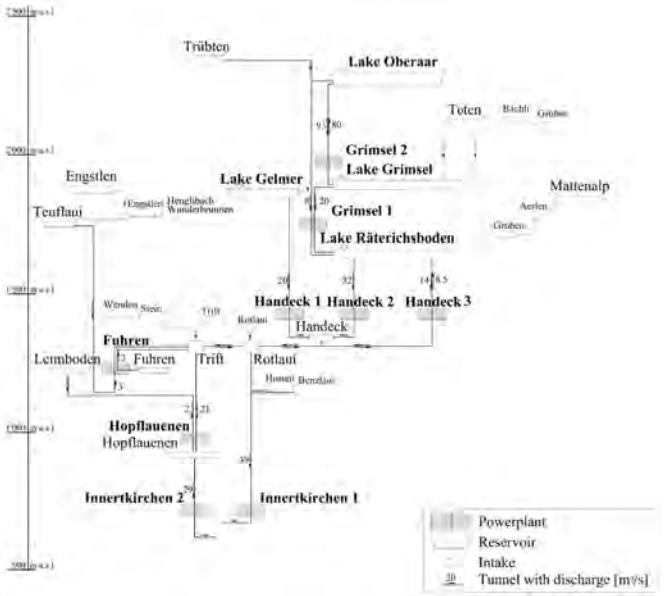

Figure 4.2. Schematic layout of the Oberhasli hydropower scheme, showing HPPs, reservoirs, intakes and water transfer tunnels with their capacities.

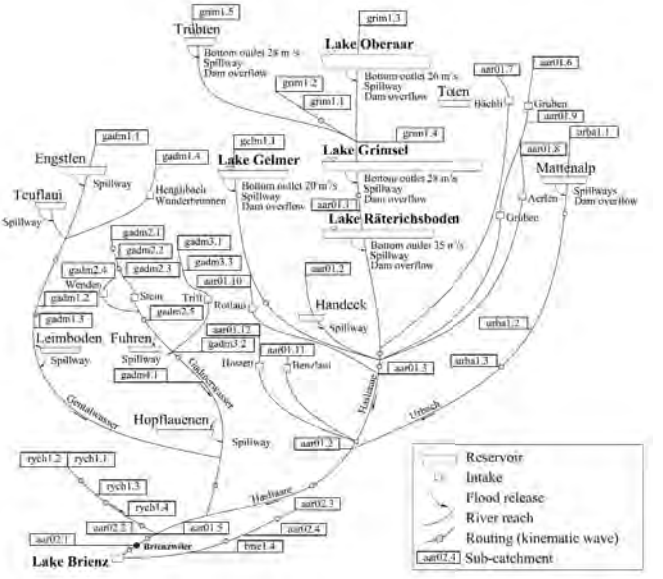

Figure 4.3. Sub-catchments and river system of the upper Aare River catchment area with KWO reservoirs, water intakes and flood release facilities as well as river reaches as modeled in *Routing System*.

The Aare River springs from Unteraar and Oberaar Glaciers at the altitude of about 2000 m a.s.l. and flows nowadays through several artificial reservoirs (Oberaar, Grimsel, Räterichsboden), in which the main part of water is temporally accumulated to be operated in the Grimsel, Handeck and Innertkirchen HPPs during peak hours of energy demand (Figure 4.3). In Innertkirchen the water is given back to the Aare River immediately downstream of the confluence with the Gadmerwasser River, draining the eastern part of the catchment area. After the Aareschlucht canyon, the Aare River reaches the main valley of Meiringen and enters Lake Brienz at Brienzwiler. The surface area of the upper Aare River basin, located between 564 m a.s.l. (Lake Brienz) and 4274 m a.s.l. (Finsteraarhorn), is 554 km^2, where about 20% was ice-covered in 2003. Seven main glaciers as well as several ice fields lie within the study area (Figure 4.4). The hydrological regime of the river is therefore glacial or glacio-nival, with an average annual discharge of 35 m^3/s at the gauging station in Brienzwiler.

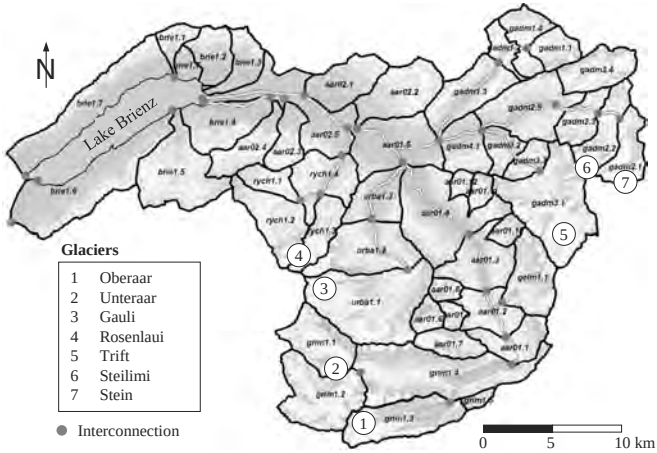

Figure 4.4. Sub-catchments division with ice-covered and non ice-covered elevation bands as well as the river network with its interconnections of the upper Aare River basin.

4.2.2 Data collection

The spatial discretization of the catchment area was carried out based on a digital elevation model with a grid size of 25 m provided by Swisstopo. For the simulation, meteorological datasets as well as discharge measurements are needed. The meteorological data is provided by the Swiss Federal Office of Meteorology and Climatology (MeteoSwiss). On the one hand, temperature and precipitation data are sampled every ten minutes by an automatic monitoring network (ANETZ) all over Switzerland. On the other hand, a large number of gauging stations (NIME) measure the daily precipitation. Five stations of the first type and nine of the second are located in and around the upper Aare River catchment and are therefore taken into account as model input (Figure 4.1).

The discharge, used to calibrate and validate the model, is measured every ten minutes at the Aare River gauging station at Brienzwiler (Figure 4.1) by the Federal Office for the Environment (FOEN).

The KWO made accessible the detailed hydraulic characteristics of the hydropower scheme, operation rules and historical operational data for the last 30 years of exploitation. Daily sums of turbine and pump operated volumes in addition to water levels in the four main reservoirs were obtained as well as hourly averages for 2005. These datasets allow the calculation of the inflow into the main lakes and compensation basins operated by KWO. Furthermore a post-analysis of the 2005 flood event could estimate the peak flow occurrences in nine river reaches downstream of the main reservoirs on the Aare, Gadmerwasser, Gentalwasser as well as on the Rychenbach and Urbachwasser Rivers (Figure 4.1).

4.3 Modeling approach

4.3.1 Hydrological model

To define runoff and its origin in a complex catchment area, where flow is only known at several control points, a hydrological model was needed. The hydrological-hydraulic *Routing System* simulation tool contains a semi-distributed conceptual model in order to simulate the runoff from glacier and snow-covered Alpine catchments using hourly or daily temperature and precipitation data as input (García Hernández *et al.*, 2007). The GSM-SOCONT approach, the Glacier Snow Melt – Soil CONTribution model (Schaefli *et al.*, 2005), combined several hydrological models for simulation of Alpine catchment areas. The modeling approach had two levels of discretization. The first distinguished between ice- and non ice-covered areas of the catchment. The surface area of the glacier-covered part was supposed to be constant during the simulation period, corresponding to rough approximation of glacier behavior in Alpine regions. The second level divided the catchment area into elevation bands of about 300 m with a homogenous hydrological behavior. For the spatial distribution of the meteorological variables, the method of Shepard (1968) was applied. Precipitation P, temperature T and evapotranspiration PET for a given elevation band were obtained by transforming the data of the weather data stations P^* and T^* in the influence zone, defined by a search radius R of 20 km. The data was weighted according to the inverse square distance to the center of gravity of the band. Because precipitation distribution in high-mountainous areas is complex due to orographic effects, a simple extrapolation is not adequate (Huss *et al.*, 2008a). The method had so been enhanced to take into account the elevation effect by considering constant altitudinal lapse rates for precipitation $grad_P$ [mm/1000 m] and temperature $grad_T$ [°C/1000 m]. Thus, hourly resolution time series are obtained for each elevation band.

The reservoir-based modeling approach defines the response of each hydrological unit and allows providing the total discharge at the outlet of the basin (Figure 4.5). The model comprises elements for (1) snowpack, (2) glacier, (3) soil infiltration and (4) surface runoff simulation as well as (5) flow routing and (6) reservoir dynamics.

Snowpack

For each elevation band, the temporal evolution of the snowpack is defined by an accumulation and melt model (Eq. 4.1 to 4.8). The inputs are temperature T [°C] and precipitation P [m/s]. The precipitation is divided by a fuzzy transition function into liquid P_{liq} and solid precipitation P_{snow} [m/s] depending on T (Eq. 4.1 and 4.2). The

separation factor α is 0 (only solid precipitation), when temperature T is lower than the low threshold temperature T_{cp1}. The separation factor α is 1 (only liquid precipitation), when temperature T is higher than the high threshold temperature T_{cp2}. When temperature T lies between T_{cp1} = 0°C and T_{cp2} = 2°C both solid and liquid precipitation occur (Eq. 4.3). Schaefli *et al.* (2005) discuss this linear transition and conclude that the threshold values vary in space and altitude

$$P_{liq} = \alpha \cdot P \tag{4.1}$$

$$P_{snow} = (1-\alpha) \cdot P \tag{4.2}$$

$$\alpha = (T - T_{cp1})/(T_{cp2} - T_{cp1}) \quad \left| T_{cp1} < T < T_{cp2} \right. \tag{4.3}$$

The solid precipitation or snowfall P_{snow} is used as input for the snowpack reservoir, which content varies depending on precipitation, snowmelt or freeze. Snowmelt or freeze M_{snow} [m/s] is computed by a degree-day approach (Eq. 4.4), where the threshold snowmelt temperature T_{cr} is set to 0°C and the melt coefficient due to rain b_p to 0.0125 h/mm

$$M_{snow} = \begin{cases} a_{snow} \cdot (1 + b_p \cdot P_{liq}) \cdot (T - T_{cr}) & \left| T > T_{cr} \right. \\ a_{snow} \cdot (T - T_{cr}) & \left| T \le T_{cr} \right. \end{cases} \tag{4.4}$$

where a_{snow} = degree-day coefficient of snowmelt [m/°C s].

The snow height H_S [m w.e.] is defined by solving the differential equation (Eq. 4.5) via the first-order Euler approach

$$\begin{aligned} &dH_S / dt = P_{snow} - M_{snow} \\ &-W_{snow} / dt \le M_{snow} \le P_{snow} + H_S / dt \end{aligned} \tag{4.5}$$

where W_{snow} = water content in the snowpack [m] and dt = time step [s].

The equivalent rainfall P_{eq} [m/s] is produced by the water content reservoir, where W_{snow} is again defined by first-order Euler approach (Eq. 4.6 to 4.8). In order to produce an equivalent precipitation, the relative water content in the snowpack θ must exceed the critical relative water content in the snowpack θ_{cr} of 0.1

$$\theta = W_{snow} / H_S \tag{4.6}$$

$$P_{eq} = \begin{cases} P_{liq} + W_{snow}/dt & \left| H_S = 0 \right. \\ 0 & \left| H_S > 0, \theta \le \theta_{cr} \right. \\ (\theta - \theta_{cr}) \cdot H_S/dt & \left| H_S > 0, \theta > \theta_{cr} \right. \end{cases} \tag{4.7}$$

$$dW_{snow} / dt = P_{liq} + M_{snow} - P_{eq} \tag{4.8}$$

Glacier

The glacier melt depends on the temperature and the snow cover of the glacier (Eq. 4.9 to 4.13). The total discharge from glacier depends on storage processes in the two linear reservoirs for snow and ice. The outflow from the linear reservoir of snow Q_{snowmelt} [m^3/s] is

$$dh_{\text{snow gl}} / dt = P_{\text{eq}} - k_{\text{snow gl}} \cdot h_{\text{snow gl}} \tag{4.9}$$

$$Q_{\text{snowmelt}} = k_{\text{snowgl}} \cdot h_{\text{snowgl}} \cdot S_{\text{gl}} \tag{4.10}$$

where $h_{\text{snow gl}}$ = snow level in the linear reservoir [m]; $k_{\text{snow gl}}$ = linear snow reservoir coefficient [1/s] and S_{gl} = surface area of glacier [m^2].

Glacier melt Q_{icemelt} [m^3/s] only happens without snow on the glacier and when the temperature is higher than the critical glacier melt temperature T_{cr}

$$P_{\text{eq ice}} = \begin{cases} 0 & \left| \; T \le T_{\text{cr}} \text{ or } \; H_S > 0 \right. \\ a_{\text{ice}} \cdot (T - T_{\text{cr}}) & \left| \; T > T_{\text{cr}} \text{ and } H_S = 0 \right. \end{cases} \tag{4.11}$$

$$dh_{\text{ice}} / dt = P_{\text{eq ice}} - k_{\text{ice}} \cdot h_{\text{ice}} \tag{4.12}$$

$$Q_{\text{icemelt}} = k_{\text{ice}} \cdot h_{\text{ice}} \cdot S_{\text{gl}} \tag{4.13}$$

where $P_{\text{eq ice}}$ = glacier flow [m/s]; a_{ice} = degree-day factor for ice melt [m/°C s]; h_{ice} = height in the glacier linear reservoir [m]; k_{ice} = linear ice reservoir coefficient [1/s] and S_{gl} = surface area of glacier [m^2].

Soil infiltration

For non ice-covered areas, soil infiltration processes have to be taken into account. The equivalent precipitation P_{eq} from the snow model and the potential evapotranspiration *PET* are used as input for the GR3 model (Edijatno and Michel, 1989; Consuegra *et al.*, 1998). Infiltration intensity i_{inf} [m/s] depends on P_{eq} as well as the soil saturation (Eq. 4.14). The model consists in an interflow and a base flow linear reservoir. If temperature T is higher than the threshold evaporation temperature T_{ETP}, real evapotranspiration RET [m/s] is defined (Eq. 4.15). The interflow reservoir reacts rapidly to precipitation. During flood events, it provides the major supply. Its outflow intensity $i_{\text{interflow}}$ [m/s] (Eq. 4.16), the transfer intensity to the base flow reservoir i_{transfer} [m/s] (Eq. 4.17) and thus the interflow $Q_{\text{interflow}}$ [m^3/s] (Eq. 4.18) are conditioned by the filling rate $h_{\text{interflow}}/h_{\text{interflow max}}$

$$i_{\text{inf}} = \begin{cases} P_{\text{eq}} \cdot (1 - (h_{\text{interflow}} / h_{\text{interflow max}})^2) & \left| \; h_{\text{interflow}} \le h_{\text{inferflow max}} \right. \\ 0 & \left| \; h_{\text{interflow}} > h_{\text{inferflow max}} \right. \end{cases} \tag{4.14}$$

$$RET = \min(PET \cdot \sqrt{h_{\text{interflow}} / h_{\text{interflow max}}}; h_{\text{interflow}} / dt - i_{\text{interflow}} - i_{\text{transfer}}) \tag{4.15}$$

$$i_{\text{interflow}} = k_{\text{interflow}} \cdot (h_{\text{interflow}} / h_{\text{interflow max}})^{a_{\text{interflow}}} \tag{4.16}$$

$$i_{transfer} = k_{transfer} \cdot (h_{interflow} / h_{interflow\,max}) \cdot (1 - h_{baseflow} / h_{baseflow\,max}) \quad (4.17)$$

$$dh_{interflow} / dt = i_{inf} - RET - i_{transfer} - Q_{interflow}/S_{ngl} \quad (4.18)$$

where $h_{interflow}$ = storage height [m]; $h_{interflow\,max}$ = maximum storage height [m]; $k_{interflow}$ = release coefficient [1/s]; $a_{interflow}$ = release factor of the interflow reservoir [-]; $k_{transfer}$ = transfer coefficient [1/s] and S_{ngl} = non ice-covered surface area [m^2].

The outflow intensity of the base flow reservoir $i_{baseflow}$ [m/s] (Eq. 4.19) in addition to the base flow $Q_{baseflow}$ [m^3/s] (Eq. 4.20) depend on the storage height of the reservoir. A nearly constant flow throughout the year should be achieved, insensitive to precipitation

$$i_{baseflow} = k_{baseflow} \cdot (h_{baseflow} / h_{baseflow\,max})^{a_{baseflow}} \quad (4.19)$$

$$dh_{baseflow} / dt = i_{transfer} - Q_{baseflow}/S_{ngl} \quad (4.20)$$

where $h_{baseflow}$ = storage height [m]; $h_{baseflow\,max}$ = maximum storage height [m]; $k_{baseflow}$ = release coefficient [1/s]; $a_{baseflow}$ = release factor [-] of the base flow reservoir and S_{ngl} = non ice-covered surface area [m^2].

Surface runoff

The surface runoff resulting from the excess equivalent rainfall is estimated with a non-linear transfer reservoir (Eq. 4.21 to 4.23). The SWMM model (Metcalf, 1971) produces the downstream hydrograph Q_{runoff} [m^3/s] using the hyetograph of net rainfall

$$i_{net} = P_{eq} - i_{inf} \quad (4.21)$$

$$dh_{runoff} / dt = i_{net} - i_{runoff} \quad | \; h_{runoff} > 0 \quad (4.22)$$

$$Q_{runoff} = \beta \cdot J^{1/2} \cdot h_{runoff}^{5/3} \cdot B \cdot S_{ngl} \quad (4.23)$$

where i_{net} = net intensity of precipitation [m/s]; h_{runoff} = water height in runoff reservoir [m]; i_{runoff} = outflow runoff intensity [m/s]; β = non-linear reservoir coefficient for direct runoff [$m^{1/3}$/s]; J = average slope of the plan [-]; B = width of the plan [m] and S_{ngl} = non ice-covered surface area [m^2].

The total runoff from the non ice-covered part of the basin is the sum of the surface runoff Q_{runoff}, the interflow $Q_{interflow}$ and the base flow $Q_{baseflow}$. From the ice-covered part, the sum of $Q_{snowmelt}$ and $Q_{icemelt}$ is computed. The total outflow of the elevation band Q_{tot} [m^3/s] is the sum of both parts.

Routing

The flood routing in channels is done by solving the Saint-Venant equations for a prismatic channel (García Hernández *et al.*, 2007). The applied kinematic wave assumption neglects the terms of inertia and pressure. Gravity and the friction forces are thus of the same magnitude, inducing an explicit relationship between flow and normal water depth. The friction slope is computed by use of Manning-Strickler's equation.

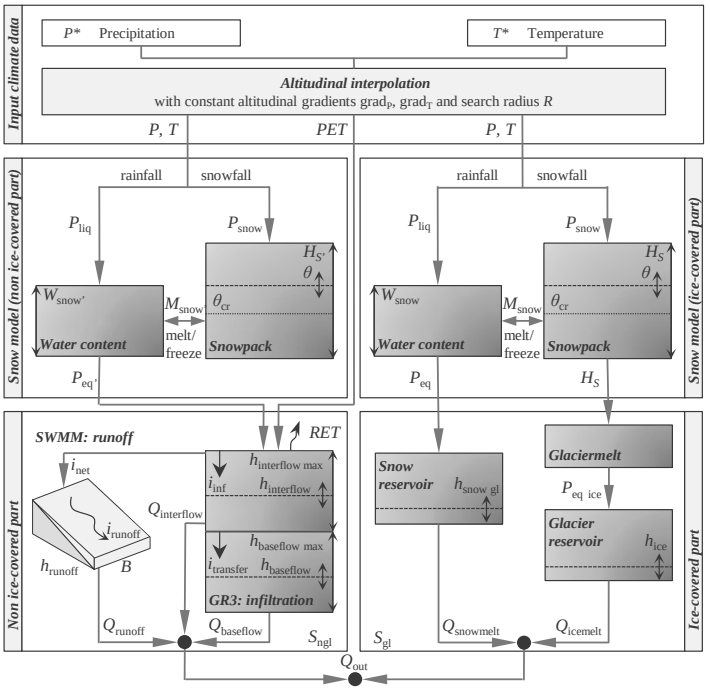

Figure 4.5. Hydrological model of *Routing System* for a glacierized elevation band containing a non ice-covered and an ice-covered part.

Reservoir dynmacis

The transient evolution of the water volume V in the reservoir is given

$$\frac{dV}{dt} = Q_{\text{inflow}} - Q_{\text{outflow}} \tag{4.24}$$

where V = reservoir storage volume [m^3], Q_{inflow} = inflow to the reservoir [m^3/s] and Q_{outflow} = outflow from the reservoir [m^3/s].

As outflow generally depends on the water level, a reservoir is characterized by its volume-level ratio for the operated storage volume. By knowing inflow, outflow as well as the initial water level (and hence the initial volume) of the reservoir, Equation 4.24 is solved via the first-order Euler approach.

4.3.2 Model calibration and validation

The catchment area of the Aare River upstream of Lake Brienz was modeled in its configuration of 2003. Related to hydrological and HPP constraints, the river basin was divided in 43 sub-catchments, which were split in 96 ice-covered and 243 non ice-covered elevation bands of 300 m (Figure 4.4). For each band, precipitation P,

temperature T and potential evapotranspiration PET were interpolated from the 14 meteorological stations, if located in the influence zone of 20 km search radius.

Temperature, precipitation, snowfall, snowmelt, ice melt, evaporation, infiltration as well as runoff were updated every 600 s. Data acquisition for all elements in the catchment area is done with hourly mean values for the total simulation period.

The usual calibration process is explained in detail in García Hernández *et al.* (2007). For large catchment areas with multiple elevation bands, the same values for the calibration parameters (a_{snow}, a_{ice}, $k_{snow\ gl}$, k_{ice} for ice-covered bands and a_{snow}, $h_{interflow\ max}$, $k_{interflow}$, $a_{interflow}$, $k_{transfer}$, $h_{baseflow\ max}$, $k_{baseflow}$, $a_{baseflow}$, β for non ice-covered bands) are adopted for the sub-catchments. The manual calibration process takes place in accordance with the hydrological cycle, allowing an independent calibration of the key parameters. The simulation starts in October when the snowpack, built up during autumn and winter, is exhausted. The degree-day factor for snowmelt a_{snow}, which mainly influences the streamflow from February to June, is first calibrated. The degree-day factor for ice melt a_{ice}, the linear ice reservoir coefficient k_{ice} and the linear snow reservoir coefficient $k_{snow\ gl}$ influence the summer runoff, when the snow is melting on the ice-covered elevation bands. The interflow depends on the infiltration of snowmelt and rainfall. The maximum storage height $h_{interflow\ max}$ and the release coefficient $k_{interflow}$ of the interflow reservoir are then calibrated. Finally the non-linear reservoir coefficient for direct runoff β, mainly influencing the time evolution of flood events, is adjusted. For flood event modeling, the base flow can be neglected and thus $k_{transfer}$, $h_{baseflow\ max}$, $k_{baseflow}$ and $a_{baseflow}$ do not need a calibration. $a_{interflow}$ was set to 1.

The model is pre-calibrated over ten 15-month periods with an hourly time step continuous simulation by using meteorological, hydrological and production datasets. The hydrological parameters of the ten sub-catchments operated by KWO are optimized independently. The results reveal the importance of glacier melt, which highlight the need for a specific for future long time scenarios (see Chapter 5).

In a second step, the model is calibrated by the historic flood event of August 2005 and validated by the flood of August 1987. The 444 m^3/s peak flow of the Aare River in 2005 (called *Measured Q*) is the highest value ever measured in Brienzwiler, corresponding statistically to a return period of about 100 years (Figure 4.6a). The valley between Meiringen and Lake Brienz was largely inundated and thus the whole discharge could not be measured at the gauging station of Brienzwiler. A post-analysis of the event allowed a reconstruction of the hydrograph and an estimation of the real peak (called *Observed Q*). As the flooding is not simulated by *Routing System*, the model is calibrated using the reconstructed hydrograph with a peak of 520 m^3/s. Further peak flow estimations in the non-influenced catchments are used for comparison. The 1987 flood event only produced insignificant inundation.

The simulated values were compared to the measured reservoir inflow, to the observed outflow in Brienzwiler and to the peak flow estimations. The simulation performance is assessed in terms of Nash and Sutcliffe (1970) efficiency NSE (Eq. 4.24) and peak flow ratio r_{peak} (Eq. 4.26). Water volume ratio r_{vol} (Eq. 4.25), related to NSE (Gupta *et al.*, 2009), is also given

$$\mathrm{NSE} = 1 - \frac{\sum_{t=1}^{n} (Q_{\mathrm{obs}\,t} - Q_{\mathrm{sim}\,t})^2}{\sum_{t=1}^{n} (Q_{\mathrm{obs}\,t} - \overline{Q_{\mathrm{obs}}})^2} \qquad (-\infty < R^2 < 1) \tag{4.25}$$

$$r_{\mathrm{vol}} = \frac{V_{\mathrm{sim}}}{V_{\mathrm{obs}}} = \frac{\sum_{t=1}^{n} (Q_{\mathrm{sim}\,t} \cdot \Delta t)}{\sum_{t=1}^{n} (Q_{\mathrm{obs}\,t} \cdot \Delta t)} \tag{4.26}$$

$$r_{\mathrm{peak}} = \frac{Q_{\mathrm{sim\ max}}}{Q_{\mathrm{obs\ max}}} \tag{4.27}$$

where $Q_{\mathrm{obs}\,t}$ = observed hourly discharge; $Q_{\mathrm{sim}\,t}$ = simulated hourly discharge; $\overline{Q_{\mathrm{obs}}}$ = mean observed discharge; V_{sim} = simulated volume; V_{obs} = observed volume, $Q_{\mathrm{sim\ max}}$ = simulated peak discharge; $Q_{\mathrm{obs\ max}}$ = observed peak discharge; T_{per} = time period and Δt = time step.

The objectives of NSE higher than 0.8, a volume ratio r_{vol} between 0.9 and 1.1 and a peak flow ratio r_{peak} between 0.9 and 1.1 should be achieved for satisfactory simulation performance. The simulated inflow to the four main reservoirs Oberaar (NSE = 0.75, r_{vol} = 0.99), Grimsel (NSE = 0.91, r_{vol} = 0.95), Gelmer (NSE = 0.91, r_{vol} = 0.94) and Räterichsboden (NSE = 0.87, r_{vol} = 1.01) shows good agreement with the observed data for the 2005 flood event. Only the calibration of the Oberaar catchment was of lower performance. Due to relatively low inflow compared to the turbine and pump capacities of Grimsel 2 HPP, the measured daily balance was adulterated.

The simulated hydrograph in Brienzwiler for the 2005 flood (Figure 4.6a) reproduces the main characteristics. Only the double-peak due to the levee breaks could not be reproduced. The performance of the simulation for the Brienzwiler gauging station A1 is satisfactory (NSE = 0.98, r_{vol} = 1.00 and r_{peak} = 1.06). Table 4.1 shows the comparison of measured/observed $Q_{\mathrm{obs\ max}}$ and simulated peak flow $Q_{\mathrm{sim\ max}}$ at the nine reference river reaches in the lower catchment for the 2005 flood event. Besides the upper Aare River in Guttannen, influenced by a high number of river water intakes, the peak flow ratios r_{peak} all fall between 0.9 and 1.1 and confirm the plausibility of the model in the downstream of KWO located part.

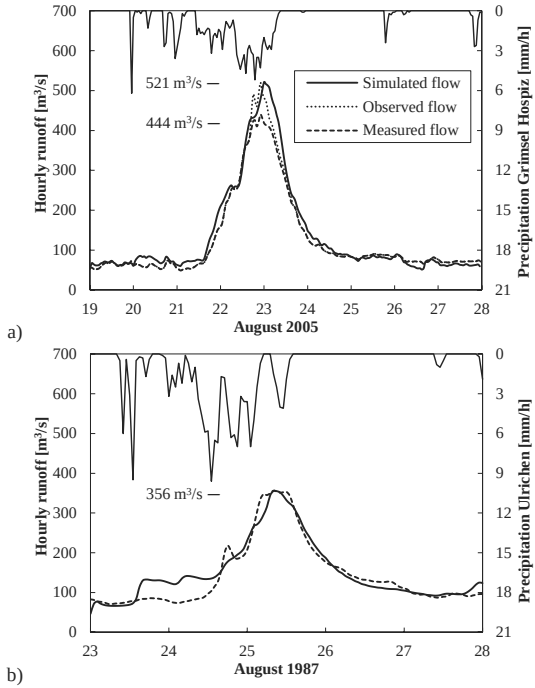

Figure 4.6. a) Calibration of 2005 flood event (NSE = 0.98, r_{vol} = 1.00, r_{peak} = 1.06), superimposed with Grimsel Hospiz precipitation series; b) Validation with 1987 flood event (NSE = 0.90, r_{vol} = 1.05, r_{peak} = 1.00), superimposed with Ulrichen precipitation series (no hourly data from Grimsel Hospiz available for 1987).

Table 4.1. Observed and simulated peak flow, $Q_{obs\ max}$ and $Q_{sim\ max}$, for the reference river reaches and flow volume, V_{obs} and V_{sim} between the 19th and 28th of August 2005, as well as peak flow ratio r_{peak}, water volume ratio r_{vol} and Nash and Sutcliffe efficiency criterion NSE for the 2005 flood event.

	Reference river reach	$Q_{obs\ max}$ [m³/s]	$Q_{sim\ max}$ [m³/s]	r_{peak} [-]	V_{obs} [10³ m³]	V_{sim} [10³ m³]	r_{vol} [-]	NSE [-]
A1	Aare River, Brienzwiler	520	521	**1.00**	100	106	**1.06**	**0.98**
A2	Aare River, Aareschlucht	340	350	**1.03**		75		
A3	Aare River, Innertkirchen	145	138	**0.95**		18		
A4	Aare River, Guttannen	60	54	**0.90**		6		
G1	Gadmerw., Innertkirchen	180	182	**1.01**		26		
G2	Gadmerw., Gadmen	80	70	**0.88**		9		
G	Gentalwasser	45	46	**1.03**		8		
R	Rychenbach	85	83	**0.97**		12		
U	Urbach	50	51	**1.02**		5		

The model was then validated with the 1987 flood event (Figure 4.6b). Without any adaptations of the calibration parameters, the measured and simulated outflow in Brienzwiler and showed with NSE = 0.90, $r_{vol} = 1.05$ and $r_{peak} = 1.00$ quite good agreement. Unfortunately no data for the other reference river reaches were available.

The model has been successfully calibrated and can be used for simulations of other scenarios as well as for flood forecasting. A particularity of the two simulated floods is the quite different distribution of rainfall. During the flood event of 2005, the maximum rainfall was measured in the north-eastern part of the river basin. For the event of 1987, the gravity center of the precipitations was located in the east. An interesting analysis could consist in scenarios with other rainfall distributions, centered for example in the southern part, where the large reservoirs are located.

4.3.3 Scenarios

Due to operational constraints the Grimsel and the downstream located Räterichsboden (Räbo) reservoirs had exceptionally low water levels on the 19th of August 2005. Their flood retention volume was therefore much higher than usual. To evaluate the retention effect of the large reservoirs of the Oberhasli scheme, several scenarios taking into account different filling degrees of the reservoirs as well as two plant operation modes are defined, simulated and compared (Table 4.2). The meteorological input data is that of August 2005 for all simulations.

Reservoir filling

Five scenarios of filling degrees based on real data, statistical analysis, maximum capacity and technical constraints are chosen:

- *Scenario I (Levels as 2005)* corresponds to the initial water levels as in 2005, as also used for the calibration process. Especially the Grimsel reservoir shows with 37% a very low filling degree.
- *Scenario II (Average levels)* considers average levels in August, calculated over the previous 10 years. This case corresponds to the most likely situation with filling degrees between 72 and 91%.
- *Scenario III (Full reservoirs)* is a worst case scenario assuming all reservoirs full on the19th of August 2005. This quite hypothetic case is the upper limit of the sensitivity analysis.
- *Scenario IV (Nearly full reservoirs)* is a more realistic upper limit of the sensitivity analysis. Due to pumped-storage activities of Grimsel 2 HPP between Oberaar and Grimsel reservoirs, $15 \cdot 10^6$ m^3 of free volume must always be available in one of the two reservoirs. In this case the filling degree of Grimsel reservoir is set to 84%.
- *Scenario V (Without HPP)* evaluates the influence of the whole hydropower scheme. By removing all reservoirs and HPPs, the non-equipped catchment is analyzed.

Table 4.2. Model conditions of the flood scenarios: Initial water levels and corresponding filling degree of the four main reservoirs for the 19th of August 2005 (00:00) and HPP operation modes.

Scenario		Initial water level [m a.s.l.] (filling degree)				HPP operation mode
		Oberaar	Grimsel	Gelmer	Räterichsboden	
a (Ref.)	Levels as 2005	2'296.9 (83%)	1'882.9 (37%)	1'847.8 (91%)	1'749.3 (55%)	Statistics (as 2005)
b	Levels as 2005	2'296.9 (83%)	1'882.9 (37%)	1'847.8 (91%)	1'749.3 (55%)	OptiProd (0 h forecast)
Ia	Average levels	2'295.7 (80%)	1'904.7 (88%)	1'847.9 (91%)	1'756.2 (72%)	Statistics (as 2005)
Ib	Average levels	2'295.7 (80%)	1'904.7 (88%)	1'847.9 (91%)	1'756.2 (72%)	OptiProd (0 h forecast)
IIa	Full reservoirs	2'303.0 (100%)	1'908.8 (100%)	1'849.7 (100%)	1'767.0 (100%)	Statistics (as 2005)
IIb	Full reservoirs	2'303.0 (100%)	1'908.8 (100%)	1'849.7 (100%)	1'767.0 (100%)	OptiProd (0 h forecast)
IVa	Nearly full reservoirs	2'303.0 (100%)	1'903.1 (84%)	1'849.7 (100%)	1'767.0 (100%)	OptiProd (0 h forecast)
IVc	Nearly full reservoirs	2'303.0 (100%)	1'903.1 (84%)	1'849.7 (100%)	1'767.0 (100%)	OptiProd (24 h forecast)
IVe	Nearly full reservoirs	2'303.0 (100%)	1'903.1 (84%)	1'849.7 (100%)	1'767.0 (100%)	OptiProd (48 h forecast)
V	not relevant	not relevant	not relevant	not relevant	not relevant	no HPP

HPP operation

The first operation scenario (a) simulates the turbine operations as applied by KWO in 2005 (called *Statistics*). For the second scenario (b) an autonomous tool for optimal HPP operation has been developed (called *OptiProd*). Figure 4.7 shows an overall sketch of its operation mode; it is explained in detail in Chapter 6. First a run without optimization is performed. For the second run, the generated data is used to define the turbine and bottom outlet activities, respecting a pre-defined forecast time horizon (24 h or 48 h). The algorithm compares data for the given time horizon with pre-defined threshold values and defines the optimal normal as well as preventive HPP operation for the next time step.

As a general rule, turbine operations should be performed during peak price hours to generate maximum revenue. Thus, the priority driving parameter is the demand by the electricity market. For this study, electricity prices are real spot market values from the European Energy Exchange (EEX). For the given forecast time horizon, the hours when the electricity price of the market is higher than the defined cost price, are set. A target level curve, defining the annual filling of the reservoir, should guarantee the seasonal water transfer from summer to the economically interesting winter hours. The algorithm follows this curve with a pre-defined tolerance.

Besides the normal operations, preventive ones are foreseen for turbines and bottom outlets in case of emergency (Figure 4.7). Bottom outlets are excluded for preventive activities in this study. If predicted inflow to a reservoir is higher than the free storage volume and thus overflow would happen, preventive emergency operations

start. This is only done, when a downstream located reservoir is not full or peak flow in the downstream river reach is lower than a pre-defined threshold value. A 0h forecast horizon corresponds to instantaneous turbine operations, whereas 24 h in scenario IVc and 48 h in scenario IVe simulate in a first run the prediction data, which is then used as a decision support for the second run.

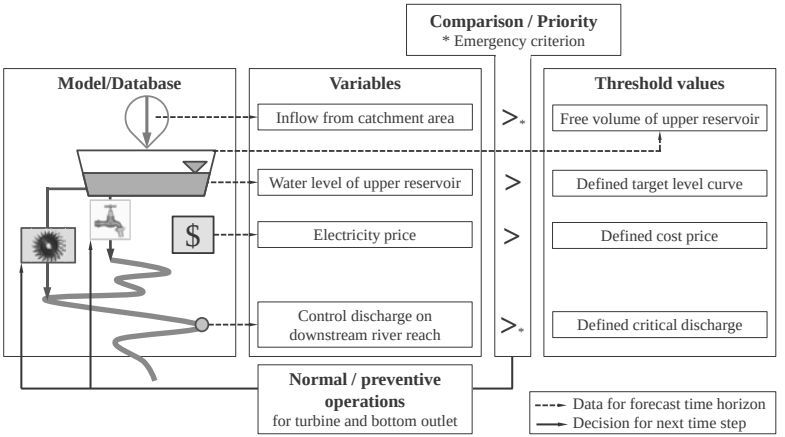

Figure 4.7. Flow chart of HPP operation for normal and preventive operations (OptiProd), containing time-dependent and pre-defined values.

4.4 Results

The results are illustrated as hydrographs of the Aare River in Guttannen, Innertkrirchen, Aareschlucht and Brienzwiler (Figure 4.8). Guttannen and Innertkirchen are located upstream of the Innertkirchen 1 and 2 HPPs and are therefore only affected by flow release of the Handeck compensation basin. Aareschlucht, downstream of the turbine outlets, and Brienzwiler, at the outlet of the upper Aare catchment, are directly influenced by the turbine operations.

The simulated curves have similar characteristics (Figure 4.8). All of them provide a local maximum in the morning of the 22nd of August and a peak around midnight the same day. Due to the different HPP operation scenarios, the peaks are slightly shifted. Thus, the difference between the peak flow of Aareschlucht A2 and Brienzwiler A1 is not always the same, although the contribution of the non-influenced catchment is identical. Flood routing in the Aare River is low due to the short distance between the reference points and not detectable for 600 s time steps. Turbine operation coming from statistics and scenario V provide smooth curves, whereas the OptiProd produces higher fluctuations due to start and stop of the full turbine capacity.

The analysis of peak flow (Figure 4.8 and Table 4.3) reveals much higher peak values than measured with a return period of 100 years. This fact points out the difficulty of statistical flood characterization in a by HPP operation affected catchment area, like for the Hasliaare River. The eastern catchment, containing the river reaches of Gentalwasser G, Gadmerwasser in Innertkirchen G1 and Gadmen G2, as well as the Rychenbach R are not influenced by the hydropower scheme due to low or not existing

retention volumes. The river reach of Urbach U is affected by the Mattenalp reservoir's flood release and varies therefore from one scenario to another.

Even though the total inflow volume is the same for every scenario, the simulated flow volume on the different river reaches for the 2005 flood scenarios between the 19th and 28th of August 2005 (Table 4.4) varies due to different turbine and flood release operations. The turbine operations are the same in scenario Ia, IIa and IIIa, but the flow release by the spillways of Handeck and Mattenalp are different and thus influence the hydrographs downstream, as seen for the river reaches Guttannen A4 and Urbach U. The volume of the cumulative precipitation for the catchment area upstream of Brienzwiler during the 2005 flood event is of 141 10^6 m^3. For Scenario Ia, the overall event runoff coefficient, the ratio of runoff and precipitation volume between the 19th and 28th of August 2005, is of 0.75. For Scenario V without HPP, a coefficient 0.88 is defined. This value is high, but quite common for extreme flood events in high-mountainous catchment areas due to rock cover of low infiltration and glacier melt.

Scenario Ia (Levels as 2005), IIa (Average levels) and IIIa (Full reservoirs) with turbine operations as in 2005 (Statistics) show different flood peak in the Hasliaare River (Table 4.3). At Aareschlucht A2, flow increases from 350 m^3/s by 12 m^3/s and 93 m^3/s, respectively. An average reservoir filling degree as in scenario IIa does not completely fill Grimsel reservoir, whereas overflow of the Räterichsboden as well as Handeck reservoirs takes place. Thus, flow derivation from the Mattenalp reservoir is stopped and peak flow in the Urbach reach U increases from 51 m^3/s to 63 m^3/s due to spillway release.

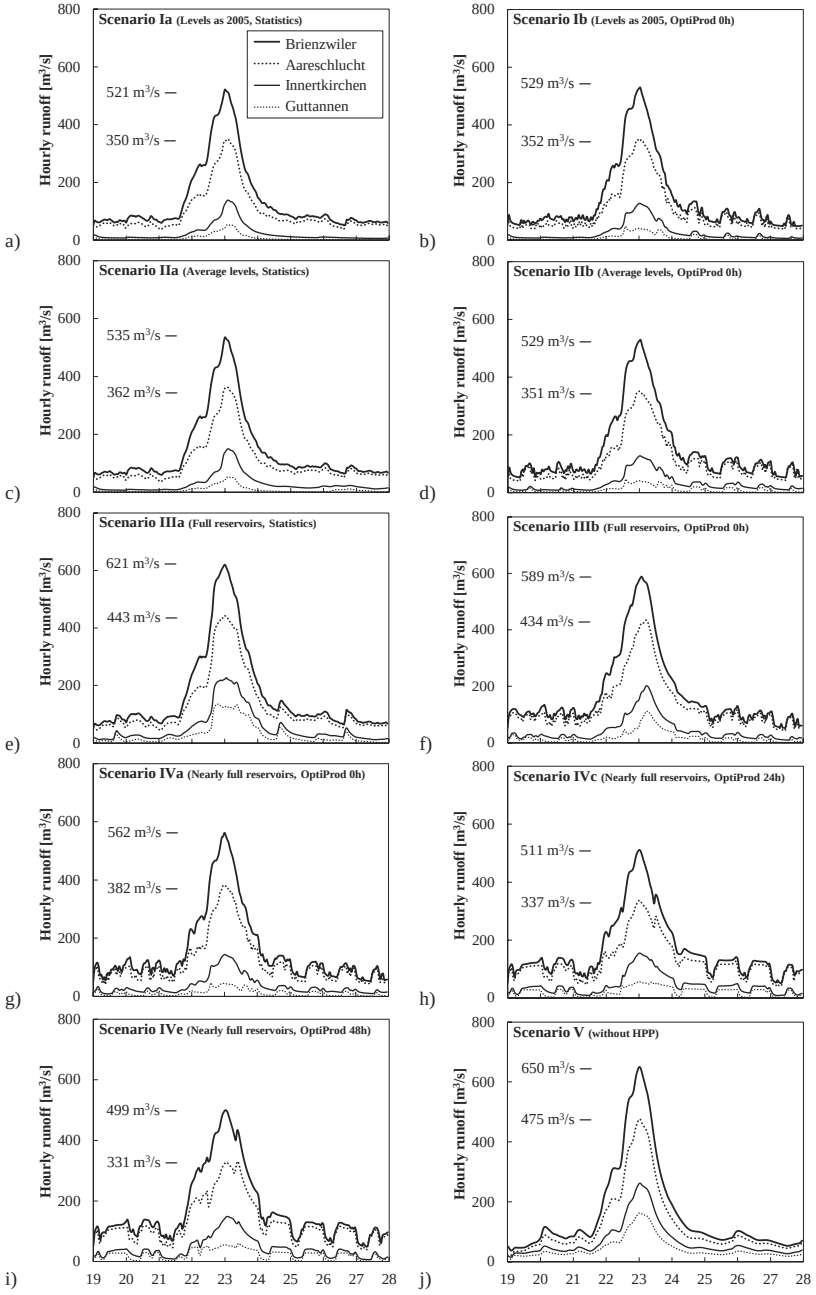

Figure 4.8. Simulated hydrographs of the flood in August 2005 at four locations on the Aare River for the scenarios Ia (a), Ib (b), IIa (c), IIb (d), IIIa (e), IIIb (f), IVa (g), IVc (h), IVe (i) and V (j).

Table 4.3. Simulated peak flow $Q_{sim\ max}$ [m^3/s] on the reference river reaches for 2005 flood scenarios.

	Reference river reach	$Q_{sim\ max}$ [m^3/s]									
		Ia	Ib	IIa	IIb	IIIa	IIIb	IVa	IVc	IVe	V
A1	Aare River, Brienzwiler	521	529	535	529	620	589	562	511	499	650
A2	Aare River, Aareschlucht	350	352	362	352	443	434	382	337	331	475
A3	Aare River, Innertkirchen	138	127	150	127	227	202	144	155	149	262
A4	Aare River, Guttannen	54	48	54	47	135	112	47	56	60	163
G1	Gadmerw., Innertkirchen	182	182	182	182	182	182	182	182	182	215
G2	Gadmerw., Gadmen	70	70	70	70	70	70	70	70	70	80
G	Gentalwasser	46	46	46	46	46	46	46	46	46	58
R	Rychenbach	83	83	83	83	83	83	83	83	83	83
U	Urbach	51	51	63	51	64	64	64	64	61	64

Table 4.4. Simulated flow volume V_{sim} [10^3 m^3] on the reference river reaches for 2005 flood scenarios between the 19th and 28th of August 2005 (00:00).

	River reach	V_{sim} [10^3 m^3]									
		Ia	Ib	IIa	IIb	IIIa	IIIb	IVa	IVc	IVe	V
A1	Aare River, Brienzwiler	106	109	110	116	130	135	123	130	131	124
A2	Aare River, Aareschlucht	75	78	79	85	99	105	92	100	101	93
A3	Aare River, Innertkirchen	18	20	22	25	42	34	28	35	34	53
A4	Aare River, Guttannen	6	7	7	9	23	16	10	18	18	34
G1	Gadmerw., Innertkirchen	26	26	26	26	26	26	26	26	26	40
G2	Gadmerw., Gadmen	9	9	9	9	9	9	9	9	9	16
G	Gentalwasser	8	8	8	8	8	8	8	8	8	9
R	Rychenbach	12	12	12	12	12	12	12	12	12	12
U	Urbach	5	6	9	9	12	12	12	10	9	12

Assuming full reservoirs at the beginning of the flood, as in scenario IIIa, only a minor decrease of reservoir levels occurs due to turbine operations as in 2005 (Statistics), when no preventive water release was undertaken. The peak of the hydrograph in Guttannen A4 increases from 54 m^3/s for scenario Ia and IIa to 135 m^3/s for IIIa. The hydrographs of the Gadmerwasser River remain unchanged.

OptiProd with 0 h prediction horizon does not reduce peak flow for scenario I (Levels as 2005). The time shift of the peak at Brienzwiler by 1 h leads even to a slightly higher peak of 529 m^3/s. The simulation of scenario IIb (Average levels) shows the same results for the peak as scenario Ib, whereas the peak at Aareschlucht A2 could be slightly reduced by 10 m^3/s compared to scenario IIa. The peak flow of scenario IIIb with completely full reservoirs could also be lowered. OptiProd generated higher volumes of the hydrographs (Table 4.4) due to higher flow release in the post-peak period, when electricity prices are high.

Scenario IVa, IVc and IVe (Nearly full reservoirs) have more realistic initial reservoir conditions than scenario III (Full reservoirs), even when they stay close to the worst case. OptiProd with a 0 h prediction horizon can reduce the peak at Aareschlucht by 52 m^3/s. By perfect prediction of flow from 24 h and 48 h, the peak can even be reduced from 382 m^3/s by 45 m^3/s and 51 m^3/s, respectively.

At the example of the Lake Räterichsboden, the lowest of the four main reservoirs in the cascade, the main differences for the full and nearly full reservoirs can be seen. Figure 4.9 shows the inflow and outflow at the reservoir for HPP operations with OptiProd. Inflow is generated by the natural, non-operated catchment area, the turbine operations of Grimsel 1 HPP, the flow derivation through the Mattenalp tunnel in addition to the spillway release of Lake Grimsel. Outflow results from the turbines of Handeck 2 and 3 HPPs and the flow release trough the spillways. Scenario IIIb with full reservoirs (Figure 4.9c) show neither turbine operations of Grimsel 1 HPP nor flow derivation during flood peak, but high release of water by the Grimsel spillways. This leads to an overflow of Lake Räterichsboden and full turbine operation during midnight of the 23rd of August. Due to the lack of retention volumes downstream, the peak discharge of 443 m^3/s in Aareschlucht is high. In scenario IVa with nearly full reservoirs (Figure 4.9d), the operation of the spillways is avoided due to equal in- and outflow from the upstream turbines. Nevertheless no flood routing occurs in Lake Räterichsboden, turbine operations are reduced to peak electricity prices (Figure 4.9a and b), dictated by the upper HPP's operation. A different behavior is simulated for scenario IVc and IVd (Figure 4.9e and f) with long turbine sequences due to preventive emptying of the reservoir. During flood peak, upstream turbine operation remains active and even water from Mattenalp reservoir is supplied. Turbine operations by Handeck 2 and 3 HPPs are stopped and thus reduce the downstream peak in the Aare River.

The comparison between scenario V without the hydropower scheme and the worst case scenario IIIa with full reservoirs reveals that the hydropower scheme reduces the peak flow of the 2005 flood event at Aareschlucht by 25%, from 475 m^3/s to 350 m^3/s. An increase of peak flow can be observed, not only in the main valley but also in the Gadmerwasser River catchment (Table 4.3). Because of the non-existence of intakes and reservoirs, the peak flow of Gadmerwasser River in Innertkirchen increases by about 20% without HPP.

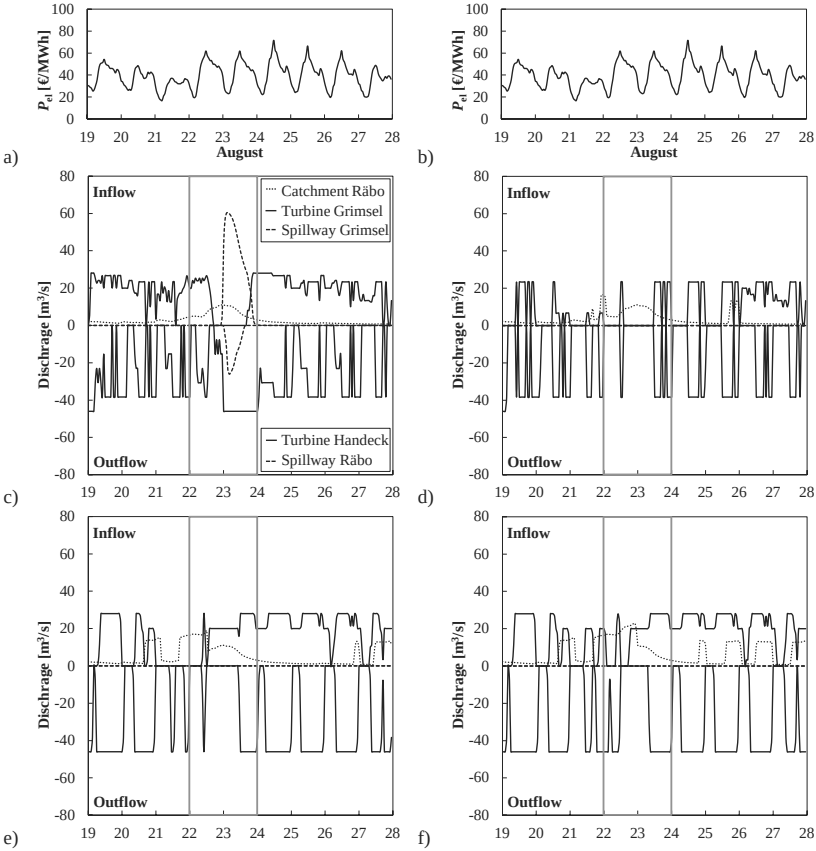

Figure 4.9. Electricity price EEX P_{el} during simulation period in August 2005 (a, b), inflow and outflow at Lake Räterichsboden during 2005 flood event with peak period in the grey box for scenario IIIb (c), IVa (d), IVc (e) IVe (f). Only scenario IIIb shows spillway operations for Grimsel and Räterichsboden.

4.5 Discussion

The chosen approach is a simple and coherent way to analyze the capacity of a complex HPP on flood reduction. Several aspects have to be discussed:

Simulation of runoff

If runoff has to be defined in catchment areas, where measured data is only available at some control points, a hydrological model is required. Deterministic models can be empirically, conceptually or physically-based, whereas the catchment area can be described as semi-distributed or distributed. The semi-distributed modeling tool *Routing System* uses a conceptual process description, taking into account the spatial variability of the meteorological and hydrological characteristics of the watershed. Small catchment areas (< 1000 km^2), like the upper Aare River basin, show short response time. The smaller the area is, the more robust a model has to be for calculating its behavior, especially during flood events. *Routing System* takes into account all relevant

hydrological processes (precipitation, evaporation, infiltration, ice and snowmelt, runoff) of an Alpine catchment for short simulation time, which would allow real-time flood prediction based on meteorological forecast in a second step.

Sources of uncertainty could come from meteorological input data (temperature and precipitation), its distribution over the catchment area as well as the initial parameter setting. Local phenomena like valley exposition and shape as well as vegetation can influence the local climate, which is not respected in the given case. The calibration process is based on runoff data provided by KWO and FOEN in addition to the peak flow estimations. The provided hourly inflow time series, available only for 2005, were provided for relatively small catchment areas. Thus, they are significantly influenced by hydropower operations and the measuring methods (reservoir level changes). The peak flows were estimated based on a post-event analysis of damage and could contain some error. Furthermore, runoff simulations are sensitive to initial soil moisture conditions. However simulated and observed data do not only show good agreement with the 2005 calibration flood event, but also with the 1987 validation one. Uncertainty due to initial conditions effects only the parameter extrapolation to catchment areas without measured data series for calibration.

Routing System has the advantage of linking the hydrological and the hydraulic environment. All hydraulic works, such as water intakes, water transfer tunnels, reservoirs with water releasing structures and power houses, are represented. Their regulation can be defined. The management of the HPP can be done by using historic data sets as well as by the autonomous operation tool OptiProd. The latter has a dynamic behavior, taking into account inflow and reservoir filling for a defined forecast time horizon. The algorithm tries to reduce peak flow in sensitive river reaches by avoiding turbine operation and spillway release during flood peak.

Filling degree

Assuming full reservoirs at the beginning of the flood, only a minor decrease of reservoir levels occurs due to normal turbine operations without preventive water release. Thus, high overflow of the four main reservoirs and the downstream located Handeck compensation basin leads to increased flood peak and volume in the Hasliaare River. Full reservoirs only influence the flow regime on the Aare River, whereas the hydrographs of the Gadmerwasser River remain unchanged.

HPP operation

Due to the inadequate turbine operations (Statistics) for scenario IIa and IIIa, overflow of Mattenalp and Handeck reservoirs occurs, increasing the discharge in the Hasliaare River. Using OptiProd with 0 h forecast horizon, the peak flow of scenario III (Full reservoirs) could be slightly lowered. OptiProd generates higher volumes due to higher flow release in the post-peak period, sometimes even with respect to advantageous electricity prices. Even with a forecast horizon of 0 h, the flood peak can be reduced. With a 24 h forecast horizon, post-flood turbine operations can create a sufficient retention volume avoiding turbine operations during the peak. A longer forecast time has only a minor influence, but can still reduce the flood peak. Thus, not only the presence of retention volume is important but it is also an appropriate management of the reservoirs and HPPs.

Presence of HPP

The scenario without the hydropower scheme increases the peak flow not only in the Aare River valley but also in the Gadmerwasser River catchment because of the missing river water intakes and storage basins. In fact, the presence of the HPP with active and passive retention has a high impact on the river discharge. This normally leads to a reduction of the peak flow. Inappropriate or emergency flow release in an unsuitable moment could even increase the river discharge.

4.6 Conclusion

To evaluate the flood reduction effect of the Oberhasli HPP, the semi-distributed modeling tool *Routing System*, containing a simple but robust hydrological approach as well as an autonomous HPP operation tool, was applied. During the calibration and validation processes, the 1987 and 2005 flood events could be accurately simulated. Inflow to the reservoirs, hydrographs at the river basin outlet as well as several estimated peak flows allowed an assessment of the simulation performance. Besides the hydrological elements, the operation of the complex hydropower scheme could also be correctly simulated.

Four scenarios with different initial filling degrees of the reservoirs were simulated for different HPP operation modes and compared to the non-operated catchment area (without HPP). Storage volume due to preventive release allows a flood peak reduction downstream. For the catchment without HPP, a peak flow of 650 m^3/s would have occurred in 2005, which is about 25% higher than the observed discharge of 520 m^3/s. Even the unrealistic scenario of full reservoirs reveals the passive retention effect of reservoirs of the Oberhasli hydropower scheme.

If initial reservoir levels are high, peak flow can only be reduced actively by an appropriate management of the HPP by using flow forecast. As simulated for the 2005 flood, with a prediction horizon of 24 h the peak flow can be reduced from 562 $m^3/$ to 511 m^3/s. Higher performance is achieved by using not only the turbines but also the bottom outlets of the dams for preventive operations to provide more retention volume in the reservoirs during peak flow. Similar simulations have been done for the extended scheme of KWO and published in Bieri *et al.* (2011).

The *Routing System* approach is an appropriate tool for multi-objective evaluation of runoff at multiple locations in operated catchment areas. The event-based calibration of the hydrological model allows the re-simulation of runoff in all the sub-catchments of the river basin. The hydraulic works are implemented and their operation optimized, taking into account flood reduction as well as economic issues. The close link between hydrological and hydraulic elements in the conceptual semi-distributed environment is promising for real-time as well as extreme events simulation in high-mountainous areas. An active flood management would require a decision-making strategy, including threshold values and constraints (legal and economic) for preventive measures. The developed modeling approach proves the potential of passive and active flood retention of storage hydropower schemes.

5

Semi-distributed conceptual modeling of effects of climate change on future runoff in glacierized Alpine catchment areas

This chapter presents the impact of climate change on runoff in Alpine catchment areas, shown for the case study area of the upper Aare River catchment in Switzerland with its large glaciers. Future runoff was assessed for the period between 2010 and 2099 using a semi-distributed conceptual hydrological model. Glacier mass balance and runoff were computed in hourly time steps for precipitation and temperature distributions. Changes in glacier volume for the elevation bands as well as runoff were simulated. The model was calibrated using ice volume changes between 1980 and 1993 as well as daily runoff at five gauging stations in the catchment area from 1980 to 2008. The scenarios for future climatic conditions up to 2099 were developed from historical temperature and precipitation data series. Annual runoff from the glacierized basins shows an initial short increase which is due to the release of melting water from glacial storage. After about two decades, depending on glacier behavior and the applied climate change scenario, runoff stabilizes and then drops below today's level because of reduced glacier size and increased evaporation. For all scenarios except one with an average temperature decrease of -2°C, the glaciers shrink. In a warmer atmosphere, runoff is increased during spring and early summer, whereas in July and August lower runoff is produced. Significant decrease of runoff related to glacier melt must be considered for future hydropower management.

5.1 Introduction

Alpine catchments are highly sensitive to climate change due to glacier shrinkage (Watson and Haeberli, 2004; UNEP, 2007). Every year 2 to 3% of the glacier volume in the European Alps is disappearing (Haeberli *et al.*, 2007). Estimations predict a reduction of the ice-covered areas by 75% already during the coming decades (Zemp *et al.*, 2006; OcCC, 2007). A change in the hydrological regime of the Alpine rivers is therefore expected (Huss, 2011). As the glaciers are readjusting to the rising temperature, higher discharges occur during the summer for a limited number of years depending on glacier size, hypsography and catchment characteristics until the glaciers either find a new equilibrium state or completely disappear. Runoff will then decrease, whereas peak flow would be shifted from summer to early summer or spring (Braun *et al.*, 2000). The annual runoff hydrograph changes from ice melt dominated (glacial) to snowmelt dominated (nival) (Horton *et al.*, 2006). In these regions, the changing hydrological regime will cause a high impact on irrigation, water supply, flood management as well as hydropower production.

More than 40% of European hydroelectric power is produced in Alpine countries (Schleiss, 2002). High-head storage hydropower plants (HPP) contribute significantly to peak energy production as well as grid regulation in central Europe. Switzerland supplies about 20% of the total Alpine hydroelectric production. Reservoirs at high altitude can store rainfall as well as snow and glacier melt during summer in order to cover energy demand in winter. The melt water runoff from the glaciers is a significant contribution to the filling of the reservoirs. These specific water resources might diminish or even run dry in partly ice-covered watersheds. An assessment of the impact of climate change and glacier retreat on runoff by hydrological modeling is needed for a sustainable use of hydropower in future.

Several modeling approaches for runoff simulation in high-mountainous catchment areas with high glacierization exist (Bergström, 1995; Schaefli *et al.*, 2005; Huss *et al.*, 2008b). As discussed in Huss *et al.* (2008b), these models simulate quite well the real hydrology, even when glaciers are assumed to remain constant in surface over time. A wide range of different modeling approaches take into account stepwise adaptation of glacial area (Schaefli *et al.*, 2007; Stähli *et al.*, 2011), combined models of glacier mass balance and ice dynamics for individual glaciers (Oerlemans and Fortuin, 1992; Schneeberger *et al.*, 2003), coupled mass balance and ice flow models (Flowers *et al.*, 2005; Huss *et al.*, 2007) as well as annual adaptation of the 3D glacier surface topography (Huss *et al.*, 2008b). These models need either high computation capacities or large input datasets and can therefore only be applied to small areas.

Routing System applies a semi-distributed conceptual approach and allows interconnecting hydrological and hydraulic elements (García Hernández *et al.*, 2007). Thus, this tool is currently applied in the field of flood as well as hydropower management in the Alps (Jordan, 2007; Bieri *et al.*, 2010; Bieri *et al.*, 2011; García Hernández, 2011). It is based on the GSM-SOCONT (Glacier Snow Melt SOil CONTribution) approach in order to simulate runoff using hourly or daily temperature and precipitation data as input (Schaefli *et al.*, 2005). To extend its applicability to climate change issues, the glacier simulation tool is improved by dynamic glacier

volume evolution. The present study focuses more on reliable prediction of long-term runoff than precise simulation of glacier behavior (Jouvet *et al.*, 2011).

Glacier thickness is estimated by using an inverse ice flow law together with a shallow ice approximation (Haeberli and Hoelzle, 1995; Linsbauer *et al.*, 2009). Inflow hydrographs for an Alpine catchment area containing a complex hydropower scheme are presented for the on-going century, taking into account four climate scenarios. Challenges for water resources management are discussed.

5.2 Case study and data

The study site is the upper Aare River catchment upstream Lake Brienz in Switzerland (Figure 5.1). The surface of the upper Aare River basin, located between 564 m a.s.l. (Lake Brienz) and 4274 m a.s.l. (Finsteraarhorn), has an area of 554 km^2. Six main glaciers as well as several ice patches lie within the study area (Table 5.1). At the end of the 19th century, hydropower development started in the Oberhasli area. The first dams were built by the Kraftwerke Oberhasli AG (KWO) hydropower company between 1925 and 1932. Since then, a complex scheme with nine hydropower plants (HPP) and several reservoirs has been developed. The largest reservoirs are Lake Grimsel ($94 \cdot 10^6$ m^3), Oberaar ($57 \cdot 10^6$ m^3), Räterichsboden ($25 \cdot 10^6$ m^3) and Gelmer ($13 \cdot 10^6$ m^3). These reservoirs are fed by several water intakes collecting the water in side valleys. The western part of the catchment is drained by the Mattenalp intake, which releases the water to Lake Räterichsboden. The water from the eastern part is collected by the Trift intake and can be pumped to Lake Räterichsboden as well.

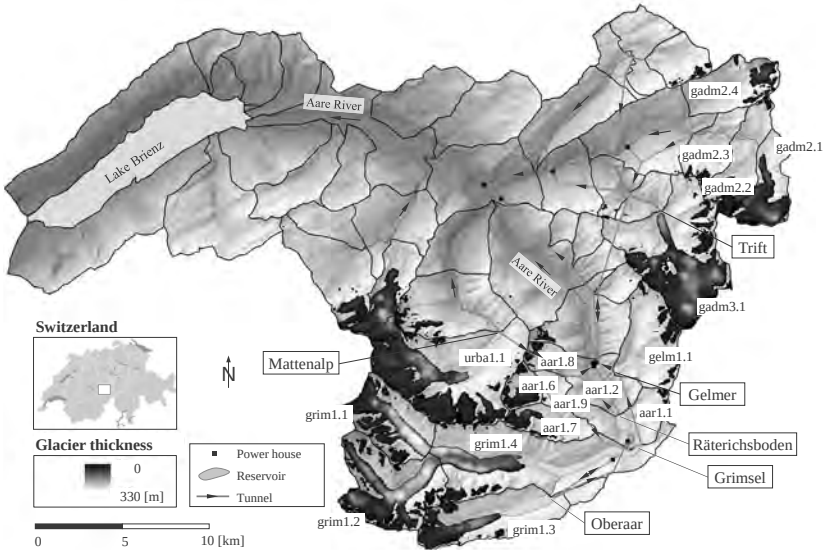

Figure 5.1. Location and overview map of the upper Aare River catchment with the Oberhasli hydropower scheme (KWO) and the glacier extensions in 1993. The sub-catchments of highest relevance for hydropower generation are indicated as well as the four main reservoirs (Oberaar, Grimsel, Räterichsboden, Gelmer) and two water intakes (Mattenalp, Trift).

Table 5.1. Characteristics of the investigated catchment areas with the six main glaciers (bold) for October 1980. Unteraar Glacier and its two tributaries Lauteraar and Finsteraar form one glacier.

Catchment	Sub-catchments	Total surface area [km^2]	Glacier name	Glacieri-zation 1980 [%]	Ice volume 1980 [10^6 m^3 w.e.]	Elevation bands [m a.s.l.]
Oberaar	grim1.3	19.2	**Oberaar**	36	301	2250-3750
Grimsel	aar01.6	4.3	Gruben	58	121	2100-3300
	aar01.7	7.7	Bächli	34	101	2100-3300
	grim1.1	15.5	**Lauteraar**	69	727	2250-4050
	grim1.2	21.9	**Finsteraar**	71	1‘000	2250-4200
	grim1.4	38.2	**Unteraar**	28	867	1800-3300
	grim1.5	2.0	-	0	0	2400-2700
Räterichsboden/ Mattenalp	aar01.1	10.3	Gärsten	5	10	2700-3300
	aar01.8	3.2	Ärlen	28	25	2400-3300
	aar01.9	2.8	-	8	4	2100-3000
	urba1.1	36.5	**Gauli**	54	825	2100-3750
Gelmer	gelm1.1	15.8	Gelmer/Alpli/ Diechter	25	103	2400-3600
Trift	gadm2.1	10.5	**Stein**	58	312	1800-3600
	gadm2.2	12.2	**Steilimi**	26	78	1950-3300
	gadm2.3	8.9	Taleggli/Gigli	8	12	2100-3000
	gadm2.4	12.8	Obertal	22	144	2100-3000
	gadm3.1	33.4	**Trift**	56	1'017	1650-3600
	gadm3.3	5.7	Tobiger	2	2	1800-2400

Simulations for the whole upper Aare River catchment were performed. For this study, only the results of the upper part are presented in Table 5.1. Lake Oberaar at 2303 m a.s.l. is the highest reservoir in the scheme and is fed by melt water from the Oberaar Glacier, a glacier with eastern aspect, which has shrunk by 1.6 km since 1930. The also east-exposed Unteraar Glacier above Lake Grimsel is with its 13 km length the fourth largest glacier in the Swiss Alps. It has two main tributaries, Lauteraar and Finsteraar Glaciers. In the western part of the catchment area, Gauli Glacier is located in the Urbach valley upstream of the Mattenalp intake. Due to substantial retreat in recent years, two main lakes appeared in the glacier forefield. A lake was also formed in the eastern drainage basin downstream of the fastly shrinking Trift and Stein Glaciers (Frey *et al.*, 2010). These glaciers as well as the Steilimi Glacier are steep, north-exposed mountain glaciers, located in the overall catchment of the Trift intake.

For the model set-up several data series were available for this study: (1) Climate data; (2) Discharge measurements; (3) Digital elevation model (DEM) and topographic maps for glacier surface area and thickness; (4) Ice thickness changes for Oberaar and Unteraar Glaciers. Homogenized time series of temperature and precipitation from 1980 to 2010 are provided by the Federal Office of Meteorology and Climatology (MeteoSwiss). On the one hand, temperature and precipitation data are collected every ten minutes by an automatic monitoring network (ANETZ) all over Switzerland. On the other hand, the daily precipitation is measured by a large number of gauging stations (NIME). For this study, the daily precipitation from NIME is split into hourly data, based on the closest ANETZ station. Five weather stations of the first type and nine of

the second are located in and close (< 20 km) to the upper Aare River catchment and are therefore taken into account for the model calibration. For the spatial distribution of the meteorological variables the method of Shepard (1968) is applied. Precipitation *P* and temperature *T* for a given elevation band are obtained by weighting the data of the weather stations *P** and *T** in the influence zone, defined by its search radius *R* of 20 km, according to their inverse square distance to the gravity center of the band. Evapotranspiration PET is computed by Turc (1961) at hourly time steps and thus mainly depend on temperature. As precipitation and temperature distribution in high-mountainous areas is complex and simple extrapolation is not adequate (Huss *et al.*, 2008a), the method has been extended to take into account the effect of altitude by constant altitudinal lapse rates $grad_P$ and $grad_T$ for precipitation and temperature, respectively. Time series in hourly resolution for each elevation band are obtained.

KWO made accessible historical exploitation data from 1980 to 2008. Daily sums of turbine and pump volumes as well as the water levels in the four main reservoirs are available. These datasets allow calculation of the inflow to the four main reservoirs Oberaar, Grimsel, Gelmer and Räterichsboden (including Mattenalp intake) as well as to the Trift intake. Due to the large volume of the reservoirs, small changes in level lead to big changes in volume. Thus, short-term (daily) balance can be biased due to HPP operation, which is not the case for long term balance.

The spatial discretization of the catchment area is carried out based on a DEM with a grid size of 25 m (Swisstopo). GIS-based analysis of topographic maps allows defining the ice thickness and surface changes between 1980 and 1993 and therefore the average annual ice thickness change over this period.

To estimate the initial ice volume, the glacier bed topography is computed using the inverse ice flow law together with a shallow ice approximation (Haeberli and Hoelzle, 1995; Linsbauer *et al.*, 2009) as discussed in Terrier *et al.* (2011). Since the basic parameter influencing ice thickness is the surface slope, the method explores the variability of glacier thickness for glacier parts with variable surface inclination in a spatially explicit way. Subtracting the ice thickness grid of 1993 from the input DEM gives the glacier bed topography.

The Oberaar as well as Unteraar Glaciers were monitored during the last 30 years focusing amongst other parameters on glaciers and their bed geometries, mass balance and surface dynamics (Huss *et al.*, 2007). Since the early 20^{th} century, surface elevation and velocities at 4 and 13 profiles have been annually measured. After 1990, aerial photographs and photogrammetric analysis recorded by *Flotron AG* allowed the computation of DEMs (VAW-ETHZ, 1980-2009; Farinotti *et al.*, 2009). All available data is used to define the average glacier thickness changes for the glacier model calibration period between 1980 and 1993.

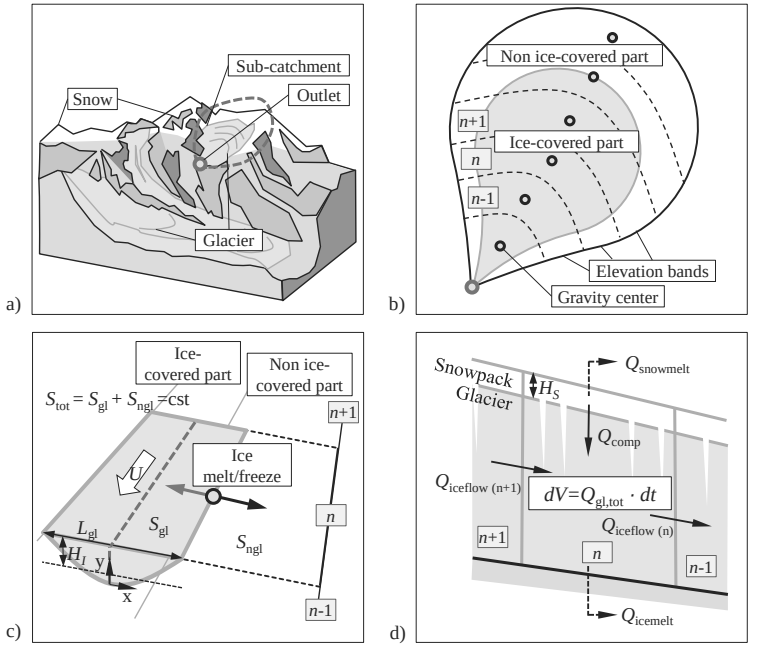

Figure 5.2. Model discretization and modeling approach: (a) Sketch of a high-mountainous catchment area containing glacier and snow; (b) Partly ice-covered sub-catchment area with subdivision in elevation bands; (c) Elevation band *n* containing glaciers with their main parameters; (d) Mass balance of a glacierized elevation band *n*; where U = glacier flow velocity [m/yr]; L_{gl} = glacier width [m]; H_I = mean ice thickness [m e.w.]; S_{gl} = surface area of glacier [m^2]; S_{ngl} = non ice-covered surface area [m^2]; S_{tot} = total surface area of elevation band [m^2]; H_S = snow height [m]; $Q_{snowmelt}$ = snowmelt [m^3/s]; $Q_{icemelt}$ = glacier melt [m^3 e.w./s]; $Q_{iceflow}$ = downstream glacier flow to next elevation band [m^3 e.w./s]; Q_{comp} = snow-to-ice transformation [m^3 e.w./s]; $Q_{gl,tot}$ = sum of glacier flows [m^3 e.w./s]; dV = glacier mass balance [m^3 e.w.] and dt = time step [s].

5.3 Methods

5.3.1 Model build-up and ice thickness

The spatial discretization of the whole upper Aare River catchment is based on a DEM with a grid size of 25 m, distinguishing glacier and non ice-covered parts at the stage of October 1980 (Figure 5.2a). The modeling approach has two levels of discretization for each defined sub-catchment. The first distinguishes between ice-covered and non ice-covered parts. The second level divides the sub-catchment into elevation bands with a homogenous hydrological behavior (Figure 5.2b), containing a non ice-covered part defined by its surface area S_{ngl}, and if present the glacierized one (Figure 5.2c). The latter is defined by its surface area S_{gl}, its width L_{gl} and the valley shape parameter *ns*. The *ns* parameter in equation $y = \alpha \cdot x^{ns}$ describes the cross-section of the glacier bed topography for every elevation band and is derived from the ice thickness grid. Values between 0.4 and 3 are achieved. The front band is semi-cone shaped. For the gravity center of the elevation band, weather data from the climatic data stations is extrapolated as mentioned in Chapter 5.2. The five main ice-covered drainage basins are divided into

elevation bands of 150 m, whereas the rest is divided into bands of 300 m. In the model, all discharges and volumes are given in water equivalent (e.w.). Thus, a correction factor of 0.9 is applied to the measured ice volumes.

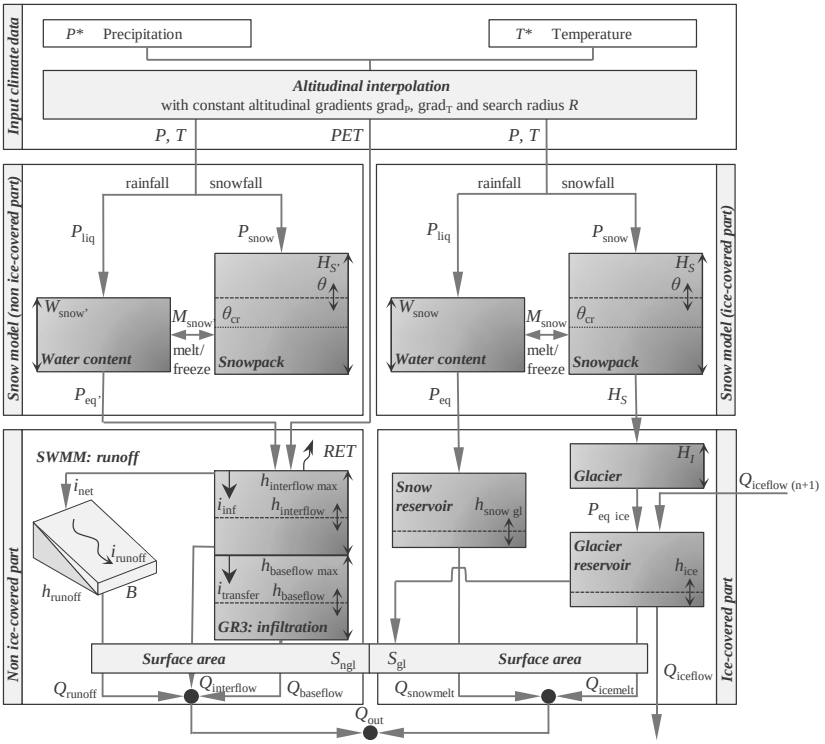

Figure 5.3. Hydrological model of *Routing System* for a partly glacierized elevation band. Abbreviations are explained in the text.

5.3.2 Hydrological model

The model contains elements for snowpack, glacier, soil infiltration and surface runoff. Except the new mass conservation glacier module, the hydrological processes are described in García Hernández *et al.* (2007) and thus not explained in detail.

In the *non ice-covered part* of the elevation band (Figure 5.3 on the left), three modules – snow, infiltration and runoff – are used. The snow model simulates the evolution of snowpack (melt and accumulation) according to temperature T and precipitation P and defines an equivalent precipitation P_{eq}. The latter and the potential evapotranspiration PET are used as input for the soil infiltration model GR3 (Edijatno and Michel, 1989; Consuegra *et al.*, 1998). The incoming precipitation or snowmelt is separated by GR3 into interflow $Q_{interflow}$, base flow $Q_{baseflow}$ and non-infiltrated flow i_{net}. This net intensity is transferred to the surface runoff model SWMM (Metcalf, 1971) where it is routed (Q_{runoff}). The total outflow is the sum of two infiltration components

$Q_{\text{interflow}}$ and Q_{baseflow} and surface runoff Q_{runoff}, taking into account the corresponding non ice-covered surface area S_{ngl}.

The *ice-covered part* of the elevation band (Figure 5.3 on the right) is composed of two elements, namely snow and glacier. The snow model is the same as in the non ice-covered part, thus providing an equivalent precipitation P_{eq}, which is transferred into the glacier model. In the glacier model, P_{eq} interacts in the linear snow reservoir, where snowmelt Q_{snowmelt} results. Moreover, the glacier melts according to a degree-day relationship when H_S is equal to zero. This glacier flow $P_{\text{eq ice}}$ enters the linear glacier reservoir and ice melt Q_{icemelt} results at the outlet of the elevation band. The sum of Q_{snowmelt} and Q_{icemelt} with respect to the surface area S_{gl} is the total outflow of the ice-covered band.

Glacier change

The purpose of the glacier model (Figure 5.2d) is to simulate the glacier mass balance and the discharge at its outlet over a long period. In a semi-distributed conceptual model with the applied discretization, glacier evolution in terms of surface area and height changes in time cannot be precisely simulated, but its general dynamics as well as the runoff are well described. In *Routing System*, the total discharge from the ice-covered part of the elevation band depends on the storage processes in the two linear reservoirs for snow and ice. The outflow from the linear snow reservoir Q_{snowmelt} [m^3/s] depends on the snow level in the linear reservoir $h_{\text{snow gl}}$ [m] as well as the linear snow reservoir coefficient $k_{\text{snow gl}}$ [1/s]:

$$dh_{\text{snow gl}} / dt = P_{\text{eq}} - k_{\text{snow gl}} \cdot h_{\text{snow gl}} \tag{5.1}$$

$$Q_{\text{snowmelt}} = k_{\text{snow gl}} \cdot h_{\text{snow gl}} \cdot S_{\text{gl}} \tag{5.2}$$

Formation of glacial ice is a complex physical process including packing, thermodynamics and deformation under load and shows exponential behavior (Paterson, 1994). In this simplified case, snow-to-ice transformation Q_{comp} [m^3 e.w./s] only depends on the transformation factor a_{comp} [1/s]. It only takes place when snow is present on the glacier ($H_S > 0$):

$$Q_{\text{comp}} = a_{\text{comp}} \cdot H_S \cdot S_{\text{gl}} \tag{5.3}$$

Ice flow Q_{iceflow} [m^3 e.w./s] from an elevation band (n) to its downstream neighbor (n-1) takes into account the glacier flow velocity U as well as the mean ice thickness H_I [m e.w.] and the width L_{gl} [m] of both bands:

$$Q_{\text{iceflow}} = U \cdot \frac{H_{I\,(n)} + H_{I\,(n\text{-}1)}}{2} \cdot \frac{L_{\text{gl}\,(n)} + L_{\text{gl}\,(n\text{-}1)}}{2} \tag{5.4}$$

Glacier melt Q_{icemelt} [m^3 e.w./s] depends on the degree-day factor for ice melt a_{ice} [m/°C s], the linear glacier reservoir coefficient k_{ice} [s], the level of the linear glacier reservoir h_{ice} [m e.w.] and the temperature T [°C]. This only happens when no snow is present on the glacier ($H_S = 0$) and when the temperature is higher than the threshold melt temperature T_{cr}:

$$P_{\text{eq ice}} = \begin{cases} 0 & \mid T \le T_{\text{cr}} \text{ or } \quad H_S > 0 \\ a_{\text{ice}} \cdot (T - T_{\text{cr}}) & \mid T > T_{\text{cr}} \text{ and } H_S = 0 \end{cases} \tag{5.5}$$

$$dh_{\text{ice}} / dt = P_{\text{eq ice}} - k_{\text{ice}} \cdot h_{\text{ice}} \tag{5.6}$$

$$Q_{\text{icemelt}} = k_{\text{ice}} \cdot h_{\text{ice}} \cdot S_{\text{gl}} \tag{5.7}$$

Glacier volume change dV [m^3 e.w.] for an elevation band (*n*) is added to the present ice volume for each time step *dt*:

$$dV_{(n)} = Q_{\text{gl,tot}\,(n)} \cdot dt = (Q_{\text{comp}\,(n)} + Q_{\text{iceflow}\,(n+1)} - Q_{\text{iceflow}\,(n)} - Q_{\text{icemelt}\,(n)}) \cdot dt \tag{5.8}$$

One part of it is transformed to glacier thickness, the other to the glacier surface area S_{gl} [m^2], corresponding to the valley shape. Because the total area of an elevation band S_{tot} [m^2] remains constant, loss or gain in the ice-covered surface has to be compensated by the non ice-covered surface area S_{ngl} [m^2]. The surface area changes linearly influence the soil infiltration model GR3 as well as the surface runoff model SWMM. The glacier surface area is therefore updated every time step Δt, which is 1 h in this study.

Model calibration

The calibration is achieved for each of the five catchments individually. *Routing System* undertakes a stepwise procedure focusing on parameter groups. They are calibrated using (1) daily runoff measurements at the outlet of each catchment (1980-2008), (2) detailed glacier volume changes from *Flotron AG* for Oberaar and Unteraar Glaciers (1980-1993) and (3) mean annual ice thickness changes from topographic maps (1980-1993).

The simulations start the 1st of October 1980, at the beginning of the hydrological year of 1981, in order to obtain parameters independent from the initial conditions. The results are compared to the observed inflow in terms of the Nash and Sutcliffe efficiency criterion NSE (Nash and Sutcliffe, 1970) in addition to water volume ratio r_{vol}:

$$\text{NSE} = 1 - \frac{\sum_{t=1}^{n} (Q_{\text{obs}\,t} - Q_{\text{sim}\,t})^2}{\sum_{t=1}^{n} (Q_{\text{obs}\,t} - \overline{Q_{\text{obs}}})^2} \qquad (-\infty < R^2 < 1) \tag{5.9}$$

$$r_{\text{vol}} = \frac{V_{\text{sim}}}{V_{\text{obs}}} = \frac{\sum_{t=1}^{n} (Q_{\text{sim}\,t} \cdot \Delta t)}{\sum_{t=1}^{n} (Q_{\text{obs}\,t} \cdot \Delta t)} \tag{5.10}$$

where $Q_{\text{obs}\,t}$ = observed hourly discharge; $Q_{\text{sim}\,t}$ = simulated hourly discharge; $\overline{Q_{\text{obs}}}$ = mean observed discharge; V_{sim} = simulated volume; V_{obs} = observed volume; T_{per} = time period observed volume and Δt = time step.

The model has several parameters to be calibrated (Table 5.2). Some of them are kept constant for the whole Aare River catchment. The two threshold temperatures T_{cp1} and T_{cp2}, defining whether precipitation is liquid, solid or mixed, depend on the location and can vary throughout the year (Rohrer *et al.*, 1994). For most stations in the Alps they lie between 0°C and 2°C (Schaefli *et al.*, 2005). Schaefli *et al.* (2005) mention, that the threshold temperature for snowmelt T_{cr} should be reconsidered with a different spatial and altitudinal discretization or for different modeling purposes (e.g., flood events). Because of the topographic as well as topologic conditions of the present study, simulation of long-time behavior allows setting of T_{cr} to 0°C. The other constant parameters are chosen as shown in Table 5.2. The altitudinal precipitation lapse rate $grad_P$ and the degree-day factor of ice melt a_{ice} are important calibration parameters which are constant for a given sub-catchment. The degree-day factor for snow melt a_{snow} and the glacier flow velocity U have to be adapted for every elevation band. U is a key parameter regulating the mass balance between the bands. Ice flow from the upper part, where new ice is formed by snow accumulation, to the glacier tongue, where glacier melt is highest ($U = 0$), has to be guaranteed without discontinuities in the intermediate bands. a_{snow} mainly influences the streamflow from February to June and is therefore first calibrated. a_{ice} as well as the linear snow and ice reservoir coefficients k_{snow} and k_{ice} influence summer runoff, when snow melts in the ice-covered elevation bands. To take into account infiltration of snowmelt and rainfall, the maximum storage height $h_{interflow\ max}$ and the release coefficient $k_{interflow}$ of the interflow reservoir are calibrated. In high-mountainous areas, base flow can be neglected and thus no calibration is needed. $a_{interflow}$ was set to 1.

Table 5.2. Parameters of hydrological model of *Routing System* with corresponding symbols, values and units applied for the upper Aare catchment simulations.

Module	Description	Symbol	Value	Units
Local climate data	Data search radius	R	20	[km]
	Altitudinal precipitation lapse rate	$grad_P$	$*^1$	[mm/1000 m]
	Altitudinal temperature lapse rate	$grad_T$	-5.4	[°C/1000 m]
Snow	Degree-day factor for snowmelt	a_{snow}	$*^2$	[m/°C s]
	Snow-ice transformation factor	a_{comp}	4	[1/s]
	Critical relative water content in the snowpack	θ_{cr}	$*^1$	[-]
	Low rain-snow threshold temperature	T_{cp1}	0	[°C]
	High rain-snow threshold temperature	T_{cp2}	2	[°C]
	Threshold melt temperature	T_{cr}	0	[°C]
	Melt coefficient due to rain	b_p	$1.08 \cdot 10^6$	[s/m]
Ice	Degree-day factor for ice melt	a_{ice}	$*^1$	[m/°C s]
	Glacier flow velocity	U	$*^2$	[m/s]
	Linear snow reservoir coefficient	k_{snow}	$*^1$	[1/s]
	Linear ice reservoir coefficient	k_{ice}	$*^1$	[1/s]
GR3	Maximum storage height of interflow reservoir	$h_{interflow\ max}$	$*^1$	[m]
	Release coefficient of the interflow reservoir	$k_{interflow}$	$*^1$	[1/s]
	Release factor of the interflow reservoir	$a_{interflow}$	1	[-]
SWMM	Strickler coefficient	K	$*^1$	[$m^{1/3}$/s]

$*^1$ to be defined for every sub-catchment; $*^2$ to be defined for every elevation band in the sub-catchment

The calibration over the time period between 1981 and 1993 shows good agreement between measured and simulated runoff (Table 5.3), especially in terms of volume. The lack of precise calibration data induces lower efficiency NSE. In particular, reservoirs with relatively low inflow compared to the turbine and pump capacities of the HPPs show lower agreement for the calibration and validation period. Lake Oberaar with an average inflow up to 7 m^3/s is heavily influenced by the Grimsel 2 pumped-storage plant ($Q_{turbine}$ = 96 m^3/s; Q_{pump} = 80 m^3/s), as well as Lake Gelmer with inflows up to 4.5 m^3/s containing a turbine outflow at Handeck 1 HPP ($Q_{turbine}$ = 20 m^3/s). Validation from 1993 to 2008 confirms the robustness of the model and reveals similar performance. Increasing pumped storage activities in Lake Oberaar affects again the results of the corresponding catchment area. It can be concluded that runoff is correctly simulated.

Table 5.3. Calibration (01.10.1981-01.10.1993) and validation (01.10.1993-01.10.2008) of the model: comparison of measured and simulated daily runoff of the catchments in terms of Nash and Sutcliffe efficiency criterion NSE [-] as well as water volume ratio r_{vol} [-].

Catchment	Calibration		Validation	
	NSE [-]	r_{vol} [-]	NSE [-]	r_{vol} [-]
Oberaar	0.72	0.98	0.66	0.85
Grimsel	0.88	1.02	0.82	1.03
Räterichsboden/Mattenalp	0.80	1.04	0.76	1.03
Gelmer	0.74	0.97	0.68	1.09
Trift	0.86	1.08	0.88	1.08

Though the calibration period for the glaciers is only 13 years, similar mass balances are reproduced as shown in Figure 5.4 for the average annual ice thickness changes for the Oberaar (Oberaar Glacier), Unteraar (Unteraar/Lauteraar/Finsteraar Glaciers), Trift (Trift/Stein/Steinlimi Glaciers) and Räterichsboden/Mattenalp (Gauli Glacier) catchments. The measured data from the Swisstopo maps shows an inhomogeneous ice thickness distribution within an elevation band, which cannot be reproduced by a semi-distributed modeling approach. Nevertheless, good agreement is obtained between the elevation bands of the Oberaar and Unteraar Galciers and the *Flotron AG* data (Figure 5.4a) (Paul and Haeberli, 2008). The shrinkage of the Trift Glacier is most difficult to calculate (Figure 5.4b). The melt of the glacier tongue of about 1.5 m/yr is slightly overestimated. Stein and Steinlimi Glaciers are well reproduced in the lower elevation bands compared to the overestimated melt in the higher bands. Gauli Glacier with its great retreat up to 2.5 m/yr of the lower zones is somewhat overestimated (Figure 5.4c).

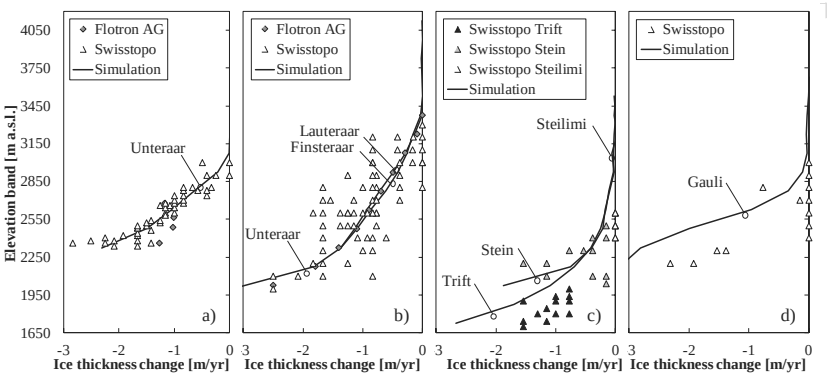

Figure 5.4. Comparison of simulated average annual ice thickness changes [m/yr] for the calibration period (01.10.1981-01.10.1993) to measured values of Swisstopo (1980-1993) and Flotron AG (1980-1993) for the Oberaar (a), Unteraar (b), Trift/Stein/Steilimi (c) and Gauli Glaciers (d).

Climate scenarios

Five different climate scenarios are considered. The first one is built using the developments of the Centre for Climate Systems Modeling (C2SM) of the Swiss Federal Institute of Technology Zurich (ETHZ) in the framework of the ENSEMBLES project. Regional Climate Models (RCM) with a 25 to 50 km resolution (Van der Linden and Mitchell, 2009) were driven by Global Circulation Models (GCM) for the A1B emission scenario (Nakicenovic and Swart, 2000). Ten different combinations were generated. In this case, the results are derived from the RCM CLM, driven by the GCM HadCM3Q0. The implemented Delta Change Method gives the difference between the reference climate period 1980-2009 and two future climate periods (Bosshard *et al.*, 2011). For every ANETZ (temperature and precipitation) and NIME (precipitation) weather station in Switzerland values have to be applied to the reference hourly time series for the temperatures and a coefficient to be multiplied for the precipitations are given for 2021-2050 and 2070-2099. Between these periods, a linear interpolation of the delta changes is applied, where for 2010-2020 the time series of 1990-2000 and for 2051-2069 the periods of 1980-1989 and 2001-2009 are used as reference. This division is based on the fact that the temperatures of the period between 1980 and 1990 are below average. A double application of this reference series for 2010-2020 and 2021-2031 would generate a very paricular behavior. The developed scenario neglects future inter- as well as intra-annual variability differing from the reference climate period. For comparison, simpler scenarios are generated using the same temperature and precipitation time series as reference. The first simple scenario, named reference (0°C), does not take into account any change and represents the climate of the past 30 years for reproduction over the next 100 years. The second -2°C, third +2°C and fourth +4°C scenarios assume a linear increase or decrease of temperature and no change in precipitation until 2099. The obtained time series for all concerned weather stations have the same resolution and a similar variability as the reference climate period.

Unfortunately the ANETZ weather station of Grimsel Hospiz is in operation only since 1989. For the time period between 1980 and 1989 the daily average of temperature and the daily sum of precipitation are available. For hourly distribution, data from neighboring meteorological stations is interpolated, taking into account the horizontal distance and elevation as well as daily values from the former weather station. As mentioned above, at the beginning of the reference climate period, low temperatures are found.

The C2SM-ETHZ scenario shows an overall increase of temperature of about +4°C by 2099. The increase of temperature compared to the reference climate period is always positive (Figure 5.5a). At the beginning of the future climate period 2021-2050, an increase of about 1.5°C is forecast, even though the reference temperatures for 1980-1990 are below average. This early temperature increase is significantly different from the scenarios with linear increase (+2°C and +4°C). A relatively steep temperature gradient results between the reference climate period and the year 2021. The annual fluctuations, only indicated for the reference scenario, vary ±1°C from the tendency curve. The intra-annual variability (Figure 5.6a) gives high increase for both future climate periods especially in summer, whereas in spring moderate increase is forecast. The increase of 2070-2099 is always higher (between 1 and 3°C) than in 2021-2050. The first future climate period has two peaks, a high one in June and July and a moderate one in December and January. For the end of the century, warming in summer and fall is predicted. Precipitation has no relevant deviation until 2099 (Figure 5.5b). However, a small decrease is predicted. The main change for the C2SM-ETHZ scenario is intra-annual. For 2021-2050 (Figure 5.6b) precipitation will slightly decrease until August, whereas a high peak up to 30% is shown in October and November. This peak is present for 2070-2099. However a second maximum of an increase of about 20% is predicted in May and June. Less precipitation is expected between July and September. The mean annual precipitation ratio is for both periods close to one, thus rain quantity does not change a lot.

The -2°C, +2°C and +4°C scenarios are used for highlighting the impact of temperature only. Intra-annual variability of the temperature and precipitation is the same as for the reference climate period. Due to the application of the low reference temperatures at the beginning of the reference climate period (1980-1990 is the reference for 2021-2031), the scenarios start with decreasing values. Thus, the reference climate scenario (0°C) as well as the -2°C, +2°C and +4°C scenarios have three significant cold periods (Figure 5.5a).

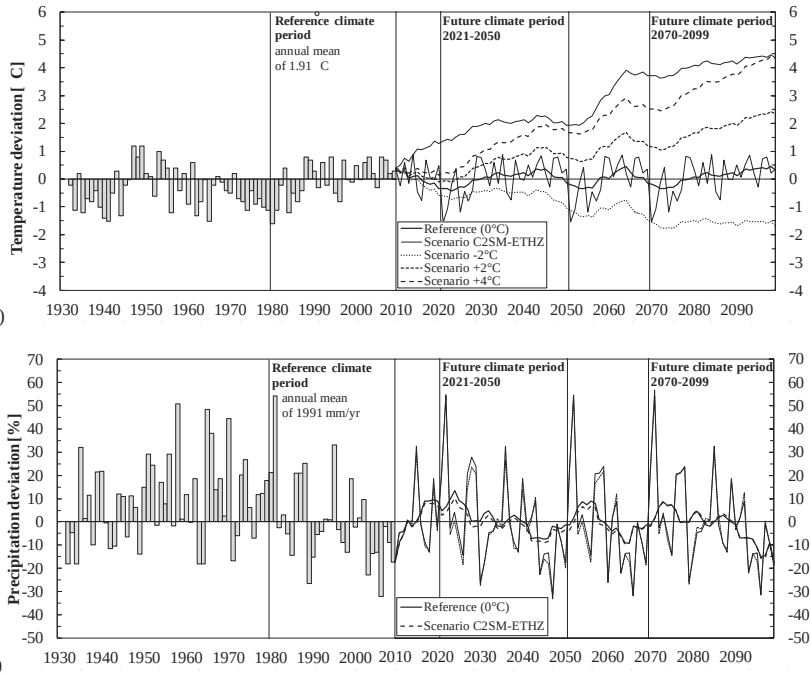

Figure 5.5. Deviation of the historic and forecasted data from the 1980-2009 reference climate period for the ANETZ weather station Grimsel Hospiz: (a) Temperature (Tendency curves of average over 11 values for scenarios; same annual inter-annual fluctuations as scenario 0°C); (b) Precipitation (Tendency curves of average over 11 values for scenarios; scenarios 0°C, -2°C, +2°C, +4°C same future precipitation).

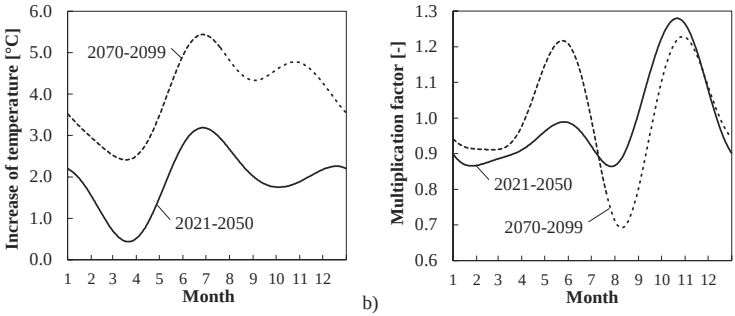

Figure 5.6. Intra-annual climate change values for the C2SM-ETHZ scenario: (a) Increase of temperature; (b) Multiplication factor for precipitation.

Modeling approach

After re-simulation of the period between 1981 and 2009, a simulation with hourly time step is run for each of the five scenarios from 2010 to 2099. Temperature, precipitation, snowfall, snowmelt, ice melt, glacier volume, evaporation, infiltration as well as runoff are updated hourly. Data analysis of all elements in the catchment areas is done with daily mean values for the total simulation period. The simulation could be repeated for other climate scenarios and sensitivity analysis could be performed. For this study, only simple scenarios are selected to evaluate the performance of the model in predicting future runoff.

5.4 Results

The results for the simulation period between 2010 and 2099 are presented for the five catchment areas (Table 5.1) and the five selected scenarios. Future hydrological values are compared to the reference climate period between 1981 and 2009. Due to the high number of data, some results are only presented for selected catchment areas.

The behavior of glaciers is shown for the Unteraar (Lauteraar/Finsteraar/ Unteraar), Gauli and Trift Glaciers. Figure 5.7a shows a past retreat of about 25% of the three glaciers. Glacier melt for the three catchment areas (Figure 5.7b) is fluctuating because of the temperature variability. Melt tendency was increasing during the last three decades, showing an accelerated melt. Similar behavior is shown for evaporation, which increases nearly constantly. For the five investigated catchments, a loss of ice-covered surface of 24% and a glacier volume loss of 33% (Table 5.4) between 1981 and 2009 is simulated.

Table 5.4. Area-weighted glacierization S_{gl}/S_{tot} [%], glacier surface $S_{gl}/S_{gl\ 1980}$ [%] and glacier volume $V_{gl}/V_{gl\ 1980}$ [%] relative to October 1980 (hydrological year of 1981) for the five catchment areas (S_{tot} = 261.0 km^2) for the reference climate scenario (0°C) (S1) and scenarios C2SM-ETHZ (S2), -2°C (S3), +2°C (S4) and +4°C (S5).

	1980	2009	2050					2099				
	real	S1	S1	S2	S3	S4	S5	S1	S2	S3	S4	S5
S_{gl}/S_{tot}	41	31	24	6	30	19	14	21	0	47	6	1
$S_{gl}/S_{gl\ 1980}$		76	59	16	74	46	33	53	0	115	16	1
$V_{gl}/V_{gl\ 1980}$		67	49	14	62	39	30	35	0	105	6	0

Due to the high temperature increase at the beginning of the future period, the C2SM-ETHZ scenario generates much higher runoff from glacier melt than the +2°C and +4°C scenarios until about 2040. This considerable initial loss of ice volume with a peak around 2020 seriously impacts the future de-glaciation process. The melt behavior is therefore widely different from the +4°C scenario, showing a similar overall increase, but with lower or even negative temperature gradient between the reference and the future climate period.

Glacierization decreases for the reference (0°C) as well as the scenarios C2SM-ETHZ, +2°C and +4°C, as shown in Figure 5.7a for the three glaciers. Disregarding the reference scenario with some stabilization of size after the loss of the lower glacier bands towards the second half of the simulation period, the glaciers are not able to reach

a steady state as the increase of temperature is too fast. For the -2°C scenario, an initial slight decrease is followed by an increase of the glacier mass. The three glaciers completely disappear until 2099 only for the C2SM-ETHZ scenario (Table 5.4). Thus, glacier melt is expected to increase for the first 10 to 15 years. Due to considerable glacier mass losses, water from ice melt decreases for the following years. For the other scenarios, the initial short cold period induces a decrease of runoff followed by a constant increase until 2050 due to ice volume losses of 38% (-2°C), 51% (0°C), 61% (+2°C) and 70% (+4°C) compared to 1980 (Table 5.4). For the +4°C scenario, glacier melt then drops to zero by the end of the century because of nearly complete de-glacierization. A similar behavior is simulated for the +2°C scenario, but with reduced glacier melt. The glacier volume gets stabilized for the reference scenario. For the -2°C scenario, glacier even grows. Thus, runoff from glacier increases in the late century. The glacier at the end of century has 105% (-2°C) and 35% (0°C), respectively, of the volume of 1980 (Table 5.4).

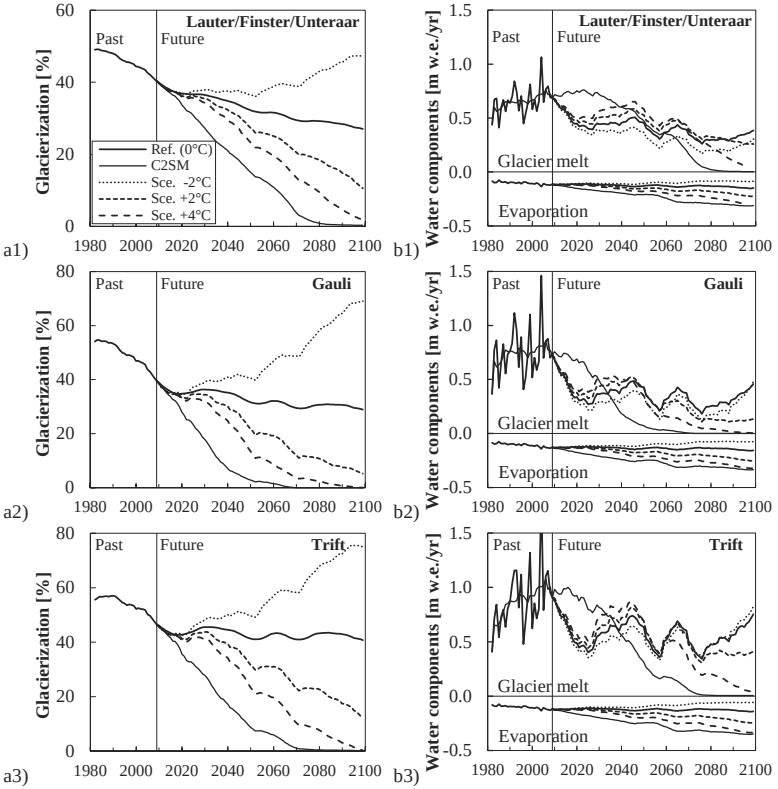

Figure 5.7. Glacierization S_{gl}/S_{tot} (a), annual glacier melt $Q_{icemelt}/S_{tot}$ and evaporation loss RET/S_{tot} (b) for the catchment areas of Grimsel with Lauteraar/Finsteraar/Unteraar Glaciers (grim1.1/1.2/1.4) (1), of Mattenalp with Gauli Glacier (urba1.1) (2) and Trift with Trift Glacier (gadm3.1) (3) for the reference climate period (past), the reference climate scenario (0°C) and scenarios C2SM-ETHZ, -2°C, +2°C and +4°C. Tendency curves (average over 11 values) normalized by the catchment surface area.

The high-mountainous catchment areas have nowadays low evaporation due to the ice-cover and the missing vegetation. During the reference climate period (1980-2009), an increase of evaporation results from the increasing temperatures, boosting evaporation losses in future. Figure 5.7 shows stabilization for the second half of the century for the reference climate scenario (0°C), whereas the -2°C scenario decreases evaporation. Transpiration is less relevant due to high altitudes of the analyzed catchment areas.

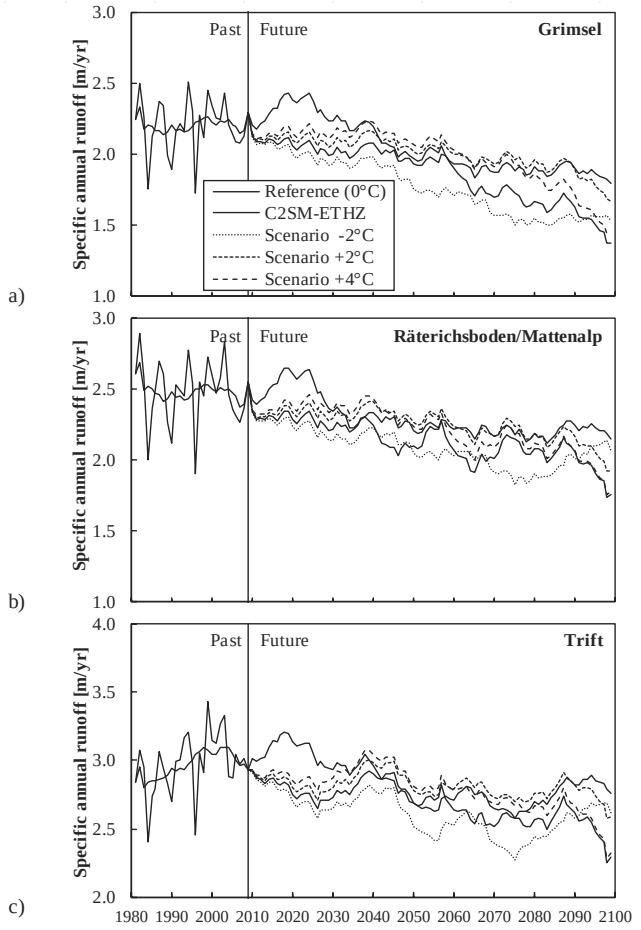

Figure 5.8. Specific annual runoff of the catchment areas of Grimsel (a), Räterichsboden/Mattenalp (b) and Trift (c) for the reference climate period (past), the reference climate scenario (0°C) and scenarios C2SM-ETHZ, -2°C, +2°C and +4°C. Tendency curves (average over 11 values) for future runoff normalized by the catchment surface area.

The future specific annual runoff of the catchment areas of Grimsel (Lauteraar/Finsteraar/Unteraar Glaciers), Räterichsboden/Mattenalp (Gauli Glacier) and Trift (Trift/Stein/Steinlimi Glaciers) shows similar behavior as for the glacier melt (Figure 5.8). The C2SM-ETHZ scenario reveals an increasing discharge until 2025, followed by a mainly decreasing period until the end of the century. Due to the relatively cold temperatures at the beginning of the simulation period, the runoff of the other scenarios is almost stable, whereas the +4°C scenario has an increasing tendency due to the fast glacier melt and the -2°C scenario a decreasing character due to ice formation. Precipitation is the same for all scenarios. In 2099, the lowest runoff is simulated for the C2SM-ETHZ and the +4°C scenarios due to the missing ice melt. The +2°C as well as the reference scenarios are influenced by slower melt of the ice mass and show therefore higher runoff at the end of the 21st century. The -2°C scenario produces low runoff during the simulation period. At the end, runoff becomes stable or even increases (Figure 5.8c) due to melt of formerly constituted glacier mass.

Intra-annual runoff distribution is shown by the mean annual hydrographs for the catchment areas of Grimsel, Räterichsboden/Mattenalp and Trift (Figure 5.9). The daily runoff is plotted as the average value over the past (1980-2009) and the two future climate periods (2021-2050 and 2070-2099) for the five scenarios. The reference climate scenario (0°C) has a similar runoff behavior to the past (Figure 5.9/1). Peak flow remains the same.

The reduction of the glacier mass influences the contribution of glacier melt. Thus, lower summer discharges are expected. The C2SM-ETHZ scenario (Figure 5.9/2) transforms today's hydrograph from glacier melt- to snowmelt-dominated. The complete loss of ice mass, the high temperatures, more rainfall in spring and less precipitation in summer lead to an increase of the runoff peak in spring, which is on average 2% for Grimsel, 24% for Räterichsboden/Mattenalp and 23% for Trift for 2021-2050 and 10%, 34% and 30%, respectively, for 2070-2099. Because of the fast melt of the glaciers and the ice mass losses, summer runoff decreases. Higher temperatures and precipitation in October and November increases winter runoff.

For the +2°C and +4°C scenarios, a similar phenomenon is shown (Figure 5.9/4 and 5). Due to invariant precipitation distribution, the peak discharge is not increased, but appears earlier. Increasing temperatures lead to an earlier start of snowmelt in spring. The higher the warming is, the faster glacier melt occurs and the lower the summer runoff is. The opposite is simulated for the -2°C scenario (Figure 5.9/3), where runoff is reduced by glacier mass constitution. Thus, water is absorbed and stored in the re-formed glaciers, as shown for the Unteraar Glacier in Figure 5.9a3.

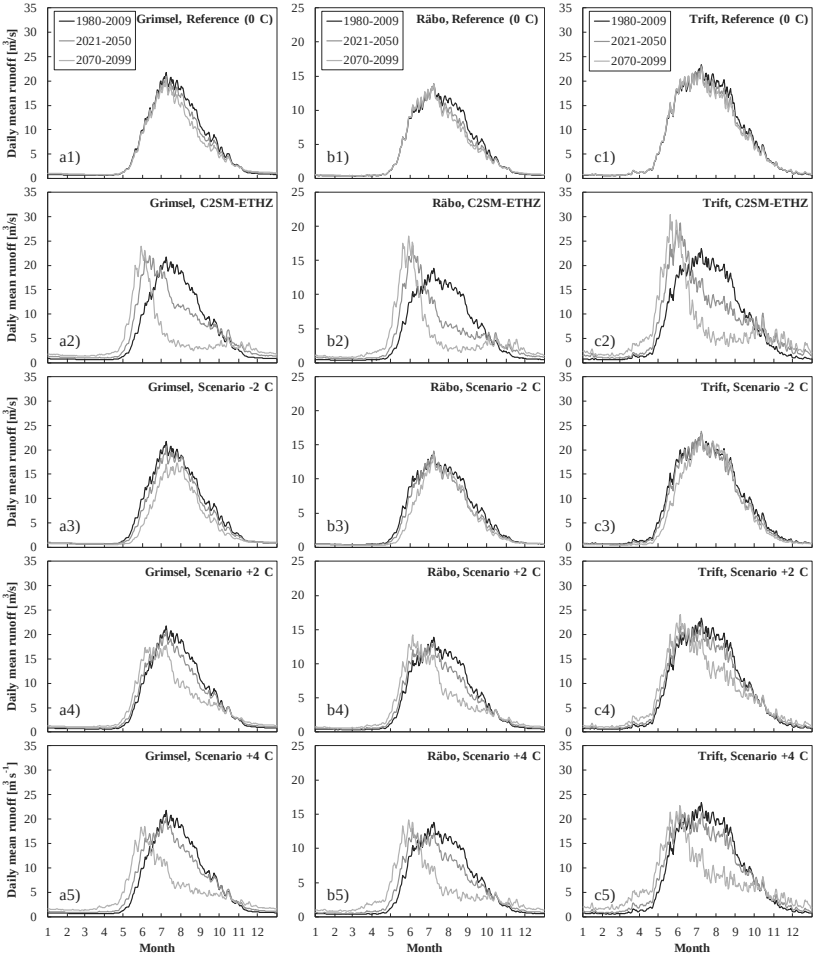

Figure 5.9. Average annual hydrograph of the catchment areas of Grimsel (a), Räterichsboden/Mattenalp (Räbo) (b) and Trift (c) over the past (1980-2009) and the two future climate periods (2021-2050 and 2070-2099) for the reference climate scenario (0°C) (1) and scenarios C2SM-ETHZ (2), -2°C (3), +2°C (4) and +4°C (5).

As shown in Figure 5.10, the model allows definition of the snow-covered area for the reference as well as the future climate periods. The average daily values are related to the five catchment areas between 1650 and 4200 m a.s.l. for the C2SM-ETHZ scenario. The last three decades (1980-2009) had a fully snow-covered area until May. Then increasing snowmelt reduces snow-cover to 15% at the end of August. The snowpack is formed until the beginning of December due to snowfall resulting from precipitation and low temperatures. The simulated climate change admits higher temperatures over the year and more rainfall in spring, producing earlier, faster and complete melt of the snow-cover. For 2070-2099 no fully snow-covered area is achieved anymore and the snow-free period lasts three months between July and September. 2021-2050 corresponds to a limit case, allowing full snow-cover in winter and almost complete snow-free area in summer.

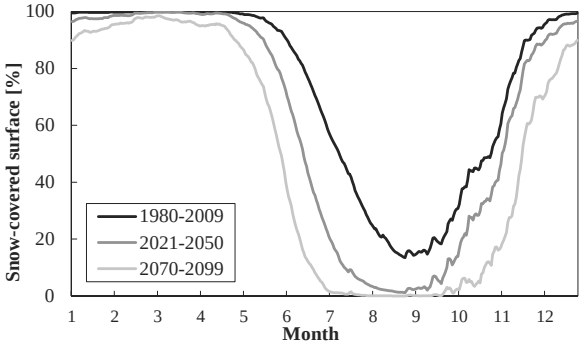

Figure 5.10. Average snow-covered surface area for the five catchment areas (S_{tot} = 261.0 km^2) over the past (1980-2009) and two future climate periods (2021-2050 and 2070-2099) for the C2SM-ETHZ scenario.

Table 5.5 summarizes the average annual values of water balance components for the simulated scenarios over the five catchment areas. As mentioned above, mean precipitation remains constant. Warming leads to an increase of evaporation and glacier melt. The latter decreases in future decades due to glacier disappearance. A decreasing temperature would even reactivate glacier formation (negative values). In any case, runoff does not only decrease but reveals a new intra-annual redistribution.

Table 5.5. Area-weighted specific annual precipitation *P* [m/yr], evapotranspiration *RET* [m/yr], ice melt $Q_{icemelt}$ [m/yr] and total runoff Q_{out} [m/yr] as well as relative runoff in July and August $Q_{out\ 7\text{-}8}/Q_{out}$ [%] for the five catchment areas (S_{tot} = 261.0 km^2) for the reference climate scenario (0°C) (S1) and scenarios C2SM-ETHZ (S2), -2°C (S3), +2°C (S4) and +4°C (S5).

		1980-2009	2021-2050					2070-2099				
		S1	S1	S2	S3	S4	S5	S1	S2	S3	S4	S5
P	[m/yr]	2.44	2.48	2.48	2.48	2.48	2.48	2.44	2.44	2.44	2.44	2.44
RET	[m/yr]	0.14	0.15	0.23	0.14	0.17	0.18	0.16	0.32	0.10	0.23	0.29
$Q_{icemelt}$	[m/yr]	0.28	0.08	0.29	-0.03	0.16	0.23	0.04	0.01	-0.28	0.10	0.06
Q_{out}	[m/yr]	2.59	2.41	2.54	2.32	2.47	2.53	2.31	2.13	2.02	2.31	2.20
$Q_{out\ 7\text{-}8}/Q_{out}$	[%]	46	44	29	47	41	38	43	14	52	32	22

5.5 Discussion

The chosen semi-distributed conceptual modeling approach is an efficient and coherent way to analyze the impact of climate change on future runoff in Alpine catchment areas. *Routing System* is an approved model for hydrological-hydraulic simulations (García Hernández, 2011). A simple dynamic glacier tool was implemented. First applications have been realized for case studies in the Swiss Alps (Jordan and Seiler, 2010; Terrier *et al.*, 2011). The transparency of the methodology allows the discussion of the main modeling uncertainties.

The model was built-up with available digital elevation models in addition to GIS applications. For high-mountainous catchments, changes in vegetation can be neglected for a time period of 100 years. The glaciers are the only relevant dynamic elements in the system. Glacier surface as well as elevation changes are topographically documented. However precise ice thickness distributions of glaciers are not easily available, requiring time-intensive measuring campaigns. The applied technique to define glacier thickness (Haeberli and Hoelzle, 1995; Linsbauer *et al.*, 2009) has an estimated precision of ±30%, influencing glacier-melt simulations considerably. Thus, a precise set-up of initial conditions for October 1980 is difficult. However, this uncertainty does not influence the tendency but the time of deglaciation. A deviation of the initial conditions impacts the moment of eventual glacier disappearance and therefore the runoff series, whereas the equilibrium state would not be temporally modified.

The calibration process is based on (1) runoff data provided by KWO and (2) the documented glacier thickness loss. It only partially contains the effects from strong albedo lowering, which occurred during the years following the extreme summer of 2003 (Paul *et al.*, 2005; Oerlemans *et al.*, 2009) and could further be developed in the future. As a consequence, the rate of ice loss could be even faster than simulated. Moreover, the daily inflow series, available from 1980, are recorded for relatively small catchment areas, but they are influenced by hydropower operations and the measuring method (reservoir level changes). Thus, they could only be corrected by avoiding negative values. Another difficulty is to define an average ice thickness loss for an elevation band for the glacier mass balance model. Statistics of glacier mass balance for long past periods are not available, unlike statistics related to glacier length. Data from 1980 to 1993 delimits the calibration period. Incorrect tendencies could influence the long simulation period. For the present case, high glacier-melt in the last three decades provided a quite robust calibration of the ice-covered catchments.

Future runoff estimations are directly linked to the climate scenarios. The simulations show that temperature and precipitation changes have the highest influence on the hydrological behavior. In Stähli *et al.* (2011) a standard deviation of 66 mm or 3% for the average annual runoff of the operated catchment is given, corresponding to a four times smaller value than the natural variability. Furthermore, sampling from rain gauges as well as inflow measurements from high-mountainous catchment areas in southern Switzerland (unpublished data) reveal a notable decrease of precipitation during the last few decades, which is not predicted by the tested climate scenarios.

The semi-distributed model allows short simulation time but not a detailed reproduction of the geometry. The division in elevation bands of 150 m does not take into account local effects of varying glacier thickness or exposition. Thus, the glacier retreat in terms of local geometry cannot be predicted exactly. The glacier mass balances of the Gauli and Oberaar Glaciers (Figure 5.11) show that in the past nearly all elevation bands were losing volume, the lower the greater, as also revealed by the results from DEM differencing by Paul and Haeberli (2008). It would continue in the same way, when applying the C2SM-ETHZ scenario with high temperature increase and therefore a considerable ice volume loss at the beginning of the simulation period. The glacier between 2100 and 2400 m a.s.l. disappears between 2020 and 2030, the highest elevation bands in the mid-century. The reference climate scenario illustrates this phenomenon even better by continuous de-glaciation of the lower bands, with the upper bands remaining stable. The model is therefore able to simulate not only the runoff correctly, but also its origin.

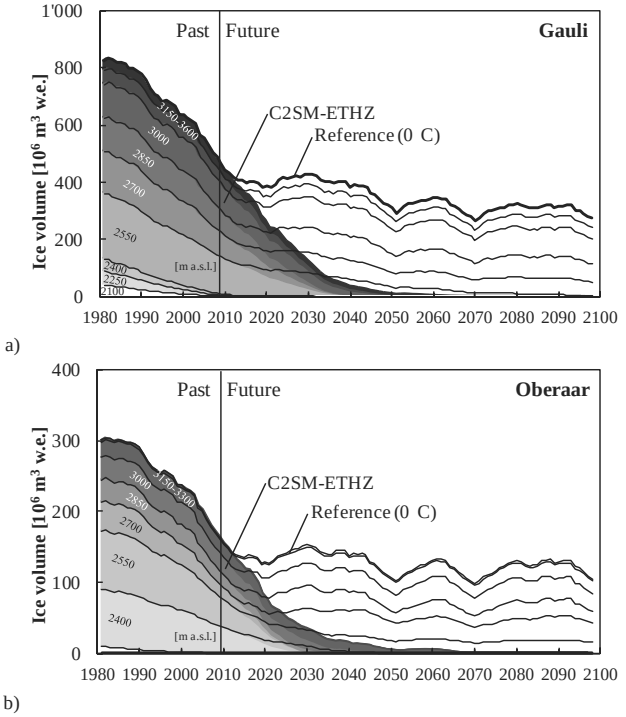

Figure 5.11. Ice volume (V_{gl}) evolution for the elevation bands of the Gauli Glacier (a) and the Oberaar Glacier (b) for the C2SM-ETHZ scenario and the reference climate scenario (0°C).

The model is based on the calibrated parameters and the initial conditions. Future behavior only depends on the climate scenarios and does not take into account special or local effects, e.g., a reduction of the albedo coefficient due to local dust cover on the glacier surface.

Similar studies of runoff from Alpine catchments in the upper Aare River catchment were done by Stähli *et al.* (2011) for the same period with a similar approach. The hydrological modeling with daily time steps was based on the semi-distributed modeling system PREVAH (Viviroli *et al.*, 2009). The glacier retreat was simulated applying the shrinkage model of Paul *et al.* (2007) in 5-year time intervals. The calibration process provided similar NSE between 0.76 and 0.83 for runoff. For a slightly different catchment (S_{tot} = 450.1 km^2) and the A1B climate scenario, glacierization of 22.9% in 1985 decreases to 14.6% in 2040 and 8.0% in 2085. The hydrograph changes from glacier-melt (glacial) to snowmelt (nival) dominated. Average annual runoff from 2.14 m (reference) decreases to 2.08 m (2021-2050) and 2.00 m (2070-99). These values, referring to another climate scenario and a different catchment, are difficult to compare directly to the present study. However, glacier-melt is generally faster and thus runoff reduction more significant. One reason of this difference could be the initial glacier volume and ice thickness distribution. The advantage of the approach proposed in this study is certainly the fact that the glacier is an integrated part of the model and is therefore updated at every time step.

5.6 Conclusion

The goal of the present study was the development of a simple but reliable approach to estimate future runoff from glacierized catchment areas. The novel formulation and modeling method allowed definition of the effects of climate change on the behavior of Alpine glaciers for different scenarios. The resulting hydrographs, highly important for future HPP operation, could be simulated.

A semi-distributed conceptual hydrological modeling approach allowed the simulation of future runoff in Alpine catchments equipped with hydropower schemes. For the period from 2010 to 2099, time series of daily resolution are calculated by hourly updating of the meteorological, glaciological and hydrological parameters for five climate scenarios. The C2SM-ETHZ scenario, assuming an overall increase of temperature of about +4°C by 2099, takes into account intra-annual change in temperature and precipitation, whereas four other scenarios only admit linearly changing temperature of -2°C, 0°C, +2°C and +4°C over the simulation period. All scenarios are based on the reference climate period 1980-2009, implementing a natural year-to-year variability to input climate data. Thus, forecast uncertainty depends directly on the input time series. The sub-division into elevation bands of 150 m is not suited for exact indication of glacier outline, but allows satisfactory results for runoff. Despite the hourly updating of all parameters in the model, the methodology is easily applicable to other case studies due to its transparent approach, short simulation time and easy accessibility to model parameters. The model is well adapted for runoff estimations in Alpine catchments, especially when containing hydropower plants. Reliable estimation and optimization of future energy production and therefore economic efficiency can be done for existing as well as new hydropower facilities.

Admitting an increase of temperature due to climate change, high glacier melt is predicted for the 21st century. The C2SM-ETHZ scenario predicts an almost complete de-glacierization of the upper Aare River basin for the period between 2050 and 2099. Runoff from glacier melt will initially slightly increase, followed by a decrease due to

ice mass losses. Total annual runoff will decrease by 2% until 2050 and by 18% until the end of the 21st century. Higher temperature increases evaporation and accelerates snowmelt. Thus, the runoff regime changes. The reduced glacier melt in summer is partly compensated by increased snowmelt in spring. For Alpine catchment areas, significant decrease of runoff related to glacier shrinkage combined with new peak flow in spring must be considered for future hydropower, irrigation but also for flood risk management.

6

Simulation of hydropower plant operation in mountainous areas considering climatic, economic and ecological issues

In Central Europe Alpine regions, high-head hydropower plants (HPP) have been used to supply peak load energy for the last few decades. Nowadays the electricity market is faced with new challenges due to new renewable energy sources, international trading and grid regulation. In addition, climate change affects meteorological and hydrological conditions. For the simulation of future hydropower management, a HPP modeling and simulation tool was developed. It is integrated in a semi-distributed conceptual hydrological model and takes into account short and long-time reservoir inflow as well as the electricity price. The approach was tested for a complex hydropower scheme in Switzerland. For three HPP outlines, different future hydrological and economic scenarios are simulated. Ecological issues were considered by an optimization tool reducing flow fluctuations in the downstream river system, the so-called hydropeaking, and estimating the subsequent operation losses. Despite the considerable reduction of future runoff, enhancements by increasing turbine and pumped-storage capacities allow compensation and could even partially restore the natural flow regime.

6.1 Introduction

15% of Europe's total power generating capacity is accounted for by hydropower. About 25% comes from more than 5000 hydropower plants in the Alps, generating about 90 TWh per year (Alpine Convention, 2011). Today's climate policies support zero-carbon power generation alternatives. Thus, hydropower will profit from the rising electricity prices, as a result of "increasing internalization of climate costs, the growth in global energy consumption and the associated increasing relative scarcity of fossil fuel sources" as well as the development of a European electricity market (Auer, 2010). High-head storage hydropower plants (HPP), especially, allow on-demand power generation. Large reservoirs at high altitudes store water from precipitation, snow and glacier melt during summer in order to use it in winter. Turbine operations are concentrated during periods of peak energy demand. High flexibility, requested due to grid regulation and electricity market issues, needs efficient planning of water storage and release. For a given hydropower scheme, the inflow from the catchment area as well as the power demand are key parameters. Their forecast is related to several uncertainties due to meteorological variability, climate change and liberalization of electricity market. Nevertheless, an appropriate tool for daily (hourly operation), annual (seasonal water transfer) as well as long-term (influence of market and climate) HPP management is needed for achieving a maximum revenue and therefore a sustainable use of water resources.

However, the sudden opening and closing of the turbines produces highly unsteady flow conditions in the river downstream of the power house outlet. The natural flow regime of the river is considerably influenced by this so-called hydropeaking and can result in the degradation of the river ecosystem. Besides or even in combination with morphological improvements, the restoration of altered and regulated flow regimes is important for sustaining the ecological integrity of rivers (Bunn and Arthington, 2002; Jungwirth *et al.*, 2002). Since 2012, the Swiss law on water protection (*GSchG*, Art. 39a) recognizes hydropeaking as a reason for river alteration.

A simple and often used indicator to express the sub-daily flow fluctuations is the ratio of the maximum $Q_{\max,j}$ and the minimum $Q_{\min,j}$ daily discharge, called drawdown range. The hydropeaking indicator HP_1 (Eq. 6.1) is a daily indicator, normalizing the ratio between $Q_{\max,j}$ and $Q_{\min,j}$ by the mean daily discharge $Q_{\text{mean},j}$ (Meile *et al.*, 2011):

$$\mathrm{HP}_{1,j} = \frac{Q_{\max,j} - Q_{\min,j}}{Q_{\text{mean},j}} \qquad \left| \; j \in [1;365(366)] \right. \tag{6.1}$$

Annual, seasonal or monthly averaged values show trends in time, e.g., the influence of seasonal and meteorological conditions in addition to hydropower operation on the flow regime.

Furthermore, the legal ordinance (*GSchV*, Art. 41d) propose the discharge analysis of a sample of 10 weeks during the low flow season (winter) for five years. To avoid single extreme events and the influence of low production during weekends, peak discharge Q_{peak} is defined as the 80$^{\text{th}}$ percentile of the daily maximum discharge series $Q_{\max,j}$ and the off-peak discharge $Q_{\text{off-peak}}$ as the 20$^{\text{th}}$ percentile of the daily minimum

discharge series $Q_{\min,j}$. The hydropeaking ratio r_{HP} (Eq. 6.2) is then the 80th percentile of the daily drawdown ranges $Q_{\max,j}/Q_{\min,j}$ over the sampling period:

$$\left.\begin{aligned} Q_{\text{peak}} &= x_{80\text{th}}(Q_{\max,j}) \\ Q_{\text{off-peak}} &= x_{20\text{th}}(Q_{\min,j}) \\ r_{\text{HP}} &= x_{80\text{th}}(Q_{\max,j}/Q_{\min,j}) \end{aligned}\right| \; j \in [1;5\cdot 70] \tag{6.2}$$

Despite an increasing knowledge of the interactions between hydropeaking and ecology, it is currently still difficult to predict and quantify biotic responses to hydropeaking (Meile *et al.*, 2011). The hydraulic indicators HP_1 and r_{HP} are therefore adequate for preliminary assessment.

To achieve the highest economic efficiency, an operation tool is developed using a heuristic approach. It is integrated in the semi-distributed conceptual hydrological-hydraulic model *Routing System* and allows simulation of the HPP operation of high-head storage hydropower schemes for different climatic, hydrological, economic and ecological scenarios. The complex interconnected network is generally of nonlinear character. A classic operational research approach was chosen. The efficiency of the optimization tool is tested for a simple case, allowing a comparison with two heuristic optimization algorithms and a sensitivity analysis of the parameters. To reduce the negative impacts on the river ecosystem, a hydropeaking coefficient can be defined and the resulting economic response estimated. The tested tool is applied to the upper Aare River catchment in Switzerland, an Alpine watershed operated by a network of several power plants. It strongly influences the natural flow regime of the river by hydropeaking. The study evaluates the operating rules regarding robustness and flexibility of today's existing scheme and two future enhancement projects faced with changing reservoir inflow and electricity demand scenarios as well as ecological constraints. Despite the complexity, an hourly or even 10-minute resolution is achieved allowing analysis of hydropeaking.

6.2 Method

Optimization techniques have revealed increasing relevance for the management and operation of complex multi-reservoir systems. Most of the optimization models are based on a mathematical programming technique (algorithm). Its choice depends on the system characteristics, the data availability and specified objectives and constraints. Yeh (1985) published a survey of state-of-the-art approaches of optimization methods and their corresponding models, like linear programming (LP), dynamic programming (DP) and their variations. Even when DP was found as more adapted to nonlinear sequential problems, its application remains difficult in complex systems. Furthermore, low computing performances at this time made nonlinear programming (NLP) cumbersome.

Thanks to an initial policy with an LP approach, a successive linear programming model (SLP) provided good results for real-time decision making of a large-scale network of 75 HPPs in Brazil (Barros *et al.*, 2003). Nowadays, thanks to developments in computer power and solvers, NLP can be applied for optimization of larger reservoir systems. Brandão (2010) reviewed several nonlinear programming packages and their application for the Brazilian electrical system.

Recently, heuristic methods show increasing application in case of nonlinear optimization with high dimensionality and higher number of equality and inequality constraints: Fuzzy Sets theories (FS) became relevant for multi-objective or multi-attribute decision making, e.g., for a complex multi-reservoir system with uncertainties of inflow (Choudhari and Anand Raj, 2010). Artificial Neuronal Networks (ANN) and Expert Systems (ES) were chosen for optimal reservoir operation in India with deterministic data (Chandramouli and Deka, 2005). Sharma *et al.* (2004) applied a two-phase neural network (TPNN) for operation of a network with ten reservoirs. Both approaches remained efficient. Genetic Algorithms (GA) are often applied in combination with other techniques. Reis *et al.* (2005) used a hybrid GA and LP for rule curves definition of a theoretical system of four reservoirs. Cheng *et al.* (2008) applied GA with Chaos algorithms for optimizing hydropower generation in the Yunnan province in China. The combination of powerful global (GA) and local (Chaos algorithms) searching abilities performed better than classic GA. Ant Colony Optimization (ACO) was successfully applied for a multipurpose reservoir system in India and compared to a GA approach (Kumar and Reddy, 2006).

Operation of high-head storage hydropower schemes has to take into account two time horizons. On the one hand, medium-term HPP production planning mainly involves the seasonal transfer of water from wet summer with low electricity prices to dry winter with high electricity prices. On the other hand, short-term management concerns the physical operation of the plant within a time horizon of a day or a week and with a time resolution of an hour or shorter, taking into account future daily peak energy demand commitments or electricity market issues such as price fluctuations. Stochastic dynamic programming can be used to deal with such conditions (Fleten and Kristoffersen, 2008). In addition, a lot of different types of heuristic approaches have been developed and applied, as done for the present study.

6.2.1 General approach

Optimization problem

The formulation of an optimization model for a hydropower system can be expressed in terms of maximization of total revenue over a given time period. In case of a high-head storage HPP, not only the total energy production is important, but also the moment of operation due to daily as well as seasonal energy price fluctuations. Thus, active storage hydropower schemes in mountainous areas contain relatively large reservoirs at high altitude feeding turbine units of relatively small discharge. A reservoir of a given volume $V_{\text{up max}}$ is supplied by inflow Q_{inflow}. The operation Q of the downstream located turbine unit of an on-off capacity Q_{turbine} has to be defined for maximum revenue (Eq. 6.3). Annual revenue depends on the power as a function of discharge Q and net head H as well as the electricity price P_{el}. The head losses and therefore the efficiency η depend on Q and H. In the case of a high head relative to the reservoir level, net head and efficiency remain approximately constant and therefore not relevant for optimization. Normally the inflow and electricity price data is given as a time series of hourly resolution, defining the discrete character of the problem. Thus, the optimization problem has as the objective function the sum of the products of electricity price and turbine operation over the given time period T_{per} (Eq. 6.3). The limited volume of the reservoir storage as well as water balance equation are considered in two constraints

(Eq. 6.4 and 6.5), defining that the stored volume V_{up}, as sum of continuous inflow and outflow, cannot be higher than $V_{up\,max}$ and that all water has to be operated avoiding release by the spillways. The definition of the storage volume is nonlinear:

$$\begin{aligned} \text{Revenue} &= \max_{Q_t}\left[\sum_{t=1}^{T_{per}}\left(\eta_t \cdot H_t \cdot Q_t \cdot P_{el,t} \cdot \Delta t\right)\right] \cdot \rho g \\ &\approx \max_{Q_t}\left[\sum_{t=1}^{T_{per}}\left(Q_t \cdot P_{el,t}\right)\right] \cdot \bar{\eta} \cdot \overline{H} \cdot \Delta t \cdot \rho g \qquad \left| \; Q_t \in Q_{turbine} \cdot \{0,1\}\right. \end{aligned} \tag{6.3}$$

$$0 \le \max_{T'}\left[\sum_{t=1}^{T'}(Q_{inflow,t} - Q_t) \cdot \Delta t\right] - \min_{T''}\left[\sum_{t=1}^{T''}(Q_{inflow,t} - Q_t) \cdot \Delta t\right] \le V_{up\,max} \tag{6.4}$$

$$\sum_{t=1}^{T_{per}} Q_{inflow,t} \cdot \Delta t = \sum_{t=1}^{T_{per}} Q_t \cdot \Delta t \tag{6.5}$$

In the case of a multi-reservoir system, the total revenue would be the sum of all HPP operations, including turbine, pump and pumped-storage activities. Constraints would be applied for all reservoirs, taking into account the storage volume as well as the sum of natural inflow and inflow from upstream facilities.

Algorithms

For the operational research problem, two heuristic algorithms A1 and A2 are developed and tested. An hourly resolution is applied to both algorithms, neglecting the net head changes. Inflow as well as electricity prices are known for the whole period, corresponding to a hydrological year from 1st of October of the previous year to 30th of September of the current year.

Algorithm A1 starts from the turbine operation series with highest revenue without respecting the given volume of the reservoir:

1. By dividing the annual inflow Q_{inflow} by the turbine capacity $Q_{turbine}$, the number of turbine operation hours n is defined.
2. The n hours of highest electricity price are chosen for initial turbine operation Q_i. The needed storage volume $V_{up,i}$ is then computed.
3. Then the operational hour of the lowest electricity price is set at the next lower non-operational hour. When the new storage volume $V_{up,i+1}$ is lower than the previous one $V_{up,i}$, the next operational hour is moved. All lower positions, also the ones of initial operation, are tested. When no position can be found, the turbine hour is set at its initial position and the next higher one is moved.
4. This procedure continues until the storage volume $V_{up,i}$ is lower than the given reservoir volume $V_{up\,max}$.

Algorithm A2 sets the initial turbine operation series with respect to a minimum reservoir volume by neglecting any economic response:

1. By dividing the annual inflow Q_{inflow} by the turbine capacity $Q_{turbine}$, the number of turbine operation hours n is defined.
2. The n hours for initial turbine operation Q_i are set, that the required storage volume $V_{up,i}$ is the lowest possible.
3. Then the operational hour of the lowest electricity price is set at the position of the highest price, when the new revenue $\Sigma(P{\cdot}Q)_{i+1}$ is higher than the previous one $\Sigma(P{\cdot}Q)_i$ and the storage volume $V_{up,i+1}$ lower than the maximum reservoir volume $V_{up\,max}$. If one of these constraints is not respected, the turbine hour is set at its initial position and the ranking of the hour of highest electricity price is lowered by one position until the suitable position for the hour of lowest electricity price is defined.
4. This procedure continues as long as $V_{up,i}$ is lower than $V_{up\,max}$ and the revenue $\Sigma(P{\cdot}Q)$ increases over a defined number of steps.

The two algorithms A1 and A2 are tested and compared for a simple standard hydropower scheme (Figure 6.1) with different input data series. Runoff from the upstream catchment Q_{inflow} is collected by a reservoir of a volume $V_{up\,max}$ of $13{\cdot}10^6$ m^3 and a quadratic volume-level relation varying between 500 ($H_{up\,min}$) and 530 m a.s.l. ($H_{up\,max}$), similar to Lake Gelmer in Switzerland (Table 6.5). The lake is operated by a power plant with one on-off turbine unit of capacity $Q_{turbine}$ of 12 m^3/s, corresponding to about 900 turbine operation hours. The power house outflow Q is released to a river reach with one upper sub-catchment, connected by a river reach.

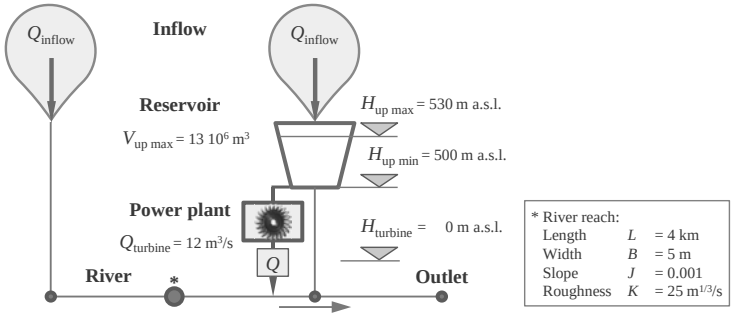

Figure 6.1. Sketch of standard high-head storage HPP in a mountainous catchment, operating one out of two sub-catchment areas. Reservoir volume of $V_{up\,max}$ is supplied by inflow Q_{inflow} and operated by a turbine of maximum on-off capacity of $Q_{turbine}$. The outlets of the sub-catchment areas are interconnected by a river reach. Outflow is generated downstream of the turbine outlet.

The simulations are performed individually for each of the six hydrological years from 2004 to 2009. Hourly inflow (Figure 6.2) is taken from an existing Alpine catchment area in the upper Aare River catchment (Gelmer) in Switzerland. It is chosen to maintain the natural and therefore fluctuating behavior of runoff from mountainous river basins with low inflow during winter and high one in spring and summer due to rainfall, snow and glacier melt. The annual mean is within the range of 1.10 and 1.19 m^3/s.

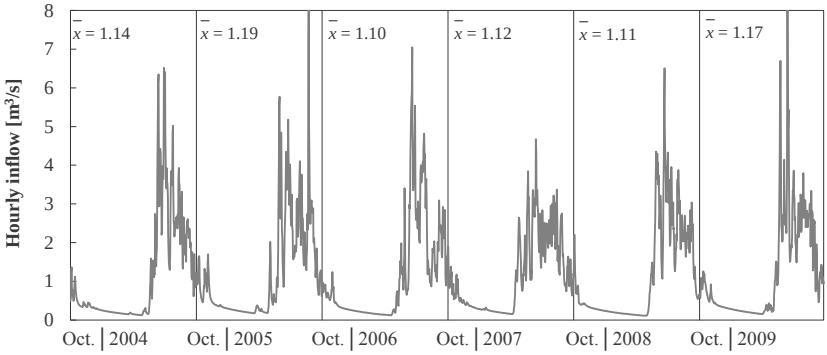

Figure 6.2. Mean hourly inflow Q_{inflow} from the Alpine catchment area of Lake Gelmer in Switzerland for the period between October 2003 and September 2009 ($\bar{x}$ = average discharge of hydrological year).

Hourly electricity prices (Figure 6.3) are from the European Energy Exchange (EEX). Nowadays, only a small amount of total produced energy is traded on the free market. Thus, the EEX prices do not show any clear tendencies. In most years except 2005 and 2008, summer prices and their volatility are lower than in winter. Extreme values from nearly 0 to higher than €200 /MWh are recorded. Thus, the annual average price is varying between €29.2 /MWh (2004) and €64.3 /MWh (2008). For the given case, this variety is welcome to test the performance of the developed algorithms in case of uncertainty.

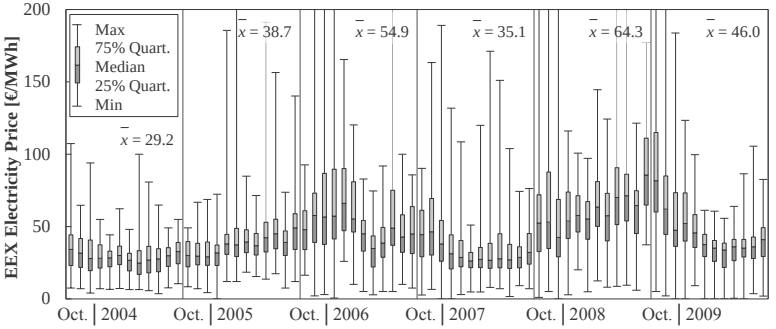

Figure 6.3. Statistics of the hourly electricity price P_{el} of the European Energy Exchange (EEX) for the period between October 2003 and September 2009 ($\bar{x}$ = average price of hydrological year). Several maximum values had to be cut for reasons of adequate presentation.

Algorithm A1 and A2 are both applied to each of the six hydrological years, taking into account the corresponding hourly inflow and electricity price time series. For the final set of turbine operation hours, the revenue is computed as the product of mainly real head, discharge and electricity price. For the start and end configuration, cumulative outflow is plotted (Figure 6.4). Computation time for A1 is several seconds, whereas A2 needed several minutes for the final set. In all cases, convergence is achieved. By taking the same inflow data and HPP outline characteristics, the duration of total turbine operation is the same for both resolution methods.

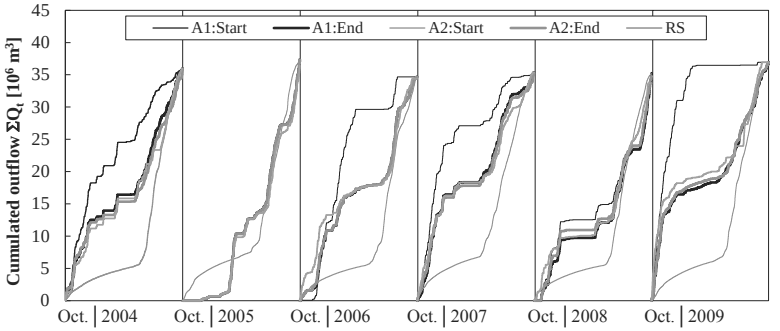

Figure 6.4. Cumulative outflow of the reservoir at initial (Start) and final (End) state of the optimization with algorithm A1 and algorithm A2 as well as for the application of *Routing System*.

Comparing the final results of A1 and A2 in terms of revenue (Table 6.1), only for 2005 both of them generate the same solution. For the other years expect 2008, A1 is able to produce higher revenue. The highest difference of 7.8% is shown for 2009. Electricity prices of 2008 of high values in summer when inflow is high have a completely different behavior than the other years. Thus, A1 is able with the initial set of high inflow hours to generate a higher economic response than A2. As far as a conclusion is possible over the small data set of realistic data, algorithm A1 accounts for higher performance, which could be proven by a more sophisticated approach, e.g., AMPL.

Table 6.1. Operational characteristics of a HPP with a reservoir of $V_{up\,tot} = 13 \cdot 10^6$ m^3 and a turbine capacity of $Q_{turbine} = 12$ m^3/s for simulations applying algorithm A1 and A2.

	Total inflow	Turbine operation	Average EEX price	Revenue Algorithm A1	Revenue Algorithm A2	Difference
	[10^6 m^3]	[h]	[€/MWh]	[M€]	[M€]	
2004	36.0	832	29.2	2.57	2.55	0.7%
2005	37.4	865	38.7	3.90	3.90	0.0%
2006	34.7	802	54.9	5.96	5.91	0.7%
2007	35.3	817	35.1	3.69	3.65	0.9%
2008	35.2	815	64.3	6.26	6.52	-4.1%
2009	36.9	855	46.0	4.53	4.18	7.8%

6.2.2 Routing System

Routing System is based on a semi-distributed conceptual modeling approach for river basin management, simulating hydrological response as well as operation of hydropower facilities (Jordan, 2007). Impact evaluation for long as well as short term behavior of climatic, hydrological, economic and ecological input variables needs a robust and efficient tool. Various modeling approaches and corresponding software exist for hydrological processes at catchment scale (Viviroli *et al.*, 2009) as well as numerous optimization strategies for multi-reservoir hydropower schemes (Alfieri *et al.*, 2006). *Routing System* links these two issues and allows global evaluation of a wide range of parameters and constraints. It is based on developments in the Object Oriented

Programming (OOP) language Visual Basic .NET (VB.NET). All elements, sub-basins in addition to the network of the water system, can be implemented and defined in the graphical user-interface. Time series are taken from a linked database. Efficient HPP operation compromises both simulation and optimization under real conditions (real-time decision making of HPP operation with perfect prediction of inflow and electricity price). In particular, the nonlinear optimization problem of maximum revenue, as defined above for the simple case (Eq. 6.3 to 6.5), is solved by a deterministic heuristic approach using an overall time step Δt of 10 minutes or 1 hour. The approach is presented for turbine operations, but it is also applied to pump or pumped-storage operations.

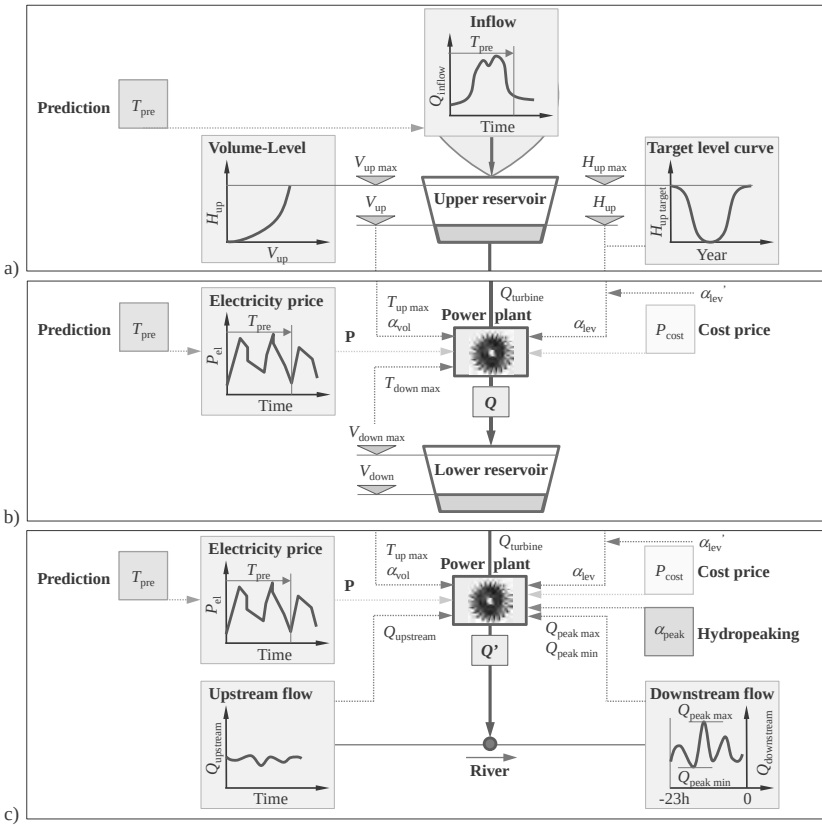

Figure 6.5. Turbine operation chart, including upper reservoir (a) and restitution to either lower reservoir (b) or downstream river, including hydropeaking concerns (c).

Each reservoir is characterized by a volume-level ratio (Figure 6.5a) for the operated storage volume. The corresponding maximum volumes of the upper and lower reservoir $V_{\text{up max}}$ and $V_{\text{down max}}$ [m a.s.l.] are defined. The power plant is defined by its technical, operational and economic characteristics, where the turbine (or pump) discharge Q_{turbine} [m^3/s] (Figure 6.5b) is the main parameter, allowing either full or no operation.

Since the short-term planning is strongly coupled to long-term, the value of current decisions must be evaluated against future consequences. For a storage HPP, the seasonal water transfer from summer to the economically interesting winter hours has to be performed by a long-term operation criterion. Thus, rough electricity price in addition to inflow estimations are used to define the target level curve of each reservoir in the network (Figure 6.5a). A heuristic algorithm, such as A1 or A2, can define the annual filling by mean monthly water level elevation $H_{\text{up target}}$ [m]. The user-defined parameter α_{lev}' [-] defines how strict the target level curve has to be followed and allows therefore to take into account the uncertainty of the predicted data series.

For the short-term operation, a prediction time horizon T_{pre} [h] has to be defined. At every given time t, inflow (Figure 6.5a) as well as electricity price (Figure 6.5b) are taken into account of the defined future period from moment t to $t + T_{\text{pre}}$. Energy price is loaded from the database, whereas inflow can come from the database to or from active storage, using data from a preliminary simulation. Thus, the chosen approach has the following main steps:

1. When, within the prediction time T_{pre}, overflow of the upper reservoir would appear (cumulative inflow $Q_{\text{inflow,t}}$ [m^3/s] is higher than available storage volume), T_{pre} is reduced to the time T_f until achieving a full reservoir. Depending on T_f, rules can be defined to start preventive or emergency turbine operations avoiding or reducing water losses:

$$T_{\text{pre}} = \begin{cases} T_{\text{pre}} & \left| V_{\text{up},t+T_{\text{pre}}} < V_{\text{up max}} \right. \\ T_{f,t} & \left| V_{\text{up},t+T_f} \geq V_{\text{up max}} \text{ and } T_{f,t} = \min\left\{1,\ldots,T_{\text{pre}}\right\} \right. \end{cases} \tag{6.6}$$

$$\text{where } V_{\text{up},t+T_f} = V_{\text{up},t} + \sum_{i=1}^{T_f} Q_{\text{inflow},t+i} \cdot \Delta t$$

2. The maximum operation time $T_{\text{up max}}$ [h] is defined to avoid emptying the upper reservoir of actual volume V_{up} [m^3] with full turbine operation Q_{turbine} [m^3/s]:

$$T_{\text{up max},t} = \frac{V_{\text{up},t}}{Q_{\text{turbine}}} \tag{6.7}$$

3. If there is a lower reservoir, the maximum operation time $T_{\text{down max}}$ [h] is defined to avoid overflow of the lower reservoir of current volume V_{down} [m^3] and maximum volume $V_{\text{down max}}$ [m^3]:

$$T_{\text{down max},t} = \frac{V_{\text{down max}} - V_{\text{down},t}}{Q_{\text{turbine}}} \tag{6.8}$$

4. The minimum of $T_{\text{up max}}$ and $T_{\text{down max}}$ is compared to the prediction time T_{pre} [h]. The lowest of the three values is chosen as limit time T_{lim} [h]:

$$T_{\text{lim},t} = \min\{T_{\text{up max},t}, T_{\text{down max},t}, T_{\text{pre}}\} \tag{6.9}$$

5. Then the limit electricity price P_{lim} [€/MWh] is defined from the hourly price series in increasing order **P** over T_{pre}, allowing full operation during $T_{\text{lim},t}$.

$$\mathbf{P}_t = \left[P_{\text{el}\,t,1},...,P_{\text{el}\,t,t},...,P_{\text{el}\,t,T_{\text{pre}}/\Delta t}\right] \quad \left| P_{\text{el}\,t,1} > P_{\text{el}\,t,n} > P_{\text{el}\,t,T_{\text{pre}}/\Delta t} \right. \tag{6.10}$$

$$P_{\text{lim},t} = \mathbf{P}_{t,m} \quad \left| \text{m} = T_{\text{lim},t}/\Delta t \right. \tag{6.11}$$

6. The level coefficient α_{lev} [-] is defined by taking into account the difference between the current H_{up} [m] and the target level $H_{\text{up target}}$ [m] of the upper reservoir as well as a user-defined level coefficient α_{lev}' [-] (Figure 6.6a):

$$\alpha_{\text{lev},t} = \max\left\{0.1, 1 - \frac{H_{\text{up},t} - H_{\text{up target},t}}{H_{\text{up target},t}} \cdot \alpha_{\text{lev}}'\right\} \tag{6.12}$$

7. The volume coefficient α_{vol} [-] is defined by taking into account the difference between the current V_{up} [m^3] and the maximum volume $V_{\text{up max}}$ [m^3] of the upper reservoir (Figure 6.6b):

$$\alpha_{\text{vol},t} = 0.9 + \frac{V_{\text{up max}} - V_{\text{up},t}}{V_{\text{up max}}} \tag{6.13}$$

8. When the electricity price P_{el} [€/MWh] is higher than P_{lim} [€/MWh] as well as the product of the cost price P_{cost} [€/MWh], the target level coefficient α_{lev} and the volume coefficient α_{vol}, turbine operation Q [m^3/s] is set to Q_{turbine} [m^3/s]:

$$Q_t = \begin{cases} Q_{\text{turbine}} & \left| P_{\text{el}\,t} \geq P_{\text{lim},t} \text{ and } P_{\text{el}\,t} \geq \alpha_{\text{lev},t} \cdot \alpha_{\text{vol},t} \cdot P_{\text{cost}} \right. \\ 0 & \left| P_{\text{el}\,t} < P_{\text{lim},t} \text{ and } P_{\text{el}\,t} < \alpha_{\text{lev},t} \cdot \alpha_{\text{vol},t} \cdot P_{\text{cost}} \right. \end{cases} \tag{6.14}$$

The cost price P_{cost} [€/MWh] and the level coefficient α_{lev}' have to be defined by the user for a reference configuration. These two parameters allow calibration of the HPP operation for a real case scenario. As shown in Figure 6.6a, high values of α_{lev}' induce stricter following of the target level $H_{\text{up target}}$. The risk of emptying reservoirs and thus interruption of HPP operation demands higher discipline related to the target level and available volumes $V_{\text{up}}/V_{\text{up max}}$ (Figure 6.6b). Thus, the level coefficient α_{lev} and volume coefficient α_{vol} are always higher for low water levels.

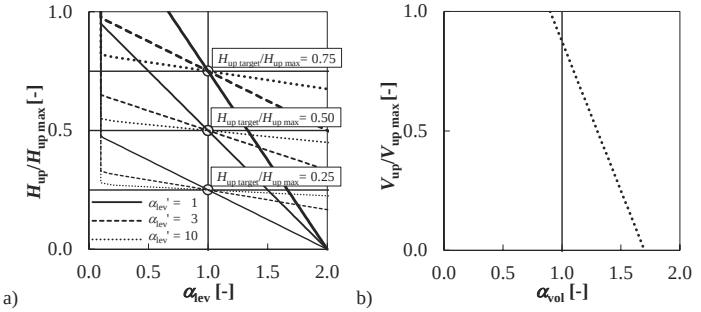

Figure 6.6. Level coefficient α_{lev} [-] as a function of dimensionless reservoir level $H_{up}/H_{up\,max}$ shown at the example of three target level ratios $H_{up\,target}/H_{up\,max}$ = 0.25, 0.50 and 0.75 and three user-defined level coefficients α_{lev}' = 1, 3 and 10 (a) and volume coefficient α_{vol} [-] as a function of dimensionless reservoir volume $V_{up}/V_{up\,max}$ (b).

In the case of a power house outflow in a river (Figure 6.5c), the HPP operation tool can be extended to assess ecological issues, hydropeaking in particular. A simple index to describe daily flow fluctuations is the ratio of the maximum $Q_{max,j}$ and the minimum $Q_{min,j}$ daily discharge, called drawdown range. In *Routing System*, this criterion is not only applied to the single days but to every time window of 24 hours and therefore called hydropeaking factor α_{peak}. For definition of the turbine operation at time step *t*, the discharge in the river after the turbine outlet of the previous 23 hours is taken into account. The defined α_{peak} can lead either to decreased turbine operation Q_{max} due to past low flow or an increase of base flow Q_{min} due to past peak release, as discussed in the following steps:

9. For the river reach downstream of the turbine outlet with $Q_{downstream}$ [m^3/s] the highest $Q_{peak\,max}$ [m^3/s] and the lowest discharge $Q_{peak\,min}$ [m^3/s] of the previous 23 hours is defined:

$$Q_{peak\,max,t} = \max\{Q_{downstream,t\text{-}s}\} \quad | \; s = [1h; 23h] \tag{6.15}$$

$$Q_{peak\,min,t} = \min\{Q_{downstream,t\text{-}s}\} \quad | \; s = [1h; 23h] \tag{6.16}$$

10. The upper $Q_{turbine\,max}$ [m^3/s] and lower turbine limit $Q_{turbine\,min}$ [m^3/s] are defined by taking into account the user-defined hydropeaking factor α_{peak} [-] and the discharge $Q_{upstream}$ [m^3/s] of the upstream river reach:

$$Q_{turbine\,max,t} = Q_{peak\,min,t} \cdot \alpha_{peak} - Q_{upstream,t} \tag{6.17}$$

$$Q_{turbine\,min,t} = Q_{peak\,max,t} / \alpha_{peak} - Q_{upstream,t} \tag{6.18}$$

11. If turbine operation Q is higher than $Q_{turbine\,max}$, $Q_{turbine\,max}$ is released. If Q is lower than $Q_{turbine\,min}$, $Q_{turbine\,min}$ is released. When Q is located between these two values, Q is released:

$$Q'_t = \begin{cases} Q_{\text{turbine min},t} & \left| Q_t < Q_{\text{turbine min},t} \right. \\ Q_t & \left| Q_{\text{turbine min},t} \le Q_t \le Q_{\text{turbine max},t} \right. \\ Q_{\text{turbine max},t} & \left| Q_t > Q_{\text{turbine max},t} \right. \end{cases} \tag{6.19}$$

The ecological criterion (Eq. 6.15 to 6.19) is applied at the end of the optimization procedure and has therefore a high impact on the HPP operation. In case of complex systems with compensation basins, smaller time steps are recommended to avoid too abrupt on-off activities leading to empty reservoirs and thus operation interruption. For the following simulations, the hydropeaking factor α_{peak} is set constant for the whole year. Intra-annually changing restrictions could be implemented in a further extension, respecting seasonal behavior of aquatic and riparian environment. Ecological performance can then be assessed by other hydraulic indicators (e.g., HP_1 or r_{HP}) or more sophisticated biologically-based approaches.

All parameters of the reservoirs (water, level, volume, spillway release), the power plants (discharge, hydraulic head, power, revenue) and the other hydraulic elements (inflow, discharge at junctions, derivations, water intakes, river reaches, etc.) are computed for every time step and saved as an hourly mean value. Total revenue is the sum of the benefits from turbine operations and the pumping costs and does not take into account any maintenance, administrative or capital costs.

6.2.3 Parameter Study

A parameter study on the simple high-head storage HPP (Figure 6.1) is performed. In a first analysis, optimal filling of the reservoir for all six hydrological years between 2004 and 2009 are achieved by algorithm A1, which are used as target level curves for analysis with *Routing System* (RS). The results of A1 are used as a reference case to analyze the performance of the RS approach (Figure 6.4 and Table 6.2).

The first two parameters analyzed in the 1-hour time step simulations with prediction time T_{pre} of 24 hours are the user-defined cost price P_{cost} and the level coefficient α_{lev}'. For the years 2004, 2005 and 2007, best performance is achieved for a P_{cost} of €50 /MWh, whereas the other years show slightly higher values with P_{cost} of €70 /MWh. If the cost price is too low, water is released during hours with low energy price, reducing revenue. If P_{cost} is set too high, only a few operations are undertaken and the reservoir target level α_{lev} becomes the driver criteria. In the present case, €50 /MWh allows satisfactory performance ratios between 0.68 and 0.80 comparing to A1. In addition, the influence of the level coefficient α_{lev}' is tested. When using the optimum target level curve as a reference, higher α_{lev}' generally leads to higher revenue. In specific cases, e.g., in 2004, high dependence on the reservoir target level can reduce flexibility and thus the ability to choose hours of highest electricity price. Furthermore, α_{lev}' of 10 does not considerably increase the revenue in comparison with a value of 3. When considering the case with P_{cost} of €50 /MWh and α_{lev}' of 3, performance ratios between 0.74 and 0.79 are achieved. Using the same values with an average target level curve for the six years, performance decreases by between 2% (2008) and 8% (2004). An opposite effect is shown by decreasing the time step from 1 hour to 10 minutes. Even when energy price and inflow time series are of hourly resolution, shorter time

steps increase flexibility and allow short turbine operations during peak-load hours and thus the revenue.

Table 6.2. Revenue for algorithm A1 and *Routing System* (RS) simulations with simple HPP for the hydrological years 2004-2009, prediction time (T_{pre}) of 24 h, different cost prices (P_{cost}) and user-defined level coefficients (α_{lev}'). As a target level curve the specifically optimized (Spec.) or the average over the six years (Aver.) is chosen. Time steps are either 1 hour (1h) or 10 minutes (10'). Performance ratio RS/A1 is the ratio between the revenue from the *Routing System* (RS) simulation and the revenue from the application of algorithm A1.

T_{pre}	[h]	A1	24	24	24	24	24	24	24	24	24	24	24
P_{cost}	[€/MWh]		25	25	25	50	50	50	75	75	75	50	50
α_{lev}'	[-]		1	3	10	1	3	10	1	3	10	3	3
Target level			Spec.	Spec.	Spec.	Spec.	Spec.	Spec.	Spec.	Spec.	Spec.	Aver.	Spec.
Time step			1h	1h	1h	1h	1h	1h	1h	1h	1h	1h	10'
2004 Revenue	[M€]	2.57	1.91	1.94	1.95	2.01	2.03	1.97	1.87	1.97	1.93	1.82	2.12
Ratio RS/A1	[-]	1.00	0.74	0.75	0.76	0.78	0.79	0.77	0.73	0.76	0.75	0.71	0.83
2005 Revenue	[M€]	3.90	2.51	2.77	2.93	2.80	2.89	2.98	2.49	2.75	2.93	2.62	3.26
Ratio RS/A1	[-]	1.00	0.64	0.71	0.75	0.72	0.74	0.76	0.64	0.71	0.75	0.67	0.84
2006 Revenue	[M€]	5.96	3.17	3.67	4.19	4.06	4.40	4.46	4.45	4.45	4.62	4.03	5.03
Ratio RS/A1	[-]	1.00	0.53	0.62	0.70	0.68	0.74	0.75	0.75	0.75	0.78	0.68	0.84
2007 Revenue	[M€]	3.69	2.39	2.60	2.71	2.71	2.79	2.82	2.64	2.72	2.73	2.56	3.08
Ratio RS/A1	[-]	1.00	0.65	0.71	0.74	0.73	0.76	0.76	0.72	0.74	0.74	0.70	0.84
2008 Revenue	[M€]	6.26	3.63	4.11	4.73	4.63	4.88	4.99	5.03	5.04	5.03	5.34	5.24
Ratio RS/A1	[-]	1.00	0.58	0.66	0.76	0.74	0.78	0.80	0.80	0.80	0.80	0.76	0.84
2009 Revenue	[M€]	4.53	3.08	3.24	3.24	3.48	3.52	3.53	3.59	3.60	3.60	3.24	3.73
Ratio RS/A1	[-]	1.00	0.68	0.71	0.71	0.77	0.78	0.78	0.79	0.79	0.79	0.72	0.82

Table 6.3. Revenue for simulations with simple HPP for the hydrological year 2004, a cost price (P_{cost}) of €50 /MWh, a user-defined level coefficients (α_{lev}') of 3, the specific target level curve (Spec.) and prediction times (T_{pre}) between 0 and 168 hours (1 week). T_{pre} of 24 hours is the reference case.

T_{pre}	[h]	0	6	12	18	24	48	72	168
P_{cost}	[€/MWh]	50	50	50	50	50	50	50	50
α_{lev}'	[-]	3	3	3	3	3	3	3	3
Target level		Spec.	Spec.	Spec.	Spec.	Spec.	Spec.	Spec.	Spec.
2004 Revenue	[M€]	1.28	1.97	2.01	2.03	2.03	2.06	2.06	2.09
Ratio to reference	[-]	0.63	0.97	0.99	1.00	1.00	1.02	1.02	1.03

Regarding the prediction time T_{pre} for 2004 with P_{cost} of €50 /MWh and α_{lev}' of 3 (Table 6.3), T_{pre} of 24 hours defines the reference case. Instantaneous production without any prediction shows a performance ratio of only 0.63. The lack of knowledge in terms of energy price and inflow makes optimization inefficient. By increasing T_{pre} to

only 6 hours, satisfactory performance of 0.97 is achieved. A T_{pre} longer than 24 hours accounts for slightly higher revenue. Regarding the unrealistic values of 48 hours and longer, the increase by only 2% and 3% is relatively low. As revealed by these results, the heuristic approach implemented in *Routing System* allows satisfactory performance for a prediction time T_{pre} of 24 h, normally relevant for day-ahead decisions.

The impact analysis regarding ecological constraints is presented for the year 2006 (Table 6.4) and refers to the reference case without any restrictions. The analysis of the impact of the hydropeaking factor α_{peak} on different hydraulic key figures, such as the mean winter daily peak Q_{peak} and low $Q_{off\text{-}peak}$ flow, the hydropeaking ratio r_{HP}, the annual means of the daily drawdown ranges Q_{max}/Q_{min} and the hydropeaking indicators HP_1, is performed. The analysis of the winter months with low residual flow in the upstream river reach reveals mainly lowered peak values Q_{peak} and only for low values of α_{peak} an increase of $Q_{off\text{-}peak}$. r_{HP} indicates respect of the implemented α_{peak}, at least in 80% of winter days. Annual values are less affected due to summer months with satisfactory flow regime, even without intervention. In consequence, the annual means of the daily drawdown ranges Q_{max}/Q_{min} is always significantly under the set hydropeaking factor α_{peak}. The ecological improvements are faced with high economic losses. Whereas for α_{peak} of 5:1 8% less revenue is generated, 3:1 makes already a difference of 17%. High operation restrictions can even induce water release by the spillways and therefore decreasing turbine volumes. The hydropeaking factor α_{peak} is an effective variable to influence flow regime. The related costs can be easily estimated.

Table 6.4. Revenue and flow regime indicators (mean winter daily peak Q_{peak} and low $Q_{off\text{-}peak}$ flow, hydropeaking ratio r_{HP}, annual means of daily drawdown ranges Q_{max}/Q_{min} and hydropeaking indicators HP_1 for simulations with the simple HPP for the hydrological year 2006, a cost price (P_{cost}) of €50 /MWh, a user-defined level coefficient (α_{lev}') of 3, the specific target level curve, a prediction time (T_{pre}) of 24 hours, a time step of 10 minutes and different hydropeaking factors (α_{peak}). The scenario without ecological restrictions (no) is the reference case.

Hydropeaking factor	α_{peak}	[-]	no	10:1	8:1	6:1	5:1	4:1	3:1	2:1	1.5:1
Revenue		[M€]	5.03	5.02	4.92	5.03	4.76	4.51	4.19	3.40	3.34
Ratio to reference		[-]	1.00	1.00	0.98	1.00	0.95	0.90	0.83	0.68	0.66
Annual operated volume		[10^6 m^3]	37.3	37.3	37.3	37.3	37.3	37.3	37.4	37.3	36.1
Average between October-December of daily	Q_{peak}	[m^3/s]	13.4	13.4	11.2	13.4	8.4	5.8	4.6	3.3	3.2
	$Q_{off\text{-}peak}$	[m^3/s]	1.3	1.3	1.3	1.3	1.3	1.3	1.4	1.4	1.4
	r_{HP}	[-]	10.2	10.0	8.0	10.2	6.0	4.0	3.0	2.0	1.5
Annual average of daily	Q_{max}/Q_{min}	[-]	4.2	4.1	3.8	4.2	3.4	2.8	2.4	1.8	1.4
	HP_1	[-]	1.67	1.62	1.45	1.67	1.29	1.06	0.82	0.55	0.34

6.3 Case study

The upper Aare River catchment is located upstream of Lake Brienz in the central part of the Swiss Alps (Figure 6.7). It is located between 564 m a.s.l. (Lake Brienz) and 4274 m a.s.l. (Finsteraarhorn) and has a surface area of about 554 km^2. Six main glaciers as well as several ice patches are located within the study area. The Aare River, also-called Hasliaare, springs in the Unteraar and Oberaar Glaciers. Nowadays, it flows through several artificial reservoirs, in which the main part of the water is temporarily stored to be operated by the turbine units. In Innertkirchen the water is given back to the Aare River immediately downstream of the confluence with the Gadmerwasser, the river draining the eastern part of the catchment area. The hydrological regime of the river is glacial or glacio-nival with an average annual discharge of 35 m^3/s.

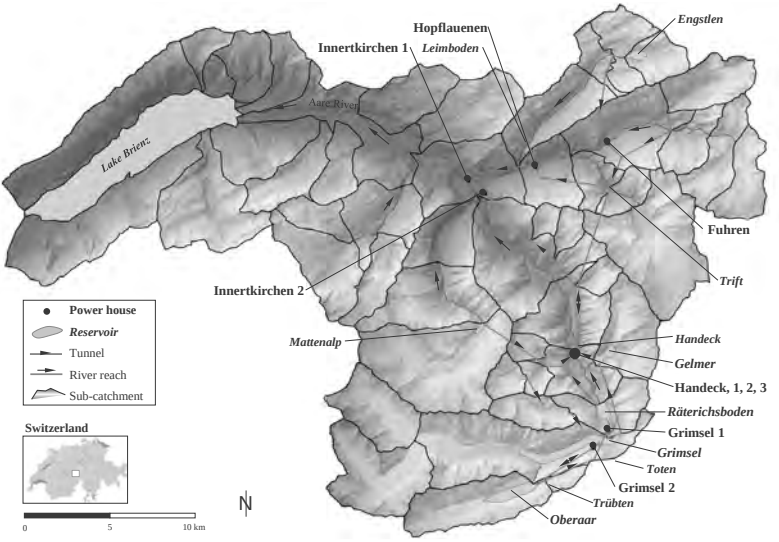

Figure 6.7. Map of the upper Aare River catchment with today's KWO hydropower scheme (reservoirs, power houses and tunnels), the sub-catchments areas and the river network with its location in Switzerland.

6.3.1 Hydropower scheme

At the end of the 19th century, the Oberhasli area was recognized appropriate for hydropower exploitation. Heavy rainfalls, large retention areas, solid granitic bedrock as well as substantial slopes provide optimal conditions for high-head storage hydropower. The first gravity and arch dams of Lake Grimsel and Gelmer were built by the Kraftwerke Oberhasli AG (KWO) hydropower company between 1925 and 1932. Since then, a complex scheme with several reservoirs (Figure 6.5) and nine power houses (Figure 6.6) has been constructed (Figure 6.8a). The largest reservoirs are Lake Grimsel, Oberaar, Räterichsboden (Räbo) and Gelmer. Lake Oberaar at 2303 m a.s.l. is the highest reservoir. Most of the reservoirs are fed by water intakes collecting the water in several side valleys. The western part of the catchment area is drained by the Mattenalp intake, which releases the water by gravity to Lake Räterichsboden. In the eastern

drainage basin, the water is collected by the Trift intake and can be pumped to Lake Räterichsboden. The main water from the Gadmerwasser and Gentalwasser Rivers is operated by the hydropower scheme providing only small compensation basins without the ability of seasonal transfer.

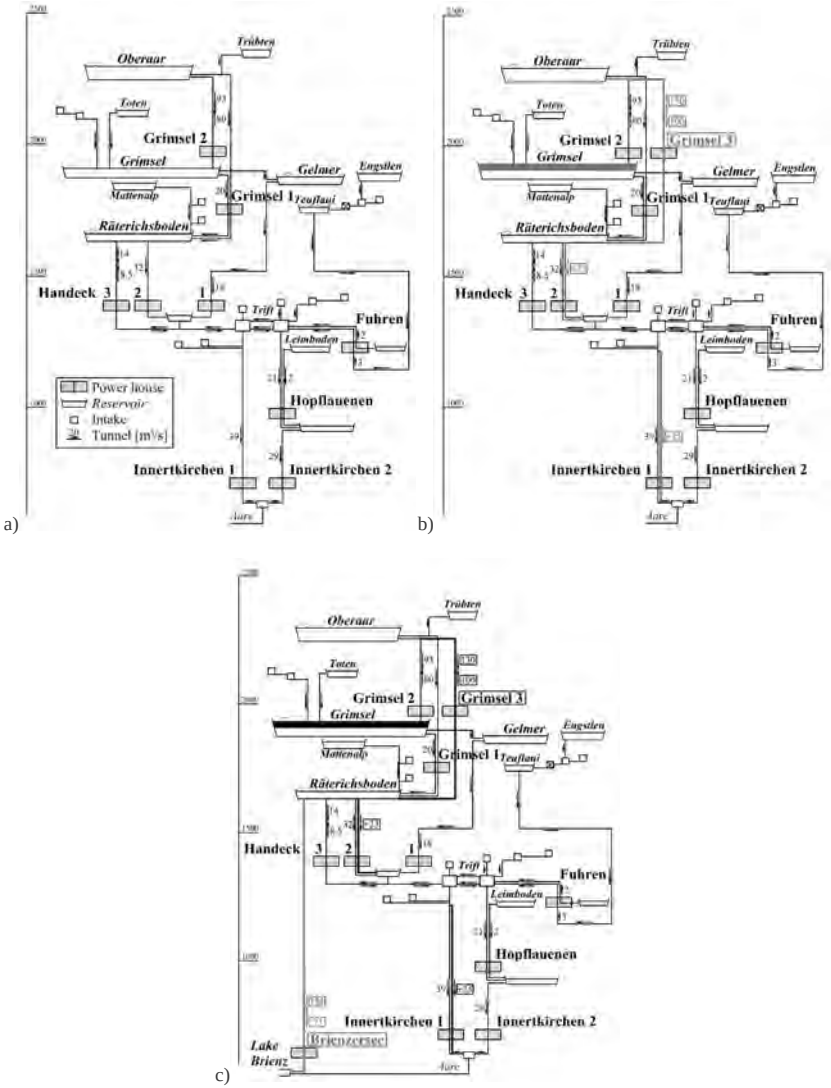

Figure 6.8. Sketch showing power houses, reservoirs and their interconnections for today's scheme (a), the enhancement project *KWOplus* (KWO+) (b), containing the upgrading of Handeck 2 and Innertkirchen 1 HPPs, the implementation of the Grimsel 3 pumped-storage plant and the increased Lake Grimsel, and the upgraded scheme with the Brienzersee pumped-storage plant (KWO++) (c).

Table 6.5. Technical characteristics of the dams and the reservoirs of KWO.

Name	Year	Type	Height [m]	Elevation [m a.s.l.]	Minimum [m a.s.l.]	V_{net} [10^6 m^3]	V_{tot} [10^6 m^3]
Oberaar	1953	Gravity dam	104	2303.0	2250.0	57.3	63.6
Grimsel				1908.7	1850.0	93.9	100.5
Seeuferegg	1932	Gravity dam	42				
Spitelamm	1932	Arch dam	114				
Räterichsboden	1950	Gravity dam	92	1767.0	1712.0	25.0	26.3
Gelmer	1929	Gravity dam	35	1849.7	1818.0	13.0	13.2
Toten	1950	Gravity dam	20	2160.0	2132.0	2.6	-
Trübten	1950	Gravity dam	48	2365.2	2346.7	1.1	-
Mattenalp	1950	Gravity dam	25	1875.2	1862.0	1.8	-
Engstlen	-	Natural lake	-	1850.5	1846.3	2.0	-
Teuflaui	1960	Compensation basin	-	1732.0	1728.0	0.023	-
Fuhren	1960	Compensation basin	-	1152.0	1150.0	0.016	-
Handeck	1942	Compensation basin	-	1301.7	1296.0	0.035	-
Handeck	1942	Comp. cavern	-	1301.7	1296.0	0.050	-
Leimboden	1967	Compensation basin	-	1201.8	1199.8	0.016	-
Hopflauenen	1967	Compensation basin	-	861.7	858.0	0.058	-
Grimsel*				1931.7	1850.0	165.6	172.2
Seeuferegg	2019	Gravity dam	65				
Spitelamm	2019	Arch dam	137				

* = *KWOplus* scheme; Height = dam height; Elevation = maximum operation level; V_{net}, V_{tot} = net/total reservoir volume

In the upgrading program *KWOplus* (KWO+), several technical, economic and ecological improvements of the actual scheme are foreseen (Figure 6.8b). An increase in storage capacity of Lake Grimsel up to $170 \cdot 10^6$ m^3 is achieved by a heightening of the Seeuferegg and Spitelamm dams by 23 m (Table 6.5). Power generation can be optimized through a better distribution of the water during the year. In parallel, the turbine capacities of Handeck 2 and Innertkirchen 1 HPPs will be increased by 23 m^3/s and 25 m^3/s, respectively, corresponding to a 240 MW power increase (Table 6.6). The new 600 MW Grimsel 3 pumped-storage plant, using the water from the two existing lakes Oberaar and Räterichsboden, has a turbine capacity of 130 m^3/s and a pump capacity of 100 m^3/s. The listed projects of *KWOplus* are under construction now and should be completed by 2019. A further idea for the enhancement of the KWO scheme is the Brienzersee pumped-storage plant, operating between Lake Brienz and Lake Räterichsboden (Figure 6.8c). A first design foresees a design discharge of 124 m^3/s for the turbines and 100 m^3/s for the pumps. This power plant would increase flexibility and could reduce hydropeaking in the Aare River by by-passing the major water directly to Lake Brienz.

Table 6.6. Technical characteristics of the hydropower plants.

Name	Year	Type	#Gr.	$P_{turbine}$ [MW]	P_{pump} [MW]	$Q_{turbine}$ [m^3/s]	Q_{pump} [m^3/s]	H [m]	Upper reservoir	Lower reservoir
Grimsel 1										
M. Oberaar	1954	P	1	35		8		533	Oberaar	Räbo
M. Grimsel	2006	P	1	32		20		182	Grimsel	Räbo
Grimsel 2	1980	F	4	348	363	93	80	400	Oberaar	Grimsel
Handeck 1	1932	P	4	100		20		547	Gelmer	Handeck
Handeck 2	1950	P	4	136		32		463	Räbo	Handeck
Handeck 3	1976									
Isogyre		F	1	55	46	14	8.5	450	Räbo	Handeck/Trift
Diagonal		F	1		4.5		7.5	30	Trift	Handeck
Innertkirchen 1	1942	P	5	255		39		672	Handeck	Aare River
Fuhren	1960									
Turbine		F	1	10		3		400	Teuflaui	Trift
Pump		F	1		5		2	184	Trift	Fuhren
Hopflauenen	1967									
M. Trift		P	2	86		21		459	Trift	Hopflauenen
M. Leimboden		P	1	6		2		336	Leimboden	Hopflauenen
Innertkirchen 2	1968	F	2	62		29		242	Hopflauen.	Aare River
Innertkirchen 1^+	2015	P	6	405		64		672	Handeck	Aare River
Handeck 2^+	2015	P	5	222		55		463	Räbo	Handeck
Grimsel 3^+	2018	F	3	660	*	130	100	*	Oberaar	Räbo
Brienzersee^{++}				*	*	124	93	*	Räbo	Lake Brienz

$^+$ = *KWOplus* scheme (to be completed), $^{++}$ = future enhancement (called KWO++); P, F = Pelton/Francis turbine; $P_{turbine}$, P_{pump} = installed turbine/pump capacity; $Q_{turbine}$, Q_{pump} = turbine/pump discharge; H = net head, * = defined in the model by corresponding reservoir elevations and efficiency factors

6.3.2 Model

Inflow

Inflow to the reservoirs and the main water intakes for the past time period 2005-2009 and the two future periods 2046-2050 and 2095-2099 is provided by the hydrological model, calibrated with precipitation, temperature, glacier melt and runoff data as mentioned in Chapter 5, for the C2SM-ETHZ scenario. It contains inflow from surface runoff as well as groundwater from infiltration. The evapotranspiration is also considered. This assumption is justified by the steep reservoirs, which would only marginally affect seasonal water surface exposition. The flow regime of the catchment area is expected to change from glacio-nival to nival during the 21st century (Figure 6.9). For all time periods, inflow data is provided as daily values from the database.

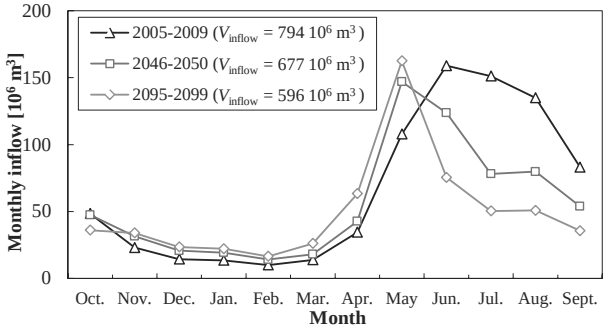

Figure 6.9. Monthly inflow volume to the catchment area operated by KWO for the three time periods of 2005-2009, 2046-2050 and 2095-2099 based on the C2SM-ETHZ scenario (V_{inflow} = volume of annual inflow).

Electricity price scenarios

Nowadays, only a small part of the electric energy is traded on the free energy market, like the European Energy Exchange (EEX). Most of the energy is delivered in conformity to long-term commitments. In future, a single European electricity market will be formed. Key infrastructure projects such as the expansion and interconnection points at the national borders are being laid. Thus, European electricity prices are expected to rise by an average of around 4% from 2010 up until 2030 (Auer, 2010). Nevertheless, it is difficult to predict future electricity price scenarios.

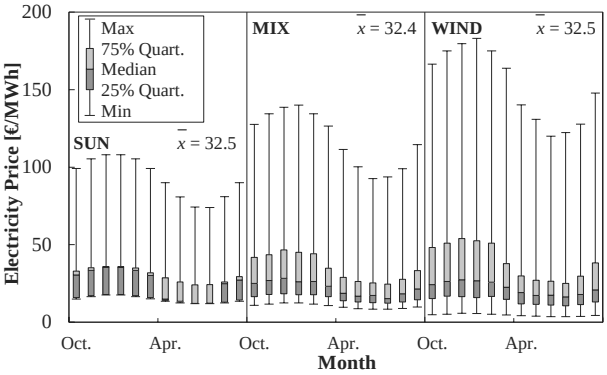

Figure 6.10. Statistical analysis of the hourly electricity price P_{el} of the scenarios with lowest (SUN), intermediate (MIX) and highest (WIND) volatility ($\bar{x}$ = average price of the hydrological year).

For this study three scenarios are developed by respecting the recently set-up environmental and climate policy readjustments (Figure 6.10). All of them have the same monthly mean values and assume higher prices in winter than in summer. The annual mean of €32.5 /MWh corresponds to the 2005 EEX scenario:

– *Scenario EEX* contains the highly unsteady market electricity prices between October 2004 and 2009 with a average price of €47.8 /MWh. It is used as reference case.

– *Scenario SUN* is based on a power supply from photovoltaic plants. High and mainly predictable solar gain during long hours in summer decreases prices and their volatility. Peak load hours are 2 in summer and 8 in winter.

– *Scenario MIX* is an intermediate case, assuming a mixture of energy suppliers and therefore slightly volatile market behavior.

– *Scenario WIND* assumes a lot of new wind power capacities in Europe. Wind turbines have the disadvantage of fluctuating and unpredictable production. Furthermore, winter production is by about 30% higher than the summer one (Pryor *et al.*, 2006). High peaking accounts for rapidly varying electricity prices with sometimes extremely high but also very low values.

Power plants

The technical data necessary for model built-up is provided by the Kraftwerke Oberhasli AG for today's (KWO) and the two future layouts (KWO+ and KWO++), as shown in Figure 6.8. For each plant (Table 6.6), turbine and pump discharge, respectively, the energy rate function (ratio between discharge, head and power) and the turbine elevation (relevant for Pelton turbines) are defined. As pump and turbine operations are either of full or no release and the high net heads are relatively indifferent to lake filling, a constant energy rate of 85% is chosen for all HPPs. For the upper and lower reservoir, the corresponding maximum and minimum storage volumes are defined. The minimum values are plant and not reservoir-dependent due to the design criteria of the intake. The western and eastern cascades from Oberaar to Innertkirchen 1 HPP and from Engstlen to Innertkirchen 2 HPP are sensitive to non-continuous operation, especially when containing small compensation basins, like in Handeck, Fuhren and Hopflauenen. The cost price P_{cost} is set to €35 /MWh as default. Those with relatively small upstream retention and therefore operation modes close to run-of-river are set to €25 /MWh (Innertkirchen 1 HPP and those located in the eastern catchment), those of high flexibility due to big reservoirs to €45 /MWh (Grimsel 1 and 2 HPPs). For the pumping mode, normally undertaken in periods of low energy demand (night, weekend and summer season), P_{cost} is set to €15 /MWh. Small upstream reservoirs remain α_{lev}' of about 10, whereas larger ones 5.

Reservoirs and their filling

Each reservoir (Table 6.5) is characterized by its volume-level relation, implemented as a discrete function, the annual target level curve with monthly values and the spillway facilities, containing the corresponding release rules. The initial filling of the 5-year simulation period is set to full. Volume losses at the end of the simulation period are taken into account for annual energy production and revenue computation.

Due to the change of inflow within the next decades, target level curves of the five main lakes Oberaar, Grimsel, Gelmer, Räterichsboden and Mattenalp have to be adapted. Algorithm A1 allows the definition of the target level curve by taking into account mean monthly inflow for the corresponding 30-year simulation periods (Figure 6.9) and price time series (Figure 6.10) as well as the reservoir volume and the turbine capacities. The changing volatility of the price scenarios makes the target level curve indifferent to them. The optimization started at the top of the cascade taking into account the discharges from the upstream HPPs. For the KWO, KWO+ and KWO++

hydropower schemes, target level curves are defined for each of the three time periods. Brienzersee HPP as all other pumped-storage plants has no major impact on the annual filling of the reservoirs. Due to their enormous turbine and pump capacities, the target level curves should allow an operation during the whole year, therefore avoiding completely empty or full reservoirs.

Hydropeaking

The Innertkirchen 1 and 2 HPPs are at the downstream end of the cascade and therefore responsible for hydropeaking in the Hasliaare River. Both of them have the same hydropeaking factor α_{peak} but are separately operated to achieve it for the corresponding downstream river reach ($Q_{downstream}$). The Aare and the Gadmerwasser River, respectively, are defined as corresponding upstream reaches ($Q_{upstream}$). The flow regime after the confluence as sum of the two discharge series also respect α_{peak}. Scenarios with turbine restrictions are only simulated for today's scheme and for one scenario and period.

For each of the three layouts (KWO, KWO+ and KWO++) and for each of the three time periods (2005-2009, 2046-2050 and 2094-2099), simulations for every price scenario (EEX, SUN, MIX and WIND) are performed with 1 h time steps. Then reference simulations are achieved with smaller time steps of 10 minutes with and without ecological requirements, defined by the hydropeaking factor. A combination of an enhanced scheme and operational mitigation measures is also presented. Different parameters are compared and reveal relevant information about computation as well as future operation.

6.4 Results and discussion

In reality, KWO had a mean annual energy production of 1.54 TWh/yr for the period between 2005 and 2009. From the 2.24 TWh initially produced energy, 0.69 TWh was used for pump operation, mainly for the Grimsel 2 pumped-storage plant. 36% of energy production and 50% of consumption was in winter. Comparing these figures with the simulation (KWO, 2005-2009) (Table 6.7), price scenario SUN with 2.2 TWh of production and 0.7 TWh of consumption shows best agreement. Nevertheless, winter operations are more similar to scenario EEX. Even when the real mean revenue of about 88 MCHF/yr (113 for production and -25 for consumption) is quite similar to the simulated value, it cannot be directly compared, without knowing the detailed legal and market issues of KWO's production policy. Despite the lack of knowledge and the given number of simplifications and hypothesis, realistic results can be produced for production scenarios in a free electricity market environment.

Table 6.7 in addition to Figure 6.12 and Figure 6.13 show the main results, which are commented and detailed with further information for the analysis. First the impact on the flow regime as well as the influence of time step, price sensitivity and target level curve are discussed. The main drivers, such as climate change, plant enhancement and hydropeaking, are the assessed:

Flow regime

The seasonal flow regime of the Aare River is analyzed at Brienzwiler, a place close to its outlet in Lake Brienz, where a gauging station of the Federal Office of the

Environment (FOEN) is located. Comparing the measured discharge series for 1926-1929 before the construction of the HPP and for 2004-2009 with today's scheme (Figure 6.11) by means of Pardé-coefficients (Meile *et al.*, 2011), a high increase of winter runoff by reduced summer discharge is shown. This shift is possible due to the large storage volume of the artificial reservoirs in the catchment area. The simulated curves for the price scenarios have a similar behavior with slightly higher discharge from October to December and therefore a lower one in spring. This gap could be explained by today's energy demand, which is higher in February and March than for the simulated scenarios. However, the seasonal impact on the river is quite similar for the measured and simulated data series.

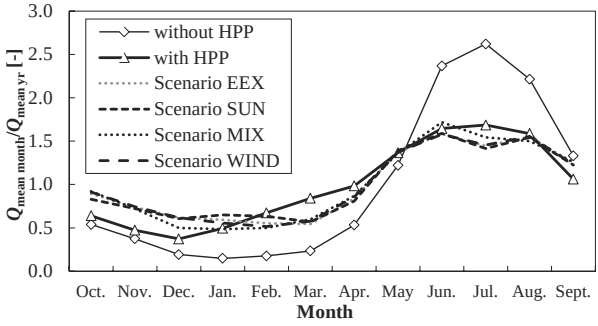

Figure 6.11. Mean values of the Pardé-coefficents as mean monthly discharge ($Q_{mean\ month}$) divided by the mean annual discharge ($Q_{mean\ yr}$) at Brienzwiler for the time period 2004-2009 and today's scheme for measured data (with HPP) as well as for simulated data for the price scenarios (EEX, SUN, MIX, WIND) compared to measured data of 1926-1929 before the construction of the HPP (without HPP).

Time step

In case of small storage volumes compared to the corresponding turbine capacities, e.g., compensation basins, the simulation time step has to be reduced from 1 hour to 10 minutes, demanding a comparison of key figures for several chosen scenarios (Table 6.7 and Table 6.8). Smaller time steps lead to slightly lower energy production due to increased consumption by pumped-storage activities. Despite the loss of energy, annual revenue can be increased by about 5% to 10%. Winter participation remains the same. Smaller time steps allow higher flexibility to operate also during short sequences when the electricity price is high. Too often start-and-stop operations seem unrealistic in terms of wear and efficiency of the turbo-machines. However, today's operation of the Grimsel 2 pumped-storage plant shows highly unsteady behavior. The definition of the short-term production timetable is done on a basis of 1 hour or 10 minutes, whereas real production is fully demand-driven and therefore instantaneous. To analyze the flow regime, smaller time steps are therefore preferred, even when averaged by hourly values for data storage reasons. In reality, lower production than the total capacity could also correspond to an operation of only some of the power units available in a plant.

Price sensitivity

Comparing the annual revenue for the three developed electricity price scenarios (Table 6.7), highest values are achieved for WIND, whereas SUN has the lowest. The difference between them is generally between 15% and 25%, except for 2005-2009, where the difference is close to 50%. Highly fluctuating energy prices with high peak and low off-peak values are an advantage for pumped-storage plants. The increasing production and consumption of energy indicate their higher activity. The energy balance is therefore decreasing. Winter operation is higher for the regular SUN scenario. The EEX scenario with the highest average price generates for today's scheme and inflow highest benefits. For future periods and HPP enhancements, it loses this ranking.

For KWO+ and KWO++, price scenario WIND generates maximum revenue independent of the time period (Figure 6.13). A similar behavior is shown for MIX. High inflow and full reservoirs as a consequence can be a problem for pumped-storage activities. The SUN scenario is less appropriate for this operation mode. It generates highest revenue for 2046-2050, having still enough runoff from glacierized catchments and allowing for lake management to conform to the rigid price scenario in addition to pumped-storage activities.

Target level curve

As shown for the parameter study, the target level curve of the reservoir has an impact on the HPP operation. By applying the curves of 2005-2009 for the period 2095-2099 for KWO and price scenario MIX, slightly different figures are found. A nival regime needs an earlier filling than the glacial one. Indeed, total energy production stays with 1.0 TWh/yr the same. But due to the incomplete filling of the reservoirs, winter production is smaller. Pump activities are similar. The lower net head as well as the higher winter energy prices decrease the total revenue from €109 to €101 M/yr. This result shows that even rough estimations of inflow as well as electricity demand can improve the profitability, when corresponding to reality. The risk of special effects like exceptionally dry or wet years is not further discussed, but is recognized as source of uncertainty.

Climate change

The loss of inflow due to glacier melt decreases the available water resources and therefore the total energy production (Table 6.7). Excluding the pumped-storage activities, total production decreases from 1.75 TWh/yr for 2005-2009 to 1.48 TWh/yr at mid-century and 1.29 TWh/yr at the end of the century. These losses of 15% and 25%, respectively, are considerable. However, the large storage capacities allow the same energy production of 0.7 TWh (KWO), 0.8 TWh (KWO+) and 1.0 TWh (KWO++) in winter for the future scenarios. Lower turbine as well as pump operation for today's scheme in future is due to the early filling of the lakes in spring and the water storage during low economic attractiveness in summer. Thanks to stable winter production, revenue is only slightly decreasing.

Table 6.7. Selected energy (electricity production and consumption) and economic (total revenue of energy trading) key figures of the parameter study on the hydropower scheme of KWO for today's (KWO) and two different extended schemes (KWO+ and KWO++) for the four electricity price scenarios (EEX, SUN, MIX, WIND) and three time periods (2005-2009, 2046-2050, 2095-2099). The simulations are performed with a time step of 1 hour.

	Period		2005-2009				2046-2050				2095-2099			
	Electricity price scenario		EEX	SUN	MIX	WIND	EEX	SUN	MIX	WIND	EEX	SUN	MIX	WIND
KWO	Production	[TWh/yr]	2.6	2.2	2.5	2.6	2.3	2.0	2.3	2.4	2.1	1.8	2.1	1.8
	Production Winter	[%]	41	46	44	44	49	57	54	52	52	59	54	59
	Consumption	[TWh/yr]	-1.2	-0.7	-1.1	-1.2	-1.2	-0.7	-1.1	-1.3	-1.2	-0.7	-1.2	-0.7
	Consumption Winter	[%]	53	71	58	54	53	70	57	52	53	66	53	66
	TOTAL	[TWh/yr]	1.4	1.5	1.4	1.4	1.1	1.3	1.2	1.1	0.9	1.1	0.9	1.1
	Revenue	[M€/yr]	128	108	118	127	115	105	112	123	105	101	109	116
	Revenue Winter	[%]	43	66	66	64	52	74	72	70	55	74	71	70
KWO+	Production	[TWh/yr]	3.9	3.1	3.7	3.9	3.6	3.1	3.6	3.7	3.5	3.0	3.7	3.8
	Production Winter	[%]	48	58	54	52	54	65	59	58	55	63	57	56
	Consumption	[TWh/yr]	-3.0	-2.0	-2.8	-3.1	-2.9	-2.2	-2.9	-3.1	-3.0	-2.4	-3.3	-3.5
	Consumption Winter	[%]	53	69	58	55	53	68	57	55	52	63	53	52
	TOTAL	[TWh/yr]	0.9	1.1	0.9	0.8	0.7	0.9	0.7	0.6	0.5	0.6	0.4	0.3
	Revenue	[M€/yr]	157	125	173	190	145	162	174	189	135	157	173	190
	Revenue Winter	[%]	51	65	74	71	58	78	77	75	60	76	75	73
KWO++	Production	[TWh/yr]	7.0	6.5	7.2	7.4	6.5	5.9	6.9	7.2	6.5	5.5	6.8	7.2
	Production Winter	[%]	50	55	52	51	54	65	57	56	54	66	57	55
	Consumption	[TWh/yr]	-7.2	-6.6	-7.5	-7.8	-6.9	-6.2	-7.5	-7.9	-7.2	-5.8	-7.6	-8.1
	Consumption Winter	[%]	52	58	53	52	53	64	55	53	52	65	54	52
	TOTAL	[TWh/yr]	-0.2	-0.1	-0.3	-0.4	-0.4	-0.3	-0.6	-0.7	-0.7	-0.3	-0.8	-0.9
	Revenue	[M€/yr]	242	232	286	345	229	292	318	349	224	282	312	350
	Revenue Winter	[%]	54	77	77	72	59	78	76	74	59	78	75	72

Plant enhancements

The enhancement of the KWO hydropower scheme by new turbine and pump capacities (KWO+) increases electricity production as well as consumption. In combination with increased storage volume of Lake Grimsel, winter production can be raised from 0.7 TWh today to 0.8 TWh and 1.0 TWh, respectively. The shift from summer to winter increases in future due to lower runoff and big storage volumes, and when enhancing the scheme due to the ability of pumping water in fall to fill the reservoirs for winter.

For the KWO++ outline with full pumped-storage on the whole cascade, energy balance is even negative, as the total efficiency is of $0.85^2 = 0.72$. However, revenue can be increased up to values between €232 and €345 M/yr with today's inflow. These values are quite resistant to climate change due to the high pumped-storage capacity. Analysis of revenues has to be completed by taking into account the capital costs of future enhancements. An investment of a billion € with an inflation rate of 1%, an interest rate of 4%, a construction time of 5 years and a redemption time of 50 years would generate capital costs of about €80 M/yr. Investments are thus only economic when price scenarios with highly fluctuating behavior make pumped-storage operation attractive.

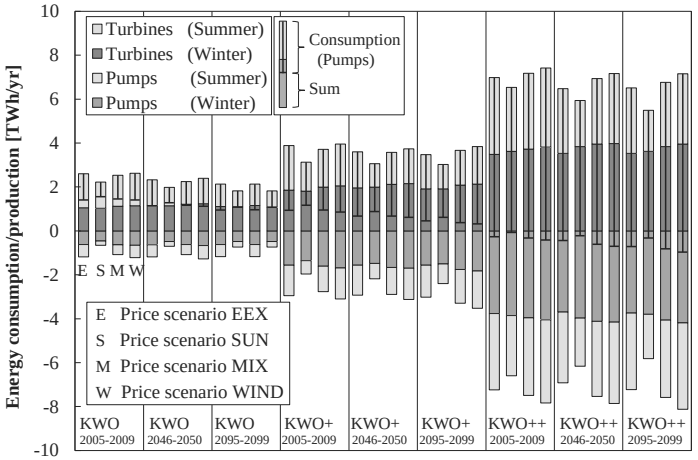

Figure 6.12. Mean annual energy consumption and production for winter (ONDJFM) and summer (AMJJAS) period as well as total energy balance (Total) for the three HPP outlines (KWO, KWO+, KWO++), the four price scenarios (EEX, SUN, MIX, WIND) and the three time periods (2005-2009, 2046-2050, 2095-2099).

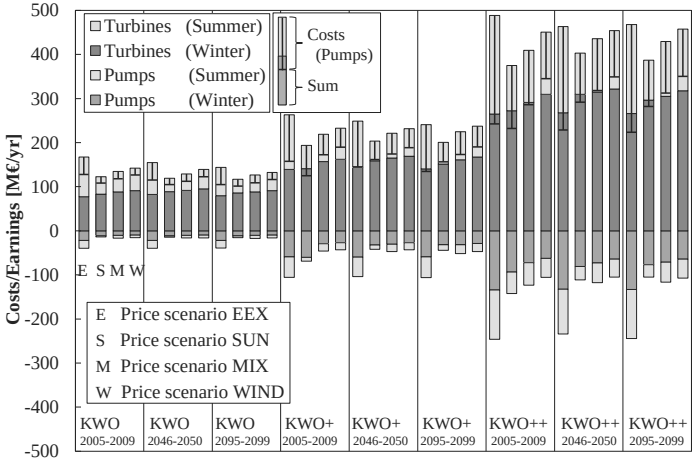

Figure 6.13. Mean annual costs from pump operations and earnings from turbine operations for winter (ONDJFM) and summer (AMJJAS) period as well as total revenue (Total) for the three HPP outlines (KWO, KWO+, KWO++), the four price scenarios (EEX, SUN, MIX, WIND) and the three time periods (2005-2009, 2046-2050, 2095-2099).

Hydropeaking

Even when ecological response to hydropeaking is not completely understood, it has been shown that a highly fluctuating flow regime disturbs the natural abiotic structure of the ecosystems (Poff *et al.*, 1997; Cowx *et al.*, 1998; Bunn and Arthington, 2002; Jungwirth *et al.*, 2002). Thus, simulations with respect to the predefined hydropeaking factor α_{peak} for Innertkirchen 1 and 2 HPPs are performed. The application of the hydropeaking factor α_{peak} at the end of the optimization procedure makes flow regime the dominant constraint. This can be justified by the legal and therefore compulsory character of this criterion. In Switzerland, the official guidance defines the hydropeaking ratio r_{HP} (Eq. 6.2) among others as official evaluation criteria. For measured discharge series at the turbine outlets in Innertkirchen, r_{HP} is between 5.3 (2008) and 9.6 (2006). These values are lower than the simulated 14.9 (Table 6.8). The reasons for this gap are again the different driving parameters. Fully market-driven production undertakes on-off operations even for short periods, whereas today's contract-based production is less fluctuating. Turbine sequences with maximum discharge were also undertaken in reality, just less frequently than simulated. The two flow regimes cannot be directly compared. The simulated scenarios stand for a future behavior corresponding to an open and electricity price-driven market.

Table 6.8. Selected energy (electricity production and consumption), economic (total revenue of energy trading) and ecological (average daily hydropeaking ratio r_{HP}, drawdown range Q_{max}/Q_{min}, parameter HP_1) key figures of the parameter study on the hydropower scheme of KWO for today's (KWO) and two different extended schemes (KWO+ and KWO++) for the electricity price scenario MIX and two time periods (2005-2009, 2095-2099). The simulations are performed with a time step of 10 minutes.

Period		2005-2009							2094-2099		
Scheme		KWO	KWO	KWO	KWO	KWO+	KWO++	KWO++	KWO	KWO+	KWO++
Hydropeaking factor α_{peak}	[-]	no	12:1	8:1	5:1	no	no	2:1	no	no	no
Production Total	[TWh/yr]	2.5	2.5	2.5	2.5	3.6	6.6	6.7	2.1	3.5	6.6
Production Winter	[%]	45	45	45	45	56	55	52	54	57	56
Consumption Total	[TWh/yr]	-1.1	-1.1	-1.1	-1.1	-2.6	-6.8	-6.9	-1.2	-3.1	-7.5
Production Winter	[%]	59	59	59	59	60	56	54	54	53	53
TOTAL	[TWh/yr]	1.4	1.4	1.4	1.4	1.0	-0.2	-0.2	0.9	0.4	-0.9
Revenue	[M€/yr]	123.7	122.8	121.7	119.8	190.8	315.7	289.7	114.1	184.0	323.0
Revenue Winter	[%]	66	66	65	65	74	75	72	71	75	74
r_{HP}	[-]	15.0	12.2	8.6	7.0	20.4	20.3	2.7	15.1	20.4	20.4
Q_{max}/Q_{min}	[-]	9.4	7.5	5.8	4.8	12.4	12.8	2.4	10.9	13.2	13.4
HP_1	[-]	2.1	1.9	1.7	1.5	2.5	2.5	0.8	2.5	2.8	2.8

Too low hydropeaking factors α_{peak} result in turbine operations during low flow periods. When no water is available in the upper reservoir, also the upstream located HPP has to undertake unplanned production. As shown in Table 6.8, α_{peak} of 12:1 and 8:1 reduce r_{HP} from initially 15.0 to 12.2 and 8.6, respectively, whereas annual mean drawdown ranges are below the target value. Higher reduction of 5:1 also allows lowering Q_{max}/Q_{min} during the year; whereat r_{HP} could be reduced to only 7.0. The related costs of €0.9, €2.0 and €3.9 M/yr are already high. Lower α_{peak} would influence also the upper power plants, including management of Lake Räterichsboden. Due to this drastic

influence, it is not possible to apply this ecological criterion without other temporal or local restrictions. This could consist in a limitation of the maximum turbine capacity of the involved plants or an increase of residual flow in a critical river reach. The increase of the turbine capacity of Innertkirchen 1 HPP from 39 to 64 m^3/s in the framework of *KWOplus* boosts r_{HP} up to 20.4. Comparison of the flow regimes of 2005-2009 and 2095-2009 reveal no relevant difference in terms of hydropeaking, as discussed in Bieri and Schleiss (2011). Future extensions of the hydropower scheme like the Brienzersee pumped-storage plant could be combined with ecological constraints on the Aare River. A hydropeaking factor α_{peak} of 2:1 allows a reduction of r_{HP} from 20.3 to 2.7, but reduces also revenue from €316 M/yr to €290 M/yr for today's inflow. An economic evaluation taking into account investment costs, legal constraints and negotiations with the authorities would allow a feasibility analysis of this ecologically probably promising alternative.

6.5 Conclusion

A simulation tool for the operation of high-head storage hydropower plants was developed, tested by a parameter study and applied to the complex Oberhasli scheme in Switzerland. The nonlinear optimization problem in response to climatic, hydrological, economic and ecological issues is solved by a deterministic heuristic approach in the semi-distributed conceptual environment of *Routing System*. Within the case study, and despite the complexity of the HPP network, the influence of climate change, electricity market issues, plant enhancements as well as hydropeaking constraints were simulated and assessed. It reveals the importance of long-term analysis for HPP operators to be prepared for future challenges. The wide range of the investigated hypothetical scenarios allows definition of several guide-lines for the sustainable use of hydropower in future.

Future climate in mountainous areas as defined in Chapter 5, with slightly higher runoff in winter and spring due to increased temperature and resulting snowmelt, but remarkably lower summer runoff, due to the diminishing glacier, will reduce annual inflow to the reservoirs. As a consequence, the total annual electricity production will decrease in the same range as the runoff by about 15% until 2050 and by about 25% by the end of the century. Thanks to the flexible operation of the pumped-storage plant in the network, revenue decreases less drastically with 4% and 8%.

An open electricity market with a lot of wind power capacities would affect volatility more than the average price. High fluctuations are an opportunity for storage as well as pumped-storage hydropower facilities to generate higher revenue. Thus, higher volatility will increase economic efficiency of hydropower in mountainous areas.

Enhancements of the hydropower scheme with new turbine in addition to pumping capacities allow increasing revenue by lowering total energy output. For pumped-storage facilities on the whole cascade (KWO++), the scheme would even consume more energy than it produces. Around 2500 hours of peak-load turbine operation allow doubling or even tripling today's annual revenue, without taking into account capital costs due to investments for scheme enhancement. As consequence, pumped-storage can be an efficient alternative to face the losses due to climate change.

Of course, further investments in electricity grid strengthening and free electricity exchange would be needed for such high amounts of injected and absorbed energy.

Regarding the impacted flow regime, only little mitigation is possible with today's scheme. A reduction of the actual hydropeaking ratio r_{HP} from 15.0 to 7.0 decreases benefits by about €4 million per year. New turbine capacities at the outlet of the river would increase this parameter to about 20 without construction mitigation measures. As mitigation of hydropeaking has become a legal constraint, the implementation of the Brienzersee pumped-storage plant in addition to restricted turbine operation of Innertkirchen 1 HPP could reduce peak flow in the Hasliaare River and may be part of negotiations with the authorities during approval procedures. Higher ecological performance could also be achieved by construction measures at the outlet of the power houses, to be tested by the same modeling tool in further studies.

Despite some potential of improvements concerning the parameter definition and the standardization of calibration, *Routing System* with the implemented HPP optimization approach is an efficient and robust tool for modeling, simulation and analysis of complex hydropower schemes in a challenging environment.

7

Mitigation measures for fish habitat improvement in Alpine rivers affected by hydropower operations

In mountainous areas, high-head storage hydropower plants (HPP) produce peak load energy. The resulting unsteady water release to rivers, called hydropeaking, alters the natural flow regime. Mitigating the adverse impacts on aquatic ecosystems has become a crucial step in recent water policies. We developed a novel economic-ecological diagnostic and intervention method to assess hydropeaking mitigation measures for fish habitat improvement. It was applied to an Alpine river downstream of a complex storage hydropower scheme. The approach comprises (1) a hydropower operation model of flow regime generation and cost estimates for different mitigation measures; (2) a 2D hydrodynamic model to simulate the flow conditions in representative river reaches; (3) a dynamic fish habitat simulation tool to assess the sub-daily changes in habitat conditions of three brown trout (*Salmo trutta fario*) life stages (adult, spawning and young of the year (YOY)). Simulations showed that operational measures, such as limiting maximum turbine discharge, increasing residual flow or limiting drawdown range, have high costs compared to their ecological effectiveness. Compensation basins and power house outflow deviation achieved the best cost-benefit ratio. Hydropeaking impact was strongly dependent on river morphology. Monotonous river reaches showed low habitat suitability for increasing discharge, whereas a braided morphology provided high instream structure and thus suitable habitat where the flow is unsteady. The interdisciplinary approach to economic and habitat rating informs decision makers how effective measures are in mitigating the environmental impacts associated with highly fluctuating hydropower operations.

This chapter is the result of an interdisciplinary project with Emilie Person, fish ecologist at EAWAG and responsible for Project B of the CTI research project. She provided fish sampling data and instream habitat modeling from the two study areas Hasliaare and Vorderrhein River. The habitat assessment tool was commonly developed and applied.

7.1 Introduction

Since 1950, a large number of high-head storage hydropower plants (HPP) in the Alps have met the demand for peak load energy in the European power grid (Schleiss, 2007). In Switzerland, for example, 32% of the total electricity in 2010 was produced by storage hydropower plants. Water retention in large reservoirs and concentrated turbine operations allow electricity to be produced on demand. Sudden opening and closing of the turbines produce highly unsteady flow conditions in the river downstream of the power house (Moog, 1993). This so-called hydropeaking is the major hydrological alteration in Alpine regions (Petts, 1984; Poff *et al.*, 1997). Due to the unpredictability and intensity they cause, sub-daily hydropeaking events disturb the natural discharge regime, which is a key factor in ecological quality and the natural abiotic structure of ecosystems (Parasiewicz *et al.*, 1998; Bunn and Arthington, 2002). These disturbances directly affect riverine biological communities (Young *et al.*, 2011). Frequent and fast fluctuations change hydraulic parameters, e.g., flow depth, velocity and bed shear stress (Petts and Amoros, 1996), and thus influence fish habitat availability, stability and quality. Salmonid populations are less abundant and have reduced population size in rivers with hydropeaking (Moog, 1993; Gouraud *et al.*, 2008). In headwaters of Alpine rivers, brown trout (*Salmo trutta fario*) is one of the species most impacted by dam operations. Without appropriate flow shelter habitat, the hydropeaking-impacted flow regime becomes energetically costly for fish and affects their over-wintering survival (Scruton *et al.*, 2003; Scruton *et al.*, 2008). Spawning areas are faced with the risk of dewatering, and young of the year (YOY) shore habitat is displaced or lost (Liebig *et al.*, 1998; Saltveit *et al.*, 2001). Success in natural reproduction and YOY survival are key factors for the fish population's natural renewal.

As part of the "Green Hydropower" assessment procedure for river management, Bratrich et al. (2004) identify hydropeaking as one of the future research priorities due to our lack of knowledge of its interaction with the riparian ecology. For impact assessment, individual investigations are recommended, as riverbed morphologies and hydropower facilities' outlines differ locally (Baumann and Klaus, 2003).

After decades of extensive use of water resources with some severe consequences for aquatic and riverine biota, the government and the administration are starting to recognize the need of a water protection policy, e.g., the European Union's Water Framework Directive. In Switzerland, Parliament adapted the Law on Water Protection in 2009, to improve the quality of Swiss waters, including hydropeaking mitigation.

To support decision makers in defining optimum restoration measures, tools are needed to define, assess and compare the associated cost and habitat improvement (Palmer and Bernhardt, 2006; Heller *et al.*, 2010). Various modeling approaches are commonly used to simulate the impact of hydropower plants. Several methods of qualitative decision support exist, such as participatory methods (Leach and Pelkey,

2001; Luyet, 2005), expert judgment (Landeta, 2006), system dynamics (Maani and Maharaj, 2004; Park *et al.*, 2004) and mixed methods such as fuzzy (Zadeh, 1965) and multicriteria analysis (Mena, 2000).

Pfaundler and Keusen (2007) and Meile *et al.* (2011) discuss several methods for flow regime analysis. Sub-daily flow variations can be expressed by the ratio between maximum (Q_{max}) and minimum (Q_{min}) daily discharge, called the *drawdown range*. Gradient in flow change is described by the *flow ramping rate* HP_2. These and other hydraulic-based parameters (Richter *et al.*, 1997; Black *et al.*, 2005) are useful for comparison and preliminary analysis. However, the interaction between hydropeaking and river ecology is complex and the current metrics are still rudimentary (Meile *et al.*, 2011).

River habitat modeling has become a powerful tool for evaluating altered flow conditions in aquatic ecosystems (Armour and Taylor, 1991; Maddock, 1999). A common instream model contains three components: (i) the hydrodynamic model, defining steady flow characteristics in river reaches; (ii) the biological input data, e.g., fish habitat preference; (iii) the habitat model. The results of both the hydraulic model and biological sampling are combined to determine habitat suitability for one or several target species. The instream habitat model CASiMiR includes a module for fish habitat suitability under steady flow conditions (Jorde *et al.*, 2000; Schneider *et al.*, 2010; Tuhtan *et al.*, 2012). García *et al.* (2011) applied this model in a conservation study to predict the habitat evolution of eight fish species under hydropeaking conditions in the Biobío River in Chile.

In common habitat modeling approaches, Weighted Usable Area (WUA) and Hydraulic Habitat Suitability (HHS) were developed within the instream flow incremental methodology (Bovee, 1982) for determining the target species' minimum flow requirement . They are calculated using the dimensionless Suitability Index (SI) and flow patterns for simulated discharges as a base. WUA is commonly defined as the sum of stream surface area weighted by multiplying area by SI for a given discharge Q. HHS is the ratio between WUA and the total wetted area for Q, representing the percentage of suitable areas over the total wetted area for the species considered. WUA and HHS integrate the overall habitat suitability on a reach for a steady state. The same WUA or HHS value can stand for many of low or a few high-quality habitat areas. They were developed for steady flow and thus are not suitable for expressing dynamic habitat conditions, such as those induced by hydropeaking.

Hydropower operation models, metrics for flow regime analysis and instream habitat models are too often developed and applied independently. Most approaches do not consider the relevant interdependency between economic and ecological concerns (Palmer and Bernhardt, 2006). Here, we propose a novel economic-ecological diagnostic and intervention method with integrated river basin and HPP modeling as well as a habitat assessment tool, to evaluate the effect of operational and construction hydropeaking mitigation projects. Several measures are implemented and tested in the *hydropower operation model*, using a semi-distributed conceptual approach for flow regime generation and economic rating. The *2D hydrodynamic model* of reference river reaches defines flow depth and velocity for the simulated flow regimes. The *dynamic habitat simulation tool* allows fish habitat suitability to be assessed. The method is

applied to the upper Aare River catchment, which comprises a complex HHP and a downstream river system with different river morphologies. Suitability and stability indices are developed for habitat rating and applied to adult, spawning and YOY brown trout (*Salmo trutta fario*). Costs and biological benefits of different mitigation strategies are correlated for comparison and assessment of their effectiveness.

7.2 Case study

Figure 7.1 shows the upper Aare River basin, located upstream of Lake Brienz in the center of the Swiss Alps. Its surface area in Brienzwiler is 554 km^2, where 21% was glaciated in 2003. The hydrological regime of the Aare River with a mean annual discharge of 35 m^3/s is glacial, with low discharge in winter and high runoff in summer due to snow and glacier melt (Weingartner and Aschwanden, 1986). Mean catchment altitude is 2150 m a.s.l. The Aare River, also called the Hasliaare in its headwaters, finds its source in the Unteraar and Oberaar Glaciers (Schweizer *et al.*, 2008). According to the Huet longitudinal zonation of 1949, the Hasliaare catchment is defined as a trout or upper grayling zone. The only widely distributed fish species is the brown trout (Haas and Peter, 2009).

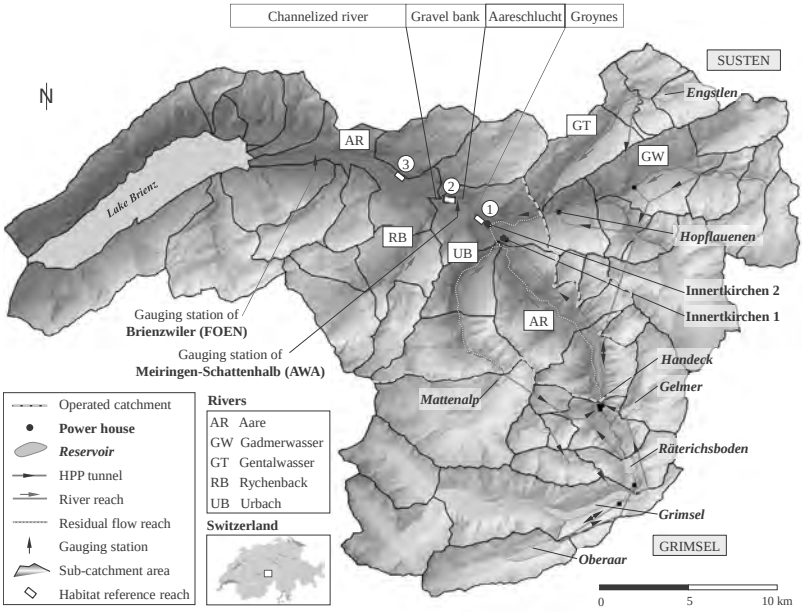

Figure 7.1. Map of the upper Aare catchment area in Switzerland with today's layout of the Oberhasli hydropower scheme (reservoirs, HPP tunnels and power houses), the limit of the operated catchment area, the sub-catchment areas, the two river gauging stations and the river network. The Hasliaare downstream of the turbine release in Innertkirchen show four main morphologies: groynes, Aareschlucht canyon, gravel bank and channelized river reach. White boxes indicate the modeled reference morphologies groynes (1), gravel bank (2) and channelized river (3).

7.2.1 Oberhasli hydropower scheme

Since the early 20th century, a hydropower scheme of nine power houses and several reservoirs and intakes has been constructed. The Kraftwerke Oberhasli (KWO) company operates 60% of the catchment area by a complex high-head storage hydropower scheme. The water from the partly glacierized catchment of Grimsel flows through the artificial reservoirs of Oberaar, Grimsel, Räterichsboden and Handeck. In Innertkirchen, the water is given back to the Hasliaare River by the Innertkirchen 1 HPP. The River Gadmerwasser drains the eastern part of the basin (Susten). Its operated water is released to the Hasliaare by the Innertkirchen 2 HPP. The substantial turbine capacities of the Innertkirchen 1 and 2 HPPs of 39 and 29 m^3/s, respectively, produce severe hydropeaking in the downstream river reaches.

The plant upgrading program *KWOplus* plans a large number of technical, economic and ecological improvements to the scheme, such as the increase of the installed capacity of several power houses and the increase of the retention volume of Lake Grimsel. To compensate for the turbine capacity increase of Innertkirchen 1 HPP by 25 m^3/s, a basin of 50'000 m^3 downstream of the power house outflow is planned for lower flow ramping.

7.2.2 Morphology

In the 19th century, the dynamic, braided river network of the Hasliaare was drained for agricultural use as well as for secure flood evacuation. Based on the three parameters of variability of water surface width, bank slope and mesohabitat, the reach downstream of the power house outlets can be divided into four reference morphologies: a reach framed by groynes (650 m); the Aareschlucht canyon (1.4 km); a reach with alternating gravel banks (1.3 km); and a monotonous and straight channel (11 km). The residual water reach upstream of Innertkirchen has a natural morphology. The river is of rhithral type, with cold water in summer, high flow velocities and a riverbed composed mainly of gravel and rocks.

7.2.3 Runoff and hydropeaking

River Hasliaare discharge series are available for 1925–1929 and 1974–2010 from the Brienzwiler gauging station (Federal Office for the Environment, FOEN), and since September 2006 from the Meiringen-Schattenhalb gauging station (Bern Canton, AWA) (Figure 7.1). Comparing the 75% non-exceedance probability of the daily drawdown ranges Q_{max}/Q_{min} in Brienzwiler before and during hydropower operation, an increase from 1.1:1 to 5:1 is observed (VAW-LCH, 2006). On 5% of the days in a year, values higher than 8:1 occur. The gauging station at Meiringen-Schattenhalb is closer to the power house outlet and thus the discharge series show higher fluctuations in flow.

7.3 Methods

A three-step approach for economic and habitat rating of hydropeaking mitigation measures was developed. Figure 7.2 presents a flowchart of the economic-ecological diagnostic and intervention method.

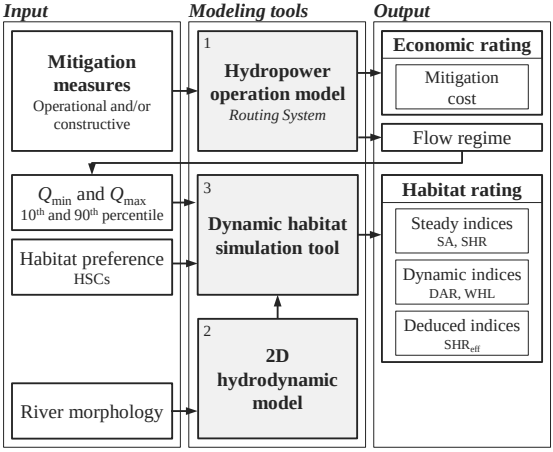

Figure 7.2. Flowchart of the economic-ecological diagnostic and intervention method for assessing the hydropeaking mitigation measures. The approach contains three modeling tools (1, 2, 3) for simulating of the flow regime and its economic and habitat rating.

7.3.1 Mitigation measures

Table 7.1 lists twelve possible operational and construction measures to mitigate the negative effects of hydropeaking:

– *Operational measures*, such as restrictions in the turbine operation mode, are probably most efficient for modifying the downstream flow regime. Nevertheless, such measures significantly reduce production flexibility and thus endanger the energetic and economic sustainability of the HPP (Baumann et al., 2005).

– *Construction measures*, such as regulated compensation basins downstream of the power house, can be located beside or on the river (Meile, 2006). Compensation basins with significant storage volumes can decrease the maximum and increase the minimum daily discharge of the downstream river reach (VAW-LCH, 2006). Multipurpose schemes can compensate construction costs (Heller et al., 2010). Underground spaces, such as tunnels or caverns, reduce visual impact and land use. Ecological issues, such as a power house outflow in a deviation tunnel, channel or directly into a lake, can be addressed in the framework of HPP enhancement projects.

– *Morphological measures* increase the flow resistance and the natural retention capacity of rivers. One goal of today's river restoration projects is to widen the riverbeds to improve both flood evacuation capacity and morphology (Willi, 2002). Such projects are ecologically effective only if the flow regime is within an acceptable range (Peter, 2004).

Table 7.1. Operational (O) and construction (C) hydropeaking mitigation measures. The power house outflow of a HPP ( ) affects the flow regime of the downstream river ( ). Detailed descriptions are given in addition to related costs and concerns.

	Measure	Type		Details	Related costs and concerns
1	Increase of residual flow	O	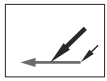	Higher base flow to increase minimum flow Q_{min} and thus to reduces drawdown range	– Legal constraints – Decline in earnings
2	Power or discharge limitation	O	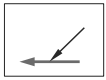	Lower peak flow to decrease daily maximum flow Q_{max} and thus to reduce drawdown range	– Legal constraints – Decline in earnings – Loss of flexibility
3	Anti-cyclical operation of the different plants	O	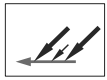	Reduce peak and increase base flow for a more constant flow regime in the whole river system	– Legal constraints – Decline in earnings due to production during low demand
4	Successive increase/decrease of discharge	O	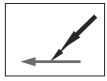	Lower flow-ramping rate HP_2 to avoid flushing of riparian species	– Legal constraints – Decline in earnings – Loss of flexibility
5	Power house outflow directly into the lake	C		Turbine outlet directly connected to a lake to avoid hydropeaking in the river reach	– Lake too far away – Construction costs
6	Power house outflow into a side channel or tunnel	C		Parallel side channel or tunnel to evacuates the turbine water without impacting the river reach	– Land use – Construction cost – Groundwater
7	Compensation basin	C		Power house outflow realised to basin of volume V_{basin} with controlled outflow to the river	– Land use – Construction cost – Fluctuating level (recreation) – Volume depending on
8	Compensation cavern	C		Power house outflow linked with underground retention space of V_{cavern} controlling outflow	– High construction cost – For reducing HP_2 – Volume depending on $Q_{turbine}$
9	Power house outflow into basin (of a run-of-river plant)	C		Basin of V_{res} located on the river controlling flow by turbines and weirs	– Legal constraints – Land use – Construction cost – Fish migration, sediment
10	Power house outflow into lake and residual run-of-river release	C	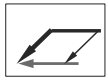	Existing plant used in run-of-river mode and new parallel system for peak production	– Construction cost – Decline in earnings due to operations during low demand
11	Morphological improvements of the river	C	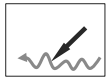	Macro-roughness or river widening to reduce Q_{max} of short turbine sequences and HP_2	– Legal and environmental constraints – Construction cost – Low performance
12	Combination of measures	O, C		Combinations of different mitigation measures (multi-reservoir).	– See above

Several operational and construction measures from Table 7.1 were chosen and implemented in the case study area (Table 7.2) to reduce the sub-daily flow fluctuations in the Hasliaare River:

– *Limitation of maximum turbine discharge*: To reduce peak flow Q_{max}, the maximum turbine releases of Innertkirchen 1 and 2 HPPs of 39 m^3/s and 29 m^3/s, respectively, are reduced by 90%, 80% and 70% (Table 7.2, D). More severe restrictions influence the operation mode of the plants up to Lake Grimsel and thus avoid on-demand production.

– *Increase of residual flow*: Constant outflow from the Handeck compensation basin is set to 1, 2 and 3 m^3/s (Table 7.2, E). These values are considerably higher than those required by law and therefore correspond to high energy losses.

– *Limited drawdown range*: Turbine operations of Innertkirchen 1 and 2 HPPs have to respect drawdown ranges Q_{max}/Q_{min} of 12:1, 8:1 and 5:1 (Table 7.2, F). It is not possible to apply lower ranges without changing the operation rules of the plants located upstream.

– *Power house outflow directly into the lake*: Through a tunnel or open channel between Innertkirchen and Lake Brienz of about 15-km length and a capacity corresponding to the total turbine discharge, the flow in the Hasliaare was reduced to the released residual flow and the inflow from the non-operated river basin (Table 7.2, G).

– *Scheme enhancements*: As part of the upgrading program *KWOplus*, the turbine capacity of the power plants downstream of Lake Räterichsboden, Handeck 2 and Innertkirchen 1, are increased by about 25 m^3/s each. Innertkirchen 1 HPP will then have a maximum discharge of 64 m^3/s (Table 7.2, H). The Brienzersee pumped-storage plant could be part of a further scheme enhancement, operating the water between Lake Brienz and Lake Räterichsboden with a capacity of 124 m^3/s for the turbines and 100 m^3/s for the pumps. This power plant would increase flexibility and could be combined with ecologically defined HPP operation rules for reducing hydropeaking in the Aare River (Table 7.2, I).

– *Compensation basins and caverns*: Retention volumes could be installed downstream of the turbine outlets in Innertkirchen. The water is temporarily stored in a basin and then released to the river by a guided system, respecting ecologically defined operation rules. Limited space availability would be the major problem for the construction. The present parameter study does not take these practical constraints into account. A cavern could be implemented as an alternative to compensation basins with an important environmental and visual impact. In this study, retention volumes V_{basin} of between 50'000 and 1'000'000 m^3 and V_{cavern} of between 20'000 and 300'000 m^3 are implemented in the model and economically rated (Table 7.2, J). The release capacity of 20 m^3/s increases with higher water levels in the reservoir or cavern up to the maximum turbine release.

Table 7.2. Flow regime characteristics of real data series and simulations with and without operational restrictions as well as for different HPP layouts and construction mitigation measures. Production losses due to operational measures as well as capital and maintenance costs for the basins are given as the mean annual mitigation cost over the 5-year period.

	Conditions and/or measure type	Details		Q_{max}*1 November	Q_{min}*2 November	Q_{max}*1 August	Q_{min}*2 August	Mean annual mitigation cost	
				[m^3/s]	[m^3/s]	[m^3/s]	[m^3/s]	[M€]	
A	Flow regime **before HPP operation** based on Brienzwiler 1926-29		A	14	14	80	60	-	
B	Measured **real data** at Meiringen-Schattenhalb for 2009		B	27	9	70	37	-	
C	Simulation under market-based conditions **without restrictions** of 2009		C	68	5	73	25	0.0	
D	Simulation of 2005–2009 with **discharge limitations** for power houses Inn 1/2 by …	90%	D1	62	5	66	29	2.9	
		80%	D2	58	5	61	30	5.8	
		70%	D3	62	5	61	30	8.5	
E	Simulation of 2005–2009 with **increase of residual flow** at Handeck by Q = … [m^3/s]	1	E1	69	6	74	26	1.8	
		2	E2	70	7	72	27	3.5	
		3	E3	67	8	75	28	5.4	
F	Simulation of 2005–2009 with **limited drawdown range** of Q_{max}/Q_{min} = … [-]	12:1	F1	61	6	69	25	0.8	
		8:1	F2	60	9	70	27	2.0	
		5:1	F3	56	10	69	27	3.9	
G	Simulation of 2009 with **only residual flow** in Hasliaare River	Residual flow	G	6	6	6	6	?	
H	Simulation of 2005–2009 by **KWOplus** without restrictions	KWO+	H	93	5	94	20	0.0	
I	Simulation of 2005–2009 by KWOplus and **Brienzersee HPP** (2:1)	KWO++	I	40	10	48	22	?	
J	Simulation of 2005–2009 with implementation of **compensation basin** immediately downstream of the turbine outlets of Inn 1/2 of volume V_{basin} = … [10^3 m^3]	1'000	J1	41	9	64	38	4.4^{wt}	4.5
		700	J2	43	7	68	34	3.3^{wt}	3.4
		400	J3	48	6	71	34	2.1^{wt}	2.2
		100	J4	68	5	73	31	0.9^{wt}	1.1
		50	J5	68	5	73	27	0.6^{wt}	0.8

*1 90th and *2 10th percentiles of 1 h flow series for November and August of the hydrological year (series of November 2008 and August 2009 are taken for the 2005–2009 period discharge).
wt with individually optimized micro-turbines at the outlet of the basin (electricity price of €0.10 /kWh)

7.3.2 Hydropower operation model

The semi-distributed conceptual hydrological-hydraulic model *Routing System* was developed to simulate the hydrological processes in Alpine river basins as well as the HPP operation (Chapter 4). Despite the complexity of the high-head storage scheme, the influence of climate change (Chapter 5), electricity market issues, plant enhancements and hydropeaking constraints can be simulated. Five climate and four electricity price scenarios were tested and the optimum HPP operation defined in Chapter 6. Comparison of today's and the future flow regimes reveal no relevant difference in terms of sub-daily discharge fluctuations. Thus, the simulation period can be limited to five hydrological years from 2005 to 2009, where the intermediate electricity price scenario MIX is applied, assuming a mix of energy suppliers and therefore a slightly volatile market behavior. The simulations are performed with a 10-minute time step. The results are saved as hourly mean values.

The optimized operation of today's Oberhasli hydropower scheme without any restrictions and mitigation measures is defined as the reference scenario (Table 7.2, C). Simulations with the implemented operational restrictions give the resulting mean annual mitigation cost in terms of production losses, where the economic efficiency of a construction measure depends on the investment cost. The basin is framed by dikes built by excavated material from reservoir construction. The cavern is realized by drill-and-blast. The annual capital costs are defined by multiplying the present investment by the annuity with an interest rate of 4% and a redemption time of 50 years. The applied method is precisely enough for a parameter study comparing different measures with each other. For further evaluation, specific design and detailed economic analysis would be required.

The *Routing System* also generates flow series in the river reaches according to the kinematic wave assumption. Off-peak (minimum: Q_{min}) and peak (maximum: Q_{max}) discharges are inferred from monthly hydrographs, correspond to 10^{th} and 90^{th} percentiles, respectively. The two percentages indicate steady flow conditions that are achieved with regularity. The simulated flow regime is compared to measured discharge series before (1926–29) and with (2009) hydropower exploitation of the upper Aare catchment.

7.3.3 2D hydrodynamic model

For habitat modeling of the river system, four morphologies are investigated. Three of them represent real habitat conditions in the Hasliaare, downstream of power house outlets in Innertkirchen. The *groynes, gravel bank* and *channelized river* reaches (Figure 7.5a, b and c) are selected, due to their diversity in width, substrate and depth. Flow depth, velocity and substrate distributions vary considerably between the three Hasliaare River morphologies and thus influence the habitat suitability for fish differently. A fourth morphology is tested to assess potential future river restoration, consisting in a transformation of parts of the channelized reach into a braided river. For this purpose, a naturally shaped section of the Vorderrhein (Person and Peter, 2012) is chosen as *braided river* (Figure 7.5d). The Vorderrhein is a Swiss Alpine river with a nivo-glacial regime, a mean annual discharge of 30.5 m^3/s and a mean catchment altitude of 2020 m a.s.l., characteristics similar to the Hasliaare. This naturally braided river is part of the trout region (Huet longitudinal zonation, 1949). The four reference morphologies are tested with the same simulated flow regime, corresponding to a location close to the power house outlets in Innertkirchen (Meiringen-Schattenhalb), to compare the influence of the bed form on fish habitat conditions.

For each morphology, riverbed elevation and drainage area topography are measured, combining a tachymeter terrestrial system (LEICA TC1102) with a GPS echo sounder (DESO 14). The grid size has to be defined in terms of the instream structure of the river. Values are sampled every 0.5 seconds, producing a grid size of 0.5 m and therefore a very detailed representation of the riverbed. Then, a 3D digital elevation model (DEM) is computed. Flow velocity is measured *in situ* by a SEBA mini current meter (type M1) for model calibration. Substrate is classified according to granulometry.

Flow depth and mean vertical velocity for every grid cell are simulated by the 2D hydrodynamic model HYDRO_AS-2D (Tolossa *et al.*, 2009) for a range of 30 discharges of between 3 and 100 m^3/s. Discharge spectrum covers the normal flow regime of 2009 at Brienzwiler, disregarding flood events. The boundary conditions are defined by measured discharge-water elevation ratios.

7.3.4 Dynamic fish habitat rating tool

To evaluate habitat response to hydropeaking, the fish module of the CASiMiR habitat model is combined with regional univariate preference curves for adult, young of the year (YOY) and spawning brown trout. The preference curves from field investigations in the Hasliaare (unpublished data) were used to define the habitat suitability of YOY and spawning brown trout. For adult fish no specific suitability curves for the Hasliaare are available and adult suitability curves from Souchon *et al.* (1989) were used. Souchon *et al.* (1989) were chosen from the literature because they show similar habitat preferences than Hasliaare data for YOY and spawning brown trout, indicating that the two populations have similar habitat preferences. The suitability curves were implemented in the CASiMiR model of the four river reaches (groynes, gravel bank, channelized and braided river). For the 30 simulated discharges, the Suitability Index (SI), ranging between 0 (unsuitable) and 1 (suitable), were computed for every grid cell using flow depth, water velocity and substrate preferences. Several mathematical methods are known to define SI from the different preference values. The geometric mean is commonly applied (Layher and Maughan, 1985). To evaluate the dynamic impact of sub-daily flow fluctuation on the target species, five indices are developed based on Suitability Index (SI) maps:

Suitable Area (SA) [m^2] considers habitat only if the associated SI achieves a defined threshold value SI_{lim}. SA for discharge Q corresponds to the total surface area, where SI is greater or equal to SI_{lim}. Here, SI_{lim} is set to 0.5, which includes middle to high SI areas. Furthermore, only water levels H achieving H_{lim}, the threshold water depth at which flow is too shallow to sustain the species of interest, are taken into account. According to the habitat preference curves and field observations of the habitat use of brown trout in Hasliaare (Person and Peter, 2012), H_{lim} is set to 5 cm for YOY and 10 cm for adult and spawning:

$$SA(Q) = \sum_{i=1}^{n} A_i \Big|_{SI_i(Q) \geq SI_{lim} \text{ and } H_i(Q) \geq H_{lim}} \tag{7.1}$$

where A_i = area of cell i [m^2]; $SI_i(Q)$ = Suitability Index for discharge Q [-]; SI_{lim} = threshold Suitability Index [-]; $H_i(Q)$ = flow depth for discharge Q [m] and H_{lim} = threshold water depth [m].

Suitable Habitat Ratio (SHR) [-] is the ratio of SA and the Relevant Wetted Area (WA_{rel}) [m^2] for Q. WA_{rel} takes into account only the wetted area with water levels achieving H_{lim} and is therefore equal to or smaller than the Total Wetted Area (WA_{tot}):

$$\mathrm{SHR}(Q) = \frac{\mathrm{SA}(Q)}{\mathrm{WA}_{\mathrm{rel}}(Q)} = \frac{\sum_{i=1}^{n} A_i\big|_{\mathrm{SI}_i(Q)\geq \mathrm{SI}_{\mathrm{lim}} \text{ and } H_i(Q)\geq H_{\mathrm{lim}}}}{\sum_{i=1}^{n} A_i\big|_{H_i(Q)\geq H_{\mathrm{lim}}}} \tag{7.2}$$

Wetted Habitat Loss (WHL) [-] indicates unstable habitat, lost between two steady flow regimes. It represents the relative area where habitat conditions change from suitable ($\mathrm{SI} \geq \mathrm{SI}_{\mathrm{lim}}$) at discharge Q_1 to unsuitable ($\mathrm{SI} < \mathrm{SI}_{\mathrm{lim}}$) at discharge Q_2. Habitats becoming dry are not considered in this index:

$$\mathrm{WHL}(Q_1, Q_2) = \frac{\sum_{i=1}^{n} A_i\big|_{\mathrm{SI}_i(Q_1)\geq \mathrm{SI}_{\mathrm{lim}} \text{ and } \mathrm{SI}_i(Q_2)<\mathrm{SI}_{\mathrm{lim}} \text{ and } H_i(Q_2)\geq H_{\mathrm{lim}}}}{\mathrm{SA}(Q_1)} \tag{7.3}$$

Drained Area Ratio (DAR) [-] also describes changing habitat conditions, indicating the relative loss of suitable habitat due to dewatering, when discharge switches from Q_1 to Q_2. It represents the relative area where habitat conditions change from suitable ($\mathrm{SI} \geq \mathrm{SI}_{\mathrm{lim}}$) at Q_1 to drained ($H < H_{\mathrm{lim}}$) at Q_2:

$$\mathrm{DAR}(Q_1, Q_2) = \frac{\sum_{i=1}^{n} A_i\big|_{\mathrm{SI}_i(Q_1)\geq \mathrm{SI}_{\mathrm{lim}} \text{ and } H_i(Q_2)<H_{\mathrm{lim}}}}{\mathrm{SA}(Q_1)} \tag{7.4}$$

Effective Suitable Habitat Ratio ($\mathrm{SHR}_{\mathrm{eff}}$) [-] is a deduced index based on DAR and SHR, defining the relative suitable habitat ($\mathrm{SI} \geq \mathrm{SI}_{\mathrm{lim}}$) remaining wetted when discharge is reduced from Q_2 to Q_1. It is useful for assessing suitable spawning conditions:

$$\mathrm{SHR}_{\mathrm{eff}}(Q_1, Q_2) = \big(1 - \mathrm{DAR}(Q_2, Q_1)\big) \cdot \mathrm{SHR}(Q_2) \tag{7.5}$$

The sum of unstable (WHL) and dewatered (DA) habitat defines the total loss of high quality habitat between Q_1 and Q_2. Consequently, the remaining suitable habitat is defined as stable. On the one hand, SA and SHR are related to a specific discharge state and present habitat suitability for steady flow conditions. On the other hand, WHL and DAR indicate the change of habitat conditions between two flow states and are therefore considered as dynamic indices.

November and August were chosen for habitat simulations. Spawning activity takes place in November. Moreover, adult brown trout are less active and therefore more vulnerable during this period (Scruton *et al.*, 2003; Scruton *et al.*, 2008). 0+ juveniles were sampled in August to avoid the first months after emergence of high density dependent mortality (Crisp, 2000). For each mitigation scenario, habitat indices for the three life stages and the four reference morphologies were computed for the corresponding Q_{min} and Q_{max}.

7.4 Results

7.4.1 Flow regime

Measured discharge series of the Hasliaare at the Brienzwiler gauging station before the construction of the Oberhasli hydropower scheme (1926–1929) show sub-daily fluctuations in August of between 80 (Q_{max}) and 60 m^3/s (Q_{min}) due to the Alpine hydrological regime. For November, no major sub-daily flow fluctuations are observed and thus the monthly average of 14 m^3/s is chosen (Table 7.2, A). For discharge series at Meiringen-Schattenhalb, runoff of the Hasliaare in November was between 27 and 9 m^3/s for 2009, whereas in August values of between 70 and 37 m^3/s were measured (Table 7.2, B).

Comparing the simulated and measured flow regimes of the Hasliaare at Meiringen-Schattenhalb (Table 7.2, B and C), both of the reference months November and August show higher sub-daily fluctuations for the *Routing System* results. This difference is caused by the different HPP operation driving parameters. Fully market-dependent production undertakes on-off operations even for short periods, while today's contract-based production fluctuates less. Turbine sequences with maximum discharge are also undertaken in reality, but less frequently than simulated. The two flow regimes cannot be directly compared. The simulated scenarios therefore represent a future behavior that corresponds to an open and electricity price-driven market. The reference scenario of optimized operation without restrictions for the 2005–2009 period gives a Q_{max} of between 63 and 68 m^3/s and Q_{min} of around 5 m^3/s in November. The peak discharge of between 73 and 96 m^3/s in August is mostly influenced by flood events. The hydrological year of 2009 with only a minor flood event in August is applied as reference year for the flow regime analysis, with a Q_{max} of 73 m^3/s and Q_{min} of 25 m^3/s (Table 7.2, C).

Limiting discharge from the turbines of Innertkirchen 1 HPP (39 m^3/s) and Innertkirchen 2 HPP (29 m^3/s) by 90%, 80% and 70% (Table 7.2, D) can reduce the flow downstream of the turbine outlet Q_{max} from 68 to 58 m^3/s in November and from 73 to 61 m^3/s in August. Q_{min} in winter remains at 5 m^3/s. Strongly limiting the outlet capacity of the HPP complex by up to 70% affects operation of the plants located upstream, e.g., Handeck and Hopflauenen. In case of the large storage volumes, such as Lake Räterichsboden, water is temporally stored and operated at another moment. Only small compensation basins are located in the eastern catchment. If there is strong inflow, this produces overflow, which increases residual flow and therefore compensates for the achieved peak reduction by limited turbine release.

Increasing outflow from the Handeck compensation basin by 1, 2 and 3 m^3/s (Table 7.2, E), raises Q_{min} for winter and summer. Q_{max} generally also increases. Due to water losses, turbine operations are shorter and the 90th percentile can be lowered.

The impact of the limited drawdown range Q_{max}/Q_{min} of 12:1, 8:1 and 5:1 was simulated (Table 7.2, F). In winter, with low residual flow in the upstream river reach, there is a decrease of 7 to 12 m^3/s of Q_{max} and an increase of Q_{min} by 1 to 5 m^3/s in November. The drawdown range is guaranteed for at least 75% of all winter days. Annual values are less affected due to summer months with a satisfactory flow regime,

even without intervention. In consequence, mean summer daily drawdown ranges are always generally lower than the set values.

For a power house outflow directly into Lake Brienz through a tunnel or open channel, the monthly average discharge in the Hasliaare would be 6 m^3/s for both November and August (Table 7.2, G). The minor natural flow fluctuations in August are neglected due to runoff retention in the reservoirs of the HPP, whereas scenario A (Table 7.2, A) contains the natural sub-daily variations of Alpine catchment areas.

The upgrading program *KWOplus* will increase the turbine capacity of Innertkirchen 1 HPP from 39 m^3/s to 64 m^3/s. Optimized simulation of HPP operation without restrictions results in a Q_{max} of 93 and 94 m^3/s in November and August, respectively. Low flow in winter is unaffected, but Q_{min} in summer is reduced to 20 m^3/s (Table 7.2, H). Further scheme extensions are under discussion to increase operation flexibility, e.g., the Brienzersee pumped-storage plant. In addition, hydropeaking in the Aare River can be limited to a drawdown range of 2:1 (Table 7.2, I). November discharge fluctuates between 40 and 10 m^3/s, irrespective of the indicated drawdown range due to a lack of storage capacities in the Susten catchment, while August flow is between 48 and 22 m^3/s.

For compensation basins or caverns downstream of the power houses in Innertkirchen, the simulations require a minimum storage volume of 100'000 m^3 to achieve a reduction of Q_{max} and/or an increase of Q_{min} (Table 7.2, J). Large reservoirs can reduce peak flow to values of 41 m^3/s in winter and 64 m^3/s in summer and low flow is increased to values of 9 and 38 m^3/s, respectively. Nearly all volumes higher than 100'000 m^3 generate lower Q_{max} and higher Q_{min} than the operational measures.

7.4.2 Economic rating

The MIX electricity price scenario and runoff from the catchment area for 2005–2009 achieves an average annual revenue of €118 M/yr for optimized turbine and pump operations of the Oberhasli hydropower scheme. Table 7.2 shows that the highest production losses of between 2.4% and 7.2% (€2.9 M and €8.5 M) are generated for discharge limitations, due to the high head of Innertkirchen 1 HPP and the impact on the power plants upstream (Table 7.2, D). An increase of residual flow leads to water losses and therefore energy losses. The corresponding annual production loss is 1.4% and 4.6% (€1.8 M and €5.4 M) for 1 and 3 m^3/s, respectively (Table 7.2, E). A drawdown range Q_{max}/Q_{min} of 12:1 generates 0.7% (€0.8 M) less revenue, whereas 5:1 makes a difference of 3.3% (€3.9 M) (Table 7.2, F). Future extensions of the hydropower scheme like the Brienzersee pumped-storage plant combined with ecologically defined HPP operation rules reduce the annual revenue by 8% from €316 M to €290 M/yr for current inflow (Table 7.2, I).

Comparing the annual costs for the compensation basins without the individually optimized micro-turbines (Figure 7.3a), the mean annual cost can be slightly reduced from €0.8 M to 0.6 M/yr for a 50'000 m^3 reservoir and from €4.5 M to €4.4 M/yr for a 1'000'000 m^3 one (Table 7.2, J). The costs for caverns (Figure 7.3b) show a nearly linear relationship between retention volume V_{cavern} and cost. The larger the cavern is, the less competitive it is compared to the reservoir. Construction costs are more than double for a storage volume of 150'000 m^3 and thus the cavern is not discussed further.

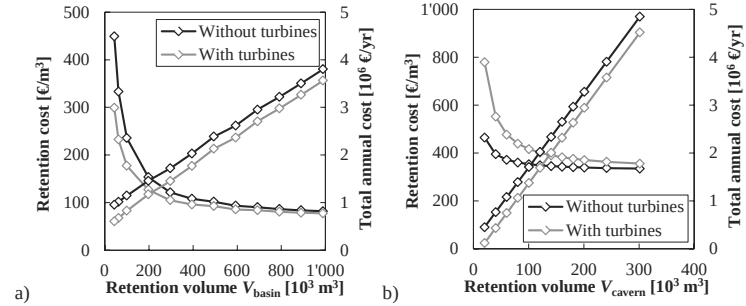

Figure 7.3. Retention cost and total annual cost as a function of the retention volume of the compensation basin (a) and cavern (b) equipped without and with turbines at their outlet. The decreasing curves represent the retention cost and the increasing curves the total annual cost.

Figure 7.4 presents the comparison of drawdown ranges Q_{max}/Q_{min} and the corresponding production losses for the different scenarios. For a mitigation type, the costliest measure normally generated the minimum drawdown range.

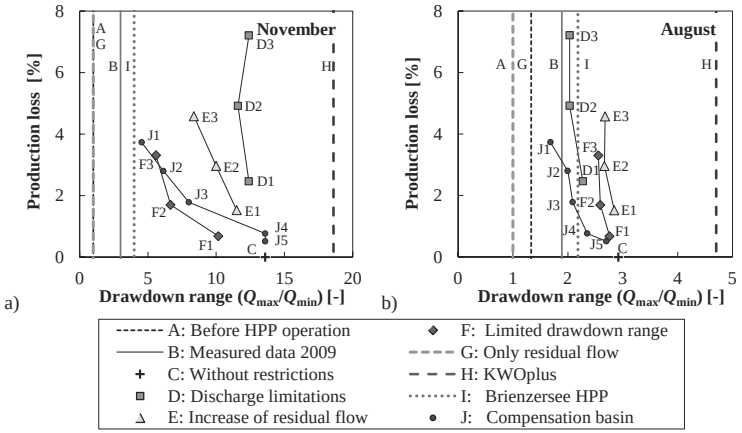

Figure 7.4. Drawdown range and mitigation cost (production loss from annual revenue without restrictions of €118 M/yr) from measured and simulated flow regimes (with and without mitigation measures) for November (a) and August (b).

7.4.3 Habitat rating

Figure 7.5 shows habitat suitability maps for spawning brown trout for the four morphologies and for a common November off-peak (5 m^3/s) and peak (68 m^3/s) discharge, as well as the mean monthly discharge of 14 m^3/s without HPP operation. For groynes (Figure 7.5a), the main flow with relatively high water depth and velocity is concentrated in the inner part of the riverbed, whereas recirculation cells are generated between the groynes. The gravel bank reach (Figure 7.5b) is characterized by a wider morphology and allows shallow flow conditions along the right riverbank. The channelized river reach (Figure 7.5c) has a monotonous morphology with no major instream structure and thus very low habitat conditions for nearly the whole range of

discharges. The braided river reach (Figure 7.5d) generates different habitat conditions compared to the three existing Hasliaare reaches. Lower discharges allow the braided structure to disappear and concentrate flow in the main riverbed, whereas higher ones increase flow velocities in the inner part of curve, reducing habitat quality in the normally shallow zone. However, the rich instream structure generates quite varying conditions and there is a risk of habitat instability with fluctuating flow. Habitat suitability decreases with increasing discharge for groynes, gravel bank and channelized river. In these three cases, habitat suitability is high for very low flow and drops rapidly when discharge is increased beyond 8 m^3/s. For the braided morphology, habitat suitability remains relatively constant for the different discharges.

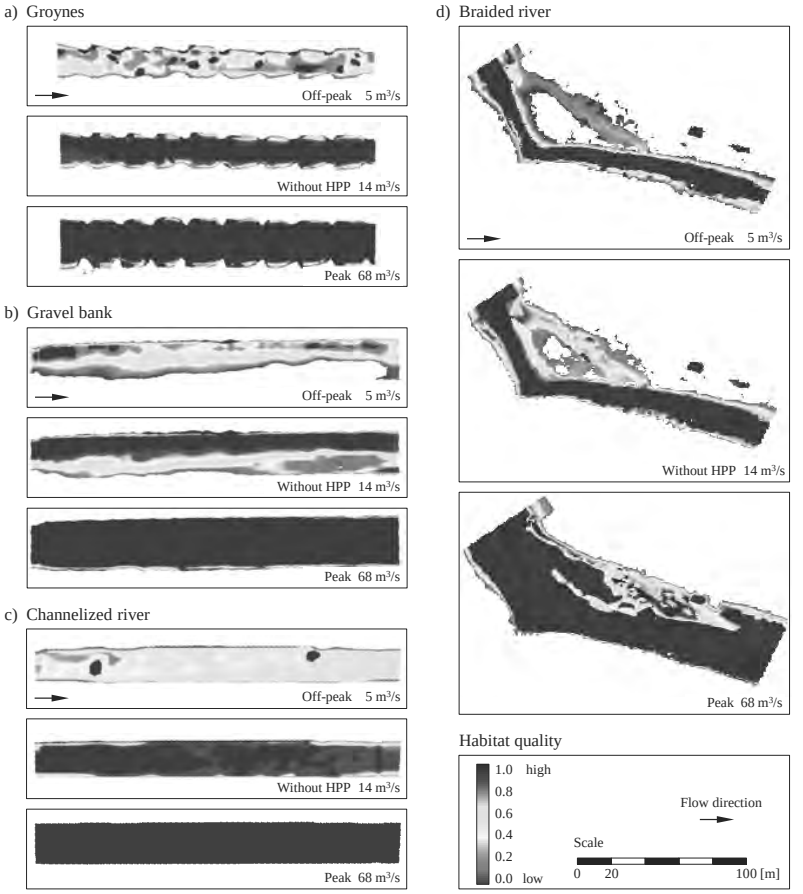

Figure 7.5. Habitat quality in terms of Suitability Index (SI) for spawning of brown trout resulting from habitat modeling for the groynes (a), gravel bank (b), channelized (c) and braided (d) river morphologies for November off-peak (Q = 5 m^3/s) and peak (Q = 68 m^3/s) of the scenario without restrictions (C) as well as the mean discharge without HPP operation (Q = 14 m^3/s). Grey presents low habitat quality and black high habitat quality.

Figure 7.6 shows the Suitable Habitat Ratio (SHR), with a threshold habitat Suitability Index of 0.5, for the three life stages and the four morphologies for the whole range of 2D simulated discharges. For adult fish, the gravel bank and channelized morphologies show correlated SHR with discharge evolution. SHR is high for very low discharge, but drastically drops to poor conditions for higher discharges. The groynes reach shows similar habitat pattern with suitable habitat stabilizing at around 20% for discharges of more than 20 m^3/s. The SHR of the braided river decreases only slightly with discharge. The highest habitat suitability for spawning is achieved in the braided river at around 40 m^3/s, corresponding to 30% of the Effective Wetted Area (WA_{eff}). For high flow, only a few shore habitats remain in the three existing Hasliaare reaches, whereas in the braided river the percentage of suitable habitat remains higher than 10% for up to 80 m^3/s. However, habitat is displaced when discharge changes. For groynes, gravel bank and channelized morphologies, the SHR for spawning and YOY (Figure 7.6b and c) rapidly decreases for discharges higher than 20 m^3/s. For adult and spawning life stages, the habitat suitability for YOY in the braided reach is more resilient to increasing discharge. At least 20% of WA_{eff} has high habitat suitability at up to 50 m^3/s.

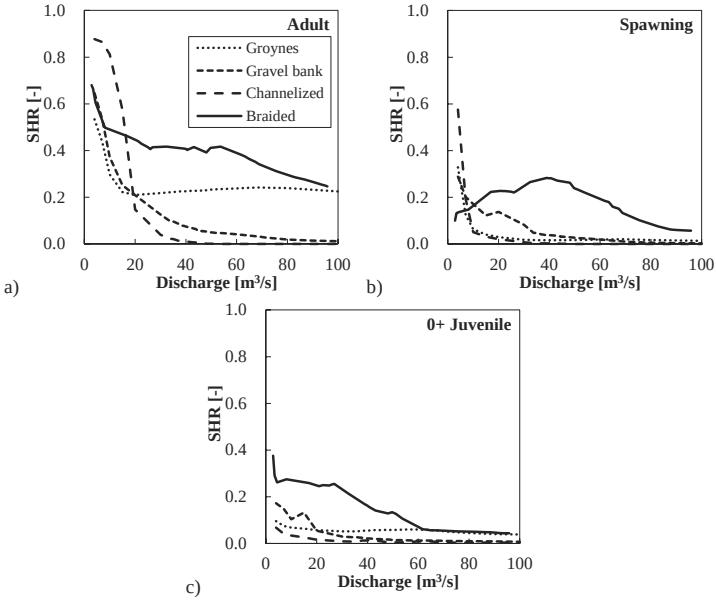

Figure 7.6. Suitability Habitat Ratio (SHR) for adult (a), spawning (b) and 0+ juvenile (c) of brown trout (*Salmo trutta fario*) for the Hasliaare as a function of discharge for the groynes (round dotted line), gravel bank (dashed line), channelized (long dashed line) and braided river reaches (solid line).

Figures 7.7, 7.8 and 7.9 show habitat suitability and stability between off-peak (Q_{min}) and peak (Q_{max}) situation for the applied scenarios with and without mitigation measures (Table 7.2) and the three brown trout life stages. Each scenario shows the percentage of SHR being lost (unstable), falling dry (dewatering), or remaining (stable) when discharge changes from Q_{min} to Q_{max} and vice versa.

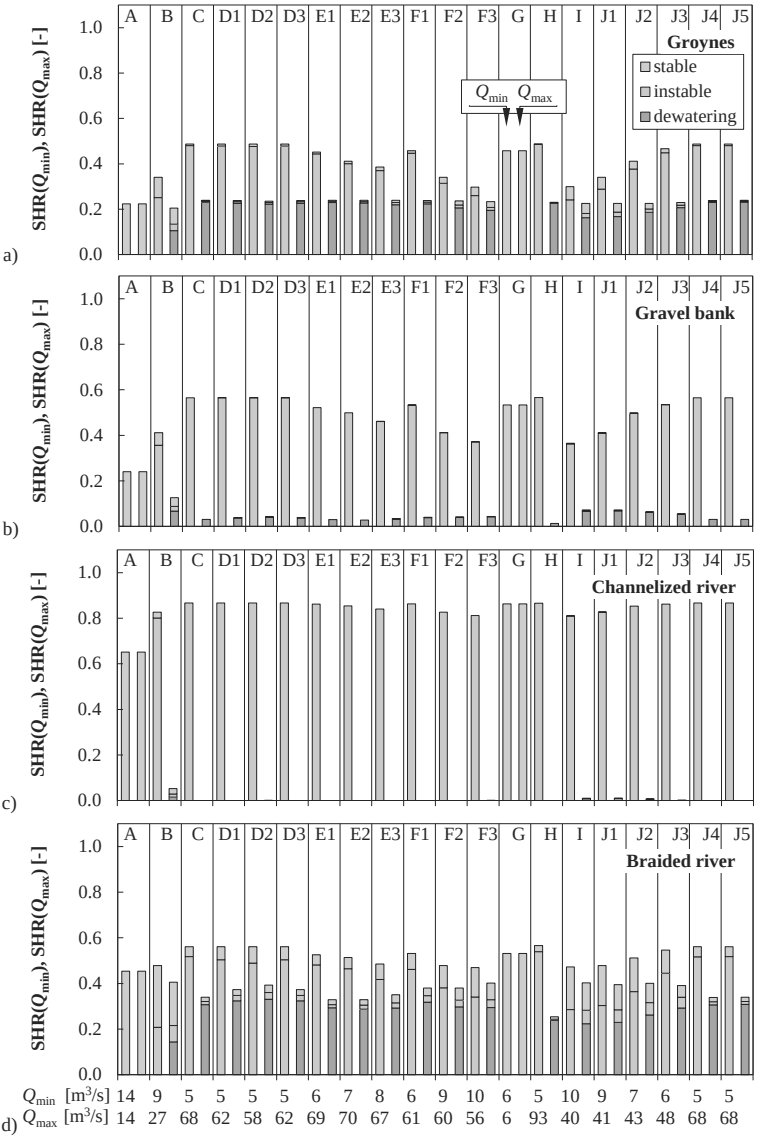

Figure 7.7. Suitability Habitat Ratio (SHR) for adult brown trout for the off-peak Q_{min} and the peak Q_{max} discharge of the measured and simulated November conditions (Table 7.2), computed for the groynes (a), gravel bank (b), channelized (c) and braided (d) river reaches. The percentage of stable (green), instable (yellow) and dewatering (red) habitat is given for discharge changes from Q_{min} to Q_{max} and Q_{max} to Q_{min}, respectively.

Results for adult fish are given in Figure 7.7. For the four morphologies, scenario A without HPP operation and scenario G with only residual flow are the only ones with a noticeable amount of stable suitable habitat. Both scenarios have a flow regime without hydropeaking and constant low discharges of up to 14 m^3/s. For all the other scenarios a considerable habitat loss is defined for discharge increase from Q_{min} to Q_{max} and a high dewatering rate for discharge decrease from Q_{max} to Q_{min}. The market-driven operation in scenario C leads to poorer conditions due to higher fluctuations than today's contract-based operation of scenario B.

The channelized river (Figure 7.6c) shows best habitat conditions for scenarios A and G without hydropeaking. For all other scenarios, the high SHR for Q_{min} completely disappears when discharge increases to Q_{max}. Almost no suitable habitat is available for Q_{max}. The gravel bank (Figure 7.7b) produces similar results, except that SHR for Q_{min} differs between the scenarios. Suitable habitat for Q_{min} is entirely unstable in changing flow conditions. A very small amount of high-quality habitat is present for Q_{max}. However, this small amount entirely dewaters when discharge decreases to Q_{min}. Groynes (Figure 7.7a) and braided river (Figure 7.7d) show similar SHR. In both cases, a small ratio of SHR remains stable under hydropeaking conditions. However, the fraction of stable SHR is slightly higher for the braided river.

Analysis for adult fish shows highly unstable habitat for all scenarios with hydropeaking, independent of morphology. Only groynes and braided river have low ratios of SHR that remain stable under fluctuating flow conditions. No major difference for SHR is found between the different scenarios for channelized river (Figure 7.7c). For groynes (Figure 7.7a), gravel bank (Figure 7.7b) and braided river (Figure 7.7d), SHR for Q_{min} does not change with discharge limitation scenarios (D1 to D3), whereas increased residual flow (E1 to E3), limited drawdown ranges (F1 to F3) and compensation basins (J1 to J5) slightly reduce suitable habitat for Q_{min}. However, habitat stability is increased for the braided river (Figure 7.7d), although SHR is slightly decreased with increasing volumes of the compensation basins (J1 to J5). For all morphologies, discharge limitations (D1 to D3) do not affect SHR.

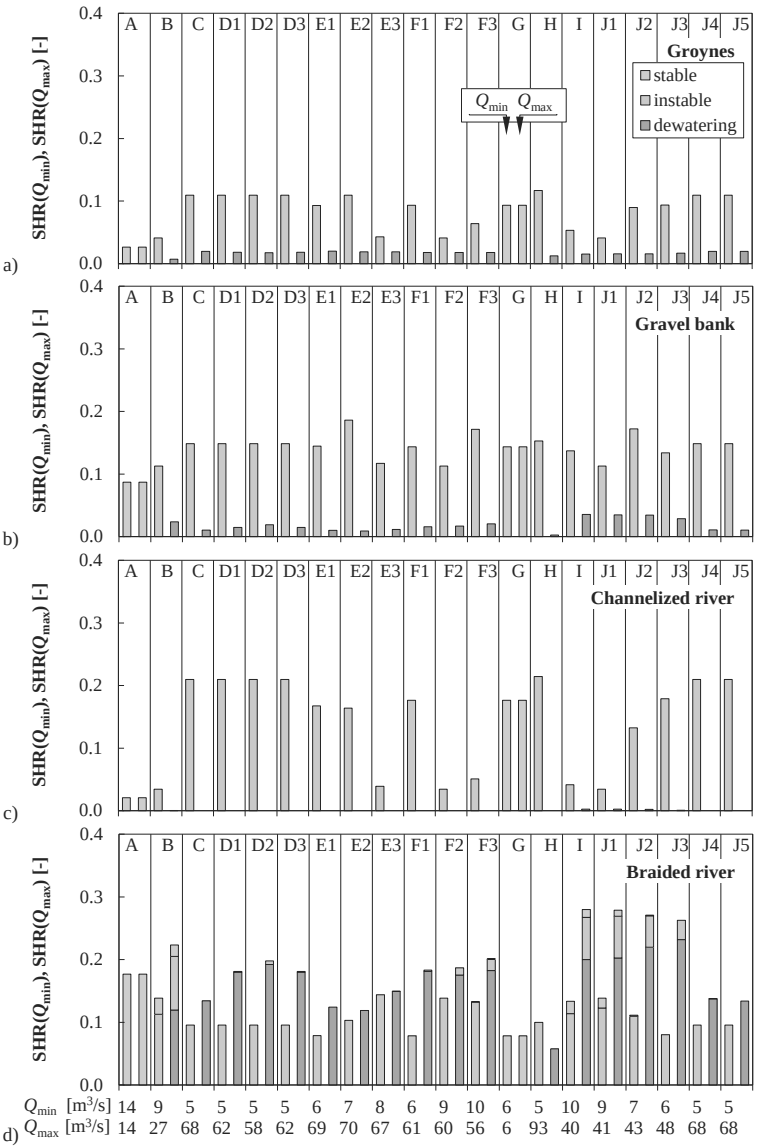

Figure 7.8. Suitability Habitat Ratio (SHR) for spawning brown trout for the off-peak Q_{min} and the peak Q_{max} discharge of the measured and simulated November conditions (Table 7.2), computed for the groynes (a), gravel bank (b), channelized (c) and braided (d) river reaches. The percentage of stable (green), instable (yellow) and dewatering (red) habitat is given for discharge changes from Q_{min} to Q_{max} and Q_{max} to Q_{min}, respectively.

Habitat conditions for spawning brown trout for the different scenarios listed in Table 7.2 are shown in Figure 7.8. The SHR for all morphologies and scenarios are lower than for the adult life stage. The SHR do not range above 30% of WA_{eff}. For adult fish, scenarios A and G without hydropeaking exclusively show some stable habitat for the four river reaches. Braided river (Figure 7.8d) is the only morphology with a small amount of stable SHR for a couple of simulated scenarios with hydropeaking, such as the measured real data for 2009 (B), the power house outflow into the lake by HPP Brienzwiler (I) and the 1'000'000 m^3 compensation basin (J1). Groynes (Figure 7.8a), gravel bank (Figure 7.8b) and channelized (Figure 7.8c) river show similar results. The SHR is higher for Q_{min} than for Q_{max}, where suitable habitat is rare, or even inexistent for the channelized river. The small amount of SHR available for Q_{max} for groynes and gravel bank falls entirely dry when discharge drops for Q_{min}. Suitable habitat at Q_{min} is lost entirely or displaced when discharge increases to Q_{max}. The braided morphology (Figure 7.8d) shows a completely different situation. The SHR is slightly higher for Q_{max} than for Q_{min}, except for *KWOplus* (H) with highest peak discharge of 93 m^3/s. Except for scenario A and G, a high percentage of SHR is lost or displaced during peak.

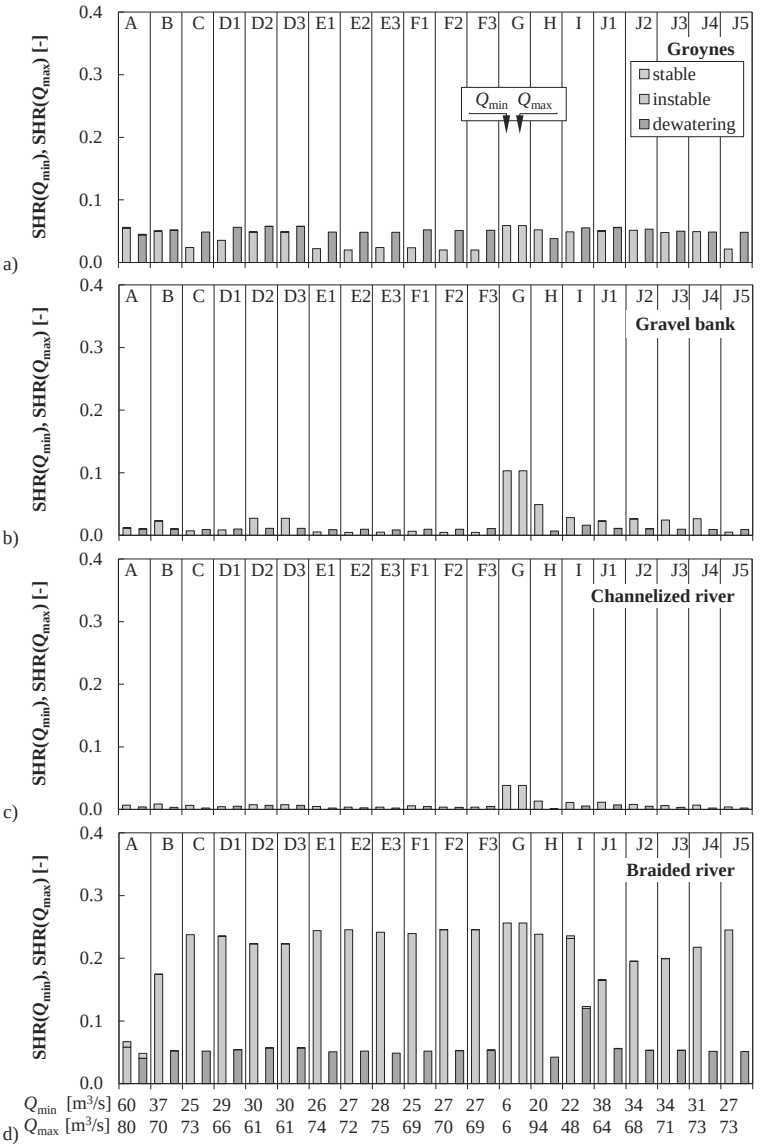

Figure 7.9. Suitability Habitat Ratio (SHR) for 0+ juvenile brown trout for the off-peak Q_{min} and the peak Q_{max} discharge of the measured and simulated August conditions (Table 7.2), computed for the groynes (a), gravel bank (b), channelized (c) and braided (d) river reaches. The percentage of stable (green), instable (yellow) and dewatering (red) habitat is given for discharge changes from Q_{min} to Q_{max} and Q_{max} to Q_{min}, respectively.

Habitat suitability and stability for YOY brown trout is shown in Figure 7.9 for all scenarios of Table 7.2. August hydrographs are used for YOY. Scenario G is the only one without sub-daily discharge fluctuations in August. SHR is very low to almost negligible for groynes (Figure 7.9a), gravel bank (Figure 7.9b) and channelized (Figure 7.9c) river reaches. Gravel bank and channelized morphologies show very low and constant SHR for all scenarios except scenario G. For groynes, SHR is relatively constant at around 2 to 4%. The braided river reach (Figure 7.9d) differs greatly from the other morphologies. Scenario G has very high and stable SHR. A low amount of stable habitat can also be found before HPP operation (A) and for the Brienzersee HPP with a limited drawdown range 2:1 (I). In general, the SHR in all the scenarios except G is either lost or displaced at Q_{max} and falls dry at Q_{min}. The SHR is higher for Q_{min} than for Q_{max} in the braided river.

The developed and applied steady and dynamic fish habitat suitability indices can be compared to the annual costs of the hydropeaking mitigation measures. Figure 7.10 presents such a cost-benefit evaluation for spawning brown trout in the Hasliaare for the channelized and braided reaches. Fish habitat is assessed in terms of SHR at the two steady states Q_{min} (Figure 7.10a1 and a2) and Q_{max} (Figure 7.10b1 and b2). In addition, dewatering risk is taken into account in the Effective Suitable Habitat Ratio $SHR_{eff}(Q_{max},Q_{min})$ (Figure 7.10c1 and c2).

For the channelized river under low flow conditions (Figure 7.10a1), the most expensive mitigation measures are not always the ecologically most effective ones. Discharge limitation (D1 to D3) as well as compensation basins of 100’000 and 50’000 m^3 (J4 and J5) show highest SHR for Q_{min} for very different costs. For increased residual flow (E1 to E3), the limited drawdown range (F1 to F3) and larger compensation basins (J1 to J3), the higher the cost of the measure is, the smaller the ecological improvement. Compared to the flow regime without restrictions (C), no mitigation potential remains. Under peak conditions (Figure 7.10b1), high flow velocities, due to the narrow riverbed and poor instream structure, largely overcome the maintenance capacity of spawning brown trout. Thus, the SHR for Q_{max} drops to zero for almost all scenarios. Independently of cost, no scenario can generate suitable spawning habitat. As shown in Figure 7.10c1, $SHR_{eff}(Q_{max},Q_{min})$ is zero as a consequence of the $SHR(Q_{max})$ zero values, except for the residual flow scenario G, where sub-daily fluctuations are low and almost negligible.

The cost-benefit analysis for the braided river shows rather different results than for the channelized one. Considering the SHR for Q_{min} (Figure 7.10a2) and for Q_{max} (Figure 7.10b2), for increased residual flow (E1 to E3), limited drawdown range (F1 to F3) and different compensation basins (J1 to J5), ecological improvements increase with increasing mitigation costs. The maximal ecological benefit is achieved for the highest residual flow (E3), the lowest drawdown range (F3) and the largest compensation basin (J1). Similar fish spawning habitat improvement can be achieved by the Brienzersee HPP (I), where evaluation of costs has to take into account the amortization costs as well as revenue from pumped-storage operation. Regarding the $SHR_{eff}(Q_{max},Q_{min})$ (Figure 7.10c2), increased residual flow (E1 to E3) and limited drawdown range (F1 to F3) lose their value in terms of improving suitable habitat for spawning. Brienzersee HHP (I) and the 1’000’000 m^3 compensation basin (J1) can

maintain almost 5% of WA_{eff} to high-quality habitat for spawning under hydropeaking conditions.

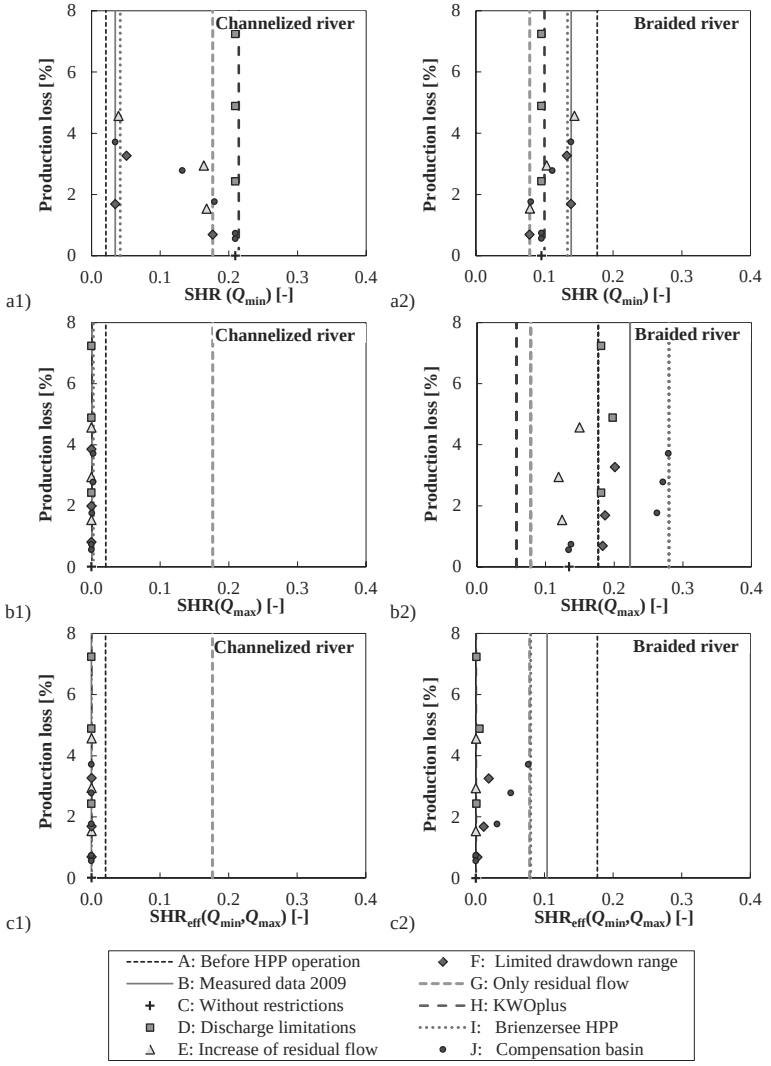

Figure 7.10. SHR indies and mitigation cost (production loss from annual revenue without restrictions of €118 M/yr) for spawning brown trout resulting from measured and simulated flow regimes (with and without mitigation measures) for the channelized (1) and braided (2) river reaches. X-axis: (a) Suitable Habitat Ratio for discharge Q_{min} SHR(Q_{min}); (b) Suitable Habitat Ratio for discharge Q_{max} SHR(Q_{max}); (c) Effective Suitable Habitat Ratio SHR$_{eff}$(Q_{min},Q_{max}). Y-axis: Annual production loss of the related scenarios.

7.5 Discussion

This paper presents a method to evaluate fish habitat improvement and the economic impact of hydropeaking mitigation measures for Alpine rivers. For complex high-head storage hydropower schemes, sophisticated hydrological-hydraulic modeling, such as *Routing System*, is needed to evaluate the financial consequences for economic rating as well as to generate the resulting flow regime. The interaction between hydropeaking and river ecology is complex (Poff *et al.*, 1997; Bunn and Arthington, 2002). The current hydraulic-based metrics are not specific enough for reliable assessment (Meile *et al.*, 2011), as shown for the drawdown ranges of the simulated scenarios. The developed simulation tool is therefore based on local biological data (Smokorowski *et al.*, 2011). The hydraulic habitat model CASiMiR (Jorde *et al.*, 2000; Schneider *et al.*, 2010; Tuhtan *et al.*, 2012) estimates the aquatic habitat quality as a function of discharge and therefore provides a better understanding of the complex aquatic conditions. In previous works (Valentin *et al.*, 1996; García *et al.*, 2011), only the steady indices WUA and HHS assessed the impact of hydropeaking. For the present study, the results of habitat modeling are post-processed by steady and dynamic fish habitat indices. The Suitable Habitat Ratio (SHR) quantifies the amount of high-quality habitat available at a steady state. In contrast to the Hydraulic Habitat Suitability (HHS), the SHR considers habitat only above a defined threshold value. The developed dynamic habitat indices quantify habitat instability (WHL), dewatering risk (DAR) and effective suitable spawning conditions (SHR_{eff}).

We applied the methodology developed to the upper Aare River catchment. The reference scenario consists of a HPP operation with no constraints or mitigation measures. Operational restrictions such as maximum and minimum turbine discharge affect the ability of peak energy production, the main advantage of storage hydropower. As a consequence, operational restrictions remain expensive compared to their effectiveness. Higher ecological effect can be achieved by construction measures. Compensation basins or caverns (J1 to J3) can be installed downstream of the turbine outlets in Innertkirchen. Nearly all volumes greater than 100’000 m^3 generate lower peak discharge and higher residual flow than the operational measures. Compensation basins reduce the sub-daily flow fluctuations for reasonable costs. Multipurpose schemes could generate synergies in terms of recreational zones or flood retention (Heller *et al.*, 2010). Furthermore, bypass tunnels as part of plant enhancement projects (G) can significantly increase fish habitat quality.

Our fish habitat simulations show that hydropeaking impact is strongly dependent on river morphology and thus the ecological mitigation effect can be increased by upgrading the altered river morphology, as discussed in previous studies (Willi, 2002; Baumann and Meile, 2004). Moreover, spawning and YOY SHR values are lower than SHR values for adult for all morphologies and simulated scenarios. These results confirm previous work establishing the evidence that spawning and YOY are particularly affected life stages (Person and Peter, 2012). To cover the relevant life stages, post-emerged fry should be included in further impact assessment on natural reproduction. However, for sampling reasons, post-emergence stadium were not considered in this study. The flow regime before HPP operation and the scenario with a power house outflow in a side channel or directly into the lake are the only ones that

provide a substantial amount of stable suitable habitat. For all scenarios generating hydropeaking regime, fish habitat is highly unstable. Groynes, gravel bank and channelized morphology showed poor habitat values when discharge increased to over 20 m^3/s. This discharge limit is unrealistic in current energy production patterns. The braided morphology provides the richest instream structure because the riverbed is wider. It is the only morphology able to absorb HHP-influenced discharges and to produce varying velocity conditions suitable at the fish scale. Such fish-suitable velocity conditions cannot be achieved under peak flow in the narrow streambeds of the three current Hasliaare morphologies. Considering the four morphologies and the three brown trout life stages, the braided river offers the better habitat conditions in terms of quantity and stability for most of the scenarios.

Several authors have discussed the YOY stranding risk in braided morphologies (Saltveit *et al.*, 2001; Tuhtan *et al.*, 2012). Fish can get used to the sub-daily downramping stressor within a few days (Flodmark *et al.*, 2002; Halleraker *et al.*, 2003). After a long period of stable flow, a gentle drop in discharge before the dewatering can significantly reduce stranding (Halleraker *et al.*, 2003). Furthermore, stranding does not equal mortality. Juvenile salmonid can survive for several hours in the substrate after dewatering (Saltveit *et al.*, 2001). YOY brown trout were sampled in considerable densities in the Vorderrhein in Switzerland, which present a natural morphology and a hydropeaking influenced flow regime (unpublished data). Stranding is strongly influenced by wetted history, ramping rate, temperature, light conditions, season, night and daytime, as well as shore slope and natural fish density (Saltveit *et al.*, 2001; Halleraker *et al.*, 2003; Irvine *et al.*, 2009; Tuhtan *et al.*, 2012). More stranding is observed in winter when juvenile are less active and the water temperature is low. Less stranding is observed at night when juvenile fish are more active. This phenomenon can thus be greatly reduced when downramping is adjusted to these parameters. Channel experiments showed that dewatering in darkness with elevation ramping rates of less than 10 cm/h, can significantly reduce stranding (Halleraker *et al.*, 2003; Irvine *et al.*, 2009). Hatchery juveniles are affected differently by stranding than wild fishes (Saltveit *et al.*, 2001). Measures to reduce stranding should therefore be adapted accordingly.

The present approach concentrates on three life stages of brown trout, a salmonid species of high economic value in Alpine streams and thus defined as an appropriate target species. Much less is known about cyprinids and other freshwater fish species, macro-invertebrates (Baumann and Klaus, 2003; Pellaud, 2007), riparian arthropods (Paetzold *et al.*, 2008), or riparian vegetation (Merritt *et al.*, 2010). Hydro-morphological conditions suitable for one salmonid species may be inappropriate for other aquatic biota (Bratrich *et al.*, 2004). In addition to further research and integration of other biological communities, extensions in terms of lateral and longitudinal (hotspots) connectivity and landscape as well as physical (water temperature, sediment load) and chemical conditions could be taken into account (Flodmark *et al.*, 2004; Olden and Naiman, 2010). The habitat rating indices should be adapted to the target species. The evaluation of the hydropeaking magnitude could then be extended to include frequency and duration as well as flow ramping analysis.

The hydropower operation tool is based on inflow and electricity price scenarios and does not generate the real contract-based production behavior precisely. The resulting on/off turbine operations produce a more fluctuating flow regime, which is

ecologically more problematic than the observed one. Thus, flow regime mitigation should be rated based on a simulated reference scenario. Flow propagation in the river network could be improved by using 1D or even 2D flow propagation models. Furthermore, costs from construction and the purchase of land for basins or channels need knowledge of local conditions, which are not easily available without detailed investigations. Conservative cost estimation with high security margins is thus recommended. The biological rating can also be affected by uncertainties regarding data sampling and expert knowledge. In addition to the commonly known problems of habitat modeling, defining a reference case for natural or initial conditions remains difficult. Natural hydro-morphological conditions do not always produce maximum habitat suitability.

7.6 Conclusion

An economic-ecological diagnostic and intervention method for mitigating fish habitat conditions in Alpine streams affected by hydropeaking was developed and applied. The approach contains a *hydropower operation model* for flow regime generation and definition of mitigation costs, a *2D hydrodynamic model* of representative river reaches and a *dynamic fish habitat simulation tool*.

Operational and constructional hydropeaking mitigation measures produce a change of the flow regime. As shown for the River Hasliaare, hydraulic-based metrics alone are unsuited to defining the ecological effectiveness of an intervention. Habitat suitability of brown trout depends highly on river morphology and life stage. Flow assessment using the developed dynamic habitat indices showed that the best ecological rating is achieved by large compensation basins or a power house outflow directly into the lake for the braided river reach. For effective flow regime mitigation, restoration of the altered morphology is essential. The method developed will facilitate science-based decision making. It can be integrated into an overall assessment tool for sustainable river management. The study may help to inform the application of the Law on Water Protection to river restoration projects at existing and newly developed hydropower facilities in Switzerland.

8 Synthesis

8.1 Achievements

This thesis combines a variety of tools to model the water cycle from a “falling raindrop” to “fish happiness” in the river. The developed approach defines the interactions between climatic, hydrological, hydraulic, economic, morphological as well as ecological parameters of Alpine river basins equipped with hydropower facilities in space and time. The novel integrative method provides a powerful instrument for sustainable water resources management.

High-head storage hydropower schemes operate in a complex and sensitive environment. Runoff from high-mountainous catchment areas, such as low flow as well as flood events, are defined by meteorological and hydrological parameters and therefore affected by climate change. The operation of hydropower plants (HPP) is mainly market-driven. Electricity prices as well as commitments define turbine and pump sequences to generate maximum economic revenue. In addition to the positive flood retention effect of the hydropower scheme, the downstream river reaches are regularly impacted by the highly fluctuating turbine operations. The sensitive aquatic ecosystems are often legally protected and/or under observation by various interest groups and stakeholders. Satisfactory water resources management, including the mitigation of the negative effects of hydropower, needs therefore an interdisciplinary approach.

The flow regime of Alpine rivers has been altered by the extensive use of storage hydropower. This results in seasonal water transfer from summer to winter and an increased frequency of daily peak discharge events. In addition, dynamic braided river

systems with rich mesohabitat gave way to straight and monotonous channelized rivers, resulting from flood protection initiatives, agriculture and urbanization. Thus, the quality of aquatic habitat has drastically decreased during many decades or centuries. Fish as well as benthos suffer from hydropeaking and poor river morphology. However, the potential for biological development of a lot of rivers, e.g., the Hasliaare River in Switzerland, remains.

In Europe and North America, the problem of highly fluctuating flow has been recognized. Governments and administrations have set up water protection policies, e.g., the European Union's Water Framework Directive or the Swiss Law on Water Protection. However, hydropeaking mitigation measures and applicable intervention strategies are still poorly developed. In Norway, the Centre for Environmental Design of Renewable Energy (SINTEF) started with detailed investigations to understand the biological response of hydropeaking. In France (Dordogne River), operational measures were implemented for river reaches of high ecological potential. In Italy, synergy projects between hydropeaking and irrigation systems are studied. Austria tries to develop the remaining hydroelectric potential in combination with river-specific mitigation measures. Switzerland focuses only on construction measures. Coordinated and integrative approaches for evaluation and mitigation of hydropeaking are often missing. Thus, the developed approach contains the appropriate modeling tools for simulation of the relevant processes:

Modeling of hydrological processes in Alpine catchment areas

The simulation of runoff in Alpine catchment areas is essential for the optimal operation of high-head storage HPP under normal flow conditions, but also for the analysis of flood events. *Routing System* undertakes hydrological modeling by a reservoir-based precipitation-runoff transformation model (GSM-SOCONT). The semi-distributed conceptual numerical approach takes into account spatial precipitation and temperature distributions for simulating the dominant hydrological processes such as glacier melt, snowpack constitution and melt, soil infiltration and runoff. Maximum data availability is required to calibrate and validate the model of the upper Aare River catchment for extreme events, e.g., the 2005 historical flood event (see Chapter 4), as well as long-term runoff estimations from glacierized Alpine catchment areas (see Chapter 5).

Climate change scenarios, based on the reference climate period 1980-2009, took into account intra-annual change in temperature and precipitation as well as long-term tendencies. Time series of the meteorological, glaciological and hydrological parameters of daily resolution were calculated by hourly updating. For a climate scenario without carbon-emission mitigation (A1B), containing an increase of temperature of about 4°C by 2099, high glacier melt is predicted for the 21st century. An almost complete de-glacierization of the upper Aare River basin for the period between 2050 and 2099 will take place. Reduction of glacier melt in summer and earlier and faster snowmelt in spring change the runoff regime from glacio-nival to nival.

The developed approach allows definition of the effects of climate change on the behavior of glacierized river basins areas for different scenarios. Despite the hourly updating of all parameters in the model, the methodology seems easily applicable to other case studies due to its transparent approach, short simulation time and easy accessibility to model parameters. *Routing System* is well adapted for runoff estimations

in Alpine catchments. Reliable estimation and optimization of future energy production and therefore economic efficiency can be done for existing and newly developed hydropower facilities.

Runoff in glacierized Alpine catchment areas will be highly impacted by climate change. Hydrological modeling is the base for sustainable future hydropower exploitation.

Modeling of hydropower operation

The heuristic hydropower modeling tool in *Routing System* allows simulation of the operating mode of a complex HPP. Within the case study of the upper Aare River catchment and despite the complexity of the HPP network, the influence of climate change, electricity market issues, plant enhancements as well as hydropeaking constraints was simulated and assessed (see Chapter 6). Reduction of future runoff by about 15% until 2050 and by about 25% by the end of the century will decrease the total annual electricity production from inflow. Thanks to the flexible operation of the pumped-storage plant in the network, revenue decreases less drastically by 4% and 8%, respectively. Open electricity market with a lot of wind power capacities will increase volatility. High fluctuations are an opportunity for storage as well as pumped-storage hydropower facilities to generate higher revenue. Enhancements of the hydropower schemes with new turbine and/or pump capacities allow increasing economic efficiency. Thus, pumped-storage can be an efficient alternative to face the losses due to climate change in mountainous areas. Of course, further investments in electricity grid strengthening and free electricity exchange would be needed for such high amounts of injected and absorbed energy. The simulations highlight the importance of long-term analysis for HPP operators to be prepared for future challenges. The wide range of the investigated hypothetical scenarios allows definition of several guide-lines for future hydropower operation.

In addition to electricity production, storage hydropower schemes can reduce flood peaks. A case study of the upper Aare River catchment operated by the Kraftwerke Oberhasli (see Chapter 4) revealed the high potential of passive and active flood retention. For the 2005 flood event and different initial reservoir filling degrees, hydropower operation was simulated and compared to the response of a catchment area without a HPP. For the non-operated catchment, a peak flow of 650 m^3/s would have occurred in 2005, which is about 25% higher than the observed discharge. Even full reservoirs still have a passive retention effect. If initial reservoir levels are high, peak flow can be reduced actively by appropriate preventive operations, using flow forecast. As simulated for the 2005 flood, with a prediction horizon of 24 h the peak flow can be reduced from 562 to 511 m^3/s. Active flood management reduces the risk of flooding in the downstream valley. Thus, the model could be applied for real-time simulations using weather forecast data as input. An agreement between the plant owner and the authorities would require a decision making strategy, including threshold values and constraints (legal and economic) for preventive measures. The developed modeling approach proves the promising capacity of passive and active flood retention of storage hydropower schemes in Alpine catchments.

Despite some potential of improvements concerning the parameter definition and the standardization of calibration, *Routing System* with the implemented heuristic HPP optimization tool is an efficient tool for modeling, simulation and analysis of complex hydropower schemes in a challenging environment.

Hydropower is faced with climate change, a changing electricity market as well as new legal and political constraints. Simulation of future operation scenarios with appropriate tools allows readiness for these challenges.

Modeling of flow regime and costs of hydropeaking mitigation

Besides the simulation of hydrological response from Alpine catchment areas as well as the operating mode of complex HPP, *Routing System* allows impact generation and analysis on the downstream river network for different scenarios (see Chapter 6). Meteorological, hydrological and morphological parameters influence the flow regime in the river for natural as well as operated catchment areas. However, turbine capacity and operation dominate it. Climate change (higher temperature and glacier melt) has only a minor impact on sub-daily fluctuations, whereas electricity market issues (higher volatility) increase them. Fully market depending peak load production undertakes on-off operations even for short periods, whereas today's contract-based production is less fluctuating. Thus, mitigation measures have to be proposed, implemented and tested.

The Oberhasli hydropower scheme is responsible for the anthropogenic hydropeaking in the Hasliaare River downstream of the Innertkirchen 1 and 2 power house outlets. The reference scenario consists of a HPP operation without any restrictions and mitigation measure. Then, several operational and construction measures were implemented in the case study area to reduce the sub-daily flow fluctuations in the Hasliaare River. Their effect on the flow regime and the related costs were defined by simulations with *Routing System.*

Regarding the impacted flow regime of the Hasliaare River, only little operational mitigation is possible with today's scheme. Measures, such as limitation of maximum turbine discharge, increase of residual flow or limited drawdown range, generate high costs relative to their effectiveness. A reduction of the actual hydropeaking ratio r_{HP} from 15.0 to 7.0 decreases benefits of initially €124 million per year by about €4 million (3%). As mitigation of hydropeaking has become a legal constraint, the implementation of new pumped-storage capacities (Brienzersee HPP) in addition to restricted turbine operation of Innertkirchen 1 HPP could reduce peak flow and may be part of negotiations with the authorities during approval procedures.

Higher ecological effect could be achieved by construction measures. Compensation basins or caverns can be installed downstream of the turbine outlets in Innertkirchen. The water is temporarily stored and then released to the river by a guided system, respecting ecologically defined operation rules. In this study, retention volumes between 50'000 and 1'000'000 m^3 for basins and between 20'000 and 300'000 m^3 for caverns were implemented and tested. Nearly all volumes higher than 100'000 m^3 generate lower peak and higher residual discharge than the operational measures. The economic efficiency of a construction measure depends on its investment cost and the related annual cost. Comparing the basins without and with the individually optimized micro-turbines at the basin outlet, the annual cost can be slightly reduced from €1.5 to

1.3 million per year for 200'000 m^3 (r_{HP} of 14.8) and from €4.5 to 4.4 million per year for 1'000'000 m^3 (r_{HP} of 6.0). Due to their high construction costs, caverns are not competitive without taking into account visual or land use assessment criteria.

Storage hydropower plants account for the main impact on the natural flow regime. Mitigation effect of operational and construction measures is simulated in terms of discharge series as well as cost.

Modeling of fish habitat suitability

The developed economic-ecological diagnostic and intervention method includes hydrological-hydraulic modeling of the HPP operation mode and a river specific habitat model for representative morphologies and target species. For the simulated and economically evaluated flow regimes, river habitat suitability is defined for fish habitat rating.

In the case study of the Hasliaare River, habitat modeling was undertaken for brown trout (*Salmo trutta fario*), based on river-specific suitability curves from *in situ* investigations. 2D hydrodynamic model simulations were performed for four reference morphologies. Their results and regional habitat suitability curves for brown trout were computed in the CASiMiR fish module, defining a reach matrix of hydraulic and habitat relevant data (flow depth and suitability indexes for specific brown trout life stages). Off-peak and peak discharges were inferred from the simulated monthly hydrograph of the fish-ecologically relevant months November (spawning and adult) and August (0+ juvenile). Habitat suitability for steady conditions is described with the steady habitat indexes. Habitat instability due to flow variations is defined by the developed dynamic habitat indexes. They are used for habitat rating and can be compared to the annual mitigation cost, as the investment costs for construction measures and production losses for operational ones, for an assessment of the implemented mitigation measures

Flow regime mitigation is only successful with suitable river morphology and vice versa. Fish habitat simulations show that hydropeaking impact is strongly dependent on river morphology. Similar to many rivers in mountainous catchment areas, the Hasliaare River has undergone considerable anthropogenic changes since the 19th century. Construction mitigation measures, such as compensation basins and HPP improvements by a direct power house outflow into Lake Brienz, show highest ecological performance for a naturally braided morphology. Achieving the same hydropeaking ratios r_{HP}, their costs are lower than for operational constraints.

The effective cost-benefit analysis of mitigation measures is a reliable and defendable approach to assess habitat suitability and financial impact and allows objective decision making.

The developed integrative approach allows operators of hydropower plants, authorities or researchers to analyze impacted catchment areas, to rate ecologically and economically construction, operational or morphological measures and thus to address hydropeaking in an optimal manner.

8.2 Concluding discussion and outlook

To define the impact of hydropower operation on the downstream river's flow regime, an interdisciplinary approach was developed. As a consequence of the wide range of modeled and analyzed fields, a certain loss of profundity has resulted. Nevertheless, congruent and coherent methodological steps contribute to a transparent approach for analysis and evaluation of operated Alpine catchment areas.

Runoff, hydropower operation as well as habitat modeling are impacted by several uncertainties, referring to upside and downside risks. They arise from wrong and incomplete data series, uncertain long-term forecasts in addition to missing knowledge and understanding of the different processes. Epistemic and stochastic uncertainties significantly influence the performance of the simulations. They stem from data, parameter estimation, model structure and state uncertainties. The main sources for the present research project are discussed hereafter:

– *Hydrological modeling*: Precipitation-runoff models are simplified representations of the hydrological cycle. Conceptual models take into account the spatial variability of the catchment area's characteristics. Detailed infiltration and evaporation processes or ice dynamics still cannot be simulated accurately.

– *Modeling of future*: Performance of climate change and runoff models may be increased. Modeling of the future is fundamentally different from reproducing the past, where interpretation and exploitation of sampled data are the main tasks. Physical back-coupling effects have to be included for reliable projections.

– *Lack of knowledge*: Besides the limits of modeling, lack of understanding of the physical processes is a major source of uncertainty. The effects of evapotranspiration or changes of albedo coefficients are not yet completely understood.

– *Data*: Reliability of data and accurate knowledge of past and actual conditions are preconditions for the simulation of future processes. Long-term forecasts are based on recent records. During calibration and validation process, quantity and quality of sampled data series are defined as accurate for simulation of future behaviors. Errors in measured data, interpretations of incomplete series and simplifications impact the reliability of modeling (Refsgaard, 1996). As an example, glacier bed geometry is still highly uncertain in several regions. Redundant monitoring and data sampling with high time and space density are therefore key factors.

– *Climate scenarios*: Climate is strongly dependent on the future greenhouse gas emission and therefore on humanity's ability to mitigation. The latter is highly dependent from social, political and economic issues, difficult to estimate or even control. Climate change scenarios are based on global and European-scale regional climate models. Future local temperature and precipitation time series are defined relative to a reference period. To meet the uncertainty due to climate forecast, the use of model ensembles is recommended. The probability of the different emission scenarios is very difficult to define. A substantial spread results. Thus, clearly defined scenarios are still the most reliable and transparent manner for future projections.

– *Electricity price scenarios*: Deregulation of the power sector increases uncertainties. In the past, estimations of only fuel price and demand level allow the definition of

reliable electricity price scenarios. Market risks due to future demand and supply parameters (e.g., weather dependency of wind and solar power) as well as regulatory risks due the lack of political and legal awareness will reduce the predictability and thus increase uncertainty.

– *Biological response*: Despite the increasing scientific body of literature investigating the interactions between flow regime and aquatic biota, skills to quantify, correlate and predict biological responses remain tenuous. For a long period, the complex riparian ecosystem has suffered from altered flow and sediment regimes. Methods to assess bio-physical processes are still rudimentary and lack the spatial and temporal complexity of the effects of hydropeaking (Meile *et al.*, 2011). Research on living organisms is always impacted by deficiencies in biological knowledge, which can only be compensated by exhaustive *in situ* data sampling.

– *Legal and political environment*: Hydropower generation is located in an area of conflict. On the one hand, renewable energy sources are promoted politically. On the other hand, construction and enhancement of big and therefore economically and energetically efficient schemes are faced with legal constraints regarding environmental protection. Uncertainties due to political and legal issues, the numerous fields of interest as well as the high number of involved stakeholders make long-term planning highly unpredictable.

A developed and applied approach can be improved by increasing knowledge to reduce uncertainties and their propagation. Several extensions could add value:

– Simulation of future operation of complex hydropower schemes in high-mountainous areas and its impact on the downstream river system is attended by several sources of uncertainty. The impact of climatic, hydrological, economic as well as biological input variables on the results could be defined by a stochastic approach. The sensitivity of the optimization procedures to uncertainty and the development of probability distributions trough the model simulations would reveal interesting – but probably also slightly disillusioning – additional value.

– In the current study, a range of operational and construction measures to mitigate hydropeaking were assessed by habitat suitability models for different river morphologies. By knowing the relationship between flow regime and habitat quality, an objective function of the biological response is defined. Multi-objective optimization could be undertaken, including economic as well as ecological criteria.

– An overall evaluation of construction measures, especially for compensation basins, would also include a range of qualitative parameters, such as political and social sensitivity, land use or agricultural issues. Heller (2007) proposes a methodology for design and management of multipurpose hydraulic schemes, taking into account a range of “soft” criteria. Qualitative methods include feedback loops between the different factors. Thus, the herein presented approach of economic-ecological assessment could be extended and completed.

– The developed method to define long-term runoff series should be applied to further Alpine catchment areas in order to obtain a comprehensive evaluation of the impact of climate change in a high-mountainous environment. Several other Swiss catchment areas with and without HPP activities have already been successfully analyzed with

the same semi-distributed conceptual approach (Terrier *et al.*, 2011). The data base of climate, glacier mass and runoff series for model calibration is exhaustive in Alpine countries. Estimation of future water availability is of substantial value for future water resources management and therefore for sustainable energy supply.

– Applications to other catchment areas with more than one hydropower plant could validate the procedure for more complex systems. Flow propagation and attenuation as well as fish migration should be included. As a consequence, not only a single hydropeaking mitigation measure, but the most effective combination could be defined by a global optimization procedure.

– *Routing System* generates the hydrograph in the river reaches with routing according to the kinematic wave assumption. Residual flow simulations with very low discharge could be improved by 1D or 2D flow propagation models for posteriori ecological assessment. Benthos, vegetation and microorganisms should also be taken into account. As a consequence, habitat indexes have to be adapted.

A

Appendix A: Simulation of hydropeaking

The hydrological-hydraulic model *Routing System* applies the GSM-SOCONT approach for simulating glacier melt, snowpack constitution and melt, infiltration and runoff. Furthermore, hydraulic structures and hydropower schemes can be implemented. The hydropower operation , the downstream flow regime and therefore the ecological impact can be computed and analyzed. In Bieri and Schleiss (2011) an analysis of the influence of meteorological, hydrological and morphological parameters on the flow regime in the river for natural as well as operated catchment areas is presented by a sensitivity analysis on a simple mountainous catchment. The approach is than applied for the upper Aare River catchment in Switzerland, operated by a high-head storage hydropower plant. The Alpine river is strongly altered by hydropeaking.

A1 Data

For the simulations, several input datasets are needed. The meteorological data are available from the Swiss Federal Office of Meteorology and Climatology (MeteoSwiss), where temperature and precipitation data is collected every ten minutes by an automatic monitoring network (ANETZ) and a large number of gauging stations (NIME) records daily precipitation. Time series of five stations of the first type and nine of the second one in and around the upper Aare River catchment are used as input data. The discharge of the Aare River in Brienzwiler is measured every ten minutes by the Federal Office of the Environment (FOEN). The Kraftwerke Oberhasli (KWO) made available historical data from the last 30 years of operation. The daily inflow datasets allow calibration of the sub-catchments operated by KWO. For the year 2005 data was collected every 10 minutes.

A2 Parameter study

A2.1 Model

The model for the parameter study contains an Alpine catchment like the upper Aare River one, but five times smaller. Three identic sub-catchments of 36 km^2 surface area each are located between 500 and 4'000 m a.s.l. (Figure A.1). The six highest elevation bands of the reference configuration are covered by glacier (17% in total). The three sub-catchment areas (SC) are connected by the main river reaches 1, 2 and 3 (MRR), with identic morphological characteristics. The calibration parameters are taken from the upper Aare River model, from the Grimsel catchment for the higher part and the Brienzwiler catchment for the lower part, leading to a mean annual discharge of 6 m^3/s.

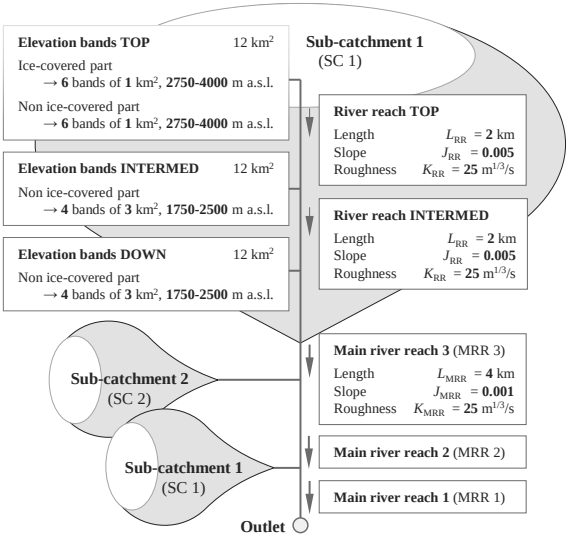

Figure A.1. Model set-up of the partly ice-covered catchment area with three identical sub-catchments (SC 1, 2, 3). Reference case with main hydrological and morphological parameters.

An autonomous turbine operation tool (see Chapter 6) is used for simulating the operation of the hydropower plant (Figure A.2). This tool is implemented at the outlet of the sub-catchment. The priority driving parameter is the electricity price. When the current price is higher than the cost price, turbine operation is undertaken. For a seasonal water transfer, the model tries to follow a preliminary defined target level curve. When inflow becomes too high compared to available storage volume, turbine operation starts to avoid water release by the spillways. The hydrological characteristics of the sub-catchments allow for a reservoir volume of $25 \cdot 10^6$ m^3 and a turbine capacity of 15 m^3/s a seasonal water transfer.

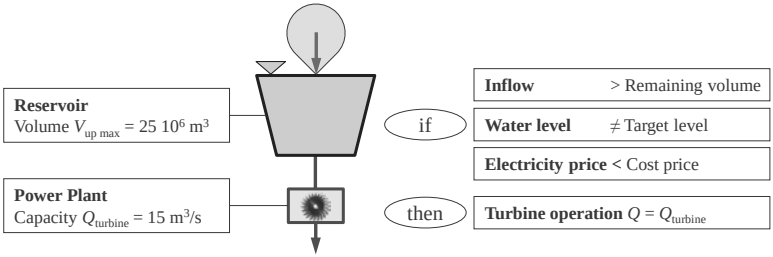

Figure A.2. Overall function chart of autonomous turbine operation tool with an upper reservoir volume of $V_{up\ max}$ and a power plant capacity of $Q_{turbine}$.

A2.2 Simulations

2005 is chosen as reference year. The simulations are run for a 15-month period, starting in October 2004 and ending in December 2005 for a 10-minute time step, using the measured precipitation and temperature series from ANETZ station Grimsel Hospiz and the electricity prices from the *European Energy Exchange* (EEX). The scenarios are simulated for the natural and the operated catchment area. Input data and the hydrological, morphological as well as hydraulic parameters are then modified for the three sub-catchments for their sensitivity analysis:

– *Position*: The power plant generally operates sub-catchment 3 (SC 3). The plant at the outlet of sub- catchment 1 (SC 1) and 2 (SC 2) is simulated for comparison.

– *Glacier*: The impact of the glacier is analyzed for different surface area of the glacier bands (GB). The total surface area of the sub-catchments does not change.

– *Climate*: The influence of increasing and decreasing precipitation is tested by an overall multiplication factor between -20% and +20% for all climate stations. Several climate change scenarios predict global warming. Overall temperature was increased by +0.5°C, +1.0°C and +1.5°C.

– *Morphology*: The influence of the three main river reaches (MRR) is tested by changing their length (L_{MRR}) and roughness (K_{MRR}).

– *Compensation basin*: To evaluate the influence of a construction hydropeaking mitigation measure, a compensation basin (CB) with different storage volumes (V_{CB}) and release capacities (Q_{CB}) is implemented downstream of the power house outflow.

A2.3 Results

Figure A.3 shows the mean annual drawdown range for 10-minute time steps for the operated and the natural catchment area. For the latter, the mean daily variations between 1.14 and 1.26, coming mostly from precipitation and snow melt, are quite small. For the operated catchment, highest drawdown ranges are simulated in winter, when residual flow is low. High magnitudes of hydropeaking occur when the power house outflow is close to the catchment outlet. A factor of nearly 2 is achieved due to the routing effect of the river, which is highest for long and rough reaches. Meteorological and hydrological parameters influence the inflow to the reservoir as well as the residual flow. The turbine unit controls the outflow of the operated sub-

catchment. When more water is available, turbine sequences are just longer, but do not have a major impact on the drawdown range. Glaciers have the highest influence on the natural flow regime. A completely ice-covered upper catchment (surface area of GB 2.0 km^2) generates slightly higher flow variations because of the higher glacier melt during the daytime.

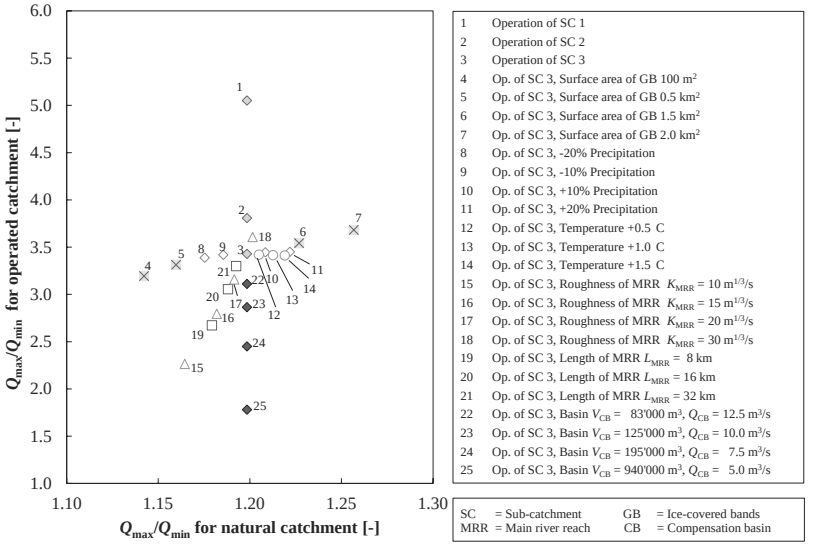

Figure A.3. Comparison of the mean annual drawdown range (Q_{max}/Q_{min}) of the simulated flow regime for the natural and operated catchment areas at the outlet for 2005 for a 10-minute time steps. Axis scales are not the same due to legibility reasons.

A3 Simulation of hydropeaking in the upper Aare River

Hydrological processes depend on a large number of parameters and their modeling is complex. Thus, the hydrological-hydraulic model's accuracy has to be tested by real case simulations. The gauging station of Brienzwiler (FOEN) at the outlet of the upper Aare River catchment is 13 km downstream of the outlets of the Innertkirchen 1 (39 m^3/s) and Innertkirchen 2 (29 m^3/s) power houses. The statistical analysis of discharge series shows that due to turbine operations, the average summer discharge decreased by 20% between 1925 and 2007, whereas winter discharge doubled. 80% of the days, hydropeaking indicators for the natural catchment between 1925 and 1928 were lower than 1.3 (Figure A.4). This value has increased by turbine operations up to 4.4.

For testing the model's ability in reproducing highly fluctuating flow, the calibrated model is first used for the simulation of the hydrological year 2005, chosen due to operation data availability in 15-minute time steps. By applying the power plant operations as done in 2005, slightly lower drawdown ranges are generated, e.g., 3.4 for the 80th percentile (Figure A.4b). The implemented basic kinematic wave theory does

not allow a better accuracy for heavily fluctuating flow. Despite this limitation, the model is able to simulate hydropeaking for different scenarios.

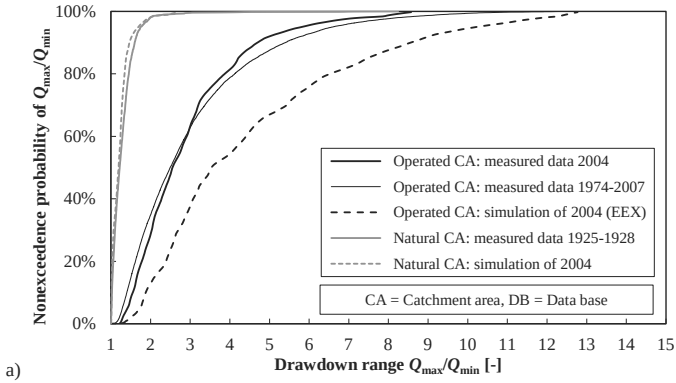

a)

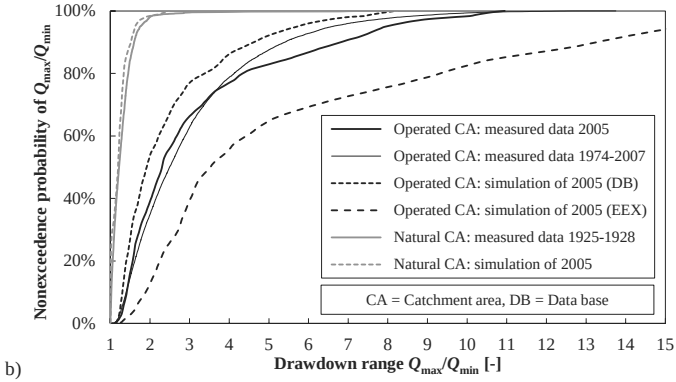

b)

Figure A.4. Statistical analysis of the daily values of the drawdown range (Q_{max}/Q_{min}) for simulated and measured hydrographs of Hasliaare River at gauging station Brienzwiler (FOEN) for operated and natural catchment for 1-hour time steps for 2004 (a) and 2005 (b).

Assuming a production only driven by the spot market (EEX), drawdown ranges would increase (Figure A.4 and Figure A.5). The reason for this difference is the Innertkirchen 2 HPP. Nowadays its production is mostly continuous like a run-of-river plant due to small upstream retention volumes. Spot market would induce short interruptions and therefore increase daily flow fluctuations. The simulation of 2005 without the hydropower scheme shows slightly lower drawdown ranges than measured between 1925 and 1928. The influence of the kinematic wave model is less important because of the more constant flow. Furthermore, the parameter study shows that larger glaciers in the past have probably generated higher flow variations because of higher melt during daytime. Another reason could be different precipitation or temperature distributions. Similar phenomenon occurred for the simulation of 2004 (Figure A.4a), where operation data of KWO was only available in daily resolution.

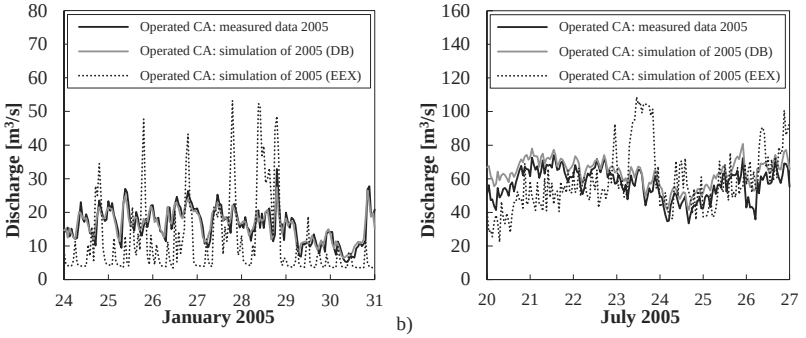

Figure A.5. Measured and simulated hydrographs of the Hasliaare River at gauging station Brienzwiler (FOEN) for chosen weeks in January 2005 (a) and July 2005 (b).

A4 Conclusion

The parameter study shows the influence of meteorological, hydrological and morphological parameters on runoff in an Alpine catchment area. It becomes more important when the turbine capacity is low or the operated catchment is small. Climate change (higher temperature and glacier melt) has only minor impact on hydropeaking, whereas electricity market issues (higher volatility) would increase it (Figure A.5). Thus, mitigation measures have to be foreseen. A restricted turbine operation mode may be theoretically an efficient measure. Construction mitigation measures are generally preferred to reduce hydropeaking downstream of the power house outflow, as shown in Figure A.3. The model is able to compare and optimize construction and operational mitigation measures and to deliver flow series for ecological rating.

B

Appendix B: Cost estimation for construction hydropeaking mitigation measures

The economic viability of a construction measure depends on its investment cost and the related annual cost. Thus, the manner of financing, the interest rate as well as the time of redemption have to be defined. The cost estimation is based on unit prices. The total costs are defined by addition of the products of the unit costs and the needed corresponding quantities. These quantities depend on the design and the size of the measure. The applied method uses a unit price which is independent from the quantity, an assumption justified by the relatively large scale of the works. The costs for environmental integration, planning and administration as well as for the equipment of the construction site are defined on pro-rata of the total costs. The planning costs take into account a percentage for miscellaneous. The investment is constantly undertaken during the construction stage. In a first step, the layout and the quantities are defined for a given case. In a second step, the product of the quantity and the corresponding unit price is calculated for defining the total investment. The presented method is only applicable for a parameter study comparing different measures between each other. For real cases, specific design and detailed economic analysis is recommended.

B1 Compensation basins

A compensation basin is generally implemented directly downstream of the turbine outlet(s). The water is temporarily stored in the basin and then released to the river by a guided system, respecting ecologically defined operation rules. The basin is realized by dikes built by extracted soil from the cutting of the reservoir.

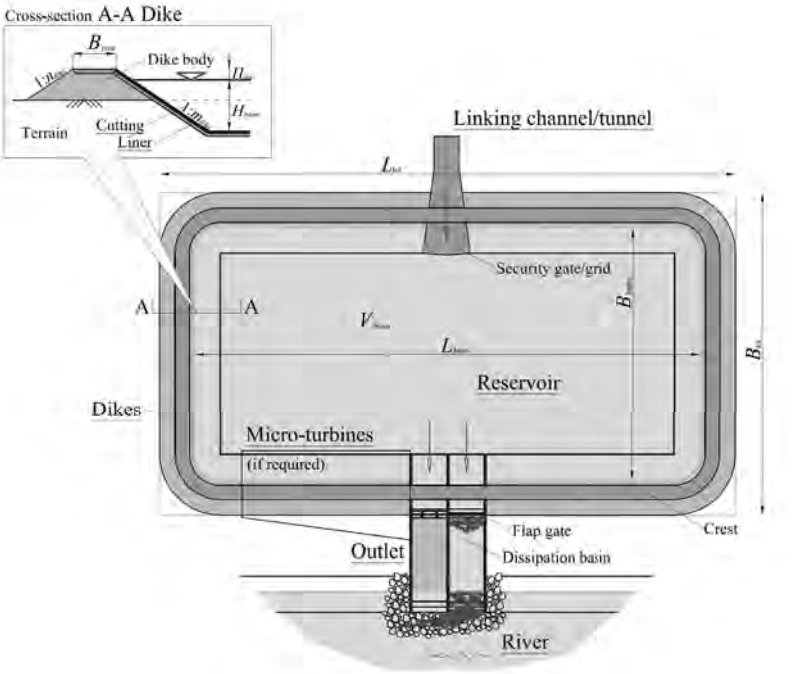

Figure B.1. Reference layout of a compensation basin with inlet and outlet facilities as well as connection to the river.

B1.1 Layout and technical key figures

The following steps explain the design details of a reference layout of the compensation basin (Figure B.1):

A. The basin is of rectangular shape. The storage volume V_{basin} [m^3] is defined by the wetted length L_{basin} [m] and width B_{basin} [m] as well as the maximum water depth H [m]. It is admitted that $L_{basin} = 1.5\ B_{basin}$.

B. For defining the use of land, the total occupied area A_{tot} [m^2] is defined by the product of the total length L_{tot} [m] and width B_{tot} [m], taking into account the crest and the outer slope of the dikes.

C. The underground part or cutting of the basin can be defined by coefficient c_{cut} [-], corresponding to the ratio of excavation depth to total depth and allowing definition of the volume of cutting V_{cut} [m^3].

D. The dikes delimit the basin and define the land use. They have the inner slope m_{dike} [-] and the outer slope n_{dike} [-]. The crest width B_{crest} [m] is normally set to 4 m. Corresponding to the coefficient c_{cut}, the dam body and the related total dike volume V_{dike} [m^3] are defined.

E. The basin has to be impermeable. Thus, a concrete or bituminous liner is placed on the inner face of the dikes and the basin ground. To avoid overtopping due to inappropriate operation and wave propagation, a security margin of H_{sec} [m] is added to the maximum water depth H_{basin} [m]. The total area A_{liner} [m^2],

corresponding to the area of the bottom and inner dike slope, takes into account this margin.

F. To link the water release of the hydropower plant (HPP) with the basin, a linking channel or tunnel is implemented. The outlet velocity of operated water $Q_{turbine}$ [m^3/s] is set to 1 m/s to avoid high flow in the basin. Depending on the position of the turbine outlet, its length $L_{channel}$ [m] can be high and the needed concrete volume $V_{channel}$ [m^3] high. Security grid or/and gate of A_{grid} [m^2] should prohibit access, avoid drift of debris and allow maintenance work.

G. Outflow is controlled by an outlet. The maximum capacity Q_{outlet} [m^3/s] corresponds to the maximum turbine discharge $Q_{turbine}$ [m^3/s]. The design consists in two parallel channels with flap gates for discharge control and a downstream located dissipation basin. The flap gates of area A_{gate} [m^2] are as high as the basin. Their unit discharge release is set to 3.5 m^3/s/m'. The needed concrete for the foundation slap V_{DB} [m^3] and the side walls V_W [m^3] depends on the corresponding areas A_{DB} [m^2] and A_W [m^2] and the thickness of 0.5 m. The dissipation basin can be connected to the river by e.g., rip-rap of an area of $A_{river} = 2\ A_{DB}$ [m^2].

H. In addition to the release control by a flap gate, micro-turbines with an efficiency of about 75% can be implemented. In reality, the technical key figures have to be defined corresponding to local conditions. For the overall analysis, the maximum operation capacity Q_{micro} [m^3/s] is set to 80% of HPP discharge $Q_{turbine}$ [m^3/s], whereas the head is $H_{micro} = 0.75\ H_{basin} + 2$ m. The 2 m take into account the elevation difference between the basin bottom and the river bed.

B1.2 Cost estimate

The cost estimations for a reference compensation basin are based on unit prices and the overall estimations of quantities (Table B.1) depending on the storage volume V_{basin}, the inlet and outlet capacities $Q_{turbine}$ and Q_{outlet} as well as the characteristics of eventually installed micro-turbines. The unit prices are based on estimations done by Heller (2007) and should be conform to realistic Swiss or European values (Table B.1):

1 The cost of land acquisition for the basin and its outlet facilities are defined by using the corresponding unit price and the areas A_{tot} and A_{DB}. The expense for excavation is defined by using the volume of cutting V_{cut}.

2 For the construction of the dikes, costs for the dam body of volume V_{dike}, the liner with an area A_{liner} and the crest of a width B_{crest} and a length corresponding to the perimeter of the wetted area have to be taken into account. These works are linked to several geotechnical and structural uncertainties; therefore a margin of 25% on the dikes' cost is applied.

3 The linking channel or tunnel between the turbine chambers and the basin is realized in concrete of volume $V_{channel}$ and ends with a security gate or grid of area A_{grid}. The price for concrete includes the material, the framework and the reinforcement in addition to the execution fees.

4 The outlet release structure with the downstream located dissipation basin generates costs related to the foundation slab of volume V_{DB} and the side walls of volume V_W. The most expensive part is the flap gate of area A_{gate}. The high unit price is related to the flexibility and reliability of use of this complex steel structure.

In case of micro-turbines, supplementary costs for the platform, the turbo-machines and the related equipment as a function of the installed power, as a product of operation capacity Q_{micro} and gross head H_{micro}, have to be included.

5 The design of the connection between the reservoir outlet and the river depends on local conditions. Often rip-rap combined with common structural works are implemented. However, the corresponding cost for an area A_{river} has to be taken into account.

6 The equipment of the construction site, including access, storage and recycling of material, electricity and water supply, etc., is estimated to 10% of the construction cost.

7 The water release to the river by the flap gate or the micro-turbines needs an autonomous intelligent remote control, depending on the release capacity Q_{outlet}.

8 The expenses for architectural and environmental integration are related to the dimensions of the dikes and therefore a percentage of their construction cost.

9 The study and administration costs include an impact analysis, the engineering as well as a certain amount for miscellaneous. They are related to the total investment.

10 Capital costs during construction depend on inflation and interim interest rates, T_{infl} and T_{int}, respectively. The investment is constantly undertaken during the 1.5 years of realization D_{constr}. The present cost can be defined by applying factor $F_{present}$:

$$F_{present} = 1 + \frac{D_{constr} \cdot T_{int}}{2} + \frac{D_{constr}{}^{2} \cdot T_{int} \cdot T_{infl}}{4} \tag{B.1}$$

The annual capital costs are defined by multiplying the present cost by the annuity $F_{annuity}$, related to a constant payment over the redemption time D_n of 50 years for civil engineering works and 25 years for the remote control and the micro-turbines:

$$F_{annuity} = \frac{T_{int} \cdot (1 + T_{int})^{D_n}}{(1 + T_{int})^{D_n} - 1} \tag{B.2}$$

11 Furthermore, expenses for maintenance work, as e.g., renovation, monitoring and remote control, have to be taken into account, depending on the construction costs.

12 Revenue from the ecologically and not economically driven operation of the micro-turbines depends on the produced energy as well as the electricity price. The number of operation hours, the corresponding heads and discharges depends on the operation rules of the basin.

The sum of the annual capital and maintenance costs as well as the revenue from turbine operation corresponds to the annual cost for flow regime mitigation.

Table B.1. Unit prices and economic assumptions for cost estimation for a reference compensation basin.

	Part	Element	Unit price	Unit
1	Basin	Land acquisition	30	[€/m^2]
		Excavation	20	[€/m^3]
2	Dikes	Body	30	[€/m^3]
		Liner	100	[€/m^2]
		Crest	150	[€/m^2]
		Margin	25% of dikes' cost (2)	
3	Linking channel	Concrete	1'000	[€/m^3]
		Security gate/grid	1'000	[€/m^2]
4.1	Outlet	Foundation slab	750	[€/m^3]
		Structures	1'000	[€/m^3]
		Flap gate	2'000	[€/m^2]
4.2	Micro-turbines	Structures	500	[€/kW]
		Machinery	1'000	[€/kW]
5	Connection to river	Rip-rap and works	250	[€/m^2]
6	Construction site	Equipment	10% of total cost (1-5)	
7	Controlling	Remote control	2'000	[€/m^3/s]
8	Integration	Architecture	5% of dikes' cost (2)	
		Environment	5% of dikes' cost (2)	
9	Study and administration	Impact analysis	3% of total cost (1-8)	
		Design engineering	15% of total cost (1-8)	
		Miscellaneous	15% of total cost (1-8)	
10	Capital costs	Inflation rate	T_{infl} = 1%	
		Construction time	D_{constr} = 1.5	[yr]
		Interest rate	T_{int} = 4%	
		Redemption time structures	D_n = 50	[yr]
		Redemption time machinery	D_n' = 25	[yr]
11	Maintenance		2% of total cost (1-5)	
12	Revenue	Electricity price for micro-turbines		[€/kWh]

B1.3 Layout and technical key figures

Applying the presented procedure to a hydropower plant (HPP) of a total turbine capacity $Q_{turbine}$ of 68 m^3/s, construction cost of the reference basin for several volumes can be computed and compared to three real cases (Figure B.2). Despite the low number of real cases, the curve for the reference layout without micro-turbines corresponds quite well to *Linthal* and *Mauvoisin II*. The costs for the layouts with micro-turbines are slightly below the known value of *KWOplus* due to a range of local conditions and detailed analysis. The smaller a basin is, the more it depends on specific particularities.

Comparing the annual cost for the reference layouts without and with micro-turbines (Figure B.3), the sensitivity concerning electricity price can be shown. Whereas as an electricity price of €0.10 /kWh reduces cost only marginally, €0.15 /kWh allow to generate between 300'000 and 500'000 €/yr depending on the volume. Such high energy prices are not realistic, unless special prices for green power or subventions can be achieved.

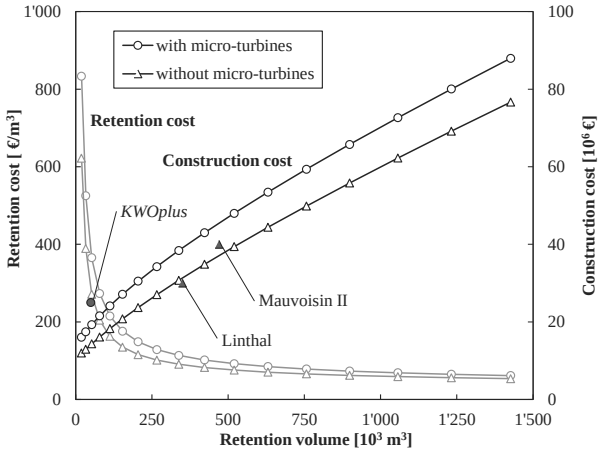

Figure B.2. Retention and construction cost in function of retention volume for reference basin layouts without and with micro-turbines for a HPP capacity of $Q_{turbine}$ = 68 m^3/s, compared to three real cases.

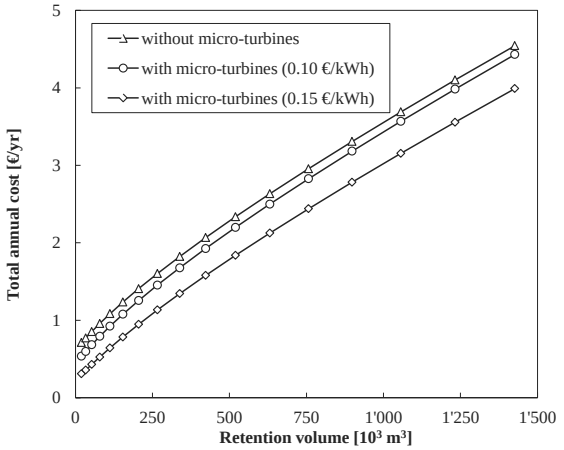

Figure B.3. Retention cost and total annual cost as a function of retention volume for reference basin layouts without and with micro-turbines (for two different electricity prices) for a HPP capacity of $Q_{turbine}$ = 68 m^3/s.

B2 Retention caverns

Instead of a compensation basin and to reduce environmental and visual impact, a retention cavern can be implemented downstream of the turbine outlet(s). The water is temporarily stored in the cavern and then released to the river by valves or turbines, ecologically defined operation rules. The cavern is realized by drill-and-blast. The storage and recycling costs of the extracted material are included in the excavation costs.

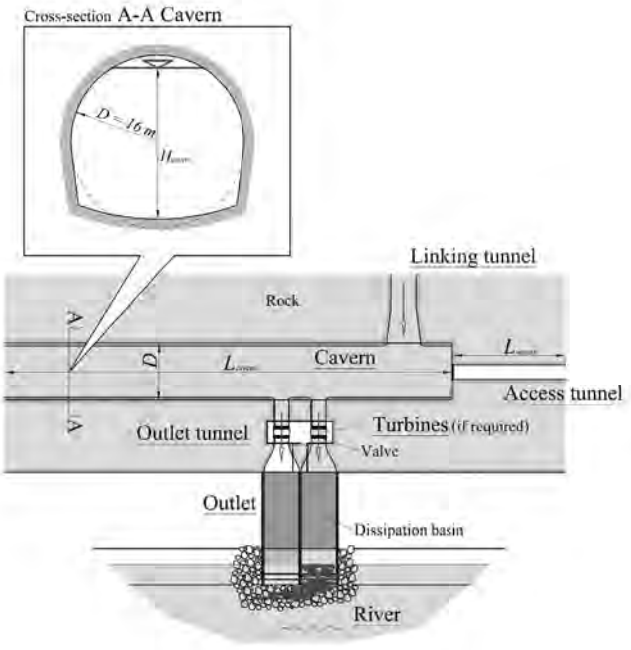

Figure B.4. Reference layout of a retention cavern with inlet and outlet facilities as well as connection to the river.

B2.1 Layout and technical key figures

The following steps explain the design details of the reference layout (Table B.2):

A. The cavern has a nearly circular cross-section of diameter D_{cavern} of 16 m, corresponding to the maximum water depth H_{cavern} [m]. The storage volume V_{caven} [m^3] is the product of the cross-section A_{cavern} [m^2] and its length L_{cavern} [m]. For greater volumes, only the cavern length is increased.

B. For construction and maintenance reasons, an access tunnel is needed. The circular gallery of diameter D_{access} of 4 m has a length L_{access} of 50 m. The excavation volume V_{access} [m^3] is therefore the product of cross-section A_{caven} [m^2] and L_{access}. The cavern can be accessed by a door with an area A_{door} of 9 m^2.

C. The water release of the hydropower plant (HPP) is connected to the cavern by a linking tunnel of diameter D_{inlet} of 4 m. The application of the length L_{inlet} of 50 m defines the excavation volume V_{inlet} [m^3].
D. Outflow is controlled by an outlet tunnel. Its maximum capacity Q_{outlet} [m^3/s] corresponds to the maximum turbine discharge $Q_{turbine}$ [m^3/s]. The design consists in two parallel tunnels with valves of section A_{valve} [m^2] for discharge control. The flow velocity through the valves is admitted to 3 m/s. Both tunnels have a diameter D_{outlet} of 4 m and a length L_{outlet} of 50 m.
E. The dissipation basin is located downstream of the outflow tunnel. The needed concrete for the foundation slab V_{DB} [m^3] and the side walls V_W [m^3] depends on the corresponding areas A_{DB} [m^2] and A_W [m^2] and their thickness of 0.5 m. The dissipation basin can be connected to the river by a rip-rap of $A_{river} = 2\ A_{DB}$ [m^2].
F. In addition to the release control by the valves, turbine units with an efficiency of about 75% can be additionally implemented. For the overall analysis, the maximum operation capacity Q_{micro} [m^3/s] is set to 80% of HPP discharge $Q_{turbine}$ [m^3/s], whereas the head is $H_{micro} = 0.66\ H_{cavern} + 2$ m.

B2.2 Cost estimate

As done for the compensation basin, the cost evaluation for the reference retention cavern is based on unit prices and the overall estimations of quantities depending on the storage volume V_{cavern}, the inlet and outlet capacities $Q_{turbine}$ and Q_{outlet} as well as the technical characteristics of the installed turbine units (Table B.2):

1 The excavation, rock stabilization and installation costs of the cavern depend on its volume V_{cavern}. Additionally a margin of 10% is applied due to several uncertainties in underground construction.
2 The access tunnel of V_{access} generates also excavation and installation costs. The latter is higher than for the cavern due to drainage system and sophisticated equipment, as e.g., the door of A_{door}.
3 The linking tunnel of V_{inlet} has to be excavated and equipped.
4 The cost of the valves for controlling flow in the two outlet tunnels of V_{outlet} is defined by their area A_{valve}.
In case of implemented turbine units, supplementary costs for the excavation, the platform, the turbo-machines and the related equipment as a function of the installed power, as a product of operation capacity Q_{micro} and gross head H_{micro}, have to be included.
5 The downstream located dissipation basin generates costs related to the foundation slab of volume V_{DB} and the side walls of volume V_W.
6 The design of the connection between the compensation basin and the river depends on local conditions. Often rip-rap combined with common structural works is implemented. However, the corresponding costs of area A_{river} have to be taken into account.
7 The equipment of construction site, including access, storage and recycling of material, electricity and water supply, etc., is estimated to 10% of the construction cost.
8 The water release to the river by the flap gate or the micro-turbines needs an autonomous remote control, depending on the release capacity Q_{outlet}.

9 The study and administration costs include an impact analysis, the engineering as well as a certain amount for miscellaneous. They are related to the total investment.
10 The assumptions for the capital costs are the same as for the compensation basin (Chapter B1.2) except the construction time of D_{contr} 2 years.
11 Furthermore, expenses for maintenance work, as e.g., renovation, monitoring and remote control, have to be taken into account, depending on the construction costs. Due to the high cost for excavation, the percentage for maintenance is with 0.2% lower than for the compensation basin.
12 The conditions for ecologically driven operation of the micro-turbines are the same as for the compensation basin (Chapter B1.2).

The sum of the annual capital and maintenance costs as well as the revenue from turbine operation corresponds to the annual fees for flow regime mitigation.

Table B.2. Unit prices and economic assumptions for cost estimation for a reference retention cavern.

	Part	Element	Unit price	Unit
1	Cavern	Excavation	200	[€/m^3]
		Interior equipment	20	[€/m^3]
		Margin	10% of cavern's cost (1)	
2	Access tunnel	Excavation	200	[€/m^3]
		Interior equipment	50	[€/m^3]
		Door	1'000	[€/m^2]
3	Linking tunnel	Excavation	200	[€/m^3]
		Interior equipment	50	[€/m^3]
		Gate	1'000	[€/m^2]
4.1	Outlet tunnel	Excavation	200	[€/m^3]
		Interior equipment	50	[€/m^3]
		Control system	5'000	[€/m^2]
4.2	Turbines	Structures	200	[€/kW]
		Machinery	750	[€/kW]
5	Outlet	Foundation slab	750	[€/m^3]
		Structures	1'000	[€/m^3]
6	Connection to river	Rip-rap and works	250	[€/m^2]
7	Construction site	Equipment	10% of total cost (1-6)	
8	Controlling	Remote control	2'000	[€/m^3/s]
9	Study and administration	Impact analysis	0.5% of total cost (1-8)	
		Design engineering	2% of total cost (1-8)	
		Miscellaneous	15% of total cost (1-8)	
10	Capital costs	Inflation rate	T_{infl} = 1%	
		Construction time	D_{constr} = 2.0	[yr]
		Interest rate	T_{int} = 4%	
		Redemption time structures	D_n = 50	[yr]
		Redemption time machinery	D_n' = 25	[yr]
11	Maintenance		0.2% of total cost (1-6)	
12	Revenue	Electricity price for turbines		[€/kWh]

B2.3 Layout and technical key figures

Applying the procedure to a hydropower plant (HPP) of a total turbine capacity $Q_{turbine}$ of 68 m^3/s, the construction cost of the reference cavern for several volumes can be computed (Figure B.5), showing an nearly linear relation between volume and cost. The only known example of the *Amsteg* HPP equipped with turbine units lies on the curve for the layout with turbines.

The retention cost decrease by increasing the retention volume and approximates a constant value (Figure B.6), explaining the linear increase of the annual cost. The linear behavior can be explained by the direct dependence on the variable cavern length L_{cavern}. The increase of the electricity price from 0.10 to 0.15 €/kWh corresponds to a shift of the line of about 300'000 €/yr, independent from the volume. The negative costs or revenue for the small volumes equipped with turbines can be explained by the relatively high constant gross head. This value depends on local conditions and cannot be always achieved.

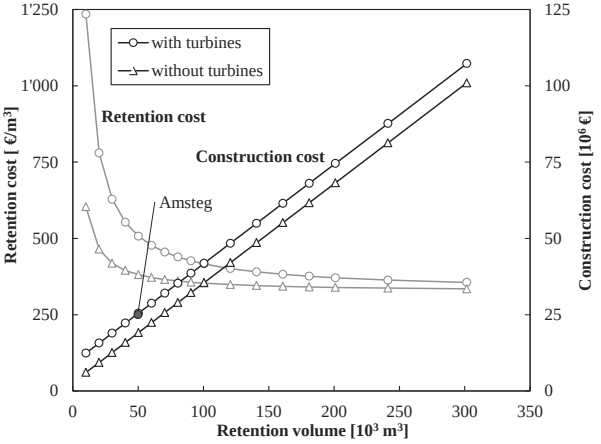

Figure B.5. Retention and construction cost in function of retention volume for reference cavern layouts without and with turbines for a HPP capacity of $Q_{turbine}$ = 68 m^3/s, compared to three real cases.

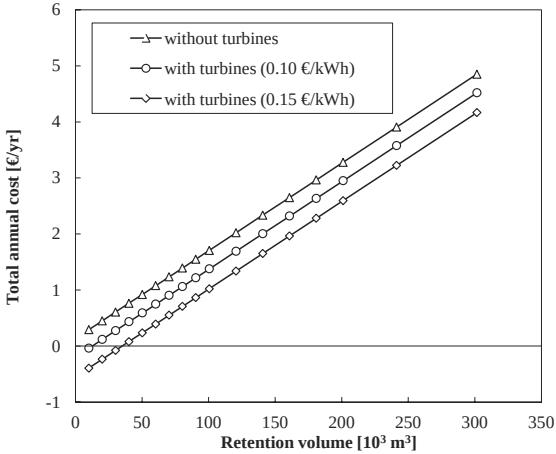

Figure B.6. Retention cost and total annual cost as a function of retention volume for reference cavern layouts without and with turbines (for two different electricity prices) for a HPP capacity of $Q_{turbine}$ = 68 m^3/s.

Bibliography

Abbott, M.B., J.C. Bathurst, J.A. Cunge, P.E. O'Connell and J. Rasmussen 1986a. An introduction to the European Hydrological System - Systeme Hydrologique Europeen, "SHE", 1: History and philosophy of a physically-based, distributed modelling system. *Journal of Hydrology* **87**(1–2): 45-59.

Abbott, M.B., J.C. Bathurst, J.A. Cunge, P.E. O'Connell and J. Rasmussen 1986b. An introduction to the European Hydrological System - Systeme Hydrologique Europeen, "SHE", 2: Structure of a physically-based, distributed modelling system. *Journal of Hydrology* **87**(1–2): 61-77.

Abbott, M.B. and J.C. Refsgaard 1996. Distributed hydrological modelling. Kluwer Academic Publishers, Dordrecht, The Netherlands.

Acreman, M.C. and A.J.D. Ferguson 2010. Environmental flows and the European Water Framework Directive. *Freshwater Biology* **55**(1): 32-48.

Ajami, N.K., H. Gupta, T. Wagener and S. Sorooshiann 2004. Calibration of a semi-distributed hydrologic model for streamflow estimation along a river system. *Journal of Hydrology* **298**: 112-135.

Alfieri, L., P. Perona and P. Burlando 2006. Optimal water allocation for an Alpine hydropower system under changing scenarios. *Water Resources Management* **20**(5): 761-778.

Alpine Convention 2011. Hydropower in the Alps focusing on small hydropower. Report. Innsbruck, Austria.

Arduino, G., P. Reggiani and E. Todini 2005. Recent advances in flood forecasting and flood risk assessment. *Hydrology and Earth System Sciences* **9**(4): 280-284.

Armour, C.L. and J.G. Taylor 1991. Evaluation of the instream flow incremental methodology by U.S. fish and wildlife service field users. *Fisheries* **16**(5): 36-43.

Arthington, A.H., R.J. Naiman, M.E. McClain and C. Nilsson 2010. Preserving the biodiversity and ecological services of rivers: New challenges and research opportunities. *Freshwater Biology* **55**(1): 1-16.

Auer, J. 2010. Hydropower in Europe: The Alps, Scandinavia and South-eastern Europe – rich in opportunities. Energy and climate change, Deutsche Bank Research, Frankfurt am Main, Germany.

Banville, C., M. Landry, J.-M. Martel and C. Boulaire 1998. A stakeholder approach to MCDA. *System Research and Behavioral Science* **15**(1): 15-32.

Barros, M.T.L., F.T.-C. Tsai, S.-l. Yang, J.E.G. Lopes and W.W.-G. Yeh 2003. Optimization of large-scale hydropower system operations. *Water Resources Planning and Management* **129**(3): 178-188.

Baumann, P., A. Kirchhofer and U. Schälchli 2012. Sanierung Schwall-Sunk - Strategische Planung: Ein Modul der Vollzugshilfe Renaturierung der Gewässer. Report. Umwelt-Vollzug, Berne, Switzerland. (in German)

Baumann, P. and I. Klaus 2003. Gewässerökologische Auswirkungen des Schwallbetriebes - Ergebnisse einer Literaturstudie. Report. Umwelt-Vollzug, Berne, Switzerland. (in German)

Baumann, P. and T. Meile 2004. Makrozoobenthos und Hydraulik in ausgewählten Querprofilen der Rhone. *Wasser Energie Luft* **96**(6): 320-325. (in German)

Baumann, P., T. Meile and M. Fette 2005. Synthesebericht Schwall/Sunk, Publikation des Rhone-Thur Projektes. Report. www.rivermanagement.ch. (in German)

Bergström, S. 1995. The HBV model. In computer models of watershed hydrology. Water Resources Publications, Highlands Ranch, Colorado, USA.

Beven, K. 1997. TOPMODEL: A critique. *Hydrological Processes* **11**(9): 1069-1085.

Beven, K.J. and M.J. Kirkby 1979. A physically based, variable contributing area model of basin hydrology / Un modèle à base physique de zone d'appel variable de l'hydrologie du bassin versant. *Hydrological Sciences Bulletin* **24**(1): 43-69.

Bieri, M. and A.J. Schleiss 2011. Modelling and analysis of hydropeaking in alpine catchments equipped with complex hydropower schemes. 34th IAHR World Congress, Brisbane, Australia: 2752-2759.

Bieri, M., A.J. Schleiss and A. Fankhauser 2010. Modelling and simulation of floods in alpine catchments equipped with complex hydropower schemes. *In:* Dittrich, Koll, Aberle & Geisheimer, eds., International Conference on Fluvial Hydraulics (River Flow 2010), Braunschweig, Germany: 1421-1428.

Bieri, M., A.J. Schleiss, F. Jordan, A.U. Fankhauser and M.H. Ursin 2011. Flood retention in alpine catchments equipped with complex hydropower schemes – A case study of the upper Aare catchment in Switzerland. *In:* Schleiss & Boes, eds., 79th ICOLD Annual Meeting, Lucerne, Switzerland: 387-394.

Black, A.R., J.S. Rowan, R.W. Duck, O.M. Bragg and B.E. Clelland 2005. DHRAM: A method for classifying river flow regime alterations for the EC Water Framework Directive. *Aquatic Conservation: Marine and Freshwater Ecosystems* **15**(5): 427-446.

Bosshard, T., S. Kotlarski, T. Ewen and C. Schär 2011. Spectral representation of the annual cycle in the climate change signal. *Hydrology Earth System Sciences Discussions* **8**: 1161–1192.

Bovee, K.D. 1982. Guide to stream habitat analysis using the instream flow incremental methodology. Instream Flow Information Paper, Washington, USA.

Brandão, J. 2010. Performance of the equivalent reservoir modelling technique for multi-reservoir hydropower systems. *Water Resources Management* **24**(12): 3101-3114.

Bratrich, C., B. Truffer, K. Jorde, J. Markard, W. Meier, A. Peter, M. Schneider and B. Wehrli 2004. Green Hydropower: A new assessment procedure for river management. *River Research and Applications* **20**(7): 865-882.

Braun, L., M. Weber and M. Schulz 2000. Consequences of climate change for runoff from Alpine regions. *Annals of Glaciology* **31**(1): 19-25.

Bunn, S.E. and A.H. Arthington 2002. Basic principles and ecological consequences of altered flow regimes for aquatic biodiversity *Environmental Management* **30**(4): 492-507.

Carpenter, T.M. and K.P. Georgakakos 2006. Intercomparison of lumped versus distributed hydrologic model ensemble simulations on operational forecast scales. *Journal of Hydrology* **329**(1–2): 174-185.

CH2011 2011. Swiss Climate Change Scenarios CH2011. Report. Zurich, Switzerland.

Chandramouli, V. and P. Deka 2005. Neural network based decision support model for optimal reservoir operation. *Water Resources Management* **19**(4): 447-464.

Chang, L.-C. 2008. Guiding rational reservoir flood operation using penalty-type genetic algorithm. *Journal of Hydrology* **354**(1-4): 65-74.

Chang, T.J. and D. Moore 1997. An expert system approach for water management in case of drought. IASTED International Conference on Intelligent Information Systems (IIS '97), Bahamas: 332-339.

Cheng, C.-T. 1999. Fuzzy optimal model for the flood control system of the upper and middle reaches of the Yangtze River. *Hydrological Sciences Journal* **44**(4): 573-582.

Cheng, C.-T. and K.W. Chau 2004. Flood control management system for reservoirs. *Environmental Modelling & Software* **19**(12): 1141-1150.

Cheng, C.-T., W.-C. Wang, D.-M. Xu and K. Chau 2008. Optimizing hydropower reservoir operation using hybrid genetic algorithm and chaos. *Water Resources Management* **22**(7): 895-909.

Choudhari, S. and P. Anand Raj 2010. Multiobjective multireservoir operation in fuzzy environment. *Water Resources Management* **24**(10): 2057-2073.

Consuegra, D., M. Niggli and A. Musy 1998. Concepts méthodologiques pour le calcul des crues - Application au bassin supérieur du Rhône. *Wasser Energie Luft* **90**(3): 223-231. (in French)

Cowx, I.G., K.T. O'Grady, P. Parasiewicz, S. Schmutz and O. Moog 1998. The effect of managed hydropower peaking on the physical habitat, benthos and fish fauna in the River Bregenzerach in Austria. *Fisheries Management and Ecology* **5**(5): 403-417.

Crisp, D.T. 2000. Trout and salmon: Ecology, conservation and rehabilitation. Wiley Online Library, Cambridge, UK.

Demeritt, D., H. Cloke, F. Pappenberger, J. Thielen, J. Bartholmes and M.H. Ramos 2007. Ensemble predictions and perceptions of risk, uncertainty and error in flood forecasting. *Environmental Hazards* **7**(2): 115-127.

Dubois, J. 2005. Simulation des systèmes hydrauliques et hydrologiques complexe : Routing System II. *In:* Schleiss, eds., Nouveaux développements dans la gestion des crues - Conférence sur la recherche appliquée en relation avec la troisième correction du Rhône, Martigny, Switzerland: 133-147. (in French)

Edijatno, N. and C. Michel 1989. Un modèle pluie-débit journalier à trois paramètres. *La Houille Blanche* **2**: 113-121. (in French)

Faber, B.A. and J.R. Stedinger 2001. Reservoiroptimization using samplingSDP with ensemblestreamflow prediction (ESP) forecasts. *Journal of Hydrology* **249**(1-4): 113-133.

Farinotti, D., M. Huss, A. Bauder and M. Funk 2009. An estimate of the glacier ice volume in the Swiss Alps. *Global and Planetary Change* **68**(3): 225-231.

Favre, H. 1935. Etude théorique et expérimentale des ondes de translation dans le canaux découverts. Dunond, Paris, France. (in French)

Feyen, L., R. Vázquez, K. Christiaens, O. Sels and J. Feyen 2000. Application of a distributed physically-based hydrological model to a medium size catchment. *Hydrology and Earth System Sciences* **4**(1): 47-63.

Finger, D., F. Pellicciotti, M. Konz, S. Rimkus and P. Burlando 2011. The value of glacier mass balance, satellite snow cover images, and hourly discharge for improving the performance of a physically based distributed hydrological model. *Water Resources Research* **47**(7): W07519.

Finger, D., M. Schmid and A. Wüest 2006. Effects of upstream hydropower operation on riverine particle transport and turbidity in downstream lakes. *Water Resources Research* **42**(8): W08429.

Fleten, S.-E. and T.K. Kristoffersen 2008. Short-term hydropower production planning by stochastic programming. *Computers & Operations Research* **35**(8): 2656-2671.

Flodmark, L.E.W., H.A. Urke, J.H. Halleraker, J.V. Arnekleiv, L.A. Vøllestad and A.B.S. Poléo 2002. Cortisol and glucose responses in juvenile brown trout subjected to a fluctuating flow regime in an artificial stream. *Journal of Fish Biology* **60**(1): 238-248.

Flodmark, L.E.W., L.A. Vøllestad and T. Forseth 2004. Performance of juvenile brown trout exposed to fluctuating water level and temperature. *Journal of Fish Biology* **65**(2): 460-470.

Flowers, G.E., S.J. Marshall, H. Björnson and G.K.C. Clarke 2005. Sensitivity of Vatnajökull ice cap hydrology and dynamics to climate warming over the next 2 centuries. *Journal of Geophysical Research* **110**: F02011.

Freeze, R.A. and R.L. Harlan 1969. Blueprint for a physically-based, digitally-simulated hydrologic response model. *Journal of Hydrology* **9**(3): 237-258.

Frey, H., W. Haeberli, A. Linsbauer and C. Huggel 2010. A multi-level strategy for anticipating future glacier lake formation and associated hazard potentials. *Natural Hazards Earth System Sciences* **10**(2): 339–352.

García, A., K. Jorde, E. Habit, D. Caamaño and O. Parra 2011. Downstream environmental effects of dam operations: Changes in habitat quality for native fish species. *River Research and Applications* **27**(3): 312-327.

García Hernández, J. 2011. Flood management in a complex river basin with a real-time decision support system based on hydrological forecasts. Thesis 5093, Ecole Polytechnique Fédérale de Lausanne.

García Hernández, J., F. Jordan, J. Dubois and J.-L. Boillat 2007. Routing System II - Flow modelling in hydraulic systems. Communication 32 du Laboratoire de Constructions Hydrauliques (ed. A. Schleiss), LCH - EPFL, Lausanne, Switzerland.

Garçon, R. 1996. Prévision opérationnelle des apports de la Durance à Serre-Ponçon à l'aide du modèle MORDOR. *La Houille Blanche* **5**: 75-82. (in French)

Gomez, P. and G. Probst 1995. Die Praxis des ganzheitlichen Problemlösens. Haupt, Berne, Switzerland. (in German)

Gouraud, V., H. Capra, C. Sabaton, L. Tissot, P. Lim, F. Vandewalle, G. Fahrner and Y. Souchon 2008. Long-term simulations of the dynamics of trout populations on river reaches bypassed by hydroelectric installations - analysis of the impact of different hydrological scenarios. *River Research and Applications* **24**(9): 1185-1205.

Grayson, R. and G. Blöschl 2001. Spatial patterns in catchment hydrology: Observations and modelling. Cambridge University Press, Cambridge, UK.

Gupta, H.V., H. Kling, K.K. Yilmaz and G.F. Martinez 2009. Decomposition of the mean squared error and NSE performance criteria: Implications for improving hydrological modelling. *Journal of Hydrology* **377**(1–2): 80-91.

Gurtz, J., A. Baltensweiler and H. Lang 1999. Spatially distributed hydrotope-based modelling of evapotranspiration and runoff in mountainous basins. *Hydrological Processes* **13**(17): 2751-2768.

Haas, R. and A. Peter 2009. Lebensraum Hasliaare 2009: Eine fischökologische Zustandserhebung zwischen Innertkirchen und Brienzersee. Report. KTI-Projekt: Nachhaltige Nutzung der Wasserkraft - Innovative Massnahmen zu Reduzierung der Schwall-Sunk Problematik, EAWAG, Kastanienbaum, Switzerland. (in German)

Haeberli, W. and M. Hoelzle 1995. Application of inventory data for estimating characteristics of and regional climate-change effects on mountain glaciers: A pilot study with the European Alps. *Annals of Glaciology* **21**: 206-212.

Haeberli, W., M. Hoelzle, F. Paul and M. Zemp 2007. Integrated monitoring of mountain glaciers as key indicators of global climate change: The European Alps. *Annals of Glaciology* **13**: 96-102.

Halleraker, J.H., S.J. Saltveit, A. Harby, J.V. Arnekleiv, H.-P. Fjeldstad and B. Kohler 2003. Factors influencing stranding of wild juvenile brown trout (salmo trutta) during rapid and frequent flow decreases in an artificial stream. *River Research and Applications* **19**(5-6): 589-603.

Heller, P. 2007. Méthodologie pour la conception et la gestion des aménagements hydrauliques à buts multiples. Thesis 3781, Ecole Polytechnique Fédérale de Lausanne. (in French)

Heller, P., E.F.R. Bollaert and A.J. Schleiss 2010. Comprehensive system analysis of a multipurpose run-of-river power plant with holistic qualitative assessment. *International Journal of River Basin Management* **8**(3-4): 295-304.

Hipel, K.W., A.I. McLeod and W.C. Lennox 1977. Advances in Box-Jenkins modeling: 1. Model construction. *Water Resources Research* **13**(3): 567-575.
Horton, P., B. Schaefli, A. Mezghani, B. Hingray and A. Musy 2006. Assessment of climate-change impacts on alpine discharge regimes with climate model uncertainty. *Hydrological Processes* **20**(10): 2091-2109.
Huss, M. 2011. Present and future contribution of glacier storage change to runoff from macroscale drainage basins in Europe. *Water Resources Research* **47**: W07511.
Huss, M., A. Bauder, D. Farinotti and M. Funk 2008a. Determination of the seasonal mass balance of four Alpine glaciers since 1865. *Journal of Geophysical Research* **113**: F01015.
Huss, M., D. Farinotti, A. Bauder and M. Funk 2008b. Modelling runoff from highly glacierized alpine drainage basins in changing climate. *Hydrological Processes* **22**(19): 3888-3902.
Huss, M., S. Sugiyama, A. Bauder and M. Funk 2007. Retreat scenarios of Unteraargletscher, Switzerland, using a combined ice-flow mass-balance model. *Antarctic and Alpine Research* **39**(9): 422-431.
Irvine, R.L., T. Oussoren, J.S. Baxter and D.C. Schmidt 2009. The effects of flow reduction rates on fish stranding in British Columbia, Canada. *River Research and Applications* **25**(4): 405-415.
Jeong, J., N. Kannan, J. Arnold, R. Glick, L. Gosselink and R. Srinivasan 2010. Development and integration of sub-hourly rainfall-runoff modeling capability within a watershed model. *Water Resources Management* **24**(15): 4505-4527.
Jordan, F. 2007. Modèle de prévision et de gestion des crues: Optimisation des opérations des aménagements hydroélectriques à accumulation pour la réduction des débits de crue. Thesis 3711, Ecole Polytechnique Fédérale de Lausanne. (in French)
Jordan, F. and K. Seiler 2010. Evolution future des apports glaciaires de la retenue de Mauvoisin en Valais. Réunion de la section de glaciologie-nivologie, Société hydrotechnique de France, Grenoble, France. (in French)
Jordan, F.M., J.-L. Boillat and A.J. Schleiss 2012. Optimization of the flood protection effect of a hydropower multi-reservoir system. *Int. Journal of River Basin Management* **10**(1): 1-8.
Jorde, K., M. Schneider and F. Zöllner 2000. Analysis of instream habitat quality - preference functions and fuzzy models. *In:* Wang & Hu, eds., Stochastic Hydraulics: 671 - 680.
Jouvet, G., M. Huss, M. Funk and H. Blatter 2011. Modelling the retreat of Grosser Aletschgletscher, Switzerland, in a changing climate. *Journal of Glaciology* **57**(206): 1033-1045.
Jungwirth, M., S. Muhar and S. Schmutz 2002. Re-establishing and assessing ecological integrity in riverine landscapes. *Freshwater Biology* **47**(4): 867-887.
Kahraman, C. 2008. Fuzzy multi-criteria decision making - Theory and applications with recent developments. Springer Science+Business Media, New York, USA.
Kapoor, I. 2001. Towards participatory environmental management? *Journal of Environmental Management* **63**(3): 269-279.
Karlsson, M. and S. Yakowitz 1987. Rainfall-runoff forecasting methods, old and new. *Stochastic Hydrology and Hydraulics* **1**(4): 303-318.
Klok, E.J., K. Jasper, K.P. Roelofsma, J. Gurtz and A. Badoux 2001. Distributed hydrological modelling of a heavily glaciated Alpine river basin. *Hydrological Sciences Journal* **46**(4): 553-570.
Koussis, A.D., A. Buzzi and P. Malguzzi 2003. Flood forecasts for urban basin with integrated hydro-meteorological model. *Journal of Hydrologic Engineering* **8**(1): 1-11.
Kumar, D. and M. Reddy 2006. Ant colony optimization for multi-murpose reservoir operation. *Water Resources Management* **20**(6): 879-898.
Landeta, J. 2006. Current validity of the Delphi method in social sciences. *Technological Forecasting and Social Change* **73**(5): 467-482.
Layher, W.G. and O.E. Maughan 1985. Spotted bass habitat evaluation using an unweighted geometric mean to determine HSI values. *Proceedings of the Oklahoma Academy of Science* **65**: 11-17.
LCH 2010. Abschwächung Schwall - Abschätzung der dämpfenden Wirkung von grossmassstäblichen Uferrauheiten auf Schwall- und Sunkerscheinungen in der Hasliaare. Report LCH 25-2010, EPFL, Lausanne, Switzerland. (in German)
Leach, W.D. and N.W. Pelkey 2001. Making watershed partnerships work: A review of the empirical literature. *Journal of Water Resources Planning and Management* **127**(6): 378-385.
Liebig, H., P. Lim and A. Belaud 1998. Influence of basic flow and hydropeaking duration on the drift of post-emergent fry of brown trout: Experiments on a semi-natural stream. *Bulletin Francais de la Pêche et de la Pisciculture* (350-51): 337-347. (in French)
Limnex 2009. Schwall/Sunk in der Hasliaare. Report. Zurich, Switzerland. (in German)
Lindström, G., B. Johansson, M. Persson, M. Gardelin and S. Bergström 1997. Development and test of the distributed HBV-96 hydrological model. *Journal of Hydrology* **201**(1–4): 272-288.

Linsbauer, A., F. Paul, M. Hoelzle, H. Frey and W. Haeberli 2009. The Swiss Alps without glaciers – A GIS-based modeling approach for reconstruction of glacier beds. Geomorphometry, Zurich, Switzerland.

Luna-Reyes, l.F. and D.L. Andersen 2003. Collecting and analyzing qualitative data for system dynamics: Methods and models. *System Dynamic Review* **19**(4): 271-296.

Luyet, V. 2005. Bases méthodologiques de la participation lors de projets ayant des impacts sur le paysage. Cas d'application: la plaine du Rhône valaisanne. Thesis 3342, Ecole Polytechnique Fédérale de Lausanne. (in French)

Maani, K.E. and V. Maharaj 2004. Links between systems thinking and complex decision making. *System Dynamic Review* **20**(1): 21-48.

Maddock, I. 1999. The importance of physical habitat assessment for evaluating river health. *Freshwater Biology* **41**(2): 373-391.

Mason, R. and I. Mitroff 1981. Challenging strategic planning assumptions. John Wiley and Sons, New York, USA.

Meile, T. 2006. Hydropeaking on watercourses. *EAWAG News* **61e**: 18-20.

Meile, T. 2008. Influence of macro-roughness of walls on steady and unsteady flow in a channel. Thesis 3952, Ecole Polytechnique Fédérale de Lausanne.

Meile, T., J.-L. Boillat and A.J. Schleiss 2011. Hydropeaking indicators for characterization of the Upper-Rhone River in Switzerland. *Aquatic Sciences* **73**: 171-182.

Mena, S.B. 2000. Introduction aux méthodes multicritères d'aide à la décision. *Biotechnologie, Agronomie, Société et Environnement* **4**(2): 83-93. (in French)

Merritt, D.M., M.L. Scott, N. LeRoy Poff, G.T. Auble and D.A. Lytle 2010. Theory, methods and tools for determining environmental flows for riparian vegetation: Riparian vegetation-flow response guilds. *Freshwater Biology* **55**(1): 206-225.

Metcalf, E. 1971. Storm water management model - Final report. Water Pollution Control Research Series, US EPA, Washington DC, USA.

Minor, H.-E. and G. Möller 2007. Schwall und Sunk, technisch-ökonomische Situation in den grösseren Flussgebieten der Schweiz. *Wasser Energie Luft* **98**(1): 19-24. (in German)

Moog, O. 1993. Quantification of daily peak hydropower effects on aquatic fauna and management to minimize environmental impacts. *Regulated Rivers: Research & Management* **8**(1-2): 5-14.

Moore, R.J., V.A. Bell and D.A. Jones 2005. Forecasting for flood warning. *Comptes Rendus Geoscience* **337**(1): 203-217.

Nakicenovic, N. and R. Swart 2000. Special report on emissions scenarios: A special report of working group III of the intergovernmental panel on climate change. Cambridge, UK.

Nash, J.E. and J.V. Sutcliffe 1970. River flow forecasting through conceptual models, part 1 - A discussion of principles. *Journal of Hydrology* **10**(3): 282-290.

Newcombe, C.P. and J.O.T. Jensen 1996. Channel suspended sediment and fisheries: A synthesis for quantitative assessment of risk and impact. *North American Journal of Fisheries Management* **16**(4): 693-727.

OcCC 2007. Klimaänderung und die Schweiz 2050 – erwartete Auswirkungen auf Umwelt, Gesellschaft und Wirtschaft. Report. OcCC and ProClim, Swiss Academy of Sciences. (in German)

Oerlemans, J. and J.P.F. Fortuin 1992. Sensitivity of glaciers and small ice caps to greenhouse warming. *Science* **258**(5079): 115-117.

Oerlemans, J., R.H. Giesen and M.R. Van Den Broeke 2009. Retreating alpine glaciers: Increased melt rates due to accumulation of dust (Vadret da Morteratsch, Switzerland). *Journal of Glaciology* **55**(192): 729-736.

Olden, J.D. and R.J. Naiman 2010. Incorporating thermal regimes into environmental flows assessments: Modifying dam operations to restore freshwater ecosystem integrity. *Freshwater Biology* **55**(1): 86-107.

Paetzold, A., C. Yoshimura and K. Tockner 2008. Riparian arthropod responses to flow regulation and river channelization. *Journal of Applied Ecology* **45**(3): 894-903.

Palmer, M.A. and E.S. Bernhardt 2006. Hydroecology and river restoration: Ripe for research and synthesis. *Water Resources Research* **42**(3): W03S07.

Parasiewicz, P., S. Schmutz and O. Moog 1998. The effect of managed hydropower peaking on the physical habitat, benthos and fish fauna in the river Bregenzerach in Austria. *Fisheries Management and Ecology* **5**: 403-417.

Pareto, V. 1896. Cours d'économie politique. Lausanne, Switzerland. (in French)

Park, M., M.P. Nepal and M.F. Dulaimi 2004. Dynamic modelling for construction innovation. *Journal for Management in Engineering* **20**(4): 170-177.

Paterson, W.S.B. 1994. The physics of glaciers. Pergamon, Oxford, UK.

Paul, F. and W. Haeberli 2008. Spatial variability of glacier elevation changes in the Swiss Alps obtained from two digital elevation models. *Geophysical Research Letters* **35**: L21502.

Paul, F., H. Machguth and A. Kääb 2005. On the impact of glacier albedo under conditions of extreme glacier melt: The summer of 2003 in the Alps. *EARSeL eProceedings* **4**(2): 139-149.
Paul, F., M. Maisch, C. Rothenbühler, M. Hoelzle and W. Haeberli 2007. Calculation and visualisation of future glacier extent in the Swiss Alps by means of hypsographic modeling. *Global and Planetary Change* **55**(4): 343–357.
Pellaud, M. 2007. Ecological response of a multi-purpose river development project using macro-invertebrates richness and fish habitat value. Thesis 3807, Ecole Polytechnique Fédérale de Lausanne.
Perona, P. and P. Burlando 2008. Mechanistic interpretation of alpine glacierized environments: Part 1. Model formulation and related dynamical properties. *Advances in Water Resources* **31**(7): 937-947.
Perona, P., N. Pasquale and D. Molnar 2008. Mechanistic interpretation of Alpine glacierized environments: Part 2. Hydrologic interpretation and model parameters identification on case study. *Advances in Water Resources* **31**(7): 948-961.
Person, E. and A. Peter 2012. Influence of hydropeaking on brown trout habitat. 9th International Symposium on Ecohydraulics, Vienna, Austria.
Peter, A. 2004. Oekologie der Rhone - Resultate aktueller Erhebungen des Forschungsprojekts "Rhone-Thur". *Wasser Energie Luft* **95**(6): 299-303. (in German)
Petts, G.E. 1984. Impounded rivers. Wiley, Chichester, UK.
Petts, G.E. and C. Amoros 1996. Fluvial hydrosystems. Chapman and Hall, London, UK.
Pfaundler, M. and M. Keusen 2007. Charakterisierung und Veränderung von Schwall-Sunk-Phänomenen in der Schweiz. *Wasser Energie Luft* **99**(1): 25-30. (in German)
Poff, N.L., J.D. Allan, M.B. Bain, J.R. Karr, K.L. Prestegaard, B.D. Richter, R.E. Sparks and J.C. Stromberg 1997. The natural flow regime. *BioScience* **47**(11): 769-784.
Pryor, S.C., R.J. Barthelmie and J.T. Schoof 2006. Inter-annual variability of wind indices across Europe. *Wind Energy* **9**(1-2): 27-38.
Refsgaard, J.C. 1996. Hydrological modelling and river basin management. Geological Survey of Danmark and Greenland, Copenhagen, Danmark.
Reis, L., G. Walters, D. Savic and F. Chaudhry 2005. Multi-reservoir operation planning using hybrid Genetic Algorithm and Linear Programming (GA-LP): An alternative stochastic approach. *Water Resources Management* **19**(6): 831-848.
Ribi, J.-M. 2011. Etude expérimentale de refuges à poissons aménagés dans les berges de rivières soumises aux éclusées hydroélectriques. Thesis 5173, Ecole Polytechnique Fédérale de Lausanne. (in French)
Richter, B., J. Baumgartner, R. Wigington and D. Braun 1997. How much water does a river need? *Freshwater Biology* **37**(1): 231-249.
Richter, B.D., A.T. Warner, J.L. Meyer and K. Lutz 2006. A collaborative and adaptive process for developing environmental flow recommendations. *River Research and Applications* **22**(3): 297-318.
Rinaldo, A., G. Botter, E. Bertuzzo, A. Uccelli, T. Settin and M. Marani 2006. Transport at basin scales: 1. Theoretical framework. *Hydrology and Earth System Sciences Discussions* **10**(1): 19-29.
Rinaldo, A. and I. Rodriguez-Iturbe 1996. Geomorphological theory of the hydrological response. *Hydrological Processes* **10**(6): 803-829.
Rohrer, M.B., L.N. Braun and H. Lang 1994. Long-term records of snow cover water equivalent in the Swiss Alps. 2. Simulations. *Nordic Hydrology* **25**(1-2): 65-78.
Rowe, G. and G. Wright 1996. The impact of task characteristics on the performance of structured group forecasting techniques. *International Journal of Forecasting* **12**: 73-89.
Saltveit, S.J., J.H. Halleraker, J.V. Arnekleiv and A. Harby 2001. Field experiments on stranding in juvenile atlantic salmon (Salmo salar) and brown trout (Salmo trutta) during rapid flow decreases caused by hydropeaking. *Regulated Rivers: Research & Management* **17**(4-5): 609-622.
Schaefli, B., B. Hingray and A. Musy 2007. Climate change and hydropower production in the Swiss Alps: Quantification of potential impacts and related modelling uncertainties. *Hydrology and Earth System Sciences* **11**(3): 1191-1205.
Schaefli, B., B. Hingray, M. Niggly and A. Musy 2005. A conceptual glacio-hydrological model for high mountainous catchments. *Hydrology and Earth System Sciences* **9**(1): 95-109.
Schärlig, A. 1985. Décider sur plusieurs critères, panorama de l'aide à la décision multicritère. Presses Polytechniques et Universitaires Romandes, Lausanne, Switzerland. (in French)
Schleiss, A. 2002. Potentiel hydroélectrique de l'arc alpin. *Bulletin SEV/VSE* **02**(2): 13-21. (in French)
Schleiss, A. 2007. L'hydraulique suisse: Un grand potentiel de croissance par l'augmentation de la puissance. *Bulletin SEV/VSE* **07**(2): 24-29. (in French)

Schneeberger, C., H. Blatter, A. Abe-Ouchi and M. Wild 2003. Modelling changes in the mass balance of the northern hemisphere for a transient 2 x CO2 scenario. *Journal of Hydrology* **182**(1-4): 145-163.

Schneider, M., I. Kopecki and J. Tuhtan 2010. Application of a habitat simulation model for the Investigation of hydropeaking effects in an Alpine river. 8th International Symposium on Ecohydraulics (ISE 2010), Seoul, South Corea.

Schweizer, S., M. Meyer, N. Heuberger, S. Brechbühl and M. Ursin 2010. Zahlreiche gewässerökologische Untersuchungen im Oberhasli. *Wasser Energie Luft* **102**(4): 289-300. (in German)

Schweizer, S., M. Meyer, T. Wagner and H.Z. Weissmann 2012a. Gewässerökologische Aufwertungen im Rahmen der Restwassersanierung und der Ausbauvorhaben an der Grimsel. *Wasser Energie Luft* **104**(1): 30-39. (in German)

Schweizer, S., J. Neuner and N. Heuberger 2009. Bewertung von Schwall/Sunk - Herleitung eines ökologisch abgestützten Bewertungskonzepts. *Wasser Energie Luft* **101**(3): 194-202. (in German)

Schweizer, S., J. Neuner, M. Ursin, H. Tscholl and M. Meyer 2008. Ein intelligent gesteuertes Beruhigungsbecken zur Reduktion von künstlichen Pegelschwankungen in der Hasliaare. *Wasser Energie Luft* **100**(3): 209-215. (in German)

Schweizer, S., H.Z. Weissmann, T. Wagner and S. Brechbühl 2012b. Oekologische Bilanzierungsmethode für die Schutz- und Nutzungsplan im Oberhasli. *Wasser Energie Luft* **104**(1): 18-29. (in German)

Scruton, D., C. Pennell, L. Ollerhead, K. Alfredsen, M. Stickler, A. Harby, M. Robertson, K. Clarke and L. LeDrew 2008. A synopsis of 'hydropeaking' studies on the response of juvenile Atlantic salmon to experimental flow alteration. *Hydrobiologia* **609**(1): 263-275.

Scruton, D.A., L.M.N. Ollerhead, K.D. Clarke, C. Pennell, K. Alfredsen, A. Harby and D. Kelley 2003. The behavioural response of juvenile Atlantic salmon (Salmo salar) and brook trout (Salvelinus fontinalis) to experimental hydropeaking on a Newfoundland (Canada) river. *River Research and Applications* **19**(5-6): 577-587.

SGHL-CHy 2011. Auswirkungen der Klimaänderung auf die Wasserkraftnutzung - Synthesebericht. Report. Beiträge zu Hydrologie in der Schweiz, Berne, Switzerland. (in German)

Sharma, V., R. Jha and R. Naresh 2004. Optimal multi-reservoir network control by two-phase neural network. *Electric Power Systems Research* **68**(3): 221-228.

Shepard, D. 1968. A two-dimensional interpolation function for irregularly-spaced data. 23rd ACM national conference, New York, USA: 517-524.

Smokorowski, K.E., R.A. Metcalfe, S.D. Finucan, N. Jones, J. Marty, M. Power, R.S. Pyrce and R. Steele 2011. Ecosystem level assessment of environmentally based flow restrictions for maintaining ecosystem integrity: A comparison of a modified peaking versus unaltered river. *Ecohydrology* **4**(6): 791-806.

Souchon, Y., F. Trocherie, E. Fragnoud and C. Lacombe 1989. Les modèles numériques des microhabitats des poissons: Application et nouveaux développements. *Revue des sciences de l'eau / Journal of Water Science* **2**(4): 807-830. (in French)

Stähli, M., M. Zappa, A. Ludwig, M. Ossiaa and A. Fankhauser 2011. Klimaänderung und Wasserkraft – Fallstudie Kraftwerke Oberhasli AG. Report. WSL, Birmensdorf, Switzerland. (in German)

Stranner, H. 1996. Schwallwellen im Unterwasser von Spitzenkraftwerken und deren Reduktion durch flussbauliche Massnahmen. Schriftenreihe zu Wasserwirtschaft, Technische Universität Graz, Graz, Austria. (in German)

Terrier, S., F. Jordan, A.J. Schleiss, W. Haeberli, C. Huggel and M. Kuenzler 2011. Optimized and adapted hydropower management considering glacier shrinkage scenarios in the Swiss Alps. *In:* Schleiss & Boes, eds., 79th ICOLD Annual Meeting, Lucerne, Switzerland: 497-508.

Thielen, J., J. Bartholmes, M.-H. Ramos and A. de Roo 2009a. The European Flood Alert System-Part 1: Concept and development. *Hydrology and Earth System Sciences* **13**: 125-140.

Thielen, J., K. Bogner, F. Pappenberger, M. Kalas, M. del Medico and A. de Roo 2009b. Monthly-, medium-, and short-range flood warning: Testing the limits of predictability. *Meteorological Applications* **16**: 77-90.

Todini, E., L. Ciarapica, V. Singh and D. Frevert 2002. The TOPKAPI model. *Mathematical models of large watershed hydrology*: 471-506.

Tolossa, H.G., J. Tuhtan, M. Schneider and S. Wieprecht 2009. Comparison of 2D hydrodynamic models in river reaches of ecological importance: HYDRO_AS-2D and SRH-W. 33rd IAHR World Congress, Vancouver, Canada: 604-611.

Truffer, B., C. Bratrich, J. Markard, A. Peter, A. Wüest and B. Wehrli 2003. Green Hydropower: The contribution of aquatic science research to the promotion of sustainable electricity. *Aquatic Sciences* **65**(2): 99-110.

Tuhtan, J., M. Noack and S. Wieprecht 2012. Estimating stranding risk due to hydropeaking for juvenile European grayling considering river morphology. *KSCE Journal of Civil Engineering* **16**(2): 197-206.
Turc, L. 1961. Estimation of irrigation-water requirements, potential evapotranspiration: A simple climatic formula evolved up to date. *Annals of Agronomy* **12**: 13-49.
Turcotte, R., P. Lacombe, C. Dimnik and J.P. Villeneuve 2004. Distributed hydrological forecast for the management of public dams in Quebec. *Canadian Journal of Civil Engineering* **31**(2): 308-320.
UNEP 2007. Global outlook for ice & snow. Arendal: UNEP/GRID.
Valentin, S., F. Lauters, C. Sabaton, P. Breil and Y. Souchon 1996. Modeling temporal variations of physical habitat for brown trout (Salmo trutta) in hydropeaking conditions. *Regulated Rivers: Research & Management* **12**(2-3): 317-330.
Van der Linden, P. and J. Mitchell 2009. ENSEMBLES: Climate change and its impacts - Summary of research and results from the ENSEMBLES project. Met Office Hadley Centre, Exceter, UK.
VAW-ETHZ 1980-2009. Die Gletscher der Schweizer Alpen - Les glaciers des Alpes suisses. Report. ETHZ, Zurich, Switzerland. (in German and French)
VAW-LCH 2006. Kraftwerksbedingter Schwall und Sunk, Eine Standortbestimmung. Report. VAW 4232, LCH 05-2006, ETHZ and EPFL, Zurich and Lausanne, Switzerland. (in German)
Vibert, R. 1939. Répercussions piscicoles du fonctionnement par éclusées des usines hydroélectriques. *Bulletin français de pisciculture* **116**: 109-115. (in French)
Viviroli, D., M. Zappa, J. Gurtz and R. Weingartner 2009. An introduction to the hydrological modelling system PREVAH and its pre- and post-processing tools. *Environmental Modelling & Software* **24**(10): 1209–1222.
Watson, R.T. and W. Haeberli 2004. Envrionmental threats, mitigation stratgies and high-mointain areas. Royal Colloquium: Maintain Areas – a Global Resoure. Ambio Special Report.
Weingartner, R. and H. Aschwanden. 1986. *Die Abflussregimes der Schweiz*. Map. Stämpfli + Cie AG, Bern. (in German)
Willi, H.-P. 2002. Synergism between flood protection and stream ecology - space as the key parameter. *EAWAG News* **51e**: 26-28.
Yeh, W.W.-G. 1985. Reservoir management and operations models: A state-of-the-art review. *Water Resources Research* **21**(12): 1797-1818.
Young, P., J. Cech and L. Thompson 2011. Hydropower-related pulsed-flow impacts on stream fishes: A brief review, conceptual model, knowledge gaps and research needs. *Reviews in Fish Biology and Fisheries* **21**(4): 713-731.
Zadeh, L.A. 1965. Fuzzy sets. *Information and Control* **8**: 338-353.
Zemp, M., W. Haeberli, M. Hoelzle and F. Paul 2006. Alpine glaciers to disappear within decades? *Geophysical Research Letters* **33**: L13504.
Zimmerman, J.K.H., B.H. Letcher, K.H. Nislow, K.A. Lutz and F.J. Magilligan 2010. Determining the effects of dams on subdaily variation in river flows at a whole-basin scale. *River Research and Applications* **26**(10): 1246-1260.
Zolezzi, G., A. Siviglia, M. Toffolon and B. Maiolini 2011. Thermopeaking in Alpine streams: Event characterization and time scales. *Ecohydrology* **4**(4): 564-576.

List of symbols and acronyms

Roman capitals

A_i	Area of cell *i* of the river morphology	[m^2]
A_{cavern}	Cross-section of cavern	[m^2]
A_{DB}	Area of foundation slab of compensation basin or cavern	[m^2]
A_{door}	Area of cavern access door	[m^2]
A_{gate}	Area of flap gates of compensation basin	[m^2]
A_{grid}	Area of security grid or gate of compensation basin	[m^2]
A_{liner}	Total area of liner of compensation basin	[m^2]
A_{river}	Area of rip-rap of compensation basin or cavern	[m^2]
A_{tot}	Total occupied area of compensation basin	[m^2]
A_{valve}	Area of outlet valve of cavern	[m^2]
A_W	Area of side walls of compensation basin or cavern	[m^2]
B	Width of runoff plan *or* of river reach	[m]
B_{basin}	Wetted width of compensation basin	[m]
B_{crest}	Crest width of dike	[m]
B_{tot}	Total width of compensation basin	[m]
D_{access}	Diameter of access tunnel to cavern	[m]
D_{cavern}	Diameter of cavern	[m]
D_{constr}	Construction time	[yr]
D_{inlet}	Diameter of linking tunnel	[m]
D_n	Redemption time	[yr]
D_n'	Redemption time for machinery	[yr]
D_{outlet}	Diameter of cavern outlet tunnel	[m]
DAR	Drained Area Ratio	[-]
$F_{annuity}$	Annuity	[-]
$F_{present}$	Factor for present construction cost	[-]
H	Net head	[m]
H_i	Flow depth of cell *i* of the river morphology	[m]
H_I	Mean ice thickness	[m e.w.]
H_S	Snow height	[m e.w.]
H_{basin}	Maximum water depth of compensation basin	[m]
H_{cavern}	Maximum water depth of cavern	[m]
H_{lim}	Threshold water depth	[m]
H_{micro}	Net head of micro-turbines	[m]
H_{sec}	Security margin for water depth of compensation basin	[m]
$H_{up\ max}$	Maximum water level of upper reservoir	[m]
$H_{up\ target}$	Target level curve of upper reservoir	[m]
HHS	Hydraulic Habitat Suitability	[-]
$HP_{1,j}$	First hydropeaking indicator of day *j*	[-]
$HP_{2,j}$	Flow-ramping rate of day *j*	[-]
J	Average slope of runoff plan *or* of river reach	[-]
K	Strickler coefficient	[$m^{1/3}/s$]
L	Length of river reach	[m]
L_{access}	Length of access tunnel to cavern	[m]
L_{basin}	Wetted length of compensation basin	[m]
L_{cavern}	Length of cavern	[m]
$L_{channel}$	Length of linking channel of compensation basin	[m]

L_{gl}	Glacier width	[m]
L_{inlet}	Length of inlet tunnel	[m]
L_{outlet}	Length of cavern outlet tunnel	[m]
L_{tot}	Total length of compensation basin	[m]
M_{snow}	Snowmelt or freeze	[m/s]
NSE	Nash and Sutcliffe efficiency criterion	[-]
P	Interpolated precipitation	[m/s]
$\mathbf{P}$	Series of decreasing electricity prices for T_{pre}	[€/MWh]
P*	Input precipitation	[m/s]
P_{cost}	Cost price	[€/MWh]
P_{el}	Electricity price	[€/MWh]
P_{eq}	Equivalent precipitation	[m/s]
$P_{eq\ ice}$	Glacier flow	[m/s]
P_{lim}	Limit operation price	[€/MWh]
P_{liq}	Rainfall	[m/s]
$P_{max,j}$	Maximum daily flow level	[m]
$P_{min,j}$	Minimum daily flow level	[m]
P_{snow}	Snowfall	[m/s]
$P_{turbine}$	Installed turbine capacity (power)	[MW]
P_{pump}	Installed pump capacity (power)	[MW]
$PC_{m,a}$	Pardé-coefficient for month *m* of year *a*	[-]
PET	Potential evapotranspiration	[m/s]
PET*	Input evapotranspiration	[m/s]
Q	Operation discharge (Chapter 6) *or* streamflow (Chapter 7)	[m^3/s]
Q'	Released discharge for hydropeaking mitigation	[m^3/s]
$Q_{baseflow}$	Base flow	[m^3/s]
Q_{comp}	Snow-to-ice transformation	[m^3 e.w./s]
$Q_{downstream}$	Discharge river downstream HPP	[m^3/s]
$Q_{gl,tot}$	Sum of glacier flows	[m^3 e.w./s]
$Q_{iceflow}$	Glacier flow to downstream elevation band	[m^3 e.w./s]
$Q_{icemelt}$	Glacier melt	[m^3 e.w./s]
Q_{inflow}	Inflow to reservoir	[m^3/s]
$Q_{interflow}$	Interflow	[m^3/s]
Q_{max}	Maximum *or* peak discharge	[m^3/s]
$Q_{max,j}$	Maximum daily discharge of day *j*	[m^3/s]
$Q_{max,j}/Q_{min,j}$	Daily drawdown range of day *j*	[-]
$Q_{mean,j}$	Mean daily discharge of day *j*	[m^3/s]
$Q_{mean\ month}$	Mean monthly discharge	[m^3/s]
$Q_{mean\ yr\ a}$	Mean annual discharge of year *a*	[m^3/s]
Q_{micro}	Maximum operation capacity of micro-turbines	[m^3/s]
Q_{min}	Minimum *or* off-peak discharge	[m^3/s]
$Q_{min,j}$	Minimum daily discharge of day *j*	[m^3/s]
$\overline{Q_{obs}}$	Mean observed runoff	[m^3/s]
$Q_{obs\ t}$	Observed hourly runoff	[m^3/s]
$Q_{obs\ max}$	Observed peak discharge	[m^3/s]
$Q_{off\text{-}peak}$	Off-peak discharge	[m^3/s]
$Q_{outflow}$	Outflow from reservoir	[m^3/s]
Q_{outlet}	Outlet capacity of compensation basin or cavern	[m^3/s]
Q_{peak}	Peak discharge	[m^3/s]

$Q_{\text{peak max}}$	Maximum discharge of the last 24 hours	[m^3/s]
$Q_{\text{peak min}}$	Minimum discharge of the last 24 hours	[m^3/s]
Q_{pump}	Full pump capacity (discharge)	[m^3/s]
Q_{runoff}	Runoff	[m^3/s]
$Q_{\text{sim } t}$	Simulated hourly runoff	[m^3/s]
$Q_{\text{sim max}}$	Simulated peak discharge	[m^3/s]
Q_{snowmelt}	Snowmelt of the glacier	[m^3/s]
Q_{tot}	Total outflow of the elevation band	[m^3/s]
Q_{turbine}	Full turbine capacity (discharge)	[m^3/s]
$Q_{\text{turbine max}}$	Upper turbine limit discharge	[m^3/s]
$Q_{\text{turbine min}}$	Lower turbine limit discharge	[m^3/s]
Q_{upstream}	Discharge river upstream HPP	[m^3/s]
R	Data search radius	[km]
RET	Real evapotranspiration	[m/s]
S_{gl}	Surface area of glacier	[m^2]
S_{ngl}	Non ice-covered surface area	[m^2]
S_{tot}	Total surface area of elevation band	[m^2]
SA	Suitable Area	[m^2]
SHR	Suitable Habitat Ratio	[-]
SHR_{eff}	Effective Suitable Habitat Ratio	[-]
SI	Suitability Index	[-]
SI_{lim}	Threshold Suitability Index	[-]
T	Interpolated temperature	[°C]
T^*	Input temperature	[°C]
T_{cp1}	Low rain-snow threshold temperature	[°C]
T_{cp2}	High rain-snow threshold temperature	[°C]
T_{cr}	Threshold melt temperature	[°C]
T_f	Reduced prediction time due to flood event	[h]
$T_{\text{down max}}$	Maximum operation time for filling the lower reservoir	[h]
T_{ETP}	Threshold evaporation temperature	[°C]
T_{lim}	Limit operation time	[h]
T_{infl}	Inflation rate	[-]
T_{int}	Interest rate	[-]
T_{per}	Time period	[h]
T_{pre}	Prediction time	[h]
$T_{\text{up max}}$	Maximum operation time for filling the upper reservoir	[h]
U	Glacier flow velocity	[m/yr]
V	Reservoir storage volume	[m^3]
V_{access}	Excavation volume of access tunnel to cavern	[m^3]
V_{basin}	Storage volume of compensation basin	[m^3]
V_{cavern}	Storage volume of cavern	[m^3]
V_{channel}	Concrete volume of linking channel of compensation basin	[m^3]
V_{cut}	Volume of cutting for compensation basin	[m^3]
V_{DB}	Concrete volume of foundation slab of compensation basin or cavern	[m^3]
V_{dike}	Total dike volume for compensation basin	[m^3]
$V_{\text{down max}}$	Maximum storage volume of lower reservoir	[m^3]
V_{down}	Volume of stored water in lower reservoir	[m^3]
V_{inflow}	Annual inflow volume to reservoir	[m^3/yr]
V_{inlet}	Excavation volume of linking tunnel	[m^3]

V_{net}	Net reservoir volume	[m^3]
V_{obs}	Observed runoff volume	[m^3]
V_{sim}	Simulated runoff volume	[m^3]
V_{tot}	Total reservoir volume	[m^3]
$V_{up\ max}$	Maximum storage volume of upper reservoir	[m^3]
V_{up}	Volume of stored water in upper reservoir	[m^3]
V_W	Concrete volume of side walls of compensation basin	[m^3]
dV	Glacier mass balance	[m^3 e.w.]
W_{snow}	Water content in the snowpack	[m]
WA_{rel}	Relevant Wetted Area	[m^2]
WA_{tot}	Total Wetted Area	[m^2]
WHL	Wetted Habitat Loss	[-]
WUA	Weighted Usable Area	[m^2]

Roman lower cases

$a_{baseflow}$	Release factor of the base flow reservoir	[-]
a_{comp}	Snow-ice transformation factor	[1/s]
a_{ice}	Degree-day factor for ice melt	[m/°C s]
$a_{interflow}$	Release factor of the interflow reservoir	[-]
a_{snow}	Degree-day factor for snowmelt	[m/°C s]
b_p	Melt coefficient due to rain	[s/m]
c_{cut}	Coefficient indicating part of cutting	[-]
$grad_P$	Altitudinal precipitation lapse rate	[mm/1000 m]
$grad_T$	Altitudinal temperature lapse rate	[°C/1000 m]
h	Storage height in the infiltration reservoir	[m]
$h_{baseflow}$	Height in base flow linear reservoir	[m]
$h_{baseflow\ max}$	Maximum storage height of base flow reservoir	[m]
h_{max}	Maximum storage capacity of infiltration reservoir	[m]
h_{ice}	Level of glacier linear reservoir	[m e.w.]
$h_{interflow}$	Height in interflow linear reservoir	[m]
$h_{interflow\ max}$	Maximum storage height of interflow reservoir	[m]
h_{runoff}	Height in runoff reservoir	[m]
$h_{snow\ gl}$	Snow level in the linear reservoir	[m]
i_{inf}	Infiltration intensity	[m/s]
$i_{interflow}$	Interflow intensity	[m/s]
i_{net}	Net intensity of precipitation	[m/s]
$i_{transfer}$	Transfer intensity	[m/s]
$k_{baseflow}$	Release coefficient of the base flow reservoir	[1/s]
k_{ice}	Linear ice reservoir coefficient	[1/s]
$k_{interflow}$	Release coefficient of the interflow reservoir	[1/s]
$k_{snow\ gl}$	Linear snow reservoir coefficient	[1/s]
$k_{transfer}$	Transfer coefficient	[1/s]
m_{dike}	Inner slope of the dike	[-]
n_{dike}	Outer slope of the dike	[-]
n	Elevation band (Chapter 5) *or* Number of turbine operation hours (Chapter 6)	[-]
ns	Valley shape parameter	[-]
r_{HP}	Hydropeaking ratio	[-]
r_{peak}	Peak flow ratio	[-]
r_{vol}	Water volume ratio	[-]

t	Time step	[h]
dt, Δt	Incremental of time step	[h; s]
$\bar{x}$	Annual mean	
x_{20th}, x_{80th}	20th and 80th percentile, respectively	

Greek symbols

α	Snow-rain separation factor	[-]
α_{vol}	Volume coefficient	[-]
α_{lev}	Level coefficient	[-]
α_{lev}'	User-defined level coefficient	[-]
α_{peak}	Hydropeaking factor	[-]
β	Non-linear reservoir coefficient for runoff	[m$^{1/3}$/s]
θ	Relative water content in the snowpack	[-]
η_t	HPP efficiency	[-]
θ_{cr}	Critical relative water content in the snowpack	[-]

Acronyms

ANETZ	Automatic measuring grid of MeteoSwiss (Automatisches MessNETZ)
AWA	Amt für Wasser und Abfall of Bern Canton
CA	Catchment area
CB	Compensation basin
CTI	Commission for Technology and Innovation
C2SM	Centre for Climate Systems Modeling
DB	Data base
DR	Drawdown range
DEM	Digital elevation model
EAWAG	Swiss Federal Institute of Aquatic Science and Technology
EEX	European Energy Exchange
EPFL	Ecole Polytechnique Fédérale de Lausanne
ETHZ	Swiss Federal Institute of Technology Zurich
FOEN	Federal Office for the Environment
GB	Glacier band
GCM	Global Circulation Models
IEA	International Energy Agency
KWO	Kraftwerke Oberhasli AG
HPP	Hydropower plant
HSC	Habitat Suitability Curve
LCH	Laboratoire de Constructions Hydrauliques
MeteoSwiss	Swiss Federal Office of Meteorology and Climatology
MRR	Main river reach
NIME	Precipitation measuring grid of MeteoSwiss (NIederschlagsMEssnetz)
Räbo	Lake Räterichsboden
RCM	Regional Climate Models
RR	River reach
RS	Routing System
SC	Sub-catchment
SFOE	Swiss Federal Office of Energy
Swisstopo	Federal Office of Topography
YOY	Young of the year

Acknowledgements

This work was conducted at the Laboratory of Hydraulic Constructions (LCH), a research unit within the Civil Engineering Institute (IIC) at the School of Architecture, Civil and Environmental Engineering (ENAC) of the Ecole Polytechnique Fédérale de Lausanne (EPFL).

During my doctoral research, I have had the opportunity to professionally and personally interact with and learn from a number of extraordinary people. I would like to acknowledge several individuals who have significantly contributed to the development of this work as well as my professional and personal perspectives.

I would first like to thank Prof. Anton J. Schleiss for the opportunity to conduct research within his laboratory, for the chance to learn his open minded perspective and for the latitude to question and research a number of domains not traditionally considered within the conventional civil engineering domain.

Secondly, I would like to thank Dr. Frédéric Jordan of *e-dric.ch Ingénieurs Conseils* for his friendship, advice and benevolent tempering of these research activities. He helped me to gain an understanding of hydrological-hydraulic modeling as well as the necessary computer skills currently developed by their innovative company.

The research project 9676.1 PFIW-IW was funded by the Swiss Innovation Promotion Agency (CTI) as well as the private and public partners. My thanks are due to the representatives of *Kraftwerke Oberhasli AG* (KWO) for following this project and for their positive attitude and encouraging interest.

I would like to thank Prof. Paolo Perona, Dr. Steffen P. Schweizer and Prof. Bernhard Wehrli for serving on my doctoral defense committee, who have honored me by evaluating and accepting this thesis, and Prof. David Andrew Barry for being the president of my thesis jury.

The colleagues from EAWAG, Emilie Person and Dr. Armin Peter, gave precious advice for the assessment of the flow regime in terms of fish habitat suitability. Comments on the manuscript about glacier by Prof. Wilfried Haeberli and about flood reduction by Dr. Jean-Louis Boillat are gratefully acknowledged. Ana Margarida Costa Ricardo supported the project with her outstanding knowledge of MATLAB coding. Special thanks go to my Irish friend Mark Treacy for acting as linguistic reviewer.

Additionally, it is a pleasure for me to acknowledge my friends and colleagues at LCH for being the surrogate family during these past years. I am proud and happy to have made wonderful friendships, especially with my long-time attender Michu Müller as well as my officemates Javier García Hernández and Stéphane Terrier. Also special thanks to our secretaries for their assistance in tackling all sorts of administrative and every-day questions as well as to the mechanics team for their strong technical support during my applied research projects. Furthermore, I would like to thank my fellow master students with whom I have had the honor and enjoyment of working with.

I wish to express my warmest thanks to my beloved family, my parents, my sister Anna and my brothers Philipp and Severin, who gave me the extra strength, motivation and love necessary to get things done.

Communications du Laboratoire de Constructions Hydrauliques ISSN 1661-1179
Ecole Polytechnique Fédérale de Lausanne
Editeur: Prof. Dr A. Schleiss

ISSN 1661-1179

Prof. Dr A. Schleiss
Laboratoire de constructions hydrauliques - LCH
EPFL, Bât. GC, Station 18, CH-1015 Lausanne
http://lch.epfl.ch
e-mail: secretariat.lch@epfl.ch